



THE HONG KONG
POLYTECHNIC UNIVERSITY

香港理工大學

Pao Yue-kong Library

包玉剛圖書館

Copyright Undertaking

This thesis is protected by copyright, with all rights reserved.

By reading and using the thesis, the reader understands and agrees to the following terms:

1. The reader will abide by the rules and legal ordinances governing copyright regarding the use of the thesis.
2. The reader will use the thesis for the purpose of research or private study only and not for distribution or further reproduction or any other purpose.
3. The reader agrees to indemnify and hold the University harmless from and against any loss, damage, cost, liability or expenses arising from copyright infringement or unauthorized usage.

If you have reasons to believe that any materials in this thesis are deemed not suitable to be distributed in this form, or a copyright owner having difficulty with the material being included in our database, please contact lbsys@polyu.edu.hk providing details. The Library will look into your claim and consider taking remedial action upon receipt of the written requests.

The Hong Kong Polytechnic University

Department of Applied Mathematics

**Co-ordinated Supply Chain Management
and Optimal Control Problems**

LEE, Yu Chung, Eugene

A thesis submitted in partial fulfillment
of the requirements for the
Degree of Doctor of Philosophy

January 2007



**Pao Yue-kong Library
PolyU · Hong Kong**

CERTIFICATE OF ORIGINALITY

I hereby declare that this thesis is my own work and that, to the best of my knowledge and belief, it reproduces no material previously published or written, nor material that has been accepted for the award of any other degree or diploma, except where due acknowledgement has been made in the text.

_____ (Signed)

LEE, Yu Chung, Eugene (Name of student)

Abstract

The thesis is divided into two parts: Supply Chain Co-ordinated Model and Optimal Control Problems.

The first part of the thesis examines co-ordinated supply chain model.

From classical inventory theory, the economic ordering quantity (EOQ) concept has been widely applied. Under EOQ, a buyer determines the optimal ordering size that minimizes its total cost. In a two-level supply chain, under individual optimal policies, the buyer orders at the EOQ and the vendor determines its own optimal production lot size, i.e. economic production quantity (EPQ). However, independent optimization may not be optimal for the whole supply chain system. Such an independent policy is known as the non-cooperation system. Many researchers, beginning in the 1970's, started to explore modes of co-ordination that performs better than the non-cooperation system in terms of total system cost. Motivated by a recently developed co-ordination model, the synchronized cycles model, this part of the thesis further explores some characteristics on this model that enhances the co-ordination between the buyers and the vendor. A hybrid heuristic is developed to solve the synchronized cycles supply chain problem.

By numerous numerical examples, the hybrid heuristic is successful in searching for a better “near-optimal” solution than the synchronized cycles algorithm developed by Chan and Kingsman (2005, 2007). Further investigations are carried out to explore the characteristics of the model and some bounds are developed on certain decision variables in order to enhance the synchronized cycles algorithm. In addition, modification to the synchronized cycles model by including vehicle scheduling is considered. The performance of the synchronized cycles model is compared to the independent policy. By the “synchronization” characteristic, the synchronized cycles model out-performs the independent policy both in shipment and delivery scheduling and total system cost. Finally, while many of the past researches emphasized on the co-ordination that minimizes the total system cost in the supply chain system, the thesis investigates how the demand heterogeneity, e.g. different values of mean demand, variance and skewness, would affect the performance of the synchronized cycles model. This is a novel investigation in the field of supply chain management. Numerical experiments are carried out to identify conditions of the demand heterogeneity that work well for the synchronized cycles model.

The second part of the thesis consists of four open optimal control problems applying to different areas. Optimal control techniques are developed in this thesis and applied to solve the mathematical and computational difficulties encountered by these problems. The optimal control software package, MISER3, is intensively used. Numerical examples are provided to demonstrate the effectiveness of the methods developed. Results obtained are significant.

1. Modeling of a supply chain system with Ornstein Uhlenbeck demand process

This demand process is seldom considered in the field of supply chain management and has not yet been analytically derived using the Pontryagin's maximum principle. A single-vendor-single-buyer supply chain system is formulated. Both co-ordinated and non-cooperative supply chain models are considered.

2. The isoperimetric pillar-construction problem

The problem is to find an enclosed cross-sectional/base region of a pillar defined by a simple closed curve of fixed perimeter, such that the volume of the pillar, bounded above by a given surface, is maximized. Solutions to the single pillar and multiple pillars cases are considered. For multiple pillars case, a novel elliptic separation constraint technique is used to

separate the overlapping of different pillars.

3. Modeling of the design of a flexible rotating beam

The problem considers a rotating beam which carries an end mass and rotates in a vertical plane under the effect of gravity by means of a time-varying driving torque. The problem is posed as a continuous-time optimal control problem for the ACLD treatment. Such a computational optimal control approach is a novel technique in the design of the ACLD treated rotating beam. In addition, the accurate time of the switching points are determined which has not been considered in previous similar researches.

4. Nonlinear model of quarter-car suspension problem

Vehicle active suspension system has been a popular issue in road vehicle applications. Many researchers have dedicated effort in the modeling and the design of controlled suspension system to ensure a smooth ride. A quarter-car suspension model with state dependent ODE system of equations is considered. Computational method with enhanced switching controls is used to solve the problem.

Publications Arising From the Thesis

1. Lee, Y.C.E., Chan, Chi Kin, and Hou, S.H., 2006, The Effects of Demand Distribution Among Buyers on Co-ordination in a Single-Vendor-Multi-Buyer Supply Chain, Conference proceedings in International Workshop on Successful Strategies in Supply Chain Management, Hong Kong, January 5-6, 157-166.
2. Lee, Y.C.E., Fung, E.H.K., Zou, J.Q., and Lee, H.W.J., 2004, A Computational Optimal Control Approach to the Design of a Flexible Rotating Beam With Active Constrained Layer Damping, Proceedings of IMECE2004, ASME International Mechanical Engineering Congress and Exposition, Anaheim, California, November 13-19, proceeding in the form of CD-ROM, IMECE2004-62205.
3. Lee, Y.C.E., Fung, E.H.K., and Lee, H.W.J., Control Parametrization Enhancing Technique and Simulation on the Design of a Flexible Rotating Beam, Journal of Optimization Theory and Applications, 136(2), 2008.
4. Lee, Y.C.E., and Lee, H.W.J., Optimal Control Solutions to the Maximum Volume Isoperimetric Pillars Problem, *Automatica*, *accepted*.
5. Lee, Y.C.E., and Lee, H.W.J., Enhanced State-dependent Switching Control for Quarter-car Suspension Model, *submitted*.
6. Wong, K.H., Lee, Y.C.E., and Lee, H.W.J., Effect of Information Sharing in a Two-Level Supply Chain with Ornstein Uhlenbeck Demand Process, *submitted*.

Acknowledgements

First and foremost, I would like to thank my chief supervisor Dr. Joseph Heung-wing Lee and two co-supervisors Dr. Chi-kin Chan and Dr. Bartholomew Ping-kei Leung. Thanks for their continuous support (both academically and personally) and mentorship in these four years of study. Dr. Lee and Dr. Chan provide me endless new and brilliant ideas on my research (especially when my ideas are all exhausted) and they also give me many opportunities to explore various field of mathematics which I have never encountered before in my undergraduate studies. At any time of the day, they are always willing to discuss and give valuable insight to my research. Thanks Dr. Leung for his dedication in sharing his wealth of knowledge and experience with me. A special thank to Prof. Shui-hung Hou for all the good advices. Many thanks to the Board of Examiners, Dr. Wai-cheung Ip as the chairman, Prof. Sui-hoi Hou and Prof. André Langevin as the external examiners, for their constructive comments and suggestions which lead to a significant improvement in the thesis.

I would like to acknowledge Dr. Eric Hoi-kwun Fung of the Department of Mechanical Engineering at the Hong Kong Polytechnic University and Prof.

Acknowledgements

Kar-hung Wong of the School of Computational and Applied Mathematics at the University of the Witwatersrand. Dr. Fung provides me an opportunity to explore the flexible rotating beam problem (Chapter 11) and guides me through the publication of all related conference and journal papers. Prof. Wong introduces me to the application of optimal control theory towards supply chain optimization (Chapter 8) and enlightens me some research areas in time-delayed optimal control problems.

To all my colleagues, academic and supporting staff of the AMA department, I appreciate their help in all kind of supports. They have made my time at the Hong Kong Polytechnic University more enjoyable. I would also like to thank the Hong Kong Polytechnic University for the postgraduate studentship.

Finally and the most importantly, I am indebted to my dad and mom, Andrew Kwok-kwan Lee and Chiu-ling Wong, for their continuous support and encouragement to me towards the completion of this degree. Further, I would like to express sincere thanks to my beloved one, Eunice Yuen-ki Ng, for her love, support and patience, allowing me to accomplish my goal and sharing with me all the happy and sad moments.

Table of Contents

Abstract		iii
Publications Arising From the Thesis		vii
Acknowledgements		viii
Table of Contents		x
List of Figures		xiv
List of Tables		xx
Chapter 1	Introduction	1
1.1	Part I: Co-ordinated Supply Chain Model	1
1.1.1	Outline: Chapter 2 – Chapter 6.....	2
1.2	Part II: Optimal Control Problems.....	4
1.2.1.	Outline: Chapter 7 – Chapter 11.....	5
PART I	CO-ORDINATED SUPPLY CHAIN MODEL	8
Chapter 2	Literature Review on Supply Chain Dynamics and Co-ordination	8
2.1	Introduction.....	8
2.2	Modeling on the Industrial Dynamic Systems.....	14
2.3	Co-ordination of Supply Chains.....	18
Chapter 3	The Synchronized Ordering and Production Cycles	31
3.1	Introduction.....	31
3.2	Assumptions and Notations.....	31
3.2.1	Assumptions.....	31
3.2.2	Notations.....	32
3.3	The Independent Policy Model.....	34
3.4	The Common Cycle Model.....	35
3.5	The Synchronized Ordering and Production Cycles Model..	37
Chapter 4	Meta-Heuristics Approach to the Synchronized Cycles Algorithm	40
4.1	Introduction.....	40
4.2	Genetic Algorithm.....	41
4.2.1	Gene Representation.....	42
4.2.2	Selection.....	42

	4.2.3	Crossover.....	43
	4.2.4	Mutation.....	44
	4.2.5	New Population.....	46
	4.2.6	Stopping Criterion.....	47
4.3		Simulated Annealing.....	47
	4.3.1	Gene Representation.....	48
	4.3.2	Initial and Final Temperature.....	48
	4.3.3	Cooling Schedule.....	49
	4.3.4	Neighborhood Moves.....	49
	4.3.5	Stopping Criterion.....	49
4.4		Numerical Results.....	50
	4.4.1	Quality of the Solutions Obtained by the Hybrid Heuristic.....	57
4.5		Discussions.....	59
Chapter 5		Further Studies on the Synchronized Ordering and Production Cycles	63
	5.1	Introduction.....	63
	5.2	Pareto Improvements.....	63
	5.3	Sensitivity Analysis.....	67
	5.3.1	Effects of Variation on Standard Parameters.....	67
	5.3.2	The Portion Borne by the Vendor Under the Independent Policy and the Synchronized Cycles Co-ordination.....	73
5.4		Establishing Bounds on N	75
	5.4.1	Synchronized Cycles Algorithm.....	75
	5.4.2	Bounds on N	76
	5.4.3	Revised Synchronized Cycles Algorithm by Establishing the Bounds on N	78
5.5		Establishing Bounds on b	84
5.6		Reduction in the Search Space on Ψ	84
5.7		Difficulties in Obtaining Analytical Solutions.....	87
5.8		Possible Extensions of the Synchronized Cycles Model.....	89
	5.8.1	Single-truck Transportation Scheduling.....	90
	5.8.2	Multi-truck Transportation Scheduling with Limited Capacity.....	90
	5.8.3	Numerical Results and Discussions.....	92

Chapter 6	The Effects of Demand Heterogeneity Among Buyers on the Three Models of Co-ordination in a Single-Vendor-Multi-Buyer Supply Chain	104
6.1	Introduction.....	104
6.2	The Three Models.....	105
6.3	Numerical Experiments.....	111
6.4	Results and Discussions.....	113
PART II	OPTIMAL CONTROL PROBLEMS	128
Chapter 7	Literature Review in Optimal Control Theory and Its Applications	128
7.1	Introduction to Control Theory.....	128
7.2	Optimal Control Theory on the Supply Chain.....	135
7.3	Optimal Control – Other Applications.....	139
7.3.1	The Isoperimetric Pillar Problem.....	139
7.3.2	The Flexible Rotating Beam.....	142
7.3.3	The Quarter–Car Suspension Model.....	143
Chapter 8	Optimal Production Schedule Problem with Ornstein Uhlenbeck Demand Process in a Two Level Supply Chain	146
8.1	Introduction.....	146
8.2	The Ornstein Uhlenbeck Demand Process.....	147
8.3	Effect of Information Sharing in a Two-Level Supply Chain.....	148
8.3.1	Lower Level’s Problem.....	148
8.3.2	Higher Level’s Problem (with full information)....	151
8.3.3	The Approximation Procedure.....	153
8.4	Vendor Managed Inventory (VMI) Co-ordination.....	156
8.5	Numerical Results and Discussions.....	157
Chapter 9	The Isoperimetric Pillar Problem	162
9.1	Introduction.....	162
9.2	The Isoperimetric Problem.....	162
9.3	The Green’s Theorem.....	164
9.4	Problem Description.....	164
9.5	Analytic Solution – One Pillar, Flat Surface.....	167

9.6	Multi-Pillar Problem.....	171
9.7	Illustrative Examples.....	175
9.8	Discussions.....	185
Chapter 10	Control Parametrization Enhancing Technique and Simulation on the Design of a Flexible Rotating Beam	187
10.1	Introduction.....	187
10.2	Optimal Control and CPET.....	188
10.3	Dynamics of the ACLD Treated Beam.....	191
10.4	Optimal Control Formulation of the ACLD Treated Beam...	195
10.5	Numerical Simulations and Results.....	196
10.5.1	Numerical Simulations of the PCLD System.....	196
10.5.2	Results of the ACLD System.....	201
Appendix 10.A	– Equation for the PCLD System.....	208
Appendix 10.B	– Derivation for Q_p	210
Chapter 11	Optimal Control Strategy for a Nonlinear Quarter–Car Suspension Model with State Depending ODE Class	212
11.1	Introduction.....	212
11.2	State Dependent Optimal Control Problem.....	212
11.3	The Computational Method with Enhanced Switching Controls.....	214
11.4	Optimal Control Formulation of the Vehicle Suspension Problem.....	216
11.5	Numerical Results and Discussions.....	219
Chapter 12	Concluding Remarks and Future Research Directions	225
12.1	Part I: Co-ordinated Supply Chain Model.....	225
12.2	Part II: Optimal Control Problems.....	229
Appendix – Datasets		234
References		245

List of Figures

Figure 2.1.1	A typical supply chain system.....	9
Figure 2.1.2	Reduction of number of shipments with an introduction of an intermediary.....	11
Figure 5.3.1.1	The effect on percentage change in demand (Set 21)....	69
Figure 5.3.1.2	The effect on percentage change in transportation cost (Set 21).....	69
Figure 5.3.1.3	The effect on percentage change in ordering cost (Set 21).....	69
Figure 5.3.1.4	The effect on percentage change in buyer's holding cost (Set 21).....	70
Figure 5.3.1.5	The effect on percentage change in vendor's set-up cost (Set 21).....	70
Figure 5.3.1.6	The effect on percentage change in vendor's holding cost (Set 21).....	70
Figure 5.3.1.7	The effect on percentage change in demand (Set 24)....	71
Figure 5.3.1.8	The effect on percentage change in transportation cost (Set 24).....	71
Figure 5.3.1.9	The effect on percentage change in ordering cost (Set 24).....	71
Figure 5.3.1.10	The effect on percentage change in buyer's holding cost (Set 24).....	72
Figure 5.3.1.11	The effect on percentage change in vendor's set-up cost (Set 24).....	72

Figure 5.3.1.12	The effect on percentage change in vendor's holding cost (Set 24).....	72
Figure 5.3.2.1	The effect on the increment of buyer's cost (Set 24, DP=0.5).....	74
Figure 5.3.2.2	The effect on vendor's cost reduction (Set 24, DP=0.5).....	74
Figure 5.3.2.3	The effect on the total cost (Set 24, DP=0.5).....	74
Figure 5.6.1	Plot of Ψ vs. j (2 cycles).....	87
Figure 5.6.2	Plot of Ψ vs. j (4 cycles).....	87
Figure 6.2.1	Total Cost vs. $\sum_{i=1}^n \sqrt{d_i}$ ($n = 10$).....	109
Figure 6.2.2	Total Cost vs. $\sum_{i=1}^n \sqrt{d_i}$ ($n = 50$).....	109
Figure 6.2.3	Total Cost vs. (Deviation) ² ($n = 10$).....	110
Figure 6.2.4	Total Cost vs. (Deviation) ² ($n = 50$).....	110
Figure 6.4.1	Total Cost vs. CV (Set 01 DP=0.5).....	114
Figure 6.4.2	Total Cost vs. CV (Set 02 DP=0.5).....	115
Figure 6.4.3	Total Cost vs. CV (Set 12 DP=0.5).....	115
Figure 6.4.4	Total Cost vs. CV (Set 22 DP=0.5).....	115
Figure 6.4.5	Saving (in %) vs. CV (Com. Cycle).....	116
Figure 6.4.6	Saving (in %) vs. CV (Syn. Cycle).....	117

Figure 6.4.7	Buyers and vendor incurred cost as a function of CV....	117
Figure 6.4.8	Total Cost vs. Skewness (Set 22, DP=0.5).....	121
Figure 6.4.9	Total Cost vs. Skewness for fixed total demand.....	125
Figure 7.1.1	The brachistochrone problem.....	130
Figure 7.1.2	Open-loop and closed-loop control system.....	131
Figure 8.2.1	Sample paths of the Ornstein Uhlenbeck process.....	147
Figure 8.5.1	Optimal Trajectory – Upper level’s production (set 04).....	160
Figure 8.5.2	Optimal Trajectory – Lower level’s production (set 04).....	160
Figure 8.5.3	Optimal Trajectory – Upper level’s inventory (set 04).....	160
Figure 8.5.4	Optimal Trajectory – Lower level’s inventory (set 04).....	161
Figure 9.4.1	A simple closed curve with positive orientation.....	166
Figure 9.6.1	Illustration of the three-pillar case.....	173
Figure 9.7.1	Optimal location of two pillars bounded above by surface S_1	176
Figure 9.7.2	Optimal location of three pillars bounded above by surface S_1	176
Figure 9.7.3	3-D plot of surface S_2	177
Figure 9.7.4	Contour plot of surface S_2	177

Figure 9.7.5	Optimal location of two pillars bounded above by surface S_2	178
Figure 9.7.6	Optimal location of three pillars bounded above by surface S_2	178
Figure 9.7.7	3-D plot of surface S_3	179
Figure 9.7.8	Contour plot of surface S_3	179
Figure 9.7.9	Optimal location of two pillars bounded above by surface S_3	180
Figure 9.7.10	Optimal location of three pillars bounded above by surface S_3	180
Figure 9.7.11	Optimal location of four pillars bounded above by surface S_3	181
Figure 9.7.12	3-D plot of surface S_4	182
Figure 9.7.13	Contour plot of surface S_4	182
Figure 9.7.14	Optimal location of two pillars bounded above by surface S_4	183
Figure 9.7.15	Optimal location of three pillars bounded above by surface S_4	183
Figure 9.7.16	Optimal location of four pillars bounded above by surface S_4	184
Figure 10.3.1	Section of Sandwiched Beam.....	192
Figure 10.3.2	Co-ordinate Systems.....	193
Figure 10.5.1	Effect of the thickness of the constraining layer with $h_2 = 1.00 \times 10^{-4} m$	197

Figure 10.5.2	Effect of the thickness of the VEM layer with $h_1 = 4.00 \times 10^{-4} m$	198
Figure 10.5.3	Effect of the ratio of the thickness of the constraining layer and the VEM layer ($h_1 / h_2 = 4$).....	199
Figure 10.5.4	Effect of the ratio of the thickness of the constraining layer and the VEM layer ($h_1 / h_2 = 1$).....	200
Figure 10.5.5	Effect of the ratio of the thickness of the constraining layer and the VEM layer ($h_1 / h_2 = 1/4$).....	200
Figure 10.5.6	Transverse Deflection w (constant gain PD controller).	203
Figure 10.5.7	Input Voltage V_c (constant gain PD controller).....	204
Figure 10.5.8	Transverse Deflection w (2-partition).....	204
Figure 10.5.9	Input Voltage V_c (2-partition).....	205
Figure 10.5.10	Optimal Control Gain u_3 (2-partition) (proportional control gain).....	205
Figure 10.5.11	Optimal Control Gain u_7 (2-partition) (derivative control gain).....	206
Figure 10.5.12	Transverse Deflection w (4-partition).....	206
Figure 10.5.13	Input Voltage V_c (4-partition).....	207
Figure 10.5.14	Optimal Control Gain u_3 (4-partition) (proportional control gain).....	207
Figure 10.5.15	Optimal Control Gain u_7 (4-partition) (derivative control gain).....	208
Figure 11.4.1	A schematic diagram for the vehicle suspension	

	model.....	216
Figure 11.5.1	The tyre deformation, $x_1(t)$ (Flat Road Surface).....	221
Figure 11.5.2	The suspension deflection, $x_2(t)$ (Flat Road Surface)..	221
Figure 11.5.3	Zoomed plot of the tyre deformation, $x_1(t)$ (Flat Road Surface).....	221
Figure 11.5.4	Zoomed plot of the enhanced switching control, $\hat{u}_1(t)$ (Flat Road Surface).....	222
Figure 11.5.5	Zoomed plot of the enhanced switching control, $\hat{u}_2(t)$ (Flat Road Surface).....	222
Figure 11.5.6	The body acceleration, $\dot{x}_4(t)$ (Flat Road Surface).....	222
Figure 11.5.7	The non-flat surface.....	223
Figure 11.5.8	The tyre deformation, $x_1(t)$ (Non-flat Road Surface)...	224
Figure 11.5.9	The suspension deflection, $x_2(t)$ (Non-flat Road Surface).....	224
Figure 11.5.10	The body acceleration, $\dot{x}_4(t)$ (Non-flat Road Surface).....	224

List of Tables

Table 4.4.1	The average percentage improvements of the GASA heuristic over SCA, GA and SA.....	52
Table 4.4.2	Minimum cost obtained by the hybrid method and its comparison with the SCA.....	53
Table 4.4.1.1	Comparison of minimum cost obtained by SCA, GASA and the “reduced enumerative search” (5-buyer case)...	58
Table 4.5.1	Minimum and maximum number of feasible combinations.....	61
Table 5.2.1	Comparison on the performances of the independent policy and the SCA	66
Table 5.4.1	The range of possible values of optimal N under SCA.	81
Table 5.8.3.1	The parameters for the 11 scenarios.....	94
Table 5.8.3.2A	The results obtained for the 11 scenarios for Set 12 (decision variables).....	100
Table 5.8.3.2B	The results obtained for the 11 scenarios for Set 12 (cost components).....	100
Table 5.8.3.3A	The results obtained for the 11 scenarios for Set 13 (decision variables).....	101
Table 5.8.3.3B	The results obtained for the 11 scenarios for Set 13 (cost components).....	101
Table 5.8.3.4A	The results obtained for the 11 scenarios for Set 22 (decision variables).....	102
Table 5.8.3.4B	The results obtained for the 11 scenarios for	

	Set 22 (cost components).....	102
Table 5.8.3.5A	The results obtained for the 11 scenarios for Set 23 (decision variables).....	103
Table 5.8.3.5B	The results obtained for the 11 scenarios for Set 23 (cost components).....	103
Table 6.4.1	Correlation of the CV and various costs.....	119
Table 6.4.2	Correlation of skewness and various costs.....	122
Table 6.4.3	Table of relationships on the total system cost for the three models.....	125
Table 6.4.4	Table of relationships on the saving for the two co-ordination models (compared to the independent policy).....	126
Table 8.5.1	Cost parameters for the four numerical examples.....	158
Table 8.5.2	Cost borne by the lower level obtained for the four numerical examples.....	159
Table 8.5.3	Cost borne by the upper level obtained for the four numerical examples.....	159
Table 8.5.4	Total Cost obtained for the four numerical examples....	159
Table 9.7.1	Equations of the elliptic separable region for surface S ₄	184
Table 9.8.1	MISER3 performance compared to the actual results...	186

Chapter 1

Introduction

This thesis is divided into two parts: Co-ordinated Supply Chain Model and Optimal Control Problems. The first part of the thesis examines co-ordinated supply chain model. The second part of the thesis consists of four projects examining the applications of optimal control theory and the software MISER3.

1.1 Part I: Co-ordinated Supply Chain Model

Supply chain management has become a critical issue in nowadays business environments. An effective supply chain policy can reduce average holding inventory level and the total expected cost. To cope with the above, co-ordination among individual members in the supply chain becomes important. In the earliest days, the economic ordering quantity (EOQ) concept has been widely applied. Under EOQ, a buyer determines the optimal ordering size that minimizes its total cost. The vendor uses the information from the buyer to determine its own optimal production schedule. In such a non-corporative system, this may not be advantageous to the whole supply chain system. From the 1970's, practitioners started to explore modes of co-ordination that performs

better than independent optimization in terms of total system cost. In these recent three decades, various integrated inventory co-ordinated models are established. Motivated by a recently developed co-ordination model, the synchronized cycles model, further exploration to the special characteristics of the synchronized cycles model is conducted, which may lead to enhancement and further development on the extension of the model. Further, hybrid meta-heuristic is designed to solve the synchronized cycles supply chain problem. In addition, investigations regarding the effect of the demand heterogeneity on the total system cost are also explored.

1.1.1 Outline: Chapter 2 – Chapter 6

Chapter 2 introduces the background and evolutions of supply chain management since the 1950s. A literature survey on the supply chain dynamics and various kinds of co-ordination models are also presented. Assumptions and notations used throughout this part of the thesis are presented in Chapter 3. Three supply chain models, the independent policy model, the common cycle model, and the synchronized cycles model, are also introduced in this chapter. Chapter 4 applies meta-heuristics to obtain “near-optimal” solutions to the synchronized cycles algorithm. A modified genetic algorithm with two sets of mutation rates

is developed and a hybrid heuristic – genetic algorithm simulated annealing (GASA) – is designed to combine the pros of the simulated annealing and the genetic algorithm. All three heuristics are capable in obtaining a better results compared to the synchronized cycles algorithm (SCA). To enhance the effectiveness of the SCA, bounds on certain decision variables are developed in Chapter 5. In addition, sensitivity of the total cost improvement with respect to two criteria are also considered: (*i*) the variation in standard parameters of the model, and (*ii*) the portion borne by the vendor under independent policy. In previous researches, practitioners suggested various kinds of co-ordination models and concluded that the models lead to reduction of total system cost. However, there were rare papers that discussed the situations when the co-ordination work in terms of vendor-buyer's cost proportion. This chapter also modifies the synchronized cycles model by including vehicle scheduling. Chapter 6 investigates how the demand heterogeneity, e.g. different values of mean demand, variance, and skewness would affect the performance of the synchronized cycles model. More importantly, the effect on the performance of the three supply chain models is examined. The datasets used in this part of the thesis is presented in the Appendix.

1.2 Part II: Optimal Control Problems

Optimal control theory is an extension to the calculus of variations with over 300 years of history. Among many ancient optimal control problems, the brachistochrone problem, posed by Johannes Bernoulli, marked the birth of optimal control. Optimal control theory gained its popularity in the 1950s for its applications to aerospace and space travel, partially due to the Cold War. The theory combines engineering and mathematical techniques to model dynamical systems. Nowadays, optimal control theory has been developed and extended to a wide variety of different areas – astronomy, chemical engineering, economics and management science, logistics, robotics, and physics.

In addition to the development on the analytic studies of optimal control theory, with the advance of computer technologies, numerical computational method and algorithms have also been developed to solve these important problems. In the early 90's, an optimal control software package, MISER3, has been developed to solve the optimal control problems. Since then, MISER3 has been used in solving various kinds of control problems in different aspects. The underlying core technique of MISER3 relies on the latest advances in the computational studies of optimal control, namely, the control parametrization as well as the control parametrization enhancing technique (CPET) which have been adopted

for numerical computation.

Motivated by the rapid growth of optimal control theory and the newly developed computational strategy, the aim of this part of the thesis is to apply optimal control strategies and techniques, as well as the software MISER3, to investigate four open problems in different areas: (*i*) the optimal production scheduling problem in supply chain management; (*ii*) the isoperimetric pillars construction problem; (*iii*) the flexible rotating beam problem with active constrained layer damping and (*iv*) the quarter-car suspension problem.

1.2.1 Outline: Chapter 7 – Chapter 11

Chapter 7 introduces the background and development from traditional calculus, calculus of variations, classical control theory to optimal control theory. Literature survey and practical issue on the four problems are also discussed in this chapter. Chapter 8 considers a supply chain system with Ornstein Uhlenbeck demand process. This demand process is seldom considered in the field of supply chain management and has not yet been analytically derived using the Pontryagin's maximum principle. Further, three different levels of information sharing practices – decentralized level (with no information sharing), co-ordinated level (with information sharing), and centralized level (vendor

managed inventory) – are compared. Motivated by the ancient Dido's problem, Chapter 9 extends the isoperimetric problem. The problem is to find an enclosed cross-sectional/base region of a pillar defined by a simple closed curve of fixed perimeter such that the volume of the constructed pillar, bounded above by a relatively smooth ceiling, is maximized. A novel elliptic separation constraint technique is developed for multiple pillars constructions. Chapter 10 considers a rotating beam which carries an end mass and rotates in a vertical plane under the effect of gravity by means of a time-varying driving torque. Both active constrained layer damping (ACLD) and passive constrained layer damping (PCLD) treatments are compared. Control parametrization enhancing technique (CPET) is used to determine the switchings of a PD controller applied to the ACLD beam. Chapter 11 investigates a nonlinear model of quarter-car suspension problem. This kind of problem is popular in road vehicle applications to ensure a smooth ride. A quarter-car model with a state dependent ODE dynamics is considered. This class of problems is difficult to solve since the dynamics of the system changes according to the state variables, and there is no information on when the system jumps from one set of dynamics to another. There does not exist any method in the literature addressing this problem. Computational method with enhanced switching controls is used to

solve the problem.

Chapter 12 summarizes the thesis and suggests possible future research opportunities arising from the results of the thesis.

PART I:

CO-ORDINATED SUPPLY CHAIN MODEL

Chapter 2

Literature Review on Supply Chain Dynamics and Co-ordination

2.1 Introduction

In a society, customers continuously demand for a particular product. Firms realize the demand and they start to source for raw materials for producing the product. Firms go through processes in designing, supplying, producing, warehousing, stockholding, pricing, packaging, scheduling, transporting, and finally distributing to the customers' side. Such a system is called a supply chain. Supply chain management refers to the management of the supply chain processes in order to satisfy customer's demand by producing the appropriate product at the right time and places with suitable quantity for the least expenses without lowering any product quality. An efficient supply chain requires a smooth logistics flow in all activities from moving the raw materials into finished products and from moving the finished products to the end customers. Such activities include logistics planning and implementation,

warehouses/facilities location, inventory management, and transportation/distribution. Each issue can be spread into chapters for detailed discussion. Most of the logistics textbooks cover these issues in details such as Ballou (1999), Coyle, Bardi, and Langley (2003) and Waters (2003).

The supply chain system mainly consists of various members: suppliers, manufacturers, distributors, retailers, and customers; various cost components: material cost, inventory cost, transportation cost, and packaging cost; and information and material flow. A typical supply chain is illustrated in Figure 2.1.1. Nowadays, supply chain has been an essential part for production firms in the competitive market. The logistics system has gone through many revolutions and developments in the past 50 years.

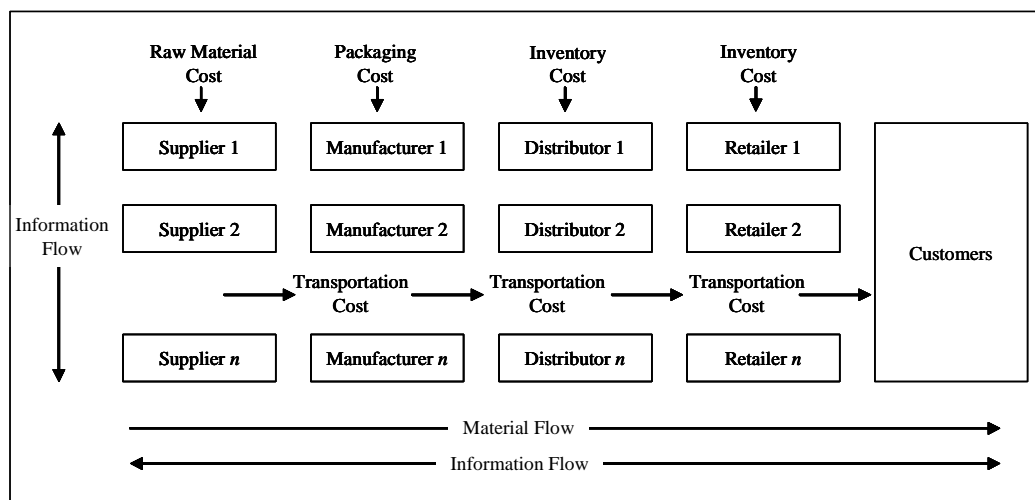


Figure 2.1.1 A typical supply chain system.

In the 1950s, firms only focus on producing products and by all means, to reach the final customers. They do not concentrate much attention on the

logistics flow. At that time, there is no concept of co-ordination. Each member (supplier, manufacturer, and retailer) in the distribution system produces solely on one's own with one's production policy. There is no communication between any distribution channels. Usually, each firm would execute a policy that minimizes one's total expenses. However, the total cost of the whole distribution system may not be optimally minimized even though each individual unit minimizes its own cost. In the 1960s, Smykay et al. (1961) suggests that there is beneficiary through co-ordination among all levels in the distribution system. The management levels, at that time, realize that some activities, such as transportation, warehousing, stock holding, and packaging, can be linked together for cost effectiveness. By the introduction of intermediary concept (Artle and Berglund, 1959), firms reorganize the physical system to adopt an intermediary, namely the wholesaler. This greatly reduces the total cost in distribution. For example, if there are 10 suppliers and 100 outlets, there would be $10 \times 100 = 1,000$ shipments to direct the goods. If an intermediary (or wholesaler) is introduced, the suppliers transport the goods to the intermediary and the intermediary ships the goods to all the outlets. Then, from the previous illustration, the total number of shipments is greatly reduced to 110 (Figure 2.1.2). Assuming the cost of each shipment is

optimized according to the economies of scale, the introduction of an intermediary can save 89% of the original cost. The reduction is more obvious as the total number of suppliers and outlets increases.

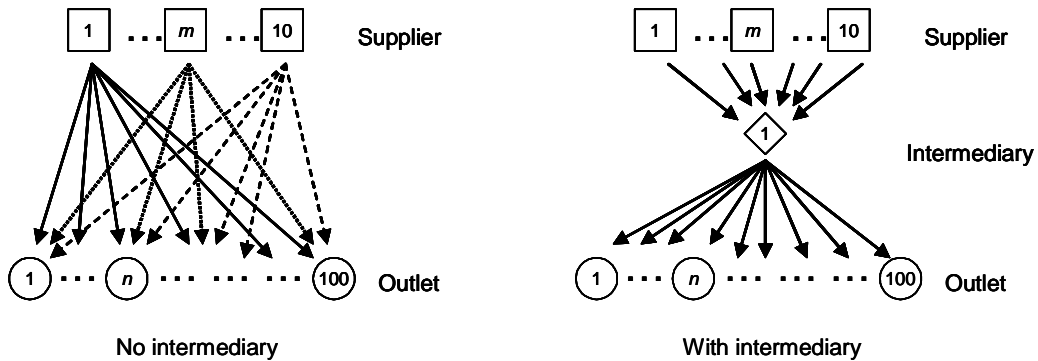


Figure 2.1.2 Reduction of number of shipments with an introduction of an intermediary.

The physical distribution concept is further developed during the 1970s. At that time, there is a major power shift in the supply chain. The power of manufacturers is greatly reduced. Before this power shift, manufacturers are the dominant section in the whole supply chain. They are large in size and most of the functions, such as product design, packaging, and distribution, are performed mainly by the manufacturers. In this early stage, manufacturers do not need to communicate with other channels in the supply chain. They carry out strategies that minimize their own expenses. However, such a monopoly activity would increase operating cost for the retailers and thus create

ineffectiveness as a whole. Therefore, economically, the retailers tend to consolidate together to form a larger retailer in order to “fight” against such situation. This consolidation may increase the size of the storage so that the retailers can order much larger quantities. Moreover, the management can handle the inventory in a more manageable and predictable manner. On the retailer’s side, the total expenses is reduced so that they can treat their customers with a better quality services and more importantly, they can offer a lower price to the customers, which will take over a larger market share from the manufacturers. In the 1980s, manufacturers realize the problem after retailers’ consolidation, and they start to change their logistics strategy. The changes improved not only the whole logistic system, but also the quality services toward customers. On the other hand, most of the firms based upon transportation for their operations, from suppliers to manufacturers, manufacturers to retailers, and retailers to customers. Transportation incurs quite a large portion of logistics expenses. During 1980s, government deregulation of transportation industry provides a good sign for the logistics industry. Transportation services become more compatible, this includes rail, air, land and water transport. Firms can independently negotiate with the transportation services providers for contractual terms. Such competition

among transportation services providers resulted in better services (in terms of timing and storage conditions) and lower prices. In addition, customers start to concern more about the quality and the design of the products during the 80s. Firms begin to concentrate on the concept of total quality management. In late 1980s and early 1990s, there are many logistics services companies that provide warehousing, inventory management, and distribution services. Many firms start to “outsource” their supply chain activities towards these logistics services companies. Outsourcing can reduce manufacturing cost and capital investment. Moreover, it allows individual firm to focus on its strength for services improvement (Simchi-Levi et al., 2003). Due to the quick development of technology, many logistics activities and strategy can be done through computers. Information technology has a great impact on the development of the supply chain. Firms start to combine the inbound activities (activities of transferring materials from the external supplier to the firm) with the outbound activities (activities of transferring materials from the firm to the final customers) through the use of computing networks. Until the 1990s, supply chain management evolves, more and more attention has been placed on this new concept. Most of the firms have focused on their supply chain for more efficiency and effectiveness. With the introduction of the

e-business, information among members in the supply chain can easily be shared and co-ordination level would be improved. Into the new millennium, organizations compete for their market share by strengthening the logistics of their supply chains. Supply chain management will continue to be an important issue in nowadays global business market.

2.2 Modeling on the Industrial Dynamic Systems

Supply Chain has many aspects that need to be considered in a supply chain model. However, by taking all concerned factors into account, the model would be of so high complexity that it would be extremely hard for analysis. Hence, there is a trade off between reality and complexity. One needs to construct a model that can simulate the real world and not very complicated to analyze. Supply chain systems can be modeled and analyzed in many distinctive ways. Researchers have a great flexibility of modeling the supply chain which is most suitable with their own interests. One can consider whether to use a deterministic or stochastic inventory model; discrete time or continuous time; infinite or finite planning horizon; the choice on the characteristics of the demand process; linearity of the costing functions, etc. Besides, there would be some conditions that restrict the supply chain, i.e.

manpower capacity, backloging allowability, allocation of material, transportation capacity, inventory level constraint, location of facilities, etc. Furthermore, as Simchi-Levi et al. (2003) mentioned, different members in the supply chain may have different and conflicting interests. As a result, in modeling the supply chain, we may need to propose multi-objective functions to cater for reality purpose. Such objectives include inventory ordering decision, production planning decision, modes of transportation, etc.

Many researchers have devoted effort in modeling the supply chain, one of the earliest researchers, Simon (1952) applied servomechanism theory to study the production control. He used Laplace transform and transfer function to structure the production system with exponential delays. The development of Industrial Dynamics was influenced to a great extent by J. Forrester (Forrester 1961). Forrester modeled the dynamical systems by sets of differential equations. He set up a highly complicated nonlinear model for simulation purpose. Due to the complexity, no sensitivity or validation was analyzed. Because of the lack of theoretical support, Forrester's results were criticized by Ansoff and Slevin (1968). Since then, a wide range of mathematical modeling and simulation techniques have been developed to model the supply chain systems. Baumol and Vinod (1970) formed an inventory model

analyzing the shipment mode of transportation. They used both deterministic and stochastic models to investigate the logistics. In the paper, Baumol and Vinod identified the trade off between the speed of the shipment and the total cost for the transportation. They deduced the equations of the cost indifference curves. Karmarkar and Patel (1977) modeled a single product single period multi-location inventory problem with stochastic demand and transshipment. By using game theory, Christy and Grout (1994) examined the relationship between buyers and suppliers in the supply chain. A supply chain relationship matrix was constructed and analyzed. A multiple objective, with mixed integer programming model, was designed to solve a relocation and phase-out problem of warehousing facilities in a multi-period planning horizon (Melachrinoudis and Min 2000).

For different industries, the consumption of different commodities follows different demand processes. Thus, it is a primary interest to study a supply chain model for various demand distributions. For example, Veinott (1965) modeled the inventory problem with a nonstationary demand process, and nonstationary cost functions (include holding cost, ordering cost and backlogging cost). Johnson and Thompson (1975) characterized the demand process by Box and Jenkins ARIMA model. Harpaz, Lee, and Winkler (1982)

considered the demand process under Bayesian framework. Miller (1986) used exponential smoothing technique to formulate the demand process. Poisson demand process was used by Zheng (1994) for a continuous review inventory system.

Stability of a supply chain system was deemed an important issue. Here, stability refers to the property that the supply chain system would gradually reverts back to equilibrium after some perturbations (i.e. a sudden change in demand process). In the 1990s, researchers started to investigate the stability and robustness properties for different models of the supply chain. Back to the 1960s, Bellman and Cooke (1963) derived the stability theory and behavior of the time-delay differential equations which served as a foundation for further stability analysis for the supply chain. Related issues can be referred to Marshall et al. (1992) for time-delay system, Niculescu et al. (1997) for stability and robustness properties and Toffner-Clausen (1996) for robust control system design.

Sterman (1989) simulated the “beer distribution game” as a stock management problem. In his paper, the total cost of the experimental result was calculated and the costs were nearly 10 times of the benchmark cost (optimal cost). Sterman explicitly identified three major characteristics from

the simulation, namely oscillation, demand amplification, and the phase lag, which caused the result far away from optimality. He estimated the system parameters through statistical analysis and established a parameter, β , the fraction that the supply line is taken into consideration, as a measure for stability. Extending Sterman's model, Riddalls and Benett (2002) further analyzed the parameter β , and identified stability regions for β . They quantified the stability and robustness properties for pure time delay system. Applying difference equations and Z transformation, Disney and Towill (2002) analyzed a two level vendor managed inventory supply chain and identified the stability criteria for the system.

Through the development of the dynamic systems, mathematical modeling becomes an essential component. Such formulation techniques include the use of continuous time differential equations, discrete time difference equations, discrete-event simulations, and operations research (Riddalls, Bennett, and Tipi, 2000).

2.3 Co-ordination of Supply Chains

From classical inventory theory, the economic ordering quantity (EOQ) concept has been widely applied. Under EOQ, a buyer determines the optimal

2.3 Co-ordination of Supply Chains

ordering size that minimizes its total cost. In a two-level supply chain, under individual optimal policies, the buyer orders at the EOQ and the vendor uses the information from the buyer to determine its own optimal production schedule, i.e. economic production quantity (EPQ). However, such a policy may not be optimal for the whole supply chain system. Such an individual policy is known as the independent optimization. Many researchers, beginning in the 1970's, started to explore modes of co-ordination that performs better than independent optimization in terms of total system cost. Goyal (1976) suggested a joint economic lot size (JELS) model between the buyer and the vendor which minimizes the total cost incurred by both parties. Under the integrated model, the buyer may need to alter the order quantity to a desired level. Such changes would increase the buyer's own cost. Thus, Goyal also suggested, but not shown in the paper, a saving-allocation scheme or a quantity discount scheme for the vendor in order to induce the buyer to make such changes. Banerjee (1986) developed a JELS model for a lot-for-lot policy. Under Banerjee's model, with a suitable saving allocation scheme, both the vendor and the buyer could be better off. Goyal (1988) further developed Banerjee's model by assuming that the vendor's lot size to be an integer multiple of the buyer's order size. Goyal's model implied that the vendor deliver to the buyer on a lot-for-lot policy. In

2.3 Co-ordination of Supply Chains

1984, Monahan developed a co-ordinated model with price discount component to increase the profits earned by the vendor. Monahan suggested that the buyer boost up the order to a higher level by a factor (K) and in return, the vendor offered a discount (d_K) for each unit ordered to the buyer. The values of K and d_K are optimally determined such that the buyer is willing to participate in the co-ordination and the vendor's profit is maximized. Based upon Monahan's model, Lee and Rosenblatt (1986) extended the model to overcome two problems that Monahan ignored: the first problem is the upper bound on the discount d_K . The maximum value of d_K should be imposed such that the purchase price of an item is non-negative; the second problem is the lot-for-lot assumption. Lee and Rosenblatt argued that the number of set-up for the vendor did not need to be the same number as the buyer ordering. The economic production quantity should be some integer multiple (k) of the buyer's economic order quantity. A thorough discussion and summary on integrated JELS models can be obtained in Goyal and Gupta (1989).

In 1990, Joglekar and Tharthare introduced the individually responsible and rational decision (IRRD) approach, which is easily to implement and is consistent with a free enterprise system. This approach suggested that the vendor should transfer the order delivery and processing costs to the buyer.

The vendor then faced a lower incurred cost and thus, the vendor can lower the unit price of an item. On the buyer's perspective, the ordering cost is higher but at the same time the unit purchasing price is lower, by rational decision the buyer would increase the ordering quantity. The authors claimed that the price reduction under IRRD is better than the joint economic lot-size model mentioned. The IRRD approach also extends to multi-buyer supply chain system. However, Goyal and Srinivasan (1992) questioned the validity of the IRRD approach by commenting that the approach contained few "conceptual errors" and not "comparing similar situations" using the JELS approach.

Lu (1995) argued that for the JELS model, the vendor must obtain the information regarding the buyer's holding cost and ordering cost. However, the buyers may not be willing to disclose such information. Even these costs are obtained, the vendor should question the validity. Therefore, the objective in Lu's model is to minimize the vendor's cost subject to the maximum cost the buyers is willing to incur. Lu developed the model under a single-vendor single-buyer supply chain first, and further extended to multiple buyers. In addition, Lu suggested the delivery of equal shipment size. Adopting Lu's Model (1995), Goyal (1995) suggested that a lower cost could be achieved by modifying the shipment policy. This shipment policy assumed that the ratio

(α) for each successive shipment, within a batch, should equal to the ratio of the production rate to the demand rate ($\alpha = P/D$). This optimal solution obtained implied that the vendor should ship all inventory that are available at each shipment. Viswanathan (1998) compared the shipment-size policy developed in Lu (1995) and Goyal (1995). The author showed, by numerous simulations, that neither policy dominated each other for all cost parameters. Hill (1997) showed that the value of α obtained in Goyal (1995) might not be an optimal value. The factor (k), as illustrated in Hill's, for each successive shipment can be any value between 1 and α . Later, Hill (1999) found that the optimal shipment sequence should be a combination of equal and unequal shipment sizes. For the first m shipments, the shipment size increases by a factor of k successively; for the remaining shipments, the shipment size remains at a constant level. Further, Goyal (2000) improved Hill's model by developing an algorithm for modifying the shipment sizes. As mentioned by Hill and Omar (2006), most of the previous research in integrated supply chain models assumed that the holding cost of the vendor to be lower than that of the buyers because of the value added concept. However, Hill and Omar (2006) raised out that the reverse can also be valid. One explanation is that the vendor faces a scarcity of storage situation and the buyers obtain low-cost bulk

storage facilities.

Valentini and Zavanella (2003) and Braglia and Zavanella (2003) introduced the Consignment Stock (CS) concept. The underlying idea of this concept is that the vendor has full authority in inventory control and the vendor would shift, as soon as possible once sufficient stock is produced, most of the stock in batches for buyers' storage. By doing that, the vendor may empty most of his storage vacancy for other uses (for example, storing raw materials, installing additional productive capacity, as Braglia and Zavanella suggested). However, the stock are still owned by the vendor and thus, the vendor would incur this part of the holding cost. The buyers are not required to pay for any holding cost until the buyers paid for the batch of stocks. This CS concept split the inventory cost into two components, the financial cost and the physical cost. The financial cost corresponds to the opportunity cost incurred by the vendor for other possible financial investment in resources; and the physical cost corresponds to the actual storage cost incurred by both the vendor and the buyers.

Lal and Staelin (1984) developed an optimal discount pricing policy for a single-vendor multi-buyer supply chain system. Analytic solutions were obtained for one group of homogenous buyers model. The author referred

“homogenous buyers” to a group of buyers with the same cost parameters as well as demand rate. Further, the study was extended to heterogeneous buyers. According to the paper, a large group of (heterogeneous) buyers was divided into groups of homogenous buyers where heterogeneity was measured based upon the item per order and the annual demand. Within each groups, all other cost parameters remained the same except the two defined heterogeneity measures. Kim and Hwang (1988) considered an incremental discount pricing schedule to a multi-buyer model with a single price break. They developed a (R, Q) discount plan for the system where R ($0 < R < 1$) is the discount rate and Q is the price break point. For order quantity larger than Q , a discount of R will be imposed to the unit price for each additional order over Q . Their results showed that both the vendor and the buyers can be better off resulting from the reduction on the frequency of set-ups. Drezner and Wesolowsky (1989) adopted similar discount plan as in Kim and Hwang (1988) but with “all-units” discount. Zahir and Sarker (1991) considered the co-ordinated problem with multiple wholesalers and a single manufacturer with price dependent demand functions. However, obtained from their numerical results, the price discount is too small such that the motivation of co-ordination may not be large enough to attract the wholesalers for such co-ordination.

Banerjee and Burton (1994) proposed a common cycle co-ordination system for a single-vendor multi-buyer supply chain system facing constant deterministic demands. Under the common cycle, the buyers are replenished at the same predetermined cycle. Since the deliveries to the buyers can be made at the same time, the order processing and shipment costs can be reduced and thus resulted at a lower system cost. Bylka (1999) extended the model by considering that the demands faced by both buyers and vendor are periodic. Algorithm is developed to solve the problem and the author recommended that some turnpike policies are suitable for dealing with periodic demands.

Similar to Banerjee and Burton (1994), Viswanathan and Piplani (2001) model the single-vendor multi-buyer supply chain through the use of common replenishment epochs (CRE). Under CRE, the vendor determined the common replenishment periods and forced all the buyers to replenish only at those time-periods. Thus, the replenishment interval for the buyers should be an integer multiple of the common replenishment period. Since not all the buyers are willing to follow the CRE policy, the vendor should offer some means of price discount to entice the buyers. While Viswanathan and Piplani (2001) offered the price discount to all buyers, Mishra (2004) generalized the CRE approach by allowing a selective discount policy. In the paper, Mishra

developed a multiple CRE model by segmenting the buyers and offering different discount policies to different segments of buyers.

Chen et al. (2001) studied the co-ordination mechanism in a single-vendor multi-buyer system. They showed that traditional order-quantity discounts scheme alone is not sufficient to guarantee co-ordination with heterogeneous buyers. Instead, they developed a co-ordination mechanism that combined three kinds of discounts, namely the traditional order-quantity discounts, the sales volume discount, and the order-frequency discount. Further, they also extended their model such that the holding cost is dependent to the unit price.

Gurnani (2001) examined three different co-ordination ordering structures in a single-supplier-two-buyers supply chain. First, the author considered order co-ordination. Under the order co-ordination, the buyers are encouraged to synchronize the timing of their orders with the supplier. Then order consolidation is considered. The orders of the two buyers are merged together as a single order with the supplier. Finally, the author considered the case when one buyer is selected as the major buyer, and only this major buyer can order directly with the supplier. For the other buyer, the order should be directly placed to the major buyer.

Banerjee and Banerjee (1992) developed a co-ordinated, orderless

inventory system through an introduction of the electronic data interchange (EDI) technology. They considered an EDI-based vendor-managed inventory (VMI) system. EDI is a system of computer-to-computer exchange of information. By using EDI, demand pattern of the buyers are revealed on the system and vendor may use such information to design a better co-ordination scheme in terms of ordering quantities, shipment schedules, planning inventory level, etc. EDI system provides a better vendor-buyer integrated co-ordination. Banerjee and Banerjee (1992) argued that, by the use of EDI, the vendor realized the buyers' demand and could make replenishment decisions for the buyers. Therefore, there would be no need for any ordering activities from the buyers, i.e. there would be no ordering cost. Woo et al. (2001) extended Banerjee and Banerjee's model (1992) to incorporate ordering cost reduction and raw material procurement into the model. From Woo's results, both the vendor and the buyers could obtain substantial cost savings.

Boyaci and Gallego (2002) considered a supply chain system with one wholesaler and multiple retailers under deterministic price-sensitive demand. Instead of providing side-payment to the buyers to entice co-ordination, the authors adopted the consignment policy. They considered two kinds of consignments: wholesaler-owned inventory with delayed payments (WOI-d)

and wholesaler-owned inventory with consignment (WOI-c). Under the WOI-d policy, the buyers immediately paid the wholesaler only when the entire lot is sold; under WOI-c policy, the buyers immediately paid the wholesaler as individual item is sold. For a co-ordinated system, they showed that WOI-c is a better option. Further, in their model, the objective is to maximize the profit of the whole supply chain system by optimally determining the price of the product and the lot-size quantity. Initially, the authors solved the problem by determining *simultaneously* the price and the lot-size quantity. However, they later showed that for high demand rate, the pricing strategy and the lot-sizing decision can be obtained sequentially. This result matched most of the companies nowadays whose marketing decisions (on pricing) usually ignores the operational decisions (on lot sizing), and vice versa.

Wang (2002) further explore the quantity discount scheme with heterogeneous buyers. A discrete all-unit quantity discount scheduling with multiple price break points is used for the model. Wang showed that larger buyers would respond to a higher break point (corresponding to larger quantity with greater discount), or at least not lower, than the break point chosen by other smaller buyers. Klastorin et. al. (2002) considered a single-manufacturer multi-buyer system with price discount scheme where the

manufacturer outsourced the production to a third party (usually an Original Equipment Manufacturer, OEM in short).

Chan and Kingsman (2005, 2007) developed a synchronized cycle model that allows each buyer to choose its ordering cycle, while the length of the cycle should be kept as a factor of the vendor's production cycle. In order to further minimize the total cost, under the synchronized cycle the vendor may schedule the time of the delivery within an ordering cycle, and this delivery time may be different from buyer to buyer, e.g. on the second day of each cycle for one buyer and on the third day of each cycle for another buyer. In their paper, the synchronized model out-performs the independent policy and the common cycle policy in a number of numerical examples with different ranges of demands and number of buyers. In addition, the paper illustrated that the common cycle policy can only outperform the independent policy in some limited cases.

Recently, a new technology in supply chain has been developed, the Enterprise Resource Planning (ERP). The ERP system unifies all data and processes into a single system. Usually, the ERP system would integrate all activities in an organization. For example, in a supply chain organization, the ERP not only involves the automation of warehousing, vehicle routing,

shipping scheduling, inventory monitoring, etc, but also include activities from other functional departments such as accounting, marketing, etc. In the research literature, the ERP system is still in its beginning stage. Kelle and Akbulut (2005) discussed the role of ERP system in supply chain information sharing, cooperation and cost optimization, as well as the opportunities and obstacles for supply chain integration.

Considered as one of the most up-to-date literature reviews on buyer-vendor co-ordination models, Sarmah et al. (2006) reviewed those integrated inventory models with quantity discount. The authors categorized single-vendor-single-buyer models into three categories: (*i*) vendor's perspective co-ordination models, which deal with objective function that maximizes the vendor's profit; (*ii*) joint buyer and vendor perspective co-ordination models, which consider the minimization of total system cost; and (*iii*) co-ordination models under game theoretic framework, which apply the concepts of game theory to model the buyer-vendor's co-ordination. The survey also provides some valuable insights and critical issues in existing supply chain management research.

Chapter 3

The Synchronized Ordering and Production Cycles

3.1 Introduction

This chapter presents mathematical derivations for the cost function of three (two-level) supply chain models (the independent policy, the common cycle model and the Chan and Kingsman (2005, 2007) synchronized cycles model). The synchronized cycles resolves the pitfalls of the common cycle model by allowing each buyer to choose its ordering cycle, while the length of the cycle is kept as an integer factor of the vendor's planning horizon. The model also allows the vendor to choose the time of the delivery within an ordering cycle so as to further reduce the system cost. Subsequent chapters further investigate the characteristics and behaviors of the synchronized cycles model.

3.2 Assumptions and Notations

3.2.1 Assumptions

Throughout the thesis, unless otherwise specified, the following assumptions are imposed.

- Demand patterns – constant and deterministic.

- No shortage allowed for both the buyers and the vendor.
- No leadtime, i.e. instantaneous arrival of orders.
- Finite planning horizon.
- Cost parameters – constant throughout the whole planning horizon.
- Production rate always greater than the demand rate.

3.2.2 Notations

General Parameters:

α	Demand-production ratio (DP ratio)
A_i	Ordering cost per order for the i^{th} buyer, for $i = 1, 2, \dots, n$
C_i	Transportation cost per delivery to the i^{th} buyer, for $i = 1, 2, \dots, n$
d_i	Demand rate faced by the i^{th} buyer, for $i = 1, 2, \dots, n$
D	Total demand rate faced by the vendor
h	Vendor's holding cost per item per unit time
h_i	The i^{th} buyer's holding cost per item per unit time, for $i = 1, 2, \dots, n$
P	Production rate setup by the vendor
S_v	Vendor's setup cost per setup

Parameters – Independent Policy:

Q_i	The i^{th} buyer's EOQ, for $i = 1, 2, \dots, n$
Q_v	Vendor's EBQ

T_i^{IND} Ordering cycle for the i^{th} buyer, for $i = 1, 2, \dots, n$

TC_i^{IND} The total cost for the i^{th} buyer, for $i = 1, 2, \dots, n$

TC_v^{IND} The total cost for the vendor

TC^{IND} The total system cost.

Parameters – Common Cycle Policy:

K Number of shipments per shipment cycle time

T^B Shipment cycle time (Common to all buyers)

$TC_i^{B\&B}$ The total cost for the i^{th} buyer, for $i = 1, 2, \dots, n$

$TC_v^{B\&B}$ The total cost for the vendor

$TC^{B\&B}$ The total system cost

Parameters – Synchronized Cycle Policy:

T Basic cycle time

$\delta_{i,t}$ 0-1 variable indicating the time of the ordering cycle for the i^{th} buyer, for $i = 1, 2, \dots, n; t = 1, 2, \dots, N$. $\delta_{i,t} = 1$ indicates that buyer i orders in period tT ; otherwise, $\delta_{i,t} = 0$.

Ψ Number of units of surplus stock at $t = 0$

b Nearest integer below F , where F is the F^{th} basic cycle time.

FT The time that the production ends

$k_i T$ Ordering cycle for the i^{th} buyer, with $k_i \in \mathbb{Z}^+$ for $i = 1, 2, \dots, n$

NT	Vendor's production cycle, where k_i is an integer factor of N
ST	The time that the production begins
TC_i^{SCA}	The total cost for the i^{th} buyer, for $i = 1, 2, \dots, n$
TC_v^{SCA}	The total cost for the vendor
TC^{SCA}	The total system cost

3.3 The Independent Policy Model

Assume there are n buyers and under the independent policy model, each buyer would determine his/her own optimal policy. The total cost per unit time incurred by the i^{th} buyer can be expressed as:

$$TC_i^{IND}(Q_i) = \frac{A_i d_i}{Q_i} + \frac{h_i Q_i}{2} \quad (3.3.1)$$

where the first term is the average ordering cost and the second term is the average holding cost. By applying the basic economic order quantity (EOQ) model, the optimal ordering quantity is

$$Q_i = \sqrt{\frac{2A_i d_i}{h_i}} \quad (3.3.2)$$

and $T_i^{IND} = \frac{Q_i}{d_i} = \sqrt{\frac{2A_i}{d_i h_i}}$ units of time.

In the perspective of the vendor, the vendor faces a demand rate of $D = d_1 + d_2 + \dots + d_n$ and needs to satisfy the delivery of Q_i units of stock to the

i^{th} buyer every T_i^{IND} units of time. The largest possible amount of ordering faced by the vendor is that all the buyers replenish at the same time totaling the ordering of $\sum_{i=1}^n Q_i$ units of stock, and this is the amount (i.e. safety stock) that the vendor must maintain at each point of time in order to 100% ensure that no stockout occurs during the whole planning horizon. The total cost per unit time incurred by the vendor can be expressed as:

$$TC_v^{IND}(Q_v) = \frac{S_v D}{Q_v} + \frac{h Q_v}{2} \left(1 - \frac{D}{P}\right) + \sum_{i=1}^n \frac{C_i d_i}{Q_i} + h \sum_{i=1}^n Q_i \quad (3.3.3)$$

where the first term is the average setup cost for the production run; the second term is the average holding cost; the third term is the order processing and shipment costs; and the last term is the holding cost for the safety stock.

By standard inventory model, the optimal economic batch production is

$$Q_v = \sqrt{\frac{2S_v D}{h \left(1 - \frac{D}{P}\right)}} \quad (3.3.4)$$

and the total system cost for the independent policy model is

$$TC^{IND}(Q_1, Q_2, \dots, Q_v) = \sqrt{2S_v h D \left(1 - \frac{D}{P}\right)} + \sum_{i=1}^n \left(\frac{C_i d_i}{Q_i} + \sqrt{2A_i d_i h_i} + h Q_i \right). \quad (3.3.5)$$

3.4 The Common Cycle Model

The common cycle model was proposed by Banerjee and Burton (1994). Under

this model, all buyers replenish at the beginning of each predetermined cycle time T^B ; and the vendor's production cycle is an integer multiple (K) of the predetermined cycle.

The cost for the i^{th} buyer is

$$TC_i^B(T^B) = \frac{A_i}{T^B} + \frac{h_i d_i T^B}{2}; \quad (3.4.1)$$

the vendor's cost is

$$TC_v^{B\&B}(T^B, K) = \frac{1}{T^B} \left(\frac{S_v}{K} + \sum_{i=1}^n C_i \right) + \left(\frac{hDT^B}{2} \right) \left[\frac{D}{P}(2-K) + K - 1 \right]; \quad (3.4.2)$$

and the joint total cost is

$$TC^{B\&B}(T^B, K) = TC_i^{B\&B}(T^B) + TC_v^{B\&B}(T^B, K). \quad (3.4.3)$$

The optimal common cycle time is

$$T^{B*} = \sqrt{\frac{2 \left(\frac{S_v}{K} + \sum_{i=1}^n (C_i + A_i) \right)}{Dh \left[\frac{D}{P}(2-K) + K - 1 \right] + \sum_{i=1}^n h_i d_i}} \quad (3.4.4)$$

and the optimal integer multiple $K = K^*$ satisfies

$$K^* (K^* - 1) \leq \frac{S \left(\frac{1}{Dh} \sum_{i=1}^n h_i d_i + 2 \frac{D}{P} - 1 \right)}{\left(1 - \frac{D}{P} \right) \left[\sum_{i=1}^n (C_i + A_i) \right]} \leq K^* (K^* + 1). \quad (3.4.5)$$

Under the common cycle approach, all the buyers are forced to order every T^{B*} units of time. This may not be economical to some buyers. For buyers who face higher demand, they would prefer to order more frequently so that they do

not need to carry too many stocks in storage which increase their holding cost. For buyers who face lower demand, they would prefer to order less frequently so that to minimize their total number of orderings and hence reduce their ordering cost. According to Banerjee and Burton (1994), since the deliveries to all the buyers can be made at the same time, the order processing and shipment costs can be reduced. This leads to a lower system cost.

3.5 The Synchronized Ordering and Production Cycles Model

This synchronized cycle model was developed by Chan and Kingsman (2005, 2007) which resolves the shortcoming in the common cycle model. The synchronized cycle model allows each buyer to choose its ordering cycle ($k_i T$), while the length of the cycle should be kept as a factor of the vendor's production cycle ($NT \bmod k_i T = 0$). Further, the model also suggests that it is not necessary for each buyer to order at the beginning of every ordering cycle. The exact time of ordering within the ordering cycle for each buyer is determined by the vendor so that the joint total cost is minimized, e.g. on the second day of each cycle for one buyer and on the third day of each cycle for another buyer. The synchronized cycle model balances the domination in the supply chain. The buyers are given choices for the length of their ordering cycle (in the common

3.5 The Synchronized Ordering and Production Cycles Model

cycle model, the buyers do not have any choices and the cycle length is determined by the vendor), while the vendor determines the time of the ordering (in the independent policy, the vendor must follow the decisions from all the buyers and adjust his/her own decision accordingly).

The total relevant cost of the whole system (See Chan and Kingsman (2005, 2007)) is given by:

$$\begin{aligned}
 TC^{SCA}(k_i, N, T, \delta_{i,j}) = & \\
 hT \left\{ \frac{1}{N} \sum_{i=1}^n \left\{ k_i d_i \left(\sum_{t=1}^N (t-1) \delta_{i,t} \right) \right\} + \frac{\Psi D}{PT} + \frac{D}{P} \sum_{i=1}^n \delta_{i,1} k_i d_i - \frac{ND^2}{2P} \right\} & \\
 + \frac{1}{2} \sum_{i=1}^n h_i d_i k_i T + \left\{ \frac{S_v}{N} + \sum_{i=1}^n \frac{(C_i + A_i)}{k_i} \right\} \frac{1}{T} & \\
 \end{aligned} \tag{3.5.1}$$

For simplicity, we assume $T = 1$.

The objective is to determine the optimal values of k_i , N , and $\delta_{i,j}$ such that

(3.5.1) is minimized with the following restrictions:

$$N \pmod{k_i} = 0 \text{ for } i = 1, 2, \dots, n \tag{3.5.2}$$

$$\delta_{it} = \delta_{i(t+k_i)} \text{ for } i = 1, 2, \dots, n; t = 1, 2, \dots, N \tag{3.5.3}$$

$$\Psi \geq \sum_{i=1}^n \left[k_i d_i T \left(\sum_{j=2}^b \delta_{i,j} \right) \right] - (j-1)PT \text{ for } i = 1, 2, \dots, n; 2 \leq j \leq b \tag{3.5.4}$$

$$\Psi \geq 0 \tag{3.5.5}$$

3.5 The Synchronized Ordering and Production Cycles Model

$$N, k_i \in \mathbb{N} \quad \text{for } i = 1, 2, \dots, n \quad (3.5.6)$$

$$\delta_{it} \in \{0,1\} \quad \text{for } i = 1, 2, \dots, n; t = 1, 2, \dots, N \quad (3.5.7)$$

Constraint (3.5.2) requires that the buyers' cycle should be a factor of the vendor's cycle. Constraint (3.5.3) guarantees that the replenishment order is placed every k_i period. To ensure no stock-outs occur for the whole planning horizon, constraints (3.5.4) and (3.5.5) determine the surplus stocks, Ψ , required at the beginning of the planning horizon. Non-negativity integer constraint for the value of N and k_i is imposed as constraint (3.5.6) and 0-1 variable for $\delta_{i,t}$ as constraint (3.5.7). Due to the high dimension and complexity of the total cost function, as well as the high dependency between the variables N and k_i , and $\delta_{i,t}$ and Ψ . It is very difficult (if not impossible) to solve the model analytically. Therefore, Chan and Kingsman (2005, 2007) developed a heuristics method to find the "near-optimal" solution of the problem.

Chapter 4

Meta-Heuristics Approach to the Synchronized Cycles Algorithm

4.1 Introduction

This chapter applies meta-heuristics to the synchronized cycles supply chain problem. Meta-heuristics are common tools for solving a wide range of complex combinatorial optimization problems. Meta-heuristics can diversify the search for an optimal solution over all feasible search space but cannot easily be trapped in any local extrema. For the SCA model, due to the high dimensional and highly complicated objective function, meta-heuristics may be capable in searching for a better solution than the one obtained by the Synchronized Cycles Algorithm. Two widely used meta-heuristics are used for this purpose: Genetic Algorithm (GA) and Simulated Annealing (SA). GA and SA have been proven over decades that they are very efficient in solving complicated combinatorial optimization problems. The experimental results show that both of the two meta-heuristics are successful in searching for a better “near-optimal” solution than the heuristics developed by Chan and Kingsman (2005, 2007). In addition, a hybrid Genetic Algorithm – Simulated Annealing (GASA) heuristic is also developed for solving the problem.

4.2 Genetic Algorithm

A genetic algorithm (GA) is a heuristic search algorithm that resembles natural selection. This algorithm was invented by Holland (1975) and developed and applied to different areas (Goldberg, 1989). As the name suggested, GA is an evolutionary algorithm inspired by reproductive biology. GA consists of a set of population of which every member (called chromosome) in the population is a feasible solution to the problem. To obtain the “best” solution, a fitness function is defined to evaluate each of the members in the population. The algorithm begins with an initial population, which is usually randomly generated. By means of a series of operators namely selection, crossover, and mutation, a new population is formed and the better members will remain in the new population due to the “survival of the fittest” concept. The effect of the crossover operation is to maintain some “good” characteristics obtained previously and at the same time to search for other solutions in the feasible search space; the effect of the mutation operation is a local search operation which avoid trapping in the local minima. The process continues until a pre-defined stopping criterion is reached. GA has been used to solve the supply chain replenishment problem (Chan et al. 2003). The idea of dynamic rates for crossover and mutation operators is adopted as described in Cheung et al. (2001

and 2005).

4.2.1 Gene Representation

For this problem, we use non-negative decimal number to code the entries of the chromosomes. The first entry of the chromosome corresponds to the value of N , where N is the vendor's planning horizon. Next, based upon the value of N , n values of k_i are generated with a restriction that k_i is an integer factor of N . Then n values of λ_i ($1 \leq \lambda_i \leq k_i$) are generated such that $\delta_{i,\lambda_i} = 1$. Thus a complete chromosome can be represented as

$$[N \ k_1 \ k_2 \ \dots \ k_n \ \lambda_1 \ \lambda_2 \ \dots \ \lambda_n].$$

4.2.2 Selection

The selection process is based on the fitness value f_i of the chromosomes. Roulette wheel selection scheme is used to randomly choose, with replacement, two chromosomes as "parents". The fitness value is calculated using objective function (3.5.1), and a fitness index is assigned to each chromosome. The fitness index is calculated as follows:

Step 1: Obtain a transformed fitness value \hat{f}_i for the i^{th} chromosome by:

$$\hat{f}_i = \left(\sum_{i=1}^n f_i \right) - f_i \quad (4.2.2.1)$$

Step 2: The fitness index \tilde{f}_i for the i^{th} chromosome is calculated by:

$$\tilde{f}_i = \frac{\hat{f}_i}{\left(\sum_{i=1}^n \hat{f}_i \right)} \quad (4.2.2.2)$$

By mapping the interval $[0,1]$ to the fitness index, we randomly choose two random numbers in $[0,1]$ and select two chromosomes which correspond to these two random numbers.

4.2.3 Crossover

After selecting “two parents”, the father and the mother, a random value from $(0,1)$ is generated to determine whether the crossover process has to be performed. The probability of performing the crossover process is completely determined by our pre-assigned dynamic crossover rate. For this problem, standard GA crossover operation is not appropriate since we need to satisfy the restrictions on k_i and λ_i . Therefore we apply different crossover operations which depend on the two chosen parents.

(i) *Case I: The two parents contain the same value of N*

If the two parents have the same value of N , the k_i can randomly crossover because we can always guarantee that k_i is an integer factor of N after the crossover. In this case, multiple-point crossover is used for the (k_i, λ_i) pairs. That is, a 0-1 variable is generated for every (k_i, λ_i) pairs to determine the resultant gene of the offspring. For instance, with $n = 5$, the crossover operator indicates a crossover at the second, fourth, and fifth (k_i, λ_i) pairs with parents

$$\text{Parent 1: } \left[N \quad k_1^{(1)} \quad k_2^{(1)} \quad k_3^{(1)} \quad k_4^{(1)} \quad k_5^{(1)} \quad \lambda_1^{(1)} \quad \lambda_2^{(1)} \quad \lambda_3^{(1)} \quad \lambda_4^{(1)} \quad \lambda_5^{(1)} \right]$$

$$\text{Parent 2: } \left[N \quad k_1^{(2)} \quad k_2^{(2)} \quad k_3^{(2)} \quad k_4^{(2)} \quad k_5^{(2)} \quad \lambda_1^{(2)} \quad \lambda_2^{(2)} \quad \lambda_3^{(2)} \quad \lambda_4^{(2)} \quad \lambda_5^{(2)} \right].$$

After the crossover, the two offsprings are obtained as follows:

$$\text{Child 1: } \left[N \quad k_1^{(1)} \quad k_2^{(2)} \quad k_3^{(1)} \quad k_4^{(2)} \quad k_5^{(2)} \quad \lambda_1^{(1)} \quad \lambda_2^{(2)} \quad \lambda_3^{(1)} \quad \lambda_4^{(2)} \quad \lambda_5^{(2)} \right]$$

$$\text{Child 2: } \left[N \quad k_1^{(2)} \quad k_2^{(1)} \quad k_3^{(2)} \quad k_4^{(1)} \quad k_5^{(1)} \quad \lambda_1^{(2)} \quad \lambda_2^{(1)} \quad \lambda_3^{(2)} \quad \lambda_4^{(1)} \quad \lambda_5^{(1)} \right].$$

(ii) *Case II: The two parents contain different values of N*

In this case, we perform a one-point crossover at which the cut places right after

the gene of k_n , denoted by the symbol “|”. For example:

$$\text{Parent 1: } \left[N^{(1)} \quad k_1^{(1)} \quad k_2^{(1)} \quad \dots \quad k_n^{(1)} \quad | \quad \lambda_1^{(1)} \quad \lambda_2^{(1)} \quad \dots \quad \lambda_n^{(1)} \right]$$

$$\text{Parent 2: } \left[N^{(2)} \quad k_1^{(2)} \quad k_2^{(2)} \quad \dots \quad k_n^{(2)} \quad | \quad \lambda_1^{(2)} \quad \lambda_2^{(2)} \quad \dots \quad \lambda_n^{(2)} \right]$$

$$\text{Child 1: } \left[N^{(2)} \quad k_1^{(2)} \quad k_2^{(2)} \quad \dots \quad k_n^{(2)} \quad | \quad \lambda_1^{(1)} \quad \lambda_2^{(1)} \quad \dots \quad \lambda_n^{(1)} \right]$$

$$\text{Child 2: } \left[N^{(1)} \quad k_1^{(1)} \quad k_2^{(1)} \quad \dots \quad k_n^{(1)} \quad | \quad \lambda_1^{(2)} \quad \lambda_2^{(2)} \quad \dots \quad \lambda_n^{(2)} \right]$$

Next, we check whether the constraint $\lambda_i \leq k_i$ is satisfied. If not, the

corresponding λ_i is also swapped; otherwise, no crossover is needed for the λ_i .

4.2.4 Mutation

Similar to the crossover process, the probability of performing the mutation process is completely determined by a pre-assigned dynamic mutation rate.

Here, we extend the dynamic concept in Cheung et. al. (2001, 2005). Instead of

having one dynamic set of mutation rate, we define two dynamic sets: a global set ($gmut$) and a local set ($lmut$). The global set is the same as described in Cheung et al. (2001, 2005) and the local set is based upon the current global mutation rate. Depending on the ranking of the chromosome within a population, a non-uniform local mutation rate is assigned to each of the chromosomes. A description of this mutation operation is described as follows:

- Step 1: Rank the chromosomes in the current population according to their fitness with the fittest as rank one.
- Step 2: Set the mutation rate for the first chromosome equal to the global mutation rate, and for each successive chromosome the corresponding mutation rate is increased linearly such that the last chromosome has a mutation rate which is 2 (arbitrarily set) times the current global mutation rate. That is, for the i^{th} chromosome in a population of M chromosomes, the local mutation rate is set equal to:

$$lmut = \left(\frac{(M + i - 2)}{M - 1} \right) \cdot gmut \quad (4.2.4.1)$$

Different chromosomes with the same fitness are ranked randomly and therefore chromosomes having the same fitness value may have different mutation rates because of their ranks.

- Step 3: Once the local mutation rate is determined, a random number in

(0,1) is drawn at each position of the k_i 's and the λ_i 's to decide whether mutation is needed. To maintain feasibility of the offspring, the mutated value of the k_i 's and the λ_i 's are restricted according to the constraint $\lambda_i \leq k_i$.

There are three reasons to use the two dynamic mutation rates, i.e. global and local:

1. Within each generation, the fittest chromosome should be the closest to the optimal one. Thus, this chromosome does not need a high mutation rate as the mutation might be destructive. For the worst chromosome, since it should be the farthest away from the optimal solution, it may need to mutate in order to “get closer” to the optimal solution.
2. As the GA evolves, and because of the concept of “survival of the fittest”, the population may become homogenous after certain iterations (i.e. after 100 generations). However, this “converged” solution may only be a solution within a local minimum region. In addition, even at this stage we do not know whether the mutation operation is constructive or destructive. So by applying non-uniform mutation rate to the same chromosome, we do not need to concern about the “constructiveness” issue.
3. More local searches are performed at each iteration.

4.2.5 New Population

A complete cycle of the selection, crossover and mutation operations forms an iteration. Once the offspring is reproduced, it is stored in a temporary population (“offspring population”). Until M offspring have been reproduced, the “offspring population” is then combined with the latest population to form a $2M$ population. Next, the $2M$ chromosomes are compared according to their fitness values. The first M chromosomes, with highest fitness (in this problem, the highest total cost), are eliminated and the remaining M chromosomes form the population of the next generation. The GA is then performed again until the stopping criterion is reached.

4.2.6 Stopping Criterion

The stopping criterion for the problem is either when 800 iterations are completed or no improvement in the best fitness value in 100 consecutive iterations, whichever comes first.

4.3 Simulated Annealing

Simulated annealing (SA) algorithm is a heuristic search algorithm that resembles a physical process, the annealing process. The annealing process is a physical process which involves heating a solid until it melts so that the atoms are fully diffused. The atoms will then be slowly cooled down at a

predetermined rate such that they will find a new and better configuration and crystallize. Kirkpatrick, Gelatt and Vecchi (1983) and Cerny (1985) introduced the concept of simulated annealing to the field of combinatorial optimization problems. SA begins with an initial feasible solution as the current solution. During each generation, a neighboring feasible solution is chosen and compared to the current solution. If the neighboring solution is better than the current solution, the neighboring solution is set as the current solution; on the contrary, if the neighboring solution is worse than the current solution by an amount ΔE , the neighboring solution can still be accepted with a Boltzmann-type probability, $e^{-\frac{\Delta E}{kT}}$, this process being also known as the Metropolis criterion. In the context of SA, T is a parameter that controls the probability of accepting a worse solution compared to the current best. Usually T is set to a high value at the very beginning to avoid being trapped at a local optimal and is gradually decreased as the process evolves.

4.3.1 Gene Representation

The gene representation for the SA is the same as for the GA.

4.3.2 Initial and Final Temperature

The initial temperature (T_0) is set equal to twice the number of buyers and the final temperature (T_f) is set to 0.005.

4.3.3 Cooling Schedule

We adopt the proportional decrement scheme as the cooling schedule. At the i^{th} iteration, the temperature is given by:

$$T_i = rT_{i-1}$$

where $r < 1$ is the annealing rate.

Suppose we want the final temperature equal to T_f at the last iteration, the annealing rate for the problem is set to

$$r = \left(\frac{T_f}{T_0} \right)^{\frac{1}{M}}$$

where M is equal to the total number of iterations performed.

4.3.4 Neighborhood Moves

A random position at the place of the k_i 's and the λ_i 's is selected and a new mutated value is randomly drawn to replace the old one while keeping the constraint $\lambda_i \leq k_i$ satisfied.

4.3.5 Stopping Criterion

Within each temperature level, the stopping criterion is either a predetermined number of iterations is completed or no improvement in 5 (for 5-buyer and 15-buyer cases) or 10 (for 30-buyer and 50-buyer cases) consecutive iterations.

For the whole SA process, the stopping criterion is set to 800 iterations or no improvement in 100 consecutive iterations, whichever comes first.

4.4 Numerical Results

We test 2,160 trials (24 datasets x 9 DP-ratios x 10 runs) with the following parameters:

GA parameters:

Population size: 80

Number of iterations: 800

Crossover rate: 0.80 for the 1st one-third of total iterations

0.60 for the next one-third of total iterations

0.40 for the remaining iterations

Global Mutation rate: 0.100 for the 1st one-third of total iterations

0.075 for the next one-third of total iterations

0.050 for the remaining iterations

SA parameters:

Number of SA iterations: 800

Number of iterations (within each temperature): 2 x number of buyers

Initial Temperature: 2 x number of buyers

Final Temperature: 0.005

To maintain the validity of the comparison between GA and SA, same initial

random population is used for each trial. In all 2,160 trials, GA out-performs the SCA in 2,101 (97.27%) trials and the average percentage improvements over the SCA for 5-buyer, 15-buyer, 30-buyer, and 50-buyer cases are 2.85%, 0.68%, 0.17%, and 0.05% respectively. SA out-performs the SCA in 2,024 trials (93.70%) and the average percentage improvements over the SCA are 1.68%, 0.43%, 0.13%, and 0.03% respectively. Compared between GA and SA, GA out-performs SA in 1,781 trials (82.45%) and the average percentage improvements over SA are 1.18%, 0.25%, 0.04%, and 0.02% respectively. Running with the Intel Pentium 4 CPU and programming in the Matlab R2006a platform, the CPU run-time for 50-buyer with DP-ratio of 0.9 is approximately 530 seconds and 250 seconds for the GA and SA respectively. Although GA yields a better solution in most of the trials, SA converges faster in terms of computational time. In order to enhance the process in terms of both the “near-optimal” solution and computational effort, a hybrid heuristics (GASA) using GA and SA is developed:

- Step 1: Due to the quick computational time of SA, run the problem with SA until the stopping criterion occurs.
- Step 2: Use the “converged” solution in Step 1 and apply the mutation

operation to construct $\frac{M}{2}$ chromosomes.

Step 3: Randomly construct the remaining $\frac{M}{2}$ chromosomes to maintain some degrees of diversification.

Step 4: Run the GA with the population in Steps 2 and 3 until the stopping criterion occurs.

The GASA heuristic out-performs the SCA, GA, and SA in 2,143 (99.21%), 1,709 (79.12%) and 2,117 (98.01%) trials respectively. The average percentage improvements over the SCA, GA and SA are depicted in Table 4.4.1. and the best results obtained by the method are shown in Table 4.4.2. The largest percentage improvement over the SCA for 5-buyer, 15-buyer, 30-buyer, and 50-buyer cases are 8.48%, 2.48%, 2.90% and 0.20% respectively. The CPU run-time of the GASA heuristic for 50-buyer with DP-ratio of 0.9 is approximately 350 seconds.

	SCA	GA	SA
5 buyers	3.58%	0.80%	1.97%
15 buyers	0.67%	0.07%	0.25%
30 buyers	0.20%	0.04%	0.08%
50 buyers	0.06%	0.01%	0.03%

Table 4.4.1 The average percentage improvements of the GASA heuristic over SCA, GA and SA.

4.4 Numerical Results

Set #	DP	SCA	Hybrid	Reduction	Set #	DP	SCA	Hybrid	Reduction
01	0.1	22.97	22.73	1.06%	04	0.1	139.45	139.26	0.14%
	0.2	23.36	22.91	1.94%		0.2	138.37	138.18	0.14%
	0.3	23.14	23.08	0.27%		0.3	137.57	137.26	0.22%
	0.4	23.92	22.62	5.42%		0.4	136.62	136.15	0.34%
	0.5	23.12	22.29	3.61%		0.5	135.67	134.25	1.05%
	0.6	24.07	22.03	8.48%		0.6	134.65	133.51	0.84%
	0.7	22.34	21.70	2.88%		0.7	133.17	132.04	0.85%
	0.8	22.36	21.16	5.38%		0.8	131.76	130.91	0.64%
	0.9	20.81	20.08	3.52%		0.9	129.15	127.33	1.41%
02	0.1	99.02	99.01	0.01%	05	0.1	133.94	133.82	0.09%
	0.2	98.13	98.13	0.00%		0.2	133.05	133.01	0.03%
	0.3	97.20	96.98	0.22%		0.3	132.38	132.15	0.17%
	0.4	96.31	96.19	0.12%		0.4	131.79	131.31	0.36%
	0.5	94.82	94.41	0.44%		0.5	130.76	129.60	0.88%
	0.6	93.61	93.32	0.30%		0.6	129.15	129.11	0.03%
	0.7	92.10	91.62	0.53%		0.7	127.75	126.51	0.97%
	0.8	90.62	89.64	1.08%		0.8	126.28	125.78	0.40%
	0.9	87.72	87.13	0.67%		0.9	123.96	122.27	1.36%
03	0.1	108.78	108.16	0.57%	06	0.1	128.54	128.34	0.16%
	0.2	107.91	107.91	0.00%		0.2	127.89	127.04	0.66%
	0.3	107.36	107.35	0.01%		0.3	127.44	127.35	0.07%
	0.4	106.71	106.46	0.24%		0.4	126.82	126.13	0.55%
	0.5	105.56	105.02	0.51%		0.5	125.29	124.95	0.27%
	0.6	104.95	104.69	0.25%		0.6	124.00	123.66	0.28%
	0.7	104.23	102.99	1.19%		0.7	123.03	122.27	0.62%
	0.8	102.84	100.77	2.02%		0.8	121.64	120.71	0.76%
	0.9	100.39	98.71	1.67%		0.9	119.47	118.23	1.04%

Table 4.4.2 Minimum cost obtained by the hybrid method and its comparison with the SCA.

4.4 Numerical Results

Set #	DP	SCA	HYBRID	Reduction	Set #	DP	SCA	Hybrid	Reduction
07	0.1	113.27	113.12	0.13%	10	0.1	119.12	119.08	0.03%
	0.2	112.34	112.34	0.00%		0.2	118.48	118.44	0.03%
	0.3	111.49	111.23	0.23%		0.3	118.22	118.07	0.12%
	0.4	110.90	110.26	0.58%		0.4	117.76	116.58	1.00%
	0.5	110.47	109.58	0.81%		0.5	116.28	115.84	0.38%
	0.6	109.58	109.52	0.05%		0.6	116.08	114.42	1.43%
	0.7	107.63	106.19	1.33%		0.7	114.55	112.81	1.52%
	0.8	105.86	105.21	0.61%		0.8	112.25	111.45	0.72%
	0.9	103.81	102.01	1.74%		0.9	111.50	108.73	2.48%
08	0.1	78.90	78.86	0.06%	11	0.1	137.58	136.51	0.78%
	0.2	78.55	78.31	0.30%		0.2	136.52	136.14	0.28%
	0.3	78.01	77.54	0.61%		0.3	135.84	135.06	0.57%
	0.4	77.86	76.42	1.85%		0.4	135.25	134.24	0.75%
	0.5	77.09	76.19	1.17%		0.5	134.33	133.15	0.88%
	0.6	75.60	75.07	0.70%		0.6	132.71	131.16	1.17%
	0.7	75.19	74.50	0.92%		0.7	131.06	130.57	0.37%
	0.8	74.69	72.98	2.28%		0.8	129.56	127.98	1.22%
	0.9	72.71	71.22	2.05%		0.9	126.34	125.52	0.65%
09	0.1	123.85	123.48	0.30%	12	0.1	111.12	110.90	0.20%
	0.2	123.13	123.09	0.04%		0.2	110.31	110.03	0.25%
	0.3	122.62	121.68	0.77%		0.3	109.80	109.48	0.29%
	0.4	121.87	121.34	0.43%		0.4	109.06	108.04	0.94%
	0.5	120.69	119.58	0.92%		0.5	108.48	106.49	1.83%
	0.6	120.24	118.96	1.06%		0.6	107.27	105.94	1.24%
	0.7	118.81	117.21	1.34%		0.7	105.82	103.08	2.59%
	0.8	117.42	115.80	1.38%		0.8	105.13	102.08	2.90%
	0.9	114.33	113.27	0.93%		0.9	101.82	99.45	2.33%

Table 4.4.2 (con't) Minimum cost obtained by the hybrid method and its comparison with the SCA.

4.4 Numerical Results

Set #	DP	SCA	Hybrid	Reduction	Set #	DP	SCA	Hybrid	Reduction
13	0.1	886.85	886.85	0.00%	16	0.1	719.93	719.61	0.04%
	0.2	880.54	880.53	0.00%		0.2	714.34	714.11	0.03%
	0.3	874.06	874.02	0.00%		0.3	708.62	708.60	0.00%
	0.4	867.38	867.37	0.00%		0.4	702.18	702.08	0.01%
	0.5	860.08	860.05	0.00%		0.5	695.55	695.12	0.06%
	0.6	851.92	851.61	0.04%		0.6	688.62	687.37	0.18%
	0.7	842.53	842.01	0.06%		0.7	679.61	678.45	0.17%
	0.8	830.72	829.92	0.10%		0.8	668.84	667.49	0.20%
	0.9	816.18	814.19	0.24%		0.9	654.81	653.42	0.21%
14	0.1	729.23	729.10	0.02%	17	0.1	749.46	749.29	0.02%
	0.2	723.13	723.12	0.00%		0.2	744.12	744.12	0.00%
	0.3	716.57	716.14	0.06%		0.3	738.64	738.61	0.00%
	0.4	709.70	709.51	0.03%		0.4	732.14	732.11	0.00%
	0.5	701.85	701.29	0.08%		0.5	725.21	725.14	0.01%
	0.6	693.85	693.24	0.09%		0.6	716.91	716.79	0.02%
	0.7	684.41	683.29	0.16%		0.7	708.78	708.65	0.02%
	0.8	672.80	671.15	0.24%		0.8	697.90	697.60	0.04%
	0.9	658.24	657.38	0.13%		0.9	684.41	683.62	0.12%
15	0.1	844.67	843.67	0.12%	18	0.1	748.63	748.63	0.00%
	0.2	838.50	838.45	0.01%		0.2	742.71	742.25	0.06%
	0.3	832.17	832.10	0.01%		0.3	736.66	736.64	0.00%
	0.4	825.69	825.65	0.00%		0.4	730.94	730.48	0.06%
	0.5	818.24	818.19	0.01%		0.5	724.14	722.40	0.24%
	0.6	810.40	810.01	0.05%		0.6	716.77	715.20	0.22%
	0.7	801.03	800.36	0.08%		0.7	708.17	706.70	0.21%
	0.8	789.37	788.07	0.16%		0.8	695.94	694.40	0.22%
	0.9	775.03	773.85	0.15%		0.9	683.38	680.42	0.43%

Table 4.4.2 (con't) Minimum cost obtained by the hybrid method and its comparison with the SCA.

4.4 Numerical Results

Set #	DP	SCA	Hybrid	Reduction	Set #	DP	SCA	Hybrid	Reduction
19	0.1	835.82	835.16	0.08%	22	0.1	1,308.61	1,308.54	0.01%
	0.2	829.82	829.16	0.08%		0.2	1,300.06	1,299.36	0.05%
	0.3	822.53	822.03	0.06%		0.3	1,290.58	1,290.31	0.02%
	0.4	815.18	815.10	0.01%		0.4	1,279.32	1,279.05	0.02%
	0.5	808.16	807.42	0.09%		0.5	1,268.57	1,264.78	0.30%
	0.6	799.29	798.06	0.15%		0.6	1,255.86	1,254.66	0.10%
	0.7	789.56	788.34	0.15%		0.7	1,241.19	1,240.60	0.05%
	0.8	777.18	776.05	0.15%		0.8	1,223.69	1,221.53	0.18%
	0.9	762.48	761.00	0.19%		0.9	1,201.27	1,198.91	0.20%
20	0.1	720.14	720.11	0.00%	23	0.1	1,976.89	1,975.16	0.09%
	0.2	715.21	715.13	0.01%		0.2	1,964.82	1,964.22	0.03%
	0.3	709.22	709.00	0.03%		0.3	1,949.68	1,947.60	0.11%
	0.4	702.97	702.18	0.11%		0.4	1,932.31	1,931.98	0.02%
	0.5	696.70	696.57	0.02%		0.5	1,914.88	1,914.31	0.03%
	0.6	689.26	689.19	0.01%		0.6	1,894.89	1,894.04	0.05%
	0.7	681.01	680.18	0.12%		0.7	1,873.56	1,872.62	0.05%
	0.8	670.76	669.59	0.17%		0.8	1,846.75	1,846.04	0.04%
	0.9	658.04	656.02	0.31%		0.9	1,812.26	1,810.03	0.12%
21	0.1	784.65	784.39	0.03%	24	0.1	2,312.07	2,311.94	0.01%
	0.2	779.79	779.38	0.05%		0.2	2,298.88	2,298.54	0.01%
	0.3	774.12	773.12	0.13%		0.3	2,283.87	2,283.05	0.04%
	0.4	768.29	768.16	0.02%		0.4	2,266.73	2,266.73	0.00%
	0.5	761.69	761.01	0.09%		0.5	2,248.14	2,248.13	0.00%
	0.6	754.31	753.82	0.07%		0.6	2,227.85	2,227.13	0.03%
	0.7	746.30	746.12	0.02%		0.7	2,204.40	2,204.21	0.01%
	0.8	736.54	736.24	0.04%		0.8	2,177.02	2,176.05	0.04%
	0.9	723.99	723.04	0.13%		0.9	2,140.60	2,139.71	0.04%

Table 4.4.2 (con't) Minimum cost obtained by the hybrid method and its comparison with the SCA.

4.4.1 Quality of the Solutions Obtained by the Hybrid Heuristic

In order to evaluate the performance of the hybrid heuristic (GASA), “enumerative search” for the optimal solution is carried out for the 5-buyer case. An enumerative search for all the combinations of (N, k_i, λ_i) is impractical since there are 1.25×10^{16} different combinations. Assume the computation rate is 30,000 combinations per second, it takes 5,783,333 days to run all the combinations! Therefore, a “reduced enumerative search” is developed for the comparison purpose. Note that the “optimal” solution obtained cannot be guaranteed as the actual optimal solution.

The procedure for the “reduced enumerative search” is described as follows:

STEP 1: Perform enumerative search on N and k_i such that the total cost function (3.5.1) is minimized. Denote the solution as (N^*, k_i^*) .

STEP 2: Use the (N^*, k_i^*) obtained in STEP 1 to perform a sub-enumerative search on λ_i , where $1 \leq \lambda_i \leq k_i$.

Sub-enumerative search on λ_i (Start with $t^* = 2$):

STEP 2.1: Perform enumerative search for all $1 \leq \lambda_i \leq t^* \leq k_i$

STEP 2.2: IF all the λ_i 's are strictly less than t^* , STOP

ELSE increase t^* by 1 and repeat STEP 2.1

The “optimal” solution for the 5-buyer case for the SCA, GASA and the “reduced enumerative search” is depicted in Table 4.4.1.1.

DP	SCA	GASA	Enum.	CPU Time
0.1	22.97	22.73	22.73	40 sec
0.2	23.36	22.91	22.88	51 sec
0.3	23.14	23.08	22.91	53 sec
0.4	23.92	22.62	22.62	56 sec
0.5	23.12	22.29	22.37	6 min 50 sec
0.6	24.07	22.03	22.49	9 min 36 sec
0.7	22.34	21.70	21.86	9 min 53 sec
0.8	22.36	21.16	21.20	10 min 33 sec
0.9	20.81	20.08	20.27	82 min 16 sec

Table 4.4.1.1 Comparison of minimum cost obtained by SCA, GASA and the “reduced enumerative search” (5-buyer case).

According to Table 4.4.1.1, for DP-ratios of 0.1 and 0.4, the “reduced enumerative search” confirms the “near-optimal” solution obtained by the GASA heuristic; for DP-ratios of 0.2 and 0.3, better solutions are obtained through enumerative search. For DP-ratios of 0.5 or above, the GASA heuristic still performs better than the enumerative search. In terms of computational time, GASA takes less than 2 minutes for the case with DP-ratio of 0.9; while the enumerative search takes 82 minutes. GASA is capable of obtaining a better solution compared to the SCA, and requires far less computational time compared to the enumerative search. Therefore, the GASA heuristic developed in this chapter is capable of validating the quality of the solutions obtained from other algorithms (i.e. the SCA) that attempt to solve this kind of supply chain

optimization problems.

4.5 Discussion

From the numerical results in section 4.4, the improvements over the SCA for all heuristics used (GA, SA, and Hybrid) decrease as the number of buyers increases.

This is because the probability of forming a better chromosome decreases dramatically as the number of buyers increases. This phenomenon is explained as below:

The total number of feasible combinations C for an n -buyer case is given by

$$C = [\sigma(N)]^n \quad (4.5.1)$$

where

$$\sigma(N) = \sum_{f|N} f \quad (4.5.2)$$

is the sum-of-divisor function with $N \equiv 0 \pmod{f}$.

Take $n = 5$ and $N = 35$ as an example:

The divisors of $N = 35$ is 1, 5, 7 and 35 and thus $\sigma(35) = 1 + 5 + 7 + 35 = 48$.

For every buyer, the buyer can choose $k_i = 1$, $k_i = 5$, $k_i = 7$ or $k_i = 35$ as the replenishment interval; and the possible number for λ (the ordering day determined by the vendor) such that $\delta_{i\lambda} = 1$ is 1 for $k_i = 1$, 5 for $k_i = 5$, 7 for $k_i = 7$ and 35 for $k_i = 35$. Thus the number of possible (k_i, λ_i) pairs, for

each buyer, equals to $1+5+7+35=48=\sigma(35)$. In the 5-buyer case, the total number of (k_i, λ_i) pairs is $C = [\sigma(35)]^5 = 48^5 = 254,803,968$.

With reference to Table 5.4.1 for the possible choices of N , Table 4.5.1 depicts the minimum and maximum number of different combinations for the 5-buyer, 15-buyer, 30-buyer, and 50-buyer examples. For example, for all 15-buyer cases the lower bound on N is 5 and the upper bound is 1388. Between the two bounds, the minimum and maximum values of the sum-of-divisor function is $\sigma(5)=6$ and $\sigma(1260)=4368$ respectively.

Comparing the two meta-heuristics, GA and SA, GA obtains a better solution in most of the trials. This is due to the additional crossover operations. However, the operation of SA is just similar to the mutation process used in GA and it has no crossover operations. In the SCA model with such a high complexity, there are many local minima and the “distance” between two minima may be “too far” such that simply applying the mutation is not enough. However, it is also the additional crossover process that nearly doubles the computational time of the GA.

	Minimum C	Maximum C
5-buyer	$[\sigma(37)]^5 \approx 7.92 \times 10^7$	$[\sigma(540)]^5 \approx 1.34 \times 10^{16}$
15-buyer	$[\sigma(5)]^{15} \approx 4.70 \times 10^{11}$	$[\sigma(1260)]^{15} \approx 4.02 \times 10^{54}$
30-buyer	$[\sigma(5)]^{30} \approx 2.21 \times 10^{23}$	$[\sigma(9240)]^{30} \approx 1.44 \times 10^{136}$
50-buyer	$[\sigma(3)]^{50} \approx 1.27 \times 10^{30}$	$[\sigma(9240)]^{50} \approx 8.49 \times 10^{226}$

Table 4.5.1 Minimum and maximum number of feasible combinations

The hybrid heuristic is designed to combine the pros of the SA and GA. The initial search using SA provides a “near-optimal” solution in a short period of time and based on the given solution, GA may further fine-tune the solution to a better “near-optimal” solution. As expected, this would shorten the computational time.

From Table 4.4.2, all the meta-heuristics (GA, SA, and GASA) give an improved solution compared to the SCA. The improvement is due to (i) Facing the large feasible combinations (Table 4.5.1) of the (k_i, λ_i) pairs, meta-heuristics still can intensively search for a “near-optimal” solutions better than the one obtained using SCA. (ii) For the sake of computational simplicity, SCA restricts the bounds on N from 1 to 365. However, there is no such restriction in the meta-heuristics. It is clear that the SCA has confirmed itself in a searching space of $N = 1$ to 365. The algorithm only searches the best solution within this

restricted space. Although the restricted space can greatly reduce the computational time, the algorithm may miss the global optimum. The meta-heuristic developed in this chapter have overcome this problem by allowing a “free” value of N . Due to the bounds imposed by the SCA, it is not so sure whether it can provide a good solution to the model. Another contribution of the meta-heuristic developed in this chapter is that they can act as benchmarks for the SCA, or other algorithms attempted to solve similar models developed in the area of supply chain management.

Chapter 5

Further Studies on the Synchronized Ordering and Production Cycles

5.1 Introduction

In chapter 3, the synchronized cycles model and the synchronized cycles algorithm (Chan and Kingsman 2005, 2007) are introduced. In this chapter, some characteristics of the synchronized cycles model is explored and reasonable bounds on certain decision variables in order to enhance the synchronized cycles algorithm is developed. Extensions to the synchronized cycles model are also introduced.

5.2 Pareto Improvements

Any buyer is willing to participate in the synchronized cycles scheme only if the scheme favors the buyer; similarly, the vendor would not execute the new scheme if the vendor cannot get any benefits from the scheme. Thus, in order to succeed in applying the synchronized cycles scheme, pareto improvements must be reached. In this context, pareto improvement refers to both the vendor and all the buyers that after participating in the new co-corporation scheme, each

involved party would not be worse off compared to the independent policy.

Under independent policy, the total cost incurred by buyer i is

$$TC_i^{IND} = \sqrt{2A_i d_i h_i}, \quad (5.2.1)$$

and the cost incurred under the synchronized cycles model is

$$TC_i^{SCA} = \frac{A_i}{k_i T} + \frac{1}{2} d_i h_i k_i T. \quad (5.2.2)$$

Consider the function

$$f(k_i) = \sqrt{2A_i d_i h_i} - \left(\frac{A_i}{k_i T} + \frac{1}{2} d_i h_i k_i T \right) \quad (5.2.3)$$

where $f(k_i)$ denotes the saving if the i^{th} buyer chooses to take part in the new

scheme. Taking the first and second derivatives with respect to k_i of (5.2.3)

yield

$$f'(k_i) = \frac{A_i}{k_i^2 T} - \frac{1}{2} d_i h_i T \quad \text{and} \quad (5.2.4)$$

$$f''(k_i) = \frac{-2A_i}{k_i^3 T} < 0 \quad \text{given that } A_i > 0. \quad (5.2.5)$$

Solving $f'(k_i) = 0$ gives the optimal value

$$k_i^* = \sqrt{\frac{2A_i}{d_i h_i T^2}} \quad (5.2.6)$$

at which $f(k_i^*)$ is a maximum. Substituting this value of k_i^* for k_i in (5.2.3),

the value of $f(k_i)$ is 0. That means the maximum saving of the i^{th} buyer is 0

if the buyer chooses to take part in the new scheme. Hence, none of the buyer

can be better off under the synchronized cycles policy. Therefore,

profit-sharing allocation and/or price-discount schemes are necessary for the vendor in order to entice the buyers to participate in the synchronized cycles scheme. For simplicity, to test for the effectiveness of the synchronized cycles, we use a straightforward repayment scheme: The vendor rebates the buyers all the losses incurred by participating in the synchronized cycles scheme rather than adopting independent optimization. The policy is considered as “effective” if

$$TC_v^{IND} - TC_v^{SCA} \geq \sum_{i=1}^n (TC_i^{SCA} - TC_i^{IND}) \quad (5.2.7)$$

or equivalently,

$$TC^{IND} - TC^{SCA} \geq 0 \quad (5.2.8)$$

Experiments have been conducted for 216 trials (24 datasets x 9 DP-ratios).

The datasets are depicted in the Appendix. All of the trials show that the synchronized cycles model is “effective”. Table 5.2.1 shows the results of 3 datasets which are the datasets used in Chan and Kingsman (2005, 2007).

5.2 Pareto Improvements

Set #	DP	Independent			SCA			Eq. 5.2.8
		B Cost	V Cost	TC	B Cost	V Cost	TC	
01	0.1	7.95	28.62	36.58	12.54	10.44	22.97	13.60
	0.2	7.95	27.97	35.92	12.33	11.04	23.36	12.56
	0.3	7.95	27.27	35.23	10.37	12.77	23.14	12.08
	0.4	7.95	26.53	34.48	10.37	13.55	23.92	10.56
	0.5	7.95	25.71	33.67	10.37	12.75	23.12	10.54
	0.6	7.95	24.81	32.77	9.37	14.70	24.07	8.70
	0.7	7.95	23.79	31.75	9.37	12.98	22.34	9.40
	0.8	7.95	22.58	30.54	9.37	13.00	22.36	8.17
	0.9	7.95	21.01	28.96	9.01	11.80	20.81	8.15
12	0.1	86.98	39.03	126.01	88.11	23.02	111.12	14.88
	0.2	86.98	37.67	124.65	87.80	22.50	110.31	14.34
	0.3	86.98	36.22	123.20	87.80	21.99	109.80	13.40
	0.4	86.98	34.67	121.64	87.70	21.37	109.06	12.58
	0.5	86.98	32.97	119.95	88.15	20.33	108.48	11.47
	0.6	86.98	31.10	118.08	87.52	19.75	107.27	10.81
	0.7	86.98	28.98	115.96	87.55	18.27	105.82	10.13
	0.8	86.98	26.46	113.44	87.43	17.70	105.13	8.31
	0.9	86.98	23.17	110.15	87.39	14.43	101.82	8.33
22	0.1	786.62	635.32	1421.94	852.61	455.99	1308.61	113.33
	0.2	786.62	625.53	1412.15	851.45	448.61	1300.06	112.09
	0.3	786.62	615.11	1401.73	850.78	439.80	1290.58	111.15
	0.4	786.62	603.92	1390.54	850.78	428.54	1279.32	111.22
	0.5	786.62	591.74	1378.36	849.63	418.94	1268.57	109.79
	0.6	786.62	578.28	1364.90	849.63	406.23	1255.86	109.04
	0.7	786.62	562.99	1349.61	850.41	390.78	1241.19	108.43
	0.8	786.62	544.86	1331.48	848.46	375.22	1223.69	107.80
	0.9	786.62	521.24	1307.86	849.00	352.27	1201.27	106.59

Table 5.2.1 Comparison on the performances of the independent policy and the SCA.

5.3 Sensitivity Analysis

From previous section, the synchronized cycles model outperforms the independent policy for all trials. In this section, to further investigate the impact on the performance of the synchronized cycles model, sensitivity analysis is performed according to two aspects: (*i*) the variation on standard parameters and (*ii*) the effect of vendor's share of the total system cost under the independent policy.

5.3.1 Effects of Variation on Standard Parameters

The effects of variation on the standard parameters (i.e. demand, transportation cost, ordering cost, buyer's holding cost, vendor's set-up cost and vendor's holding cost) are examined. For each parameter, a percentage change from -50% to +50%, with an increment of 10%, is added-on to its original value.

With a newly assigned parameter, the total cost is evaluated for both the independent policy and the synchronized cycles policy. Figures 5.3.1.1 – 5.3.1.12 reveals the plot of the percentage savings vs. the parameter's percentage change, of which figures 5.3.1.1 – 5.3.1.6 correspond to dataset 21 (30 buyers) and figures 5.3.1.7 – 5.3.1.12 correspond to dataset 24 (50 buyers). The following results are observed from the plots:

- For such a wide range of parameters' values, the synchronized cycles policy

performs better than the independent policy.

- The savings increase as the transportation cost increases.
- The savings decrease as the ordering cost increases or the vendor's set-up cost increases.
- The vendor's "optimal" planning horizon (N) decreases as the demand or the vendor's holding cost increases; while it increases as the set-up cost increases. The "optimal" planning horizon is not sensitive to the change in the transportation cost, the ordering cost, or the buyer's holding cost.

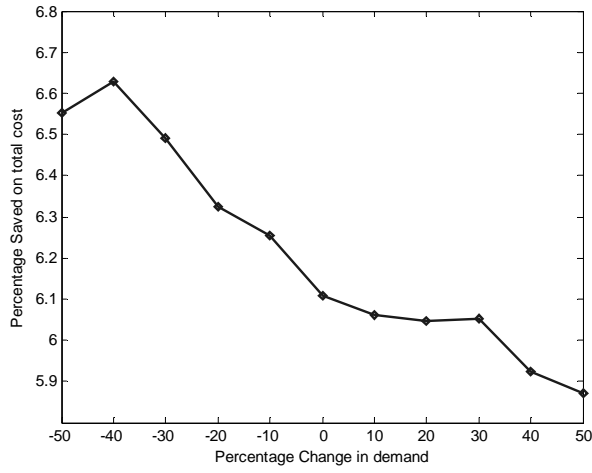


Figure 5.3.1.1 The effect on percentage change in demand (Set 21).

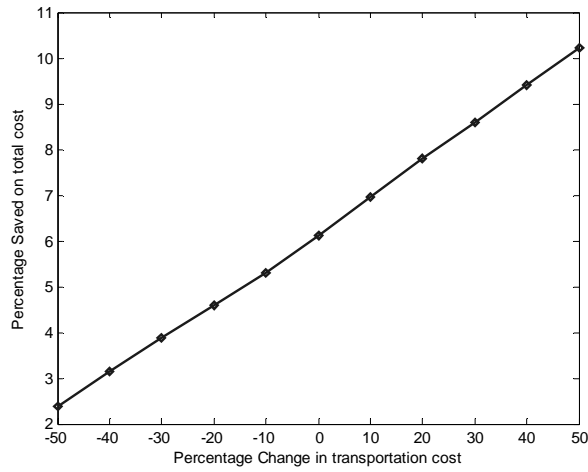


Figure 5.3.1.2 The effect on percentage change in transportation cost (Set 21).

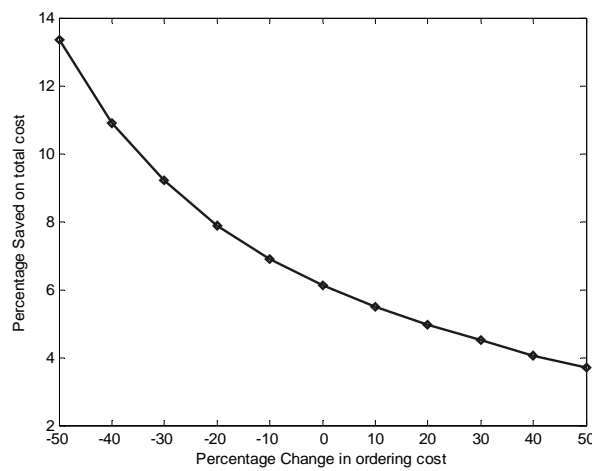


Figure 5.3.1.3 The effect on percentage change in ordering cost (Set 21).

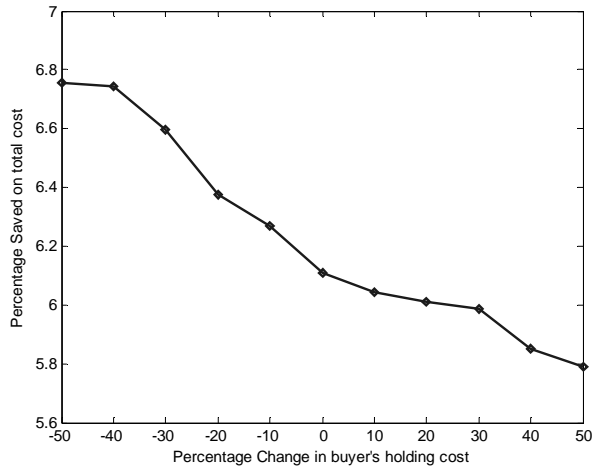


Figure 5.3.1.4 The effect on percentage change in buyer's holding cost (Set 21).

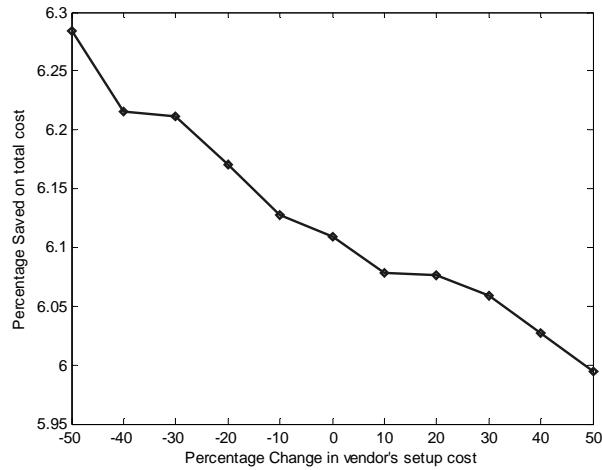


Figure 5.3.1.5 The effect on percentage change in vendor's set-up cost (Set 21).

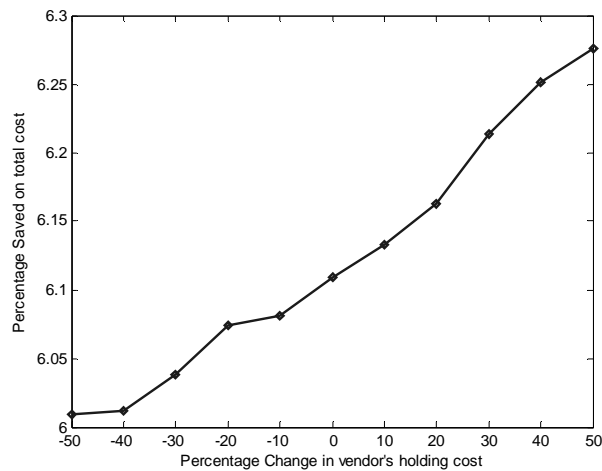


Figure 5.3.1.6 The effect on percentage change in vendor's holding cost (Set 21).

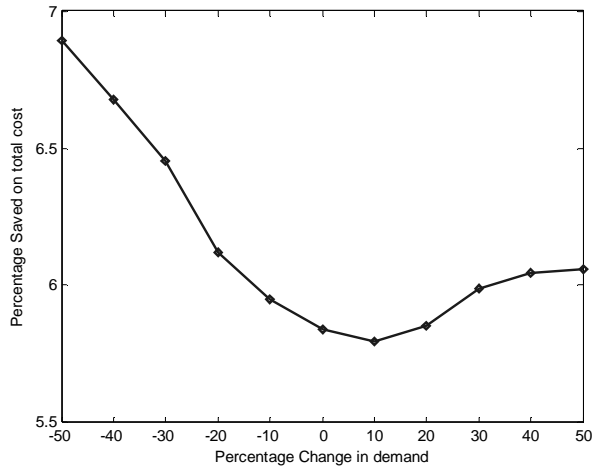


Figure 5.3.1.7 The effect on percentage change in demand (Set 24).

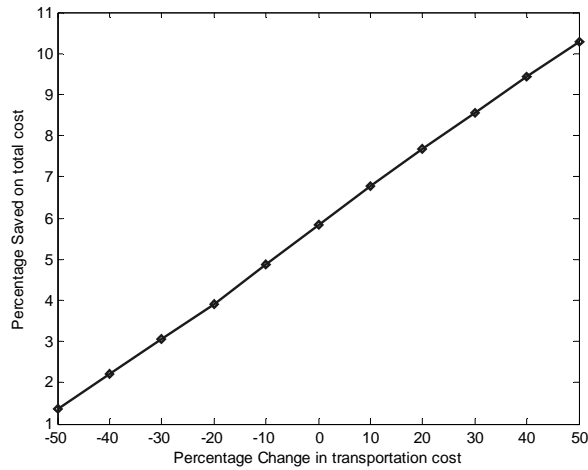


Figure 5.3.1.8 The effect on percentage change in transportation cost (Set 24).

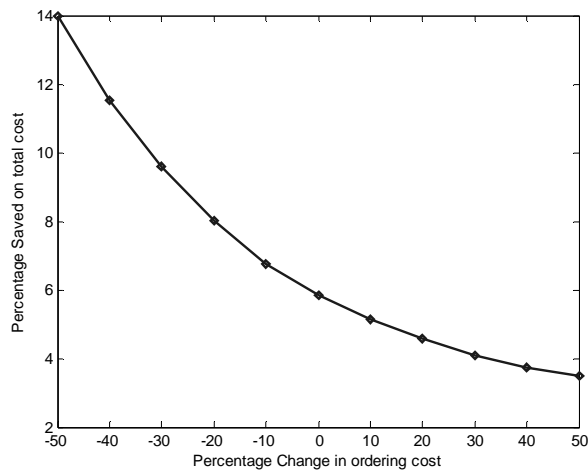


Figure 5.3.1.9 The effect on percentage change in ordering cost (Set 24).

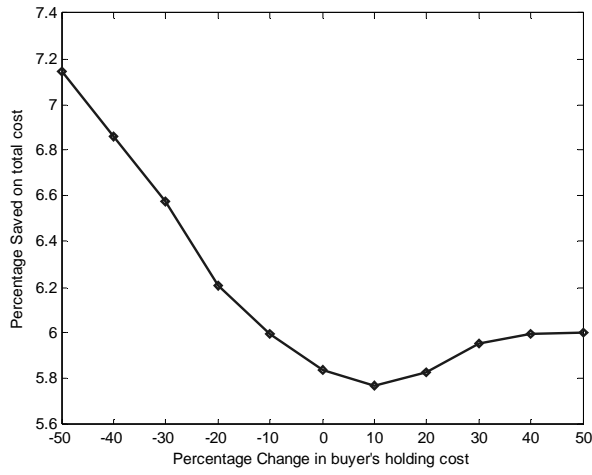


Figure 5.3.1.10 The effect on percentage change in buyer's holding cost (Set 24).

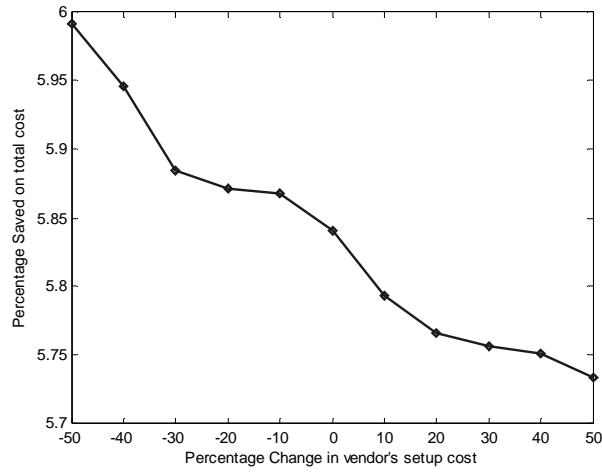


Figure 5.3.1.11 The effect on percentage change in vendor's set-up cost (Set 24).

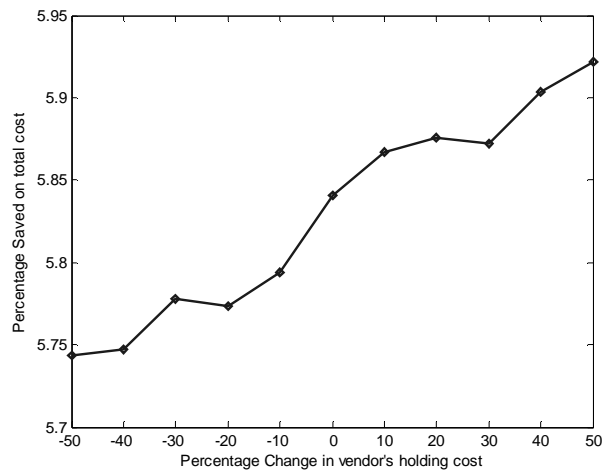


Figure 5.3.1.12 The effect on percentage change in vendor's holding cost (Set 24).

5.3.2 The Portion Borne by the Vendor Under the Independent Policy and the Synchronized Cycles Co-ordination

All 216 trials are tested and the results can be summarized as follows:

Over a wide range of vendor's share of total system cost under the independent policy, the synchronized cycles model out-performs the independent policy. In addition, as the vendor's share under the independent policy increases, the percentage increment in the buyer's cost, the percentage reduction in both the vendor's cost and the total cost increases. All three measurements have a strong relationship (an average of 0.92, 0.93 and 0.98 respectively) with the vendor's share. These findings suggest that if the vendor realizes himself that he is bearing a "large" portion of the system cost when independent optimization is adopted in the supply chain, it is more beneficial to the vendor if he could persuade the buyers to participate in the synchronized cycles co-ordination system.

Figures 5.3.2.1 – 5.3.2.3 show the percentage increase in buyer's cost, the percentage decrease in vendor's cost, and the percentage reduction in total cost respectively as the vendor's share changes for dataset 24 with DP ratio equal to 0.5.

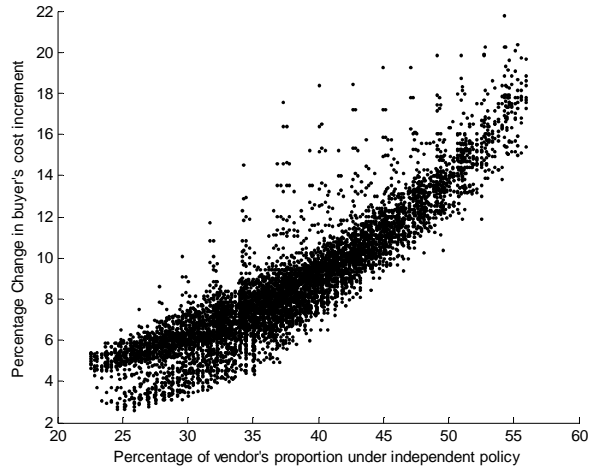


Figure 5.3.2.1 The effect on the increment of buyer's cost (Set 24, DP=0.5).

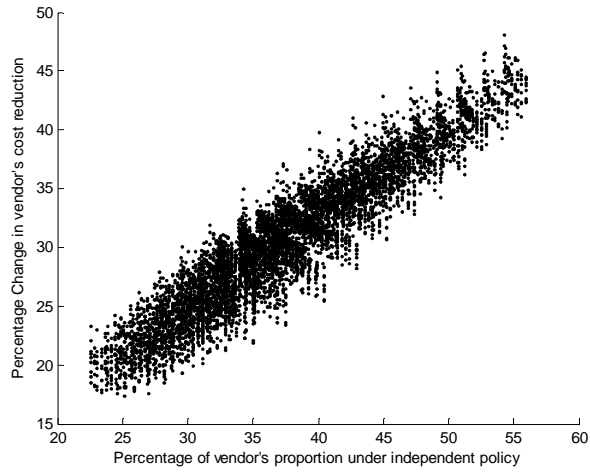


Figure 5.3.2.2 The effect on vendor's cost reduction (Set 24, DP=0.5).

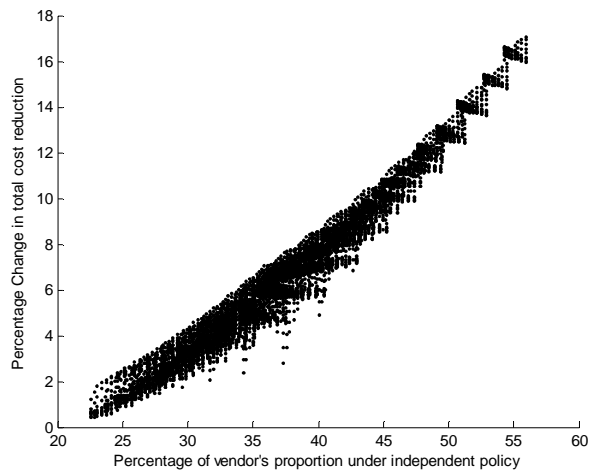


Figure 5.3.2.3 The effect on the total cost (Set 24, DP=0.5).

5.4 Establishing Bounds on N

Consider the total relevant cost function:

$$TC(N, k_i) = \frac{S_v}{NT} + NT \left(\frac{hD}{2} (1 - \alpha) \right) + \sum_{i=1}^n \left[\frac{C_i + A_i}{k_i T} + d_i k_i T \left(h\alpha - \frac{1}{2} (h - h_i) \right) \right] \quad (5.4.1)$$

which is a convex function of k_i , for a particular value of N . Thus, an “optimal” solution of (5.4.1) for each N can be obtained by finding the minimum point at $k_i = k_i^*$, where k_i^* is a factor of N , using the synchronized cycles algorithm developed by Chan and Kingsman (2005, 2007).

5.4.1 Synchronized Cycles Algorithm

In this sub-section, the synchronized cycles algorithm is introduced.

STEP 1: Set $N = 1$ and $T = 1$

STEP 2.1: Determine all factors of N .

STEP 2.2: IF $\left(h\alpha - \frac{1}{2} (h - h_i) \right) d_i > 0$, GO TO STEP 2.3

ELSE set $k_i^* = N$ and GO TO STEP 3

STEP 2.3: Calculate $\Phi = \frac{C_i + A_i}{d_i \left[h \left(\alpha - \frac{1}{2} \right) + \frac{1}{2} h_i \right] T^2}$

STEP 2.4: Find k_i^* such that $k_i^* (k_i^* - 1) \leq \Phi \leq k_i^* (k_i^* + 1)$

STEP 2.5: IF $k_i^* \geq N$, set $k_i^* = N$ and GO TO STEP 3

ELSE IF k_i^* is a factor of N , then GO TO STEP 3

ELSE Find two consecutive factors of N , k_i^1 and k_i^2 ,
such that $k_i^1 < k_i^* < k_i^2$.

STEP 2.6: Substitute k_i^1 and k_i^2 into the function

$$f(k_i) = \frac{C_i + A_i}{k_i T} + d_i \left[h \left(\alpha - \frac{1}{2} \right) + \frac{1}{2} h_i \right] k_i T$$

and set $k_i^* = k_i^1$ if $f(k_i^1) < f(k_i^2)$, otherwise set $k_i^* = k_i^2$.

STEP 2.7: Substitute N and the k_i 's into (5.4.1) to obtain the total system
cost.

STEP 3: IF $N < 365$, set $N = N + 1$ and repeat STEP 2.1 – 2.7

ELSE GO TO STEP 4

STEP 4: Take the $(n + 1)$ -tuple, $(N, k_1, k_2, \dots, k_n)$, which gives the least
total system cost.

In the next sub-section, the bounds on N are established in order to enhance the
performance of the synchronized cycles algorithm.

5.4.2 Bounds on N

Relaxing the constraints on k_i and N , we define the relaxed sets as:

$$\{k_i, N \in \mathbb{R}^+ \mid 1 \leq k_i \leq N\} \quad (5.4.2.1)$$

For fixed N , $TC(N, k_i^*)$ is a minimum when:

$$(i) \quad k_i^* = \sqrt{\frac{C_i + A_i}{d_i T^2 \left(h\alpha - \frac{1}{2}(h - h_i) \right)}} \quad \text{for } h\alpha - \frac{1}{2}(h - h_i) > 0 \quad (5.4.2.2)$$

$$(ii) \quad \text{Or else assume } k_i^* = N \quad (\text{i.e. for } h\alpha - \frac{1}{2}(h - h_i) \leq 0) \quad (5.4.2.3)$$

The lower bound of the total cost function (5.4.1), for fixed N , becomes:

$$TC_L(N) = \frac{S_v}{NT} + NT \left(\frac{hD}{2}(1 - \alpha) \right) + \sum_{i=1}^n f_i(k_i^*) \quad (5.4.2.4)$$

where

$$f_i(k_i^*) = \frac{C_i + A_i}{k_i^* T} + d_i k_i^* T \left(h\alpha - \frac{1}{2}(h - h_i) \right) \quad (5.4.2.5)$$

A reasonable upper bound of the total cost is attained when $k_i^* = N$ for all i ,

which can be expressed as:

$$\begin{aligned} TC_U(N) &= \frac{S_v}{NT} + NT \left(\frac{hD}{2}(1 - \alpha) \right) + \sum_{i=1}^n f(N) \\ &= \frac{S_v + \sum_{i=1}^n (C_i + A_i)}{NT} + \frac{NT}{2} \left(hD\alpha + \sum_{i=1}^n h_i d_i \right). \end{aligned} \quad (5.4.2.6)$$

(5.4.2.6) is a convex function of N and we may obtain an upper bound at $N =$

N^* :

$$TC_U(N^*) = 2 \sqrt{\frac{1}{2} \left(S_v + \sum_{i=1}^n (C_i + A_i) \right) \left(hD\alpha + \sum_{i=1}^n h_i d_i \right)} \quad (5.4.2.7)$$

where

$$N^* = \sqrt{\frac{\left(S_v + \sum_{i=1}^n (C_i + A_i) \right)}{\frac{1}{2} T^2 \left(hD\alpha + \sum_{i=1}^n h_i d_i \right)}}. \quad (5.4.2.8)$$

Consider (5.4.2.4) and (5.4.2.7), we can eliminate some values of N in

applying the Synchronised Cycles Algorithm. We only need to take into account the values of N if

$$TC_L(N) \leq TC_U(N^*) \quad (5.4.2.9)$$

Let

$$TC_L(N) = \frac{W}{N} + XN + Y \quad (5.4.2.10)$$

where

$$W = \frac{S_v}{T}, \quad X = T \left(\frac{hD}{2} (1 - \alpha) \right),$$

$$Y = \sum_{i=1}^n f_i(k_i^*) \quad \text{and} \quad Z = TC_U(N^*).$$

(5.4.2.9) becomes:

$$\frac{W}{N} + XN + Y \leq Z$$

implies

$$XN^2 - MN + W \leq 0, \quad M = Z - Y.$$

\therefore X is always positive.

$$\therefore \frac{M - \sqrt{(-M)^2 - 4XW}}{2X} \leq N \leq \frac{M + \sqrt{(-M)^2 - 4XW}}{2X}. \quad (5.4.2.11)$$

5.4.3 Revised Synchronized Cycles Algorithm by Establishing the Bounds

on N :

An algorithm to establish the bounds on N

STEP 1: Calculate $TC_L(N)$ by evaluating the k_i^* using (5.4.2.2) and

(5.4.2.3).

STEP 2: Calculate $TC_U(N^*)$ by (5.4.2.6), (5.4.2.7) and (5.4.2.8).

STEP 3: Obtain a feasible set of N by (5.4.2.9) – (5.4.2.11).

IF $(-M)^2 - 4XW \leq 0$, $\{N \in \mathbb{Z}^+ \mid 1 \leq N \leq \infty\}$

ELSE

let $N_{MIN} = \max \left\{ 1, \left\lceil \frac{M - \sqrt{(-M)^2 - 4XW}}{2X} \right\rceil \right\}$ and

let $N_{MAX} = \left\lfloor \frac{M + \sqrt{(-M)^2 - 4XW}}{2X} \right\rfloor$

$\{N \in \mathbb{Z}^+ \mid N_{MIN} \leq N \leq N_{MAX}\}$

END

Revised Synchronized Cycles Algorithm

The revised synchronized cycles algorithm is similar to the one introduced in sub-section 5.4.1 with the following modifications:

STEP 1: Set $N = N_{MIN}$ and $T = 1$

STEP 2.1 – 2.7: Same routine as original.

STEP 3: IF $N < N_{MAX}$, set $N = N + 1$ and repeat STEP 2.1 – 2.7

ELSE GO TO STEP 4

STEP 4: Same routine as original.

Table 5.4.1 shows the lower and upper bounds on N for all of the 24 sample datasets. The first few steps of the synchronized cycles algorithm suggests to find the least total relevant cost by trying all values of N from 1 to 365. However, as depicted in table 5.4.1, for most of the datasets 1 – 12 (with fewer buyers and low value of demand-production ratio α), there is no need to test for all values of N from 1 to 365 and this could save a little bit of computational time; but for more buyers or high values of demand-production ratio α , the upper bound on N exceeds far beyond 365. Thus, the SCA should test all the integer values of N within the bounds. Nevertheless, if the bounds are too far apart, this is just similar to enumerative search for N which violates the purpose of the design of the SCA – for the sake of simplicity. In this case, meta-heuristics may be more appropriate.

5.4 Establishing Bounds on N

Set	D/P	N min	N max	Set	D/P	N min	N max	Set	D/P	N min	N max
01	0.1	37	53	04	0.1	7	94	07	0.1	5	156
	0.2	38	57		0.2	7	106		0.2	5	175
	0.3	37	67		0.3	7	121		0.3	5	200
	0.4	36	80		0.4	7	141		0.4	5	232
	0.5	35	99		0.5	7	169		0.5	5	279
	0.6	34	128		0.6	7	212		0.6	5	348
	0.7	33	176		0.7	7	282		0.7	5	463
	0.8	32	273		0.8	7	423		0.8	5	694
	0.9	31	561		0.9	7	847		0.9	5	1388
02	0.1	5	140	05	0.1	6	91	08	0.1	9	150
	0.2	5	158		0.2	6	102		0.2	9	168
	0.3	5	181		0.3	6	116		0.3	9	192
	0.4	5	211		0.4	6	136		0.4	9	224
	0.5	5	254		0.5	6	163		0.5	9	269
	0.6	5	318		0.6	6	203		0.6	9	336
	0.7	5	424		0.7	6	271		0.7	9	448
	0.8	5	637		0.8	6	406		0.8	9	672
	0.9	5	1277		0.9	6	813		0.9	9	1344
03	0.1	6	137	06	0.1	6	119	09	0.1	7	97
	0.2	6	154		0.2	6	134		0.2	7	109
	0.3	6	175		0.3	6	152		0.3	7	125
	0.4	6	204		0.4	6	177		0.4	7	146
	0.5	6	244		0.5	6	212		0.5	7	175
	0.6	6	305		0.6	6	265		0.6	7	220
	0.7	6	406		0.7	6	353		0.7	7	293
	0.8	6	608		0.8	6	529		0.8	7	440
	0.9	6	1216		0.9	6	1057		0.9	7	882

Table 5.4.1 The range of possible values of optimal N under SCA.

5.4 Establishing Bounds on N

Set	D/P	N min	N max	Set	D/P	N min	N max	Set	D/P	N min	N max
10	0.1	8	75	13	0.1	4	750	16	0.1	4	905
	0.2	8	84		0.2	4	844		0.2	4	1018
	0.3	8	95		0.3	4	965		0.3	4	1163
	0.4	8	111		0.4	4	1126		0.4	4	1358
	0.5	8	133		0.5	4	1352		0.5	4	1630
	0.6	8	166		0.6	4	1690		0.6	4	2037
	0.7	8	222		0.7	4	2255		0.7	4	2717
	0.8	8	332		0.8	4	3384		0.8	4	4077
	0.9	8	665		0.9	4	6771		0.9	4	8155
11	0.1	5	89	14	0.1	4	734	17	0.1	4	904
	0.2	5	100		0.2	4	826		0.2	4	1017
	0.3	5	114		0.3	4	944		0.3	4	1163
	0.4	6	133		0.4	4	1102		0.4	4	1357
	0.5	6	159		0.5	4	1323		0.5	4	1630
	0.6	6	199		0.6	4	1654		0.6	4	2038
	0.7	6	264		0.7	4	2206		0.7	4	2718
	0.8	6	396		0.8	4	3310		0.8	4	4080
	0.9	6	792		0.9	4	6623		0.9	4	8163
12	0.1	6	84	15	0.1	4	864	18	0.1	4	842
	0.2	5	110		0.2	4	973		0.2	4	948
	0.3	5	125		0.3	4	1112		0.3	4	1083
	0.4	5	144		0.4	4	1298		0.4	4	1263
	0.5	5	172		0.5	4	1558		0.5	4	1516
	0.6	5	214		0.6	4	1948		0.6	4	1895
	0.7	5	284		0.7	4	2598		0.7	4	2527
	0.8	5	425		0.8	4	3897		0.8	4	3791
	0.9	5	848		0.9	4	7797		0.9	4	7582

Table 5.4.1 (con't) The range of possible values of optimal N under SCA.

Set	D/P	N min	N max	Set	D/P	N min	N max	Set	D/P	N min	N max
19	0.1	4	773	21	0.1	4	1062	23	0.1	3	602
	0.2	4	870		0.2	4	1195		0.2	3	677
	0.3	4	994		0.3	4	1366		0.3	3	774
	0.4	4	1160		0.4	4	1594		0.4	3	904
	0.5	4	1392		0.5	4	1914		0.5	3	1085
	0.6	4	1740		0.6	4	2393		0.6	3	1356
	0.7	4	2321		0.7	4	3192		0.7	3	1809
	0.8	4	3481		0.8	4	4790		0.8	3	2714
	0.9	4	6963		0.9	4	9583		0.9	3	5430
20	0.1	5	852	22	0.1	4	1109	24	0.1	3	598
	0.2	5	959		0.2	4	1248		0.2	3	673
	0.3	5	1097		0.3	4	1426		0.3	3	770
	0.4	5	1280		0.4	4	1664		0.4	3	899
	0.5	5	1537		0.5	4	1997		0.5	3	1079
	0.6	5	1922		0.6	4	2497		0.6	3	1349
	0.7	5	2563		0.7	4	3330		0.7	3	1800
	0.8	5	3846		0.8	4	4996		0.8	3	2701
	0.9	5	7696		0.9	4	9993		0.9	3	5404

Table 5.4.1 (con't) The range of possible values of optimal N under SCA.

5.5 Establishing Bounds on b

The search on Ψ , the number of units of surplus stock at the beginning of the production, depends on the value of $b = \lfloor F \rfloor$ where F is the time at which the production terminates.

To satisfy the demand at the first ordering time, we have

$$(1+S)PT = \Psi + D_1 \quad (5.5.1)$$

and this implies

$$S = \frac{\Psi + D_1}{PT} - 1 \geq \frac{D_1}{PT} - 1. \quad (5.5.2)$$

Further, total production must satisfy

$$(F+S)PT = NDT \quad (5.5.3)$$

and this implies

$$F = N\alpha - S = N\alpha - \left(\frac{\Psi + D_1}{PT} - 1 \right) \leq N\alpha - \left(\frac{D_1}{PT} - 1 \right). \quad (5.5.4)$$

With $D_1 \geq 0$ and $b = \lfloor F \rfloor$, we obtain

$$b \leq \lfloor N\alpha + 1 \rfloor. \quad (5.5.5)$$

Since $b \leq N$, we obtain two choices of b depending on the value of α :

$$b \begin{cases} \leq \lfloor N\alpha + 1 \rfloor & \text{for } \alpha < \frac{N-1}{N} \\ \leq N & \text{for } \alpha \geq \frac{N-1}{N} \end{cases}. \quad (5.5.6)$$

5.6 Reduction in the Search Space on Ψ

Recall from (3.5.3) and (3.5.4), the value of Ψ must satisfy

$$\Psi \geq \sum_{i=1}^n \left[k_i d_i T \left(\sum_{i=2}^j \delta_{i,j} \right) \right] - (j-1)PT \quad \text{for } i = 1, 2, \dots, n; \quad 2 \leq j \leq b, \quad (5.6.1)$$

with the result obtained in section 5.5, $b = \min\{\lfloor N\alpha + 1 \rfloor, N\}$, and

$$\Psi \geq 0 \quad (5.6.2)$$

Given all the value of the $\delta_{i,j}$, define Ψ_j as the value of

$$\sum_{i=1}^n \left[k_i d_i T \left(\sum_{i=2}^j \delta_{i,j} \right) \right] - (j-1)PT \quad \text{for } 2 \leq j \leq b. \quad \text{The value of } \Psi \text{ satisfying both}$$

(5.6.1) and (5.6.2) is equal to

$$\max\{\max\{\Psi_2, \Psi_3, \dots, \Psi_b\}, 0\}. \quad (5.6.3)$$

Based on (5.6.1), the value of

$$f(\delta_{i,j}) = \sum_{i=1}^n \left[k_i d_i T \left(\sum_{i=2}^j \delta_{i,j} \right) \right] - (j-1)PT$$

should be decreasing at a constant rate of PT along j , if there is no order

placement at a new j . If there is any order, at a new j , $f(\delta_{i,j})$ will be

increased by an amount of $\sum_{i=1}^n (k_i d_i T \delta_{i,j}) - PT$. Hence, the possible values of

Ψ should locate at the time when there is an order placement from any buyer.

In addition, since all the buyers replenish at a regular intervals according to their

own k_i 's, an ordering cycle that the vendor perceives would repeat every

$t_1 = LCM\{k_i\} \cdot T$ unit of time, and the graph of Ψ vs t has a period of t_1 .

Two sample graphs are depicted in Figs. 5.6.1 and 5.6.2.

To determine the location and the value of Ψ , let the time $t_p = (LCM\{k_i\}) \cdot p \cdot T$

denote the end of the p^{th} ordering cycle.

If $\Psi_{t_1+1} \leq 0$, then $\Psi_{t_1+1} \leq \Psi_{t_2+1} \leq \dots$ and subsequent cycles of the graph of

Ψ vs t is lower than or at the same level as the previous one. Hence, the

value of $\Psi = \max\{\max\{\Psi_2, \Psi_3, \dots, \Psi_b\}, 0\}$ would be located within the first

cycle at time $j = 2, 3, \dots, (t_1 + 1)$; otherwise if $\Psi_{t_1+1} > 0$, then $\Psi_{t_1+1} > \Psi_{t_2+1} > \dots$

subsequent cycles is higher than the previous one and the value of Ψ would be

located at the final cycle at time $j = b - t_1 + 1, b - t_1 + 2, \dots, b$.

In section 5.5, the bounds of b is established which shorten the search for Ψ .

The bound $b \leq \lfloor N\alpha + 1 \rfloor$ indicates that less computational effort is required for

lower values of demand-production ratio. This section further demonstrates

that the possible locations of Ψ are either $t = 2, 3, \dots, (t_1 + 1)$ or

$t = b - t_1 + 1, b - t_1 + 2, \dots, b$.

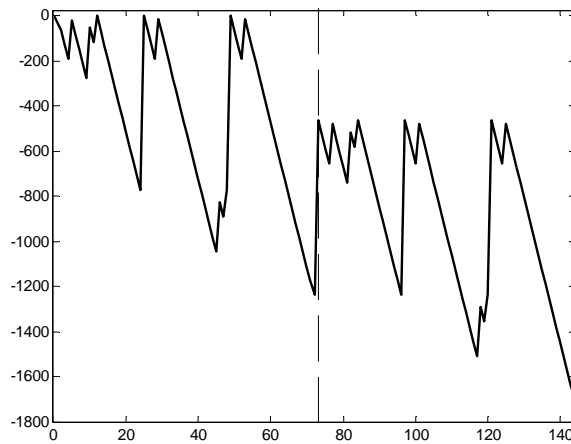


Figure 5.6.1 Plot of Ψ vs. j (2 cycles)

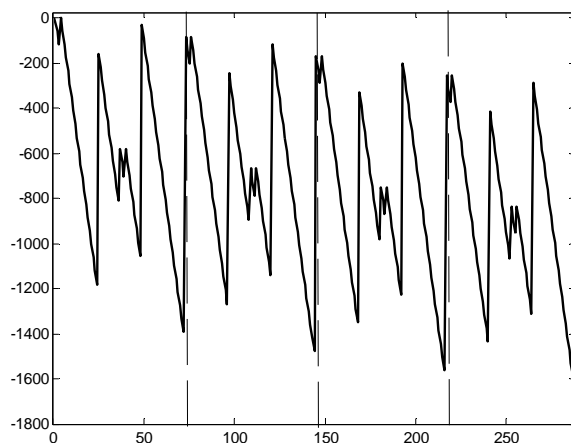


Figure 5.6.2 Plot of Ψ vs. j (4 cycles)

5.7 Difficulties in Obtaining Analytical Solutions

Due to the complexity of the problem, it is very difficult, if not impossible, to find an analytical optimal solution. The major difficulty arises in two-fold: (*i*) the “modular” relationship of N and k_i ; and (*ii*) the high dependency

between the variables $\delta_{i,t}$ and Ψ is also a barrier to finding the optimal replenishment time. To obtain the optimal values of the $\delta_{i,t}$'s the total cost

(3.5.1) can be arranged as

$$\begin{aligned}
 TC^{SCA} = hT \left\{ \frac{1}{N} \sum_{i=1}^n \left\{ k_i d_i \left(\sum_{t=1}^N (t-1) \delta_{i,t} \right) \right\} + \frac{\Psi \alpha}{T} + \alpha \sum_{i=1}^n \delta_{i,1} k_i d_i \right\} \\
 - \frac{NhTD\alpha}{2} + \frac{1}{2} \sum_{i=1}^n h_i d_i k_i T + \left\{ \frac{S_v}{N} + \sum_{i=1}^n \frac{(C_i + A_i)}{k_i} \right\} \frac{1}{T}
 \end{aligned}
 \tag{5.7.1}$$

Given N and k_i 's, optimization of (5.7.1) is the same as the optimization of the first term of (5.7.1) since the other 3 terms are constants. In matrix notation, the problem can be formulated as a 0–1 integer programming:

$$\min_{\delta_{it}} f(\delta_{it}) \quad \text{with } i = 1, 2, \dots, n; t = 1, 2, \dots, N$$

where

$$f(\delta_{it}) = hT \left[\alpha \quad \frac{1}{N} \quad \frac{2}{N} \quad \frac{3}{N} \quad \dots \quad \frac{N-1}{N} \right] \begin{bmatrix} \delta_{11} & \delta_{21} & \dots & \delta_{n1} \\ \delta_{12} & \delta_{22} & \dots & \delta_{n2} \\ \vdots & \vdots & \ddots & \vdots \\ \delta_{1N} & \delta_{2N} & \dots & \delta_{nN} \end{bmatrix} \begin{bmatrix} k_1 d_1 \\ k_2 d_2 \\ \vdots \\ k_n d_n \end{bmatrix} + \alpha h \Psi$$

(5.7.2)

subject to

$$\delta_{it} = \delta_{i(t+k_i)} \tag{5.7.3}$$

$$\delta_{it} \in \{0, 1\}. \tag{5.7.4}$$

From the constraints (5.6.1) and (5.6.2), the solution of Ψ that satisfied both

constraints could be expressed in the following matrix notation:

Denote

$$\mathbf{A} = \begin{bmatrix} 1 & 0 & 0 & \cdots & 0 \\ 1 & 1 & 0 & \cdots & 0 \\ 1 & 1 & 1 & \cdots & 0 \\ \vdots & \vdots & \vdots & \ddots & \vdots \\ 1 & 1 & 1 & \cdots & 1 \end{bmatrix} \begin{bmatrix} \delta_{12} & \delta_{22} & \delta_{32} & \cdots & \delta_{n2} \\ \delta_{13} & \delta_{23} & \delta_{33} & \cdots & \delta_{n3} \\ \delta_{14} & \delta_{24} & \delta_{34} & \cdots & \delta_{n4} \\ \vdots & \vdots & \vdots & \ddots & \vdots \\ \delta_{1b} & \delta_{2b} & \delta_{3b} & \cdots & \delta_{nb} \end{bmatrix} \begin{bmatrix} k_1 d_1 \\ k_2 d_2 \\ k_3 d_3 \\ \vdots \\ k_n d_n \end{bmatrix} - \begin{bmatrix} 1 \\ 2 \\ 3 \\ \vdots \\ b-1 \end{bmatrix} \mathbf{P} \quad (5.7.5)$$

and

the solution of $\Psi = T \cdot \max \{ \max(\mathbf{A}_i), 0 \}$.

To solve the problem analytically, we need to establish optimization methods to

(i) determine Ψ using (5.7.5) by the known δ_{it} 's; and (ii) find optimal solution of $f(\delta_{it})$ by the known N and k_i 's.

5.8 Possible Extensions of the Synchronized Cycles Model

This section modifies the synchronized cycles model by introducing transportation costs of trucks with and without limited capacities. In the synchronized cycles model discussed earlier, the order processing and shipment cost is evaluated on a number-of-order basis. This evaluation perhaps can only take into account those activities such as order processing, loading and unloading of each order. In real-life situations, goods are delivered by trucks and therefore

this actual delivery cost, evaluated on truck basis, has to be reflected in the model.

5.8.1 Single-truck Transportation Scheduling

At the first place, single-truck transportation is considered and no capacity restriction is applied. Let C_{op} be the operating cost (i.e. the hourly wages for the drivers/workers, fuel cost, etc.) for each shipment. For every time t , if there is at least one buyer placing the order, there will be an operation cost. In terms of the model's notation, define indicator variable I_t as follows:

$$I_t = \prod_i (1 - \delta_{i,t}) = \begin{cases} 0 & \text{at least one order from any buyer} \\ 1 & \text{no order from all buyers} \end{cases} \quad (5.8.1.1)$$

From (5.8.1.1), if buyer i orders at time t_1 , then δ_{i,t_1} for buyer i equals 1 and the whole product I_{t_1} equals 0. The value of I_t equals to 1 only if all $\delta_{i,t}$'s equal 0 for all I , which indicates no shipment at time t . Thus as a counting indicator,

$$I_t^c = 1 - I_t = 1 - \prod_i (1 - \delta_{i,t}) = \begin{cases} 0 & \text{no shipment at time } t \\ 1 & \text{shipment at time } t \end{cases} \quad (5.8.1.2)$$

Hence the value of $\sum_{t=1}^N I_t^c$ represents the total number of shipments during the

whole planning horizon. The total system cost becomes:

$$TC_{SHIP}^{SCA01} = TC^{SCA} + \left(\sum_t I_t^c \right) \frac{C_{op}}{NT} \quad (5.8.1.3)$$

where TC^{SCA} is the same total cost function defined in (3.5.1).

5.8.2 Multi-truck Transportation Scheduling with Limited Capacity

5.8 Possible Extensions to the Synchronized Cycles Model

As an extension of sub-section 5.8.1, this sub-section imposes the capacity of a truck in terms of the number of items delivered. The costs of truck deliveries include overhead cost (i.e. maintenance cost). Suppose each truck can be used to deliver orders to any buyer, let C_R be the overhead cost of each truck and L be the maximum capacity of the truck. The parameter C_{op} is, again, denoted as the operating cost for each shipment. In addition, the vendor should determine the number of trucks needed before the production starts. Thus, the trucks are available from time 0 until the end of the planning horizon. For every time t , the expression

$$\sum_i \delta_{i,t} k_i d_i \quad (5.8.2.1)$$

denotes the total number of items to be delivered at time t . Since a truck has a limited capacity, the number of trucks needed for this delivery is

$$U_t = \left\lceil \frac{\sum_i \delta_{i,t} k_i d_i}{L} \right\rceil \quad (5.8.2.2)$$

where $\lceil x \rceil$ denotes the least integer greater than or equal to x . For the whole planning horizon, the number of trucks needed is

$$m = \max_t \{U_t\} \quad (5.8.2.3)$$

and the value of

$$\sum_{t=1}^N U_t \quad (5.8.2.4)$$

represents the total number of separate shipments for the whole planning horizon.

The total system cost becomes:

$$TC_{SHIP}^{SCA02} = TC^{SCA} + \left(\sum_t U_t \right) \frac{C_{op}}{NT} + \frac{mC_R}{NT} \quad (5.8.2.5)$$

5.8.3 Numerical Results and Discussions

The extension in sub-section 5.8.1 tries to minimize the number of shipments needed in addition to the original total system cost; while the extension in sub-section 5.8.2 further tries to “diversify” the orders, in a manner that no extremely large order is placed at any single time t .

For the first extension, a small value of k_i (i.e. $k_i = 1$ or 2) may not be a good choice (depends on the value of C_{op}) as this will increase the number of shipments. In applying the SCA, smaller value of the k_i 's should be avoided.

However, the cut-off point for the elimination of the first few k_i 's is not clear nor easily estimated (except $k_i = 1$). Thus the first few steps of the SCA may not be a good starting point in determining the k_i 's.

For the second extension, in order to “diversify” the orders, different values of k_i 's, or same k_i 's with different values of $\delta_{i,t}$'s are preferable. Again, in applying the SCA, the determination of the k_i 's is still a problem. Further, the improvement sub-algorithm of the SCA is not appropriate for this model. The improvement sub-algorithm starts with the values for all $\delta_{i,1} = 1$ and applies the

5.8 Possible Extensions to the Synchronized Cycles Model

incremental search as follows:

Increment, sequentially for each buyer, t to $t + 1$ for $\delta_{i,t} = 1$ for a total of n new solutions. The best of these n solutions is compared to the best solution of the last increment. If the new solution is better, the procedure will continue; otherwise, the algorithm terminates and take the current best solution as the optimal solution.

By this stopping criteria, the SCA would most likely be terminated at an earlier stage, resulting a large value of m , the number of trucks needed for the deliveries.

As discussed in section 5.7, the optimal values of $\delta_{i,t}$'s cannot easily be analytically determined. Here, additional terms with $\delta_{i,t}$'s have been imposed.

Apparently, there is again no systematic solution procedure to obtain the optimal solution, and therefore meta-heuristic is applied in this research to get the “near-optimal” solution. For the numerical experiments, 11 scenarios are considered (depicted in Table 5.8.3.1). Scenario $P1$ is the original formulation.

$P2$ and $P3$ are the scenarios for the single-truck transportation problem described in sub-section 5.8.1. $P4$ to $P11$ are the scenarios for the multi-truck transportation problem described in sub-section 5.8.2.

5.8 Possible Extensions to the Synchronized Cycles Model

Scenario	C_{op}	C_R	L	Scenario	C_{op}	C_R	L
P1	0	0	∞	P7	150	300	1,500
P2	50	0	∞	P8	50	600	750
P3	150	0	∞	P9	50	600	1,500
P4	50	300	750	P10	150	600	750
P5	50	300	1,500	P11	150	600	1,500
P6	150	300	750				

Table 5.8.3.1 The parameters for the 11 scenarios.

Comparison to the Independent Policy

Under the independent policy, the optimal ordering quantity for each buyer is

$$Q_i = \sqrt{\frac{2A_i d_i}{h_i}} \text{ every } T_i^{IND} = \sqrt{\frac{2A_i}{d_i h_i}} \text{ units of time. For each delivery, } \left\lceil \frac{Q_i}{L} \right\rceil$$

trucks are required. Hence, for each buyer, there are $\frac{d_i}{Q_i} \cdot \left\lceil \frac{Q_i}{L} \right\rceil$ shipments per unit time. The vendor, then, needs a total of $\sum_i \frac{d_i}{Q_i} \cdot \left\lceil \frac{Q_i}{L} \right\rceil$ shipments per unit

time. In practice, if the time between any separate orders is “close”, the vendor

would deliver the orders at the same time (e.g. at the end of each day). In

addition, if a buyer has a replenishment cycle of 0.28 units, it is not common for

the vendor to deliver items to that buyer three times in a unit of time ($t = 0.28T$,

0.56T, and 0.84T).

5.8 Possible Extensions to the Synchronized Cycles Model

In order to make an equivalent comparison, few assumptions are needed for the independent policy to match the situation as in the synchronized cycles model:

- (i) In the independent policy, any separate orders within each time unit, T , are aggregated for deliveries at the end of this time unit. For example, if a buyer has an ordering cycle of 0.28 units (with ordering quantity Q_i for each order), then there will be three orders at time 1 ($t = 0.28T$, $0.56T$, and $0.84T$) i.e. between 0 to T . These three orders will be aggregated together for deliveries at $t = T$.
- (ii) To compare with the synchronized cycles model, the final time $\tilde{N}T$ of the independent policy is required. For the synchronized cycles model, the optimal production schedule is based on the optimization in determining the values of N , k_i 's, $\delta_{i,t}$'s, and Ψ . The total system cost (3.5.1) obtained can be re-interpreted as the average cost per unit time T in producing and delivering a total of NDT units of item in NT units of time. For a comparable situation, set the final time $\tilde{N}T$ of the independent policy as the time the $(NDT)^{\text{th}}$ item is delivered and the total obtained is then averaged over the $\tilde{N}T$ units of time. The total cost obtained for the independent policy can be re-interpreted as the average cost per unit time in producing and delivering a total of NDT

5.8 Possible Extensions to the Synchronized Cycles Model

units of item in $\tilde{N}T$ units of time, the same interpretation of the synchronized cycles model.

According to the above assumptions, the shipment operation cost and the rental and maintenance cost can be formulated.

The number of orders for buyer i at the end of unit time tT , O_{it} , can be expressed as

$$O_{it} = \left\lfloor \frac{t}{T_i^{IND}} \right\rfloor - \left\lfloor \frac{t-1}{T_i^{IND}} \right\rfloor \quad (5.8.3.1)$$

and the total number of items to be delivered to buyer i at the end of unit time tT is

$$\tilde{D}_{it} = O_{it} Q_i. \quad (5.8.3.2)$$

Hence, the total number of items the vendor needs to deliver at time tT is

$$\sum_i \tilde{D}_{it} \quad (5.8.3.3)$$

and the number of trucks needed for this delivery is

$$\tilde{U}_t = \left\lceil \frac{\sum_i \tilde{D}_{it}}{L} \right\rceil \quad (5.8.3.4)$$

To deliver all NDT units of items, the number of trucks needed is

$$\tilde{m} = \max_t \{ \tilde{U}_t \} \quad (5.8.3.5)$$

and the value of

$$\sum_{t=1}^{\tilde{N}} \tilde{U}_t \quad (5.8.3.6)$$

5.8 Possible Extensions to the Synchronized Cycles Model

represents the total number of separate shipments for delivering all *NDT* units of items. The total system cost becomes:

$$TC_{SHIP}^{IND} = TC^{IND} + \left(\sum_{t=1}^{\tilde{N}} \tilde{U}_t \right) \frac{C_{op}}{\tilde{NT}} + \frac{\tilde{m}C_R}{\tilde{NT}} \quad (5.8.3.7)$$

where TC^{IND} is the same total cost function defined in (3.3.5).

Numerical results are depicted in tables 5.8.3.2 – 5.8.3.5 for the 30-buyer (Set 12, 13) and 50-buyer cases (Set 22, 23), respectively. Tables in panel A shows the relevant “optimal” decision variables, i.e. the time needed to produce and deliver *NDT* items (NT and \tilde{NT}), the total number of deliveries throughout the whole planning horizon, the number of trucks required at the beginning of the planning horizon, the average number of shipments per unit time, and the saving on the average shipments of the synchronized cycles model over the independent policy. From the tables, the independent policy requires longer time to complete the production and delivery than the synchronized cycles model ($\tilde{NT} > NT$), but the difference is small (within 1 – 6 units of time). As expected, the total shipments required and the average shipments of the independent policy are higher than the synchronized cycles model. For the independent policy, the buyers make replenishment for the sake of minimizing their own total cost. Hence, the orders may not be synchronized thus resulting in an inevitably increase in the number of shipments. Further, more trucks are required for the independent

5.8 Possible Extensions to the Synchronized Cycles Model

policy. The buyers only order at their desired optimal ordering quantity and disregard the capacity of the truck, as long as they receive the replenishment from the vendor on time. By synchronizing the orders of the buyers, as in the synchronized cycles model, there are substantial savings on the number of shipments. Depicted in the four tables, panel A of tables 5.8.3.2 – 5.8.3.5, the savings can be approximately up to 65% of the shipments for the 30-buyer cases and up to 20% for the 50-buyer cases.

Tables in panel B show the total system costs and the shipment and delivery cost for the two supply chain models. Savings on each of the cost of the synchronized cycles model over the independent policy are also revealed. For scenario P1, the total cost obtained for the independent policy should be the same as depicted in chapter 4 since there is no additional cost imposed. For the synchronized cycles model, the cost might be a bit different from those previously obtained since meta-heuristics (GASA) are re-run for the 4 cases.

The maximum saving on the total system cost is approximately up to 35% for the 30-buyer case and up to 10% for the 50-buyer case. Since the average number of shipments and the number of trucks required are large for the independent policy, there are substantial savings on the shipment and delivery cost for the synchronized cycles model as well. The maximum saving on the shipment and

5.8 Possible Extensions to the Synchronized Cycles Model

delivery cost is approximately up to 65% for the 30-buyer case and up to 20% for the 50-buyer case.

In this section, a more generalized model is developed by imposing the shipment and delivery cost to the supply chain model. There are substantial savings on the shipment and delivery costs by adopting the synchronized cycles model instead of using independent optimization. For the 30-buyer case, even in the scenario that these costs are not imposed (scenario *P1*), the synchronized cycles model still synchronizes the orders of the buyers so that there is no need to carry out any delivery per unit time. Despite the fact that the numerical results are data/parameters dependent, the synchronized cycles model out-performs the independent policy in terms of both shipment scheduling and the total system cost by its “synchronization” characteristic.

5.8 Possible Extensions to the Synchronized Cycles Model

Scenario	Synchronized Cycles Model				Independent Policy				Save on shipments
	NT	total shipments	total trucks	shipment per unit time	$\tilde{N}T$	total shipments	total trucks	shipment per unit time	
P1	90	86	1	0.96	95	94	1	0.99	3.43%
P2	90	54	1	0.60	95	94	1	0.99	39.36%
P3	108	36	1	0.33	112	111	1	0.99	66.37%
P4	96	74	1	0.77	101	105	2	1.04	25.85%
P5	120	66	1	0.55	125	124	1	0.99	44.56%
P6	80	56	1	0.70	84	88	2	1.05	33.18%
P7	126	48	1	0.38	130	129	1	0.99	61.61%
P8	156	119	2	0.76	161	168	2	1.04	26.90%
P9	119	67	1	0.56	125	124	1	0.99	43.24%
P10	84	66	1	0.79	87	91	2	1.05	24.88%
P11	154	76	2	0.49	159	158	1	0.99	50.34%

Table 5.8.3.2A The results obtained for the 11 scenarios for Set 12 (decision variables).

Scenario	Synchronized Cycles Model		Independent Policy		Save (Total Cost)	Save (Ship/Delivery Cost)
	Total Cost	Ship/Delivery Cost	Total Cost	Ship/Delivery Cost		
P1	106.93	0.00	119.95	0.00	10.86%	NA
P2	138.25	30.00	169.43	49.47	18.40%	39.36%
P3	169.38	50.00	268.61	148.66	36.94%	66.37%
P4	155.21	41.67	177.87	57.92	12.74%	28.06%
P5	141.37	30.00	171.95	52.00	17.79%	42.31%
P6	223.00	108.75	284.24	164.29	21.54%	33.80%
P7	192.22	59.52	271.11	151.15	29.10%	60.62%
P8	161.55	45.83	179.58	59.63	10.04%	23.13%
P9	146.83	33.19	174.35	54.40	15.79%	38.98%
P10	243.43	125.00	290.64	170.69	16.24%	26.77%
P11	204.35	81.82	272.78	152.83	25.09%	46.46%

Table 5.8.3.2B The results obtained for the 11 scenarios for Set 12 (cost components).

5.8 Possible Extensions to the Synchronized Cycles Model

Scenario	Synchronized Cycles Model				Independent Policy				Save on shipments
	NT	total shipments	total trucks	shipment per unit time	$\tilde{N}T$	total shipments	total trucks	shipment per unit time	
P1	72	60	1	0.83	74	74	1	1.00	16.67%
P2	72	56	1	0.78	74	74	1	1.00	22.22%
P3	84	66	1	0.79	86	86	1	1.00	21.43%
P4	72	96	2	1.33	74	123	2	1.66	19.78%
P5	60	56	1	0.93	62	62	1	1.00	6.67%
P6	84	105	2	1.25	86	144	2	1.67	25.35%
P7	72	60	1	0.83	74	74	1	1.00	16.67%
P8	84	104	2	1.24	86	144	2	1.67	26.06%
P9	84	70	1	0.83	86	86	1	1.00	16.67%
P10	80	96	2	1.20	82	136	2	1.66	27.65%
P11	80	64	1	0.80	82	82	1	1.00	20.00%

Table 5.8.3.3A The results obtained for the 11 scenarios for Set 13 (decision variables).

Scenario	Synchronized Cycles Model		Independent Policy		Save (Total Cost)	Save (Ship/Delivery Cost)
	Total Cost	Ship/Delivery Cost	Total Cost	Ship/Delivery Cost		
P1	859.96	0.00	917.09	0.00	6.23%	NA
P2	907.48	38.89	967.09	50.00	6.16%	22.22%
P3	997.60	117.86	1076.09	150.00	7.29%	21.43%
P4	944.47	75.00	1008.30	91.22	6.33%	17.78%
P5	912.57	51.67	971.93	54.84	6.11%	5.78%
P6	1074.32	194.64	1175.23	258.14	8.59%	24.60%
P7	994.92	129.17	1071.14	154.05	7.12%	16.15%
P8	940.02	76.19	1014.76	97.67	7.37%	22.00%
P9	910.55	48.81	974.07	56.98	6.52%	14.33%
P10	1068.24	195.00	1180.50	263.41	9.51%	25.97%
P11	995.41	127.50	1074.41	157.32	7.35%	18.95%

Table 5.8.3.3B The results obtained for the 11 scenarios for Set 13 (cost components).

5.8 Possible Extensions to the Synchronized Cycles Model

Scenario	Synchronized Cycles Model				Independent Policy				Save on shipments
	NT	total shipments	total trucks	shipment per unit time	$\tilde{N}T$	total shipments	total trucks	shipment per unit time	
P1	90	90	1	1.00	92	92	1	1.00	0.00%
P2	84	84	1	1.00	86	86	1	1.00	0.00%
P3	60	60	1	1.00	62	62	1	1.00	0.00%
P4	72	129	2	1.79	74	152	3	2.05	12.77%
P5	84	84	1	1.00	86	91	2	1.06	5.49%
P6	84	140	3	1.67	86	176	3	2.05	18.56%
P7	84	84	1	1.00	86	91	2	1.06	5.49%
P8	90	164	2	1.82	92	189	3	2.05	11.30%
P9	60	60	1	1.00	62	67	2	1.08	7.46%
P10	96	159	3	1.66	97	199	3	2.05	19.27%
P11	72	72	1	1.00	74	79	2	1.07	6.33%

Table 5.8.3.4A The results obtained for the 11 scenarios for Set 22 (decision variables).

Scenario	Synchronized Cycles Model		Independent Policy		Save (Total Cost)	Save (Ship/Delivery Cost)
	Total Cost	Ship/Delivery Cost	Total Cost	Ship/Delivery Cost		
P1	1265.74	0.00	1378.36	0.00	8.17%	NA
P2	1317.65	50.00	1428.36	50.00	7.75%	0.00%
P3	1421.85	150.00	1528.36	150.00	6.97%	0.00%
P4	1369.45	97.92	1493.23	114.86	8.29%	14.75%
P5	1325.89	53.57	1438.25	59.88	7.81%	10.54%
P6	1535.32	260.71	1695.81	317.44	9.46%	17.87%
P7	1424.24	153.57	1544.06	165.70	7.76%	7.32%
P8	1378.33	104.44	1500.65	122.28	8.15%	14.59%
P9	1334.70	60.00	1451.75	73.39	8.06%	18.24%
P10	1556.95	267.19	1704.65	326.29	8.66%	18.11%
P11	1428.04	158.33	1554.71	176.35	8.15%	10.22%

Table 5.8.3.4B The results obtained for the 11 scenarios for Set 22 (cost components).

5.8 Possible Extensions to the Synchronized Cycles Model

Scenario	Synchronized Cycles Model				Independent Policy				Save on shipments
	NT	total shipments	total trucks	shipment per unit time	$\tilde{N}T$	total shipments	total trucks	shipment per unit time	
P1	48	48	1	1.00	49	49	1	1.00	0.00%
P2	60	60	1	1.00	62	62	1	1.00	0.00%
P3	60	60	1	1.00	62	62	1	1.00	0.00%
P4	60	229	5	3.82	62	250	6	4.03	5.35%
P5	60	120	2	2.00	62	134	3	2.16	7.46%
P6	64	236	5	3.69	65	265	6	4.08	9.55%
P7	60	114	3	1.90	62	134	3	2.16	12.09%
P8	60	224	5	3.73	62	250	6	4.03	7.41%
P9	60	120	2	2.00	62	134	3	2.16	7.46%
P10	64	228	4	3.56	65	265	6	4.08	12.62%
P11	60	112	2	1.87	62	134	3	2.16	13.63%

Table 5.8.3.5A The results obtained for the 11 scenarios for Set 23 (decision variables).

Scenario	Synchronized Cycles Model		Independent Policy		Save (Total Cost)	Save (Ship/Delivery Cost)
	Total Cost	Ship/Delivery Cost	Total Cost	Ship/Delivery Cost		
P1	1914.31	0.00	2039.66	0.00	6.15%	NA
P2	1966.45	50.00	2089.66	50.00	5.90%	0.00%
P3	2066.44	150.00	2189.66	150.00	5.63%	0.00%
P4	2144.76	215.83	2270.31	230.65	5.53%	6.42%
P5	2088.31	110.00	2162.24	122.58	3.42%	10.26%
P6	2567.86	576.56	2678.89	639.23	4.14%	9.80%
P7	2219.05	300.00	2378.37	338.71	6.70%	11.43%
P8	2155.88	236.67	2299.34	259.68	6.24%	8.86%
P9	2046.66	120.00	2176.76	137.10	5.98%	12.47%
P10	2567.72	571.88	2706.59	666.92	5.13%	14.25%
P11	2293.12	300.00	2392.89	353.23	4.17%	15.07%

Table 5.8.3.5B The results obtained for the 11 scenarios for Set 23 (cost components).

Chapter 6

The Effects of Demand Heterogeneity Among Buyers on the Three Models of Co-ordination in a Single-Vendor-Multi-Buyer Supply Chain

6.1 Introduction

While many of the past researches emphasized on the co-ordination that reduces the total system cost in a supply chain network, in this chapter the effect of the demand heterogeneity among buyers on the total cost of a single-vendor-multi-buyer supply chain system is investigated. The demand heterogeneity includes different values of mean demand, variance and skewness. For the numerical experiments performed in this chapter, the performance on three policies, i.e. the individual optimal policy (classical inventory theory), the common cycle co-ordination policy (Banerjee and Burton, 1994) and the synchronized cycle co-ordination policy (Chan and Kingsman 2005, 2007) are investigated. How the demand heterogeneity would affect the total cost and more importantly, the effect on the performance of the three models are examined.

The main reference for this chapter is Ref. 102.

6.2 The Three Models

The independent policy

The independent policy model is given by

$$TC^{IND} = \sqrt{2SDh(1-\alpha)} + \sum_{i=1}^n \left(\frac{C_i d_i}{Q_i} + \sqrt{2A_i d_i h_i} \right) + h \sum_{i=1}^n Q_i \quad (6.2.1)$$

where

$$Q_i = \sqrt{\frac{2A_i d_i}{h_i}} \quad (6.2.2)$$

is the economic ordering quantity (EOQ) from classical inventory theory.

Substitute Q_i from (6.2.2) into (6.2.1) and rearrange the equation as follows:

$$TC^{IND} = \sqrt{2SDh(1-\alpha)} + \sum_{i=1}^n \left(\sqrt{2A_i h_i} + \sqrt{\frac{C_i^2 h_i}{2A_i}} + h \sqrt{\frac{2A_i}{h_i}} \right) \sqrt{d_i} \quad (6.2.3)$$

Assuming $h_i = h_B$ for all buyers, (6.2.3) becomes

$$TC^{IND} = \sqrt{2SDh(1-\alpha)} + \left(\sqrt{2Ah_B} + \sqrt{\frac{C^2 h_B}{2A}} + h \sqrt{\frac{2A}{h_B}} \right) \sum_{i=1}^n \sqrt{d_i} \quad (6.2.4)$$

Total cost incurred by all buyers is given by

$$TC_B^{IND} = \sqrt{2Ah_B} \sum_{i=1}^n \sqrt{d_i} \quad (6.2.5)$$

and the remaining cost portion

$$TC_v^{IND} = \sqrt{2SDh(1-\alpha)} + \left(\sqrt{\frac{C^2 h_B}{2A}} + h \sqrt{\frac{2A}{h_B}} \right) \sum_{i=1}^n \sqrt{d_i} \quad (6.2.6)$$

is borne by the vendor.

The common cycle co-ordination model

Assuming again $h_i = h_B$ for all buyers, the Banerjee and Burton model is given

by

$$TC^{B\&B} = \sqrt{2 \left[\frac{S}{K} + n(C+A) \right] \left[Dh((2-K)\alpha + K - 1) + h_B \sum_{i=1}^n d_i \right]} \quad (6.2.7)$$

where K is a positive integer that satisfies

$$K(K-1) \leq \frac{S \left[(1/Dh) h_B \sum_{i=1}^n d_i + 2\alpha - 1 \right]}{n(1-\alpha)(C+A)} \leq K(K+1) \quad (6.2.8)$$

The synchronized cycles co-ordination model

For simplicity, we relax the assumption that the ordering cycle, k_i , to be the

factor of N . Assuming again $h_i = h_B$ for all buyers,

$$k_i = \sqrt{\frac{C+A}{\left[h\alpha - \frac{1}{2}(h-h_B) \right] d_i T^2}} \quad (6.2.9)$$

The total cost obtained is

$$TC^{SCA} = \left[\frac{S}{NT} + \left(\frac{hD}{2} (1-\alpha) \right) NT \right] + \left\{ \sum_{i=1}^n \left(\frac{C+A}{k_i T} + d_i \left[h\alpha - \frac{1}{2} (h-h_B) \right] k_i T \right) \right\} \quad (6.2.10)$$

By substituting (9) into (10) and rearranging the terms yields

$$TC^{SCA} = \left[\frac{S}{NT} + \left(\frac{hD}{2} (1-\alpha) \right) NT \right] + \left(2\sqrt{C+A} \sqrt{h\alpha - \frac{1}{2} (h-h_B)} \right) \sum_{i=1}^n \sqrt{d_i} \quad (6.2.11)$$

Total cost of all buyers is given by

$$TC_B^{SCA} = \sum_{i=1}^n \left(\frac{A}{k_i T} + \frac{1}{2} h_B d_i k_i T \right) \quad (6.2.12)$$

and can be rearranged as a linear function of $\sum_{i=1}^n \sqrt{d_i}$. Similarly, the cost incurred by the vendor can also be shown as a linear function of $\sum_{i=1}^n \sqrt{d_i}$.

Compare equations (6.2.4) and (6.2.11), the total costs obtained by the independent policy and the synchronized cycle co-ordination are characterized as

a linear function of $\sum_{i=1}^n \sqrt{d_i}$. Of course, there will be some fluctuations for the

synchronized model when the relaxed constraint is “re-imposed”. However, the

fluctuations do not deteriorate the underlying trend. In addition, as long as we

fix the mean demand, the value of $\sum_{i=1}^n d_i = n\bar{d} = D$ remains unchanged.

Therefore the optimal value of K obtained in (6.2.8) and the total cost in (6.2.7)

do not change as the individual demand changes. This implies that the total

cost of the common cycle policy only depends on the cost parameters. Once the

cost parameters are specified, the total cost remains constant for the common cycle co-ordination model. These relationships are shown in Fig. 6.2.1 (10 buyers) and Fig. 6.2.2 (50 buyers). Both figures plot the total system cost against $\sum_{i=1}^n \sqrt{d_i}$. The crossed line represents the total cost from the independent policy (Eqn (6.2.4)); the horizontal line from the common cycle policy equation (Eqn (6.2.7)); and the dotted line from the synchronized cycles policy (Eqn (6.2.11)). Note that none of the three policies is better than the other two for all values of $\sum_{i=1}^n \sqrt{d_i}$. Consider the function

$$f(d_1, d_2, \dots, d_n) = \sum_{i=1}^n \sqrt{d_i}. \quad (6.2.13)$$

The function attains its maximum when all demands are the same, given that $\sum_{i=1}^n d_i$ is a constant. This implies that any buyer whose demand deviates from the mean demand would reduce the value of $f(d_1, d_2, \dots, d_n)$ from the maximum.

The function $\sqrt{d_i}$ is concave, it can be deduced that, although not linearly, the total cost would decrease as the d_i 's deviate further from the mean demand.

Fig. 6.2.3 and Fig. 6.2.4 depict this relationship. The dotted line and the solid line represent the independent policy and the synchronized cycles co-ordination model respectively. As mentioned, the common cycle does not respond to the “deviation effect”.

In order to eliminate the deviation effect, we equate the sensitivity to $\sum_{i=1}^n \sqrt{d_i}$

for equations (6.2.4) and (6.2.11), i.e.

$$\sqrt{2Ah_B} + \sqrt{\frac{C^2 h_B}{2A}} + h\sqrt{\frac{2A}{h_B}} = 2\sqrt{C+A}\sqrt{h\alpha - \frac{1}{2}(h-h_B)} \quad (6.2.14)$$

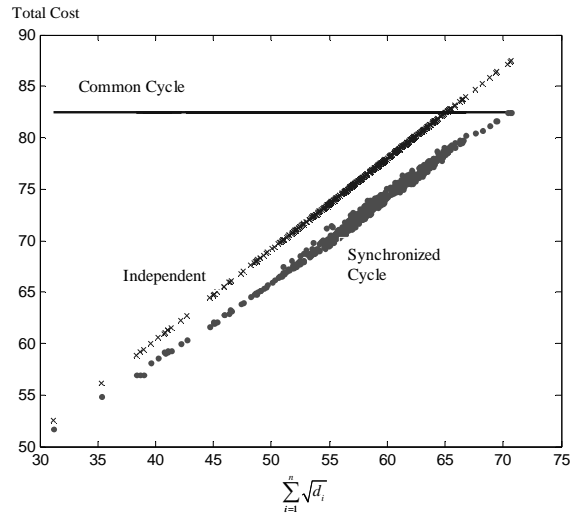


Figure 6.2.1 Total Cost vs. $\sum_{i=1}^n \sqrt{d_i}$ ($n = 10$)

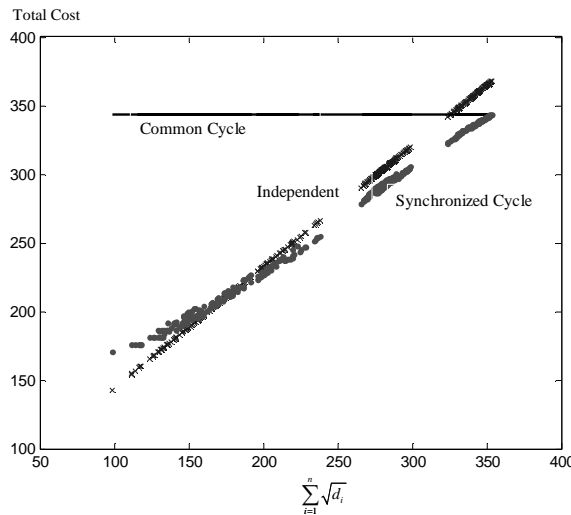


Figure 6.2.2 Total Cost vs. $\sum_{i=1}^n \sqrt{d_i}$ ($n = 50$)

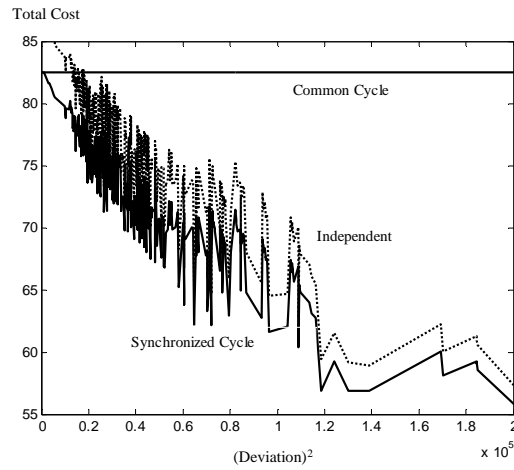


Figure 6.2.3 Total Cost vs. (Deviation)² (n = 10)

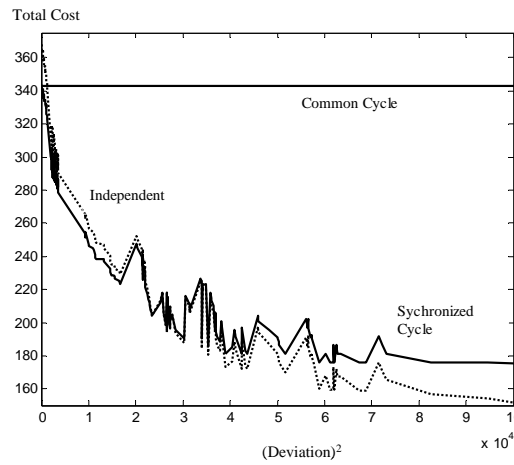


Figure 6.2.4 Total Cost vs. (Deviation)² (n = 50)

Rearrange the terms in (6.2.14) and make α as the subject of the function

$$\alpha = f(A, C, h_B, h) = \frac{1}{h} \left[\frac{1}{8} \frac{(2Ah_B + Ch_B + 2Ah)^2}{(C + A)Ah_B} + \frac{1}{2}(h - h_B) \right]. \quad (6.2.15)$$

Given all the cost parameters, if the vendor could adjust his production rate

according to (6.2.15), then the deviation effect could be somehow eliminated.

However, by further examination, the minimum value of $\alpha = f(A, C, h_B, h)$

occurs at $f(A^*, C^*, h_B^*, h^*) = f\left(A^*, C^*, h_B^*, \left(\frac{C}{2A}\right)h_B^*\right)$ which yields a value of

$\alpha = 1.5$. This violates our assumption of $0 < \alpha < 1$. Moreover, in practice a

rational vendor would not set his production process with rate $\alpha > 1$ since the

production is less than the demand per unit time and stockout is certain to occur.

The deviation effect cannot be eliminated and this motivates the following

investigation: Under what conditions of the demand heterogeneity among

buyers the synchronized cycle co-ordination performs better than the

independent policy?

6.3 Numerical Experiments

Throughout the numerical experiments, instead of using homogeneous buyers

(same cost parameters and demand rate), we use the cost parameters in our

dataset. We are interested in quantifying, or identifying the relationship among

the mean demand, the variance, and the skewness towards the total cost of the

supply chain. A factorial design of experiments is set-up as follows:

Test for the effect of variance

Number of buyers (n): 5 (Set 01), 15 (Set 02), 30 (Set 12), 50 (Set 22)

Mean Demand (\bar{d}): 10, 30, 50, 80

DP Ratio: 0.1, 0.5, 0.9

Test for the effect of skewness

Number of buyers (n): 5 (Set 01), 15 (Set 02), 30 (Set 12), 50 (Set 22)

Mean Demand (\bar{d}): 10, 30, 50, 80

Coefficient of Variance (CV): 0.50, 0.75, 1.00

DP Ratio: 0.5

To test the relationship between the variability and the total cost, 600 sets of data were generated for every combination of n , \bar{d} and DP ratio. There are altogether 48 combinations, i.e. 4 levels of buyer x 4 levels of mean demand x 3 levels of DP Ratio. Similarly, to test the relationship between the skewness and the total cost, 600 sets of data were also generated for every combination of n , \bar{d} and CV. The number of combination is again 48, i.e. 4 levels of buyer x 4 levels of mean demand x 3 levels of CV.

6.4 Results and Discussions

In this section, the effect of the variability on the three models will be investigated first; next, the effect of skewness; and finally a summary of the results are presented in a table.

Figs. 6.4.1 – 6.4.4 depict the relationship of the total cost and the coefficient of variation for 5-buyer, 15-buyer, 30-buyer, and 50-buyer cases with mean demand of 50 and DP Ratio of 0.5. As discussed in section 6.2, the total cost of the common cycle policy is not affected by the variance of the data and thus does not exhibit any upward or downward trends; while the total cost for the independent policy and the synchronized cycles policy tends to decrease as coefficient of variation (CV) increases. Further, the trend of the synchronized cycles policy follows closely to the trend of the independent policy. From the figures, we can see that the common cycle model only works in a very limited case (i.e. Set01 which is illustrated in Banarjee and Burton (1994)). The choice of the cost parameters seems to “make” the common cycle works better than the independent policy in this case. From figure 6.4.1, the independent policy is far worse than the common cycle policy at $CV = 0$ and outperforms the independent policy for a wide range of CV values (i.e. $CV < 2$). Nevertheless, the synchronized cycles policy provides a lower cost than the common cycle

throughout the whole range of CVs. For a wide range of other cost parameters as illustrated in figures 6.4.2 – 6.4.4, the common cycle policy is not appropriate, not even at a low CV. On the other hand, the synchronized cycles model is more competitive than the common cycle policy. The synchronized cycles model is better than the independent model at lower CV. For higher CV ($CV > 3$), the independent policy outperforms the synchronized cycles model. However, a CV larger than 3 is deemed a very extreme case of variation of demands among buyers.

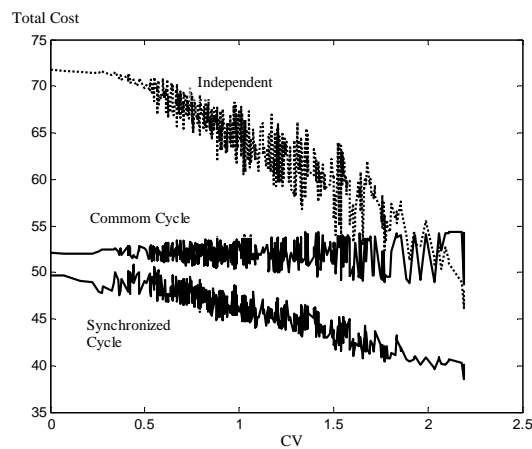


Figure 6.4.1 Total Cost vs. CV (Set 01 DP=0.5)

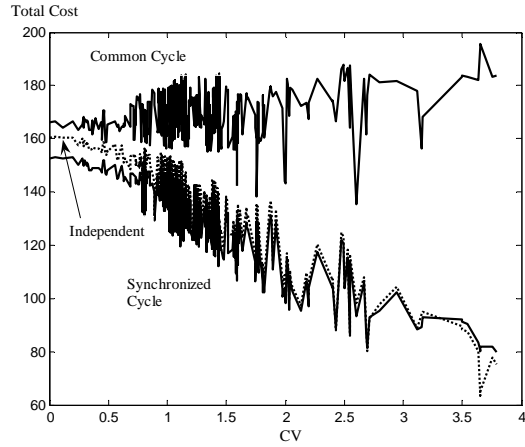


Figure 6.4.2 Total Cost vs. CV (Set 02 DP=0.5)

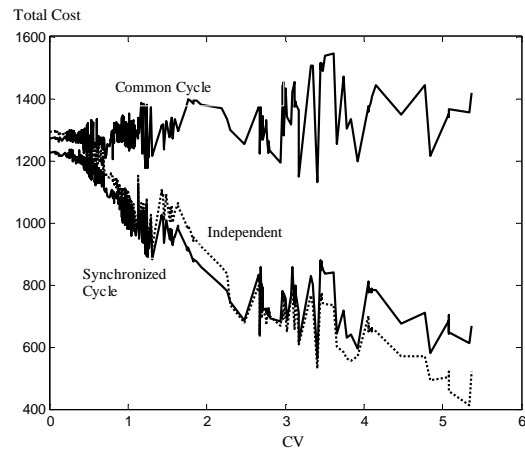


Figure 6.4.3 Total Cost vs. CV (Set 12 DP=0.5)

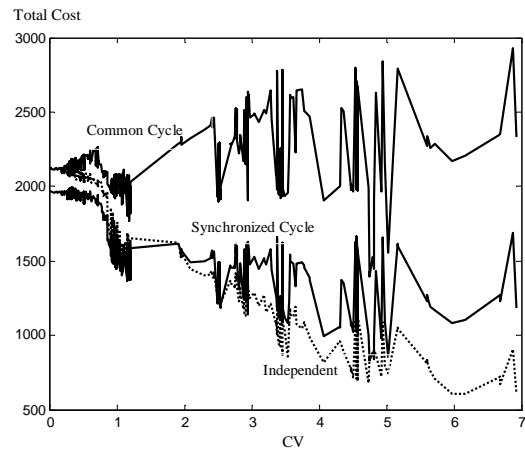


Figure 6.4.4 Total Cost vs. CV (Set 22 DP=0.5)

Fig. 6.4.5 depicts the saving (in %, compared to the independent policy) of the common cycle policy as a function of CV with different levels of mean demand.

Fig. 6.4.6 reveals the same information for the synchronized cycles policy.

These two figures show that: (*i*) A negative relationship prevails between the percentage saved and the CV. (*ii*) The negative relationship becomes stronger for higher mean demand. (*iii*) The common cycle model has a stronger negative relationship than the synchronized cycle model. (*iv*) At the same level of CV, for most of the time the saving is better for lower mean demand than higher mean demand.

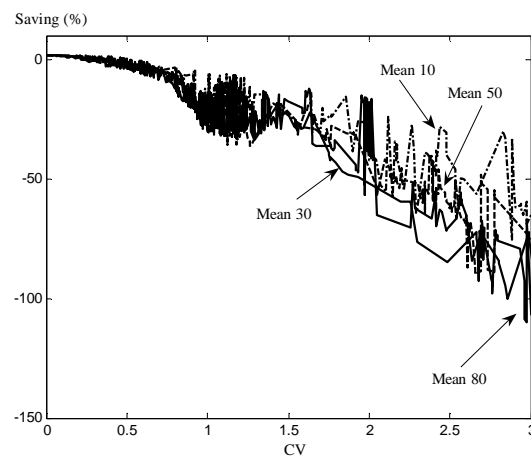


Figure 6.4.5 Saving (in %) vs. CV (Com. Cycle)

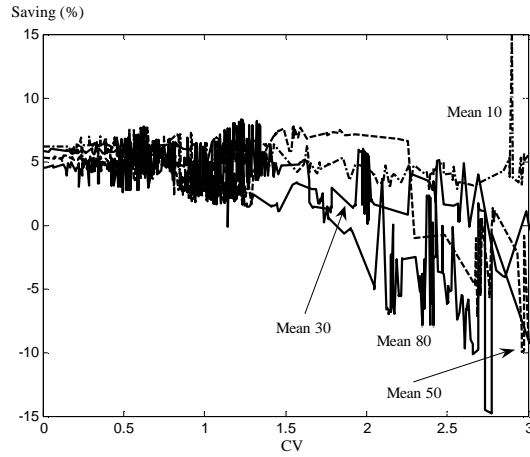


Figure 6.4.6 Saving (in %) vs. CV (Syn. Cycle)

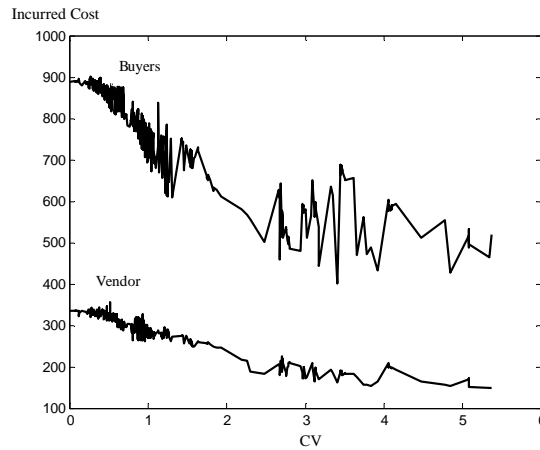


Figure 6.4.7 Buyers and vendor incurred cost as a function of CV

Fig. 6.4.7 shows the buyers' and vendor's costs as a function of the CV for the synchronized cycles model. Both parties show a negative relationship between their cost and CV. This relationship is stronger for the buyers. This implies that if we can look for a way to increase the CV of the buyer's demand, even the vendor controls the delivery scheduling, the buyers should welcome such a

co-ordination system since they benefit more than the vendor does.

Table 6.4.1 shows the correlation between the buyers' cost, the vendor's cost and the total cost and the CV for all three models. For most of the experiments, the relationship has a strong negative correlation for the independent policy and the synchronized cycle policy. The magnitude of the correlation is stronger for the independent policy. As mentioned previously, the common cycle is not quite affected by the variance, thus most of the correlations are of low magnitude. In addition, for the common cycle policy, the effect on the buyers and the vendor are nearly the same. For the independent policy, the relationship on the buyers' cost is slightly higher than the vendor's for any size of the number of buyers involved. For the synchronized cycles policy, the magnitude of the buyers' cost stays sensitive to CV with correlation around $r = 0.7 - 0.9$; for the vendor's, the relationship tends to increase as the number of buyers increases.

6.4 Results and Discussions

Set #	Mean	DP	Independent Policy			Common Cycle			Synchronized Cycle		
			B	V	TC	B	V	TC	B	V	TC
01	10	0.1	-0.794	-0.755	-0.901	0.036	0.038	0.037	-0.771	0.531	-0.637
	30	0.1	-0.754	-0.860	-0.924	-0.105	-0.104	-0.105	-0.768	0.516	-0.724
	50	0.1	-0.728	-0.772	-0.859	-0.059	-0.057	-0.058	-0.747	0.499	-0.633
	80	0.1	-0.735	-0.778	-0.882	0.020	0.022	0.021	-0.769	0.478	-0.595
	10	0.5	-0.751	-0.750	-0.906	-0.013	-0.002	-0.010	-0.800	-0.290	-0.817
	30	0.5	-0.798	-0.777	-0.890	0.034	0.043	0.036	-0.820	-0.252	-0.841
	50	0.5	-0.779	-0.746	-0.871	0.159	0.171	0.162	-0.763	-0.268	-0.839
	80	0.5	-0.770	-0.774	-0.874	0.012	0.022	0.014	-0.782	-0.169	-0.856
	10	0.9	-0.781	-0.798	-0.917	0.023	0.035	0.026	-0.862	-0.517	-0.816
	30	0.9	-0.803	-0.766	-0.892	-0.016	0.000	-0.013	-0.870	-0.561	-0.819
	50	0.9	-0.748	-0.825	-0.891	-0.288	-0.275	-0.285	-0.829	-0.564	-0.803
	80	0.9	-0.711	-0.838	-0.905	-0.121	-0.107	-0.119	-0.803	-0.669	-0.830
02	10	0.1	-0.775	-0.785	-0.817	0.051	0.081	0.053	-0.777	-0.105	-0.789
	30	0.1	-0.721	-0.753	-0.773	0.118	0.121	0.118	-0.714	-0.408	-0.735
	50	0.1	-0.852	-0.846	-0.879	0.217	0.264	0.220	-0.855	-0.160	-0.861
	80	0.1	-0.732	-0.833	-0.783	0.258	0.296	0.260	-0.747	0.042	-0.742
	10	0.5	-0.710	-0.783	-0.756	0.281	0.285	0.282	-0.719	-0.252	-0.732
	30	0.5	-0.749	-0.810	-0.792	0.242	0.277	0.243	-0.751	-0.653	-0.773
	50	0.5	-0.824	-0.812	-0.847	0.200	0.211	0.200	-0.826	-0.360	-0.836
	80	0.5	-0.594	-0.853	-0.667	0.337	0.340	0.337	-0.630	-0.346	-0.641
	10	0.9	-0.652	-0.760	-0.696	0.123	0.147	0.123	-0.655	-0.160	-0.670
	30	0.9	-0.784	-0.825	-0.828	0.415	0.441	0.415	-0.785	-0.680	-0.809
	50	0.9	-0.830	-0.826	-0.859	0.003	0.046	0.003	-0.837	-0.533	-0.848
	80	0.9	-0.764	-0.896	-0.806	0.156	0.185	0.157	-0.776	-0.641	-0.803

Table 6.4.1 Correlation of the CV and various costs.

6.4 Results and Discussions

Set #	Mean	DP	Independent Policy			Common Cycle			Synchronized Cycle		
			B	V	TC	B	V	TC	B	V	TC
12	10	0.1	-0.816	-0.480	-0.771	0.502	0.505	0.503	-0.793	-0.698	-0.814
	30	0.1	-0.892	-0.650	-0.877	-0.374	-0.375	-0.374	-0.880	-0.774	-0.881
	50	0.1	-0.467	-0.523	-0.529	0.469	0.467	0.469	-0.425	-0.590	-0.502
	80	0.1	-0.904	-0.626	-0.864	-0.018	-0.017	-0.018	-0.903	-0.612	-0.887
	10	0.5	-0.778	-0.741	-0.835	0.087	0.087	0.087	-0.794	-0.736	-0.815
	30	0.5	-0.801	-0.710	-0.810	-0.107	-0.110	-0.108	-0.803	-0.711	-0.808
	50	0.5	-0.930	-0.666	-0.890	-0.410	-0.412	-0.410	-0.910	-0.825	-0.911
	80	0.5	-0.816	-0.770	-0.858	0.107	0.107	0.107	-0.808	-0.815	-0.835
	10	0.9	-0.759	-0.728	-0.825	-0.012	-0.012	-0.012	-0.765	-0.794	-0.806
	30	0.9	-0.863	-0.546	-0.840	-0.092	-0.091	-0.092	-0.859	-0.628	-0.856
	50	0.9	-0.839	-0.564	-0.804	-0.056	-0.055	-0.056	-0.823	-0.728	-0.830
	80	0.9	-0.885	-0.480	-0.804	0.301	0.301	0.301	-0.792	-0.766	-0.810
22	10	0.1	-0.844	-0.678	-0.791	-0.035	-0.038	-0.036	-0.837	-0.635	-0.797
	30	0.1	-0.909	-0.733	-0.845	-0.525	-0.521	-0.524	-0.879	-0.797	-0.859
	50	0.1	-0.876	-0.874	-0.884	-0.340	-0.333	-0.338	-0.820	-0.907	-0.862
	80	0.1	-0.926	-0.886	-0.919	-0.691	-0.691	-0.691	-0.851	-0.933	-0.899
	10	0.5	-0.873	-0.658	-0.797	-0.407	-0.411	-0.408	-0.834	-0.740	-0.822
	30	0.5	-0.888	-0.829	-0.874	-0.437	-0.436	-0.437	-0.885	-0.832	-0.881
	50	0.5	-0.909	-0.763	-0.895	-0.680	-0.680	-0.680	-0.867	-0.902	-0.898
	80	0.5	-0.810	-0.848	-0.842	0.175	0.172	0.174	-0.493	-0.916	-0.715
	10	0.9	-0.826	-0.788	-0.822	-0.121	-0.120	-0.121	-0.812	-0.757	-0.803
	30	0.9	-0.918	-0.901	-0.925	-0.537	-0.537	-0.537	-0.907	-0.914	-0.919
	50	0.9	-0.817	-0.800	-0.828	-0.514	-0.513	-0.513	-0.746	-0.896	-0.812
	80	0.9	-0.752	-0.721	-0.745	-0.219	-0.218	-0.219	-0.545	-0.821	-0.655

Table 6.4.1 (con't.) Correlation of the CV and various cost

Fig. 6.4.8 depicts the total cost (Set22 with mean demand of 50 and DP ratio of 0.5) of the synchronized cycles policy as a function of skewness with different levels of CV (similar relationship for the independent policy). The figure further confirms that as the CV increases the system cost decreases. The figure also shows that for a fixed CV, there is an increasing trend of the total system cost as skewness increases. This positive relationship becomes stronger at higher CV.

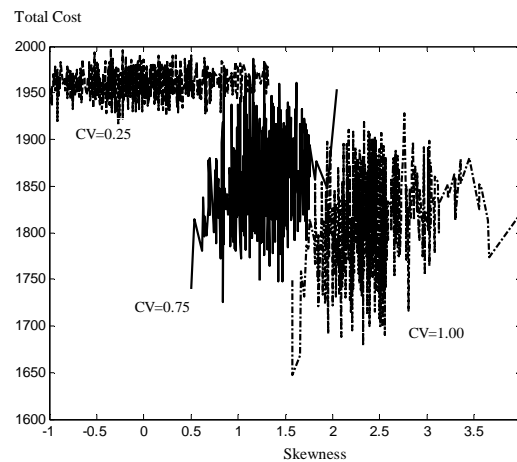


Figure 6.4.8 Total Cost vs. Skewness (Set 22, DP=0.5)

Table 6.4.2 reveals the correlation between the total cost and skewness. Based on the numerical examples, however, the relationship is quite low (around 0.2 – 0.3) between total cost and skewness. For independent policy, this relationship is strong for fewer buyers and then decreases to moderately low as the number of buyers increases. This relationship is also presented for the two co-ordination policies, but the magnitude is very low for the synchronized cycles policy and

6.4 Results and Discussions

Set #	Mean	CV	Independent Policy			Common Cycle			Synchronized Cycle		
			B	V	TC	B	V	TC	B	V	TC
01	10	0.50	0.571	0.336	0.753	-0.278	-0.279	-0.279	0.395	-0.381	-0.235
	10	0.75	0.470	0.496	0.766	0.074	0.071	0.073	0.551	-0.214	0.087
	10	1.00	0.507	0.545	0.740	0.127	0.123	0.126	0.449	-0.109	0.202
	30	0.50	0.590	0.356	0.770	-0.245	-0.246	-0.245	0.448	-0.425	-0.205
	30	0.75	0.506	0.478	0.777	-0.010	-0.012	-0.011	0.473	-0.186	0.098
	30	1.00	0.494	0.571	0.776	0.131	0.128	0.130	0.353	-0.011	0.280
	50	0.50	0.455	0.356	0.746	-0.142	-0.143	-0.142	0.502	-0.340	-0.080
	50	0.75	0.509	0.354	0.692	-0.068	-0.070	-0.069	0.418	-0.164	0.200
	50	1.00	0.511	0.482	0.724	0.038	0.035	0.037	0.250	0.106	0.323
	80	0.50	0.463	0.301	0.707	-0.182	-0.183	-0.183	0.341	-0.209	0.005
	80	0.75	0.449	0.416	0.713	0.015	0.014	0.015	0.521	-0.199	0.255
	80	1.00	0.471	0.547	0.759	0.110	0.106	0.109	0.318	0.025	0.353
02	10	0.50	0.322	0.198	0.348	0.291	0.289	0.291	0.323	0.111	0.341
	10	0.75	0.307	0.205	0.334	0.161	0.148	0.161	0.305	0.121	0.327
	10	1.00	0.306	0.317	0.339	0.116	0.111	0.116	0.302	0.019	0.311
	30	0.50	0.268	0.188	0.293	0.191	0.189	0.191	0.250	0.184	0.281
	30	0.75	0.240	0.273	0.271	0.231	0.213	0.231	0.231	0.128	0.250
	30	1.00	0.198	0.291	0.231	0.139	0.132	0.138	0.214	0.126	0.233
	50	0.50	0.308	0.129	0.330	0.214	0.210	0.214	0.310	0.115	0.324
	50	0.75	0.269	0.258	0.296	0.205	0.188	0.205	0.322	0.007	0.329
	50	1.00	0.184	0.373	0.222	0.073	0.060	0.073	0.153	0.168	0.174
	80	0.50	0.331	0.093	0.351	0.297	0.289	0.297	0.367	0.250	0.402
	80	0.75	0.261	0.272	0.290	0.206	0.196	0.206	0.243	0.106	0.258
	80	1.00	0.301	0.250	0.329	0.090	0.082	0.089	0.285	0.050	0.294

Table 6.4.2 Correlation of skewness and various costs.

6.4 Results and Discussions

Set #	Mean	CV	Independent Policy			Common Cycle			Synchronized Cycle		
			B	V	TC	B	V	TC	B	V	TC
12	10	0.50	0.197	0.060	0.192	0.034	0.035	0.034	0.192	0.131	0.215
	10	0.75	0.163	0.066	0.170	0.000	0.001	0.000	0.164	0.069	0.168
	10	1.00	0.124	0.096	0.162	-0.073	-0.072	-0.073	0.153	0.089	0.162
	30	0.50	0.239	-0.005	0.175	0.000	0.000	0.000	0.192	0.113	0.229
	30	0.75	0.135	0.069	0.156	-0.003	-0.003	-0.003	0.096	0.103	0.129
	30	1.00	0.172	0.016	0.144	-0.086	-0.087	-0.086	0.137	0.056	0.141
	50	0.50	0.173	-0.006	0.129	-0.025	-0.023	-0.025	0.120	0.017	0.119
	50	0.75	0.130	0.050	0.130	-0.032	-0.033	-0.032	0.106	0.059	0.115
	50	1.00	0.158	0.134	0.206	0.018	0.021	0.019	0.172	0.174	0.208
	80	0.50	0.170	0.000	0.134	-0.058	-0.060	-0.058	0.209	-0.083	0.147
	80	0.75	0.154	0.001	0.117	-0.045	-0.043	-0.044	0.155	0.022	0.144
	80	1.00	0.197	0.057	0.187	0.007	0.008	0.007	0.199	0.148	0.221
22	10	0.50	0.194	0.050	0.170	0.091	0.087	0.090	0.134	0.186	0.181
	10	0.75	0.169	0.076	0.168	0.021	0.021	0.021	0.194	0.023	0.166
	10	1.00	0.113	0.040	0.109	0.002	0.003	0.003	0.134	0.031	0.120
	30	0.50	0.285	0.104	0.272	0.115	0.116	0.115	0.161	0.249	0.263
	30	0.75	0.191	0.157	0.232	0.110	0.109	0.109	0.191	0.104	0.204
	30	1.00	0.135	0.151	0.187	0.016	0.014	0.015	0.122	0.097	0.137
	50	0.50	0.270	0.088	0.256	0.084	0.084	0.084	0.255	-0.010	0.222
	50	0.75	0.199	0.075	0.195	0.053	0.054	0.054	0.201	0.078	0.204
	50	1.00	0.264	0.231	0.337	0.028	0.028	0.028	0.230	0.235	0.283
	80	0.50	0.250	0.139	0.270	0.096	0.094	0.096	0.217	0.088	0.251
	80	0.75	0.168	0.027	0.146	0.083	0.083	0.083	0.168	0.055	0.178
	80	1.00	0.160	0.150	0.209	0.008	0.010	0.009	0.099	0.194	0.150

Table 6.4.2 (con't) Correlation of skewness and various costs.

even near zero for the common cycle policy.

Based upon the numerical experiments performed, the results are summarized in Table 6.4.3. The table depicts the relationship of total system cost and in four kinds of measurements: (*i*) number of buyers in the supply chain, the (*ii*) mean (*iii*) coefficient of variance and (*iv*) skewness of the demand among buyers.

In terms of total system cost, all three models have a strong positive relationship with the number of buyers (with mean demand fixed) and the mean demand (with the number of buyers fixed). That means the total cost tends to increase with increasing number of buyers and/or increasing mean demand. This is obvious since additional costs are involved. In addition to the above, numerical experiments of fixing the total demand $n\bar{d} = D$ as depicted in Fig. 6.4.9 are also conducted (For comparison purpose, the cost parameters are the same for all buyers). Results show that the total cost increases as the number of buyers increases (or as the mean demand decreases).

For the independent and synchronized cycles models, a high degree of demand heterogeneity is preferred; while the common cycle policy is unaffected by the measure. Compared to the independent policy, a summary is presented in Table 6.4.4. From the table, the common cycle policy is less worse off if there are relatively more buyers and lower demand heterogeneity. There is no clear

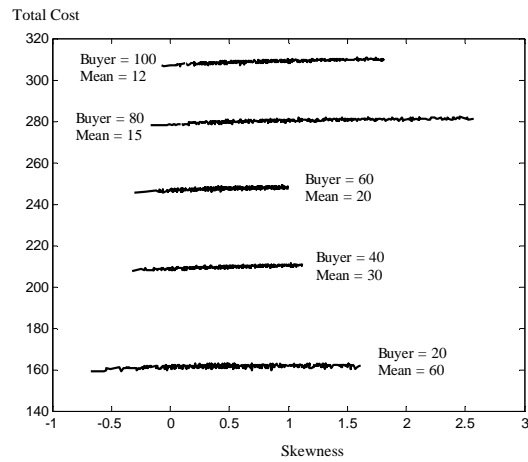


Figure 6.4.9 Total Cost vs. Skewness for fixed total demand

Factor	Policy	Relationship	Remedial Strategy
Number of Buyers	Independent	Strong positive correlation	Decrease
	Common Cycle	Strong positive correlation	Decrease
	Synchronized	Strong positive correlation	Decrease
Mean Demand	Independent	Strong positive correlation	Decrease
	Common Cycle	Strong positive correlation	Decrease
	Synchronized	Strong positive correlation	Decrease
Coef. of Var.	Independent	Strong negative correlation	Increase
	Common Cycle	Weak in magnitude, not clear in direction	Unaffected
	Synchronized	Strong negative correlation	Increase
Skewness	Independent	Weak positive correlation	Unaffected
	Common Cycle	Correlation near zero	Unaffected
	Synchronized	Weak positive correlation	Unaffected

Table 6.4.3 Table of relationships on the total system cost for the three models

implication on the effect of the mean demand, and the skewness of the demand does not affect the performance of the common cycle policy. Compared to the independent policy, the synchronized cycles model is much better off if there are relatively more buyers, lower mean demand, and lower demand heterogeneity. The skewness, again, does not affect the differences between the independent policy and the synchronized cycles policy.

Factor	Policy	Relationship	Remedial Strategy
Number of Buyers	Common Cycle	Strong positive correlation	Increase
	Synchronized	Strong positive correlation	Increase
Mean Demand	Common Cycle	Not clear in both magnitude and direction	??
	Synchronized	Strong negative correlation	Decrease
Coef. of Var.	Common Cycle	Strong negative correlation	Decrease
	Synchronized	Moderate to strong negative correlation	Decrease
Skewness	Common Cycle	Weak positive correlation	Unaffected
	Synchronized	Weak positive correlation	Unaffected

Table 6.4.4 Table of relationships on the saving for the two co-ordination models (compared to the independent policy)

The objective of any co-ordination system is to further reduce the total cost of the whole supply chain. Based upon the above findings, a new co-ordination system by extending the synchronized cycles policy is suggested. Once the vendor knows all the demand faced by every buyer, the vendor may merge (keep the buyers un-noticed) the demand to vary the demand heterogeneity to a desired

pattern. By merging the demand, the coalition of buyers as one “group” of buyers can be considered. The collated group would share the same ordering schedule (same k_i and δ_{it}). This is similar to the common cycle policy. The system will consist of a reduced “groups” of buyers. Within each “group” of buyers, one buyer acts as the major buyer who directly deals with the vendor. The major buyer collects all the other buyers’ demand and this aggregate demand is the only demand that the vendor perceives. Then the vendor would apply the synchronized cycles model to determine an “optimal” delivery schedule. Once the major buyer receives the replenishment from the vendor, the major buyer will transship the desired demand to all other buyers in the group. This co-ordination is an extension of the synchronized cycles model.

PART II:

OPTIMAL CONTROL PROBLEMS

Chapter 7

Literature Review in Optimal Control Theory and Its Applications

7.1 Introduction to Control Theory

Mathematical modeling has been extensively used in many different aspects, like astronomy, chemistry, economics, physics, and logistics. Many of these models concern with minimizing the total expenses/effort, or maximizing total benefits. These models are categorized as optimization problem. When time is involved, the system would change its state as time evolves and is classified as dynamic system. Suppose we manipulate some behavior of a dynamical system through the control of external inputs, this comprises a control problem. The combination of optimization and control is known as optimal control problem.

In traditional calculus, invented by Newton and Leibniz, one would solve the optimization problem by finding the maxima or minima of a particular function, possibly with a set of constraints. A further development of such a

problem gives rise to the maximization or minimization of an integral of another function. Finding a function optimizing a functional is an infinite dimensional problem. This kind of problem is known as the calculus of variation. The development of calculus of variation can be traced back in late 17th century when Johannes Bernoulli posed the brachistochrone problem (Figure 7.1.1). The problem required to find a path, joining two points, so that a bead sliding along the path, under normal gravitational pull travels in minimum time. Bernoulli himself and his brother, Jacob Bernoulli successfully solved the problem (The solution is a cycloid). However, it is Euler and Lagrange who applied the concept of variation to formulate and solve functional optimization problem systematically. The development of control theory, however, comes quite independently initially. For a typical control problem, to describe the dynamics, an extra set of state differential equations is required.

Automatic control has a long history in engineering science and it became acknowledged when, in late 1780s, James Watts developed a speed governor for a steam engine. Following Watts, other control theorists like Maxwell, Liapunov, Nyquist, and Wiener etc. have contributed significantly to the field.

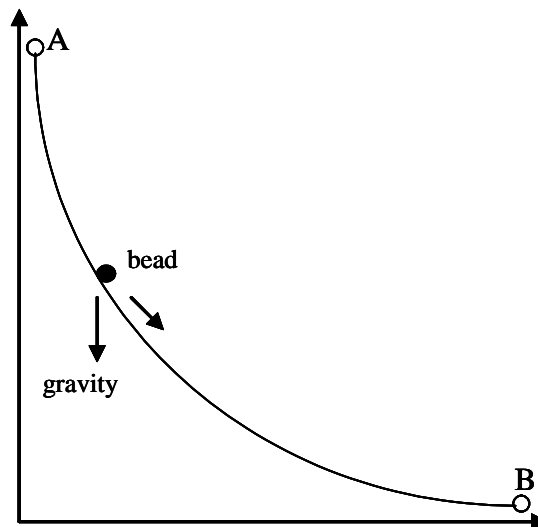


Figure 7.1.1 The brachistochrone problem.

A constructional convention we now termed as feedback control is widely developed among the early researchers. Simply speaking, the concept of feedback control is to use the signal of the difference between the actual output and the desired output (generated from known input) to construct the control to the whole system. A closed-loop control system uses feedback to adjust the input signal by comparing the system's output (control as a function of output). Due to the feedback adjustment, close-loop control system would not be sensitive to external disturbances, any deviation to nominal behavior would be adjusted to reduce system error. In contrast to closed-loop control system, open-loop control system does not involve any feedback action comparing to its input (Figure 7.1.2). External disturbances may cause the actual output to be different from the desired output. Despite the accuracy of the output, open-loop control

system is cheaper to construct since the system does not need a feedback controller. The design of open-loop control very much relies on the assumption that the model is accurate, and all future behaviors are known in advance. Thus, the control is a function of time.

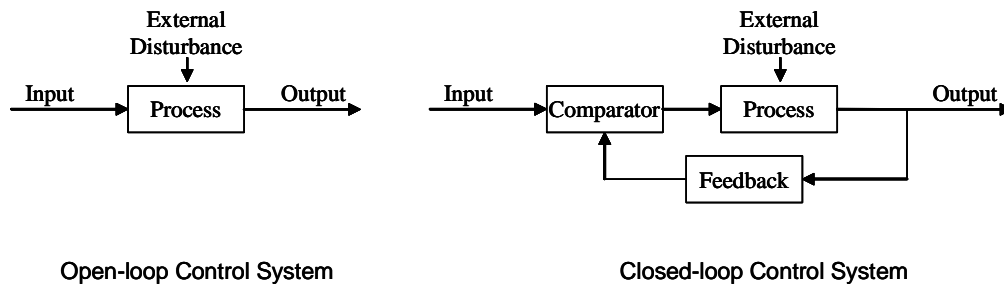


Figure 7.1.2 Open-loop and closed-loop control system.

There are mainly two classes of control theory: classical control theory and modern control theory. Classical control theory uses Laplace transform and the complex plan (s -plane) to describe the control systems. The study of transfer function (impulse response in time domain) facilitates the calculation of the output with a given input (convolution in time domain). Many other classical control theorists developed various methods to analyze the control system. For instances, Nyquist established the stability criterion in 1932; Bode developed frequency response plot in 1938; Ziegler-Nichols enhanced the proportional integral derivative (PID)-tuning in 1942; and Evans developed root-locus method in 1948 (Franklin et al., 1994). Such frequency domain techniques are easy to construct and to analyze, so they form an essential part in control theory in the

1930s. However, the classical control techniques are only best suitable for linear time-invariant single-in-single-out (LTI SISO) systems. To cope with the development of engineering systems, modern control theory emerges. Modern control theory tackles the modeling of multiple-input-multiple-output (MIMO) systems, caters for linear or non-linear, time-invariant or time-variant designs. The early foundation includes Pontryagin's maximum principle in 1956; dynamic programming techniques in 1957 by Bellman; and controllability and observability criteria of a control system developed by Kalman in 1960. Modern control theory uses ordinary differential equations to describe the control system and this is known as the state space design. In the 1960s, modern control theory came into prominence. Related issues can be referred to Leigh (1992), Lewis (1992), Dorf and Bishop (2001), and Ogata (2002).

In the 1950s, the development of aerospace systems and space travel arouse engineers' and mathematicians' attention in modeling such systems by using modern control theory together with a set of differential equations governing the systems. When using modern control techniques, a wide range of mathematical tools are required. For example, multivariate functions, ordinary and partial differential equations, linear algebra, polynomial matrices, and extensive use of set notations. Therefore, a new branch of mathematics is developed - the

optimal control theory. The theory combines engineering and mathematical techniques to tackle dynamical systems. Nowadays, optimal control theory has been applied to a wide variety of areas, such as astronomy, chemistry, economics, logistics, management science, and physics.

Traditionally, optimal control problem is formulated as:

$$J = \Phi_0(x(t_1)) + \int_{t_0}^{t_1} g_0[x(t), u(t)] dt \quad (\text{The cost functional})$$

where $x(t)$ is the state vector and $u(t)$ is the control vector. Φ_0 is a continuously differentiable function and g_0 is continuously differentiable with respect to the state and control and piecewise continuous with respect to t .

The problem is subject to a set of state equations

$$\frac{dx_i(t)}{dt} = f_i[x(t), u(t)] \quad \text{for } i = 1, 2, \dots, n \quad \forall t \in [t_0, t_1]$$

with initial state and target terminal state

$$x(t_0) = x^{(t_0)}, \quad x(t_1) = x^{(t_1)}$$

subject to canonical equality constraints

$$J_i = \Phi_i(x(t_1)) + \int_{t_0}^{t_1} g_i(x(t), u(t)) dt = 0$$

for $i = 1, 2, \dots, N_e \quad \forall t \in [t_0, t_1]$

and canonical inequality constraints

$$J_i = \Phi_i(x(t_1)) + \int_{t_0}^{t_1} g_i(x(t), u(t)) dt \geq 0$$

for $i = N_e + 1, \dots, n \quad \forall t \in [t_0, t_1]$

where

$$u(t) \in \Omega, \forall t \in [t_0, t_1)$$

with Ω denotes the set of admissible controls.

The objective of the problem is to find a control $u^*(t)$, from an admissible control set Ω , that optimizes J from the position $x(t_0) = x^{(t_0)}$ to $x(t_1) = x^{(t_1)}$.

A common problem in optimal control is, like the brachistochrone problem, to bring a system from its initial position $x(0) = x^{(0)}$ to possibly a target position $x^{(t_1)}$ with minimal time or minimum effort.

The mechanism of deriving the solution of the optimal control problem arises in many optimal control textbooks such as Hocking (1991), Teo, Goh and Wong (1991), Craven (1995), and Sethi and Thompson (2000). In addition to the development on optimal control theory, computational method and algorithms have also been developed to solve the optimal control problems, with the aid of the ever emerging computer technologies. In the 1990s, an optimal control software package, MISER3, has been developed by Jennings et al. (1990, 2004) to solve the optimal control problems. MISER3 has been used in solving various kinds of control problems which in different aspects can be found in Teo, Goh and Wong (1991). Moreover, the latest advances in the computational studies of optimal control, namely, the control parametrization as well as the

control parametrization enhancing technique (CPET) have been adopted (Lee et al. 1997). CPET allows the exact computation of the switching times using the control parametrization technique. This technique maps all the switching points of the original problem onto the set of integers, so that the time of the switching points can be exactly determined (up to machine precision). Using CPET the optimal values of the design parameters can be computed with reasonable computational efforts. CPET provides accurate solutions for optimal control problems (Lee et al. 1997, 1998, 1999, 2001a, 2001b, 2001c, 2003, 2004).

7.2 Optimal Control Theory on the Supply Chain

From the very beginning, Tustin (1953) and Elmaghraby (1966) introduced transform techniques and control theory concept in modeling the production inventory systems. Since then, in the 70s, optimal control theory has been rapidly developed to solve the supply chain issue. Midler (1969) formulated a discrete time stochastic control problem with quadratic cost function in a multi-period planning horizon. Schneeweiss (1971) modeled the inventory planning decision by the use of Wiener filtering theory. He set up a continuous linear stochastic inventory model with stationary stochastic demand process and quadratic cost criterion. Lieber (1973) used continuous differential equations,

7.2 Optimal Control Theory on the Supply Chain

with deterministic demand, to formulate the problem over a finite time horizon with linear holding and backlogging cost functions. Lieber established a sufficient condition allowing forecasting error on the actual demand. Gonedes and Lieber (1974) formulated the production planning model for a stochastic demand process. A stochastic programming problem is formulated and solved by deriving the problem to a deterministic equivalent form. In addition, the paper had a discussion on imposing a chance constraint to the model, with parameter $\alpha \in [0,1]$ where $(1-\alpha)$ is the maximum probability of allowing a negative terminal inventory. Bensoussan et al. (1975) considered deterministic and stochastic deterioration rate inventory models. Moreover, Porter and Taylor (1972), Porter and Bradshaw (1974), and Bradshaw and Daintith (1976) studied modal control theory on piecewise constant control policies. These papers and other control theory concepts were discussed in Axsater (1985). Dohi et al. (1995) derived the optimal production schedule in a two-level supply chain with two demand processes, the Ornstein-Uhlenbeck process and the geometric Brownian motion process. Using linear quadratic theory, Aliyu and Andijani (1999) developed an optimal policy for a multi-item inventory model with capacity constraint, with consideration of the large-scale production inventory system. Riddalls and Bennett (2001) studied the batch size effect on demand

7.2 Optimal Control Theory on the Supply Chain

amplification. Riddalls et al. (2002) studied the effects of trust in a multi-level supply chain system. Both Riddalls and Bennett's and Riddalls et al.'s papers examined the conditions of the stability supply chain models with time-delay differential equations. Kogan, Leu, and Perkins (2002) used the maximum principle to model continuous production scheduling problem. They derived algorithms for multiple parallel machines with variable planning horizon. Disney and Towill (2003) and Dejonckheere et al (2003) used control theory to analyze the bullwhip effect. Dejonckheere et al. (2003) used control system engineering approach, transfer function, frequency response plot and spectral analysis to quantify the bullwhip effect caused by the order-up-to policies. In the paper, the authors summarized that, for order-up-to policy, the bullwhip effect is always present. In addition, Dejonckheere et al. derived new general replenishment rules such that the demand amplification can be greatly reduced. Disney and Towill (2003) further confirmed that the use of the vendor management inventory strategy on the supply chain greatly reduced the bullwhip effect compared to the original "serial link" supply chain.

Supply chain systems are classified as dynamical systems which could be analyzed by optimal control theory. Compare to other modeling techniques, the use of optimal control in formulating the production inventory systems is rather

new. Thus, there are many research opportunities for this field of mathematics in the supply chain systems. In many supply chain models, the following basic inventory balance equations, originated by Porter and Taylor (1972), are used:

$$\begin{aligned}\frac{di(t)}{dt} &= p_a(t) - d(t) \\ \frac{dp_a(t)}{dt} &= \alpha(p_d(t) - p_a(t))\end{aligned}\tag{7.2.1}$$

where $i(t)$ and $d(t)$ are the inventory level and the demand respectively, $p_a(t)$ and $p_d(t)$ are the actual production rate and desired production rate respectively, and α is the exponential production lag. To modify the formulation including time-delay, equation (7.2.1) becomes:

$$\begin{aligned}\frac{di(t)}{dt} &= p_a(t-h) - d(t) \\ \frac{dp_a(t)}{dt} &= \alpha(p_d(t) - p_a(t))\end{aligned}\tag{7.2.2}$$

where $p_a(t-h)$ is the production time delay that the production is initiated at h time units before time t . Equations (7.2.1) and (7.2.2) represent a one-level supply chain, whereas to generalize to n -level system, equation (7.2.1) becomes:

$$\begin{aligned}\frac{di_1(t)}{dt} &= p_{a_1}(t) - d_1(t), & \frac{dp_{a_1}(t)}{dt} &= \alpha_1(p_{d_1}(t) - p_{a_1}(t)) \\ \frac{di_2(t)}{dt} &= p_{a_2}(t) - p_{a_1}(t), & \frac{dp_{a_2}(t)}{dt} &= \alpha_2(p_{d_2}(t) - p_{a_2}(t)) \\ & & & \vdots \\ \frac{di_n(t)}{dt} &= p_{a_n}(t) - p_{a_{n-1}}(t), & \frac{dp_{a_n}(t)}{dt} &= \alpha_n(p_{d_n}(t) - p_{a_n}(t))\end{aligned}\tag{7.2.3}$$

where the subscript j of each variable denotes the j^{th} level in the supply chain.

This formulation can be found in Riddalls et al. (2002). Analogous to the

continuous cases, discrete time difference inventory balance equations are also used to model the supply chain as in Tzafestas and Kapsiotis (1994):

$$\begin{aligned}
 i_1(t+1) &= i_1(t) + u_1(t - h_1) - d(t) \\
 i_2(t+1) &= i_2(t) + u_2(t - h_2) - u_1(t) \\
 &\vdots \\
 i_n(t+1) &= i_n(t) + u_n(t - h_n) - u_{n-1}(t)
 \end{aligned}
 \tag{7.2.4}$$

where $i_j(t)$ is the inventory level at the j^{th} level of the supply chain, $d(t)$ is the demand, $u_j(t - h_j)$ is the production at the j^{th} level with h_j units of time delayed.

Most recently, Wong et. al. (2006) further extended the model in Riddalls and Bennett (2001) and Riddalls et al. (2002) to obtain the vendor's optimal production policy. The authors modelled the dynamics of a supply chain as an infinite-horizon time-delayed optimal control problem and solved by the control parametrization method.

7.3 Optimal Control – Other Applications

7.3.1 The Isoperimetric Pillar Problem

The isoperimetric problem is one of the earliest problems that lead to the invention of calculus of variation, the optimization of functionals. The isoperimetric problem stated that, given a fixed length of perimeter, find among all shapes in \mathbb{R}^2 the one that encloses the greatest area. Zenodorus proved, later fine-tuned by Pappus, that given a fixed perimeter the circle enclosed the

largest area (Heath, 1956; Suzuki, 2002). However, the isoperimetric problem had long been posed in 850 B.C. in the legend of Queen Dido of Carthage. Dido was a princess, who fled from Tyrus to North Africa where she requested the North African ruler Jarbas to buy some area of land. Jarbas agreed that she could purchase all the land she could surrounded by the hide of the cow. Dido then cut the cow's hide into many narrow strips, tied them up to form a long ribbon. With this long ribbon, Dido is to encompass the largest area. Facing the isoperimetric problem, Dido enclosed the area with a semicircle, where the diameter was the coast along North Africa. The enclosed area by Dido was then known as Carthage.

However, in the field of applied mathematics, significant progress of the isoperimetric problem had not been made until the late 17th century when Johannes Bernoulli posed the brachistochrone problem. Euler extended the brachistochrone problem in 1734. Instead of minimizing time, Euler minimized the cost functional with respect to other aspects, i.e. in terms of energy in a dynamical system. By extensive work, Euler successfully derived a necessary condition (later known as Euler-Lagrange first necessary condition of calculus of variation) for the extremal that minimizes the cost functional, and he published the results in 1736. In 1744, Euler published a book that generalized his

findings and worked out substantial examples and applications to illustrate the usefulness of his results. Following the work of Euler's, Lagrange applied pure analytical method and developed the concept of "variation" to prove Euler's results, and arrived at the necessary condition that Euler had obtained. In addition, Lagrange developed the transversality conditions to the problems with variable end points and he also extended the problems to higher dimensions. Euler and Lagrange laid down the principles of a new branch of mathematics, officially then known as calculus of variation (Kline, 1972). Since then, calculus of variation becomes the concentrated area by most of the mathematicians in the 19th century: including Poisson, Hamilton, Jacobi, Legendre, and Weierstrass (Kolmogorov and Yushkevich, 1998).

As an extension to Dido's problem, researchers considered the isoperimetric problem in \mathbb{R}^3 : Given a fixed surface area, find the one among all surfaces in \mathbb{R}^3 that forms the greatest volume. In 1884 Schwarz proved that the sphere is the solution to this three-dimensional isoperimetric problem. Recently, there are researchers working on the variation of the isoperimetric problems: Siegel (2002) discussed Dido-type problem posed by Fejes Tóth; Ritoré and Ros (2002) summarized the recent advances related to the isoperimetric problems in \mathbb{R}^3 ; Apostol and Mnatsakanian (2004) studied on the isoparametric problems, which

considered different plane regions having equal perimeters and equal areas.

7.3.2 The Flexible Rotating Beam

Flexible multi-link systems have attracted a great attention in the spacecraft design and robotics literature (Xu and Bainum, 1995; Bainum and Xu, 1995; Yang et al., 2001; Gouliaev and Zavrazhina, 2001) in the past two decades. Rotating flexible beam covered with constrained layer damping treatment is developed recently to minimize structure vibration. Constrained layer damping treatment can be divided mainly into two kinds of treatments: active constrained layer damping (ACLD) and passive constrained layer damping (PCLD) treatments. ACLD treatment is usually a three-layer beam-like structure with a beam as the bottom layer, visco-elastic layer sandwiched in the middle, and covered with a piezo-electric constraining layer on top. Input voltage is applied through the piezo-electric layer for the ACLD treated beam. If there is no voltage applied to the piezo-electric layer, the ACLD beam is simply a PCLD beam. Both active constrained layer damping (ACLD) and passive constrained layer damping (PCLD) treatments have been extensively studied in the past: Baz and Ro (1995) applied optimal control method to obtain optimal parameter values for the active constrained layer damping treatment. Lesieutre and Lee

(1996) and Baz and Ro (2001) applied finite element method to model the flexible rotating beam with active constrained layer damping; Lam et al. (2001) used Golla-Hughes-McTavish method to model the frequency-dependent damping of the vibrating beam; Fasana and Marchesiello (2001) applied Rayleigh-Ritz analysis to the sandwiched beam; Zou et al. (2003) and Fung et al. (2004) derived the PCLD and the ACLD treatment, respectively, by using Lagrangian formulation; Fung and Yau (2004) investigated the vibration behavior of a flexible rotating arm under ACLD treatment; Hau and Fung (2004) studied the effect of different ACLD treatment configurations on the damping behavior of a flexible rotating beam.

7.3.3 The Quarter-Car Suspension Model

Vehicle suspension systems have been a popular issue in road vehicle applications in recent decades. In the past years, many researchers have dedicated effort in the modeling and the design of controlled suspension system (Fruhauf et al., 1985, Sharp and Crola, 1987, Hrovat, 1990, Gordon et al., 1991, Alleyne and Hedrick, 1992, Ali and Storey, 1996, Ando and Suzuki, 1996, Hrovat, 1997, Esmailzadeh and Taghirad, 1998, Ali, 2000, Bouazara and Richard, 2001). Traditionally, most vehicles use the springs and the dampers system

which are passive in nature. Due to the increasing demand on ride-comfortness and better road-handling facilities, semi-active and fully-active computer-controlled systems are developed. Semi-active systems include devices such as air springs and switchable shock absorbers, self-leveling systems, and hydroelastic suspension systems etc. Fully-active systems include an autonomous electronic system that fully control the dynamics and motions of the vehicle.

Although the quarter-car model is much simpler than the full-vehicle model (four-wheel vehicle model), many researchers still worked on the development of the quarter-car model since the quarter-car model can capture most of the basic features and has been proven useful for designing control strategies in the real vehicle problem. Most of the previous formulations implemented linear optimal control theory to tackle the problem (Hac, 1985, Wilson et al., 1986, Frost et al., 1996). However, such a formulation involving only linear system of equation is not realistic, even though analytical solution can be obtained. Hac (1987) introduced an adaptive linear strategy with a quadratic cost function of both the state and the control variables. Gordon et al. (1991) used the adaptive LQG system to study the quarter-car problem. Gordon and Best (1994) further extended the model in Gordon et al. (1991) by imposing various

7.3 Optimal Control – Other Applications

constraints on the model and the introduction of the clipped linear controllers applying to the suspension system. More recently in the quarter-car model literature, Elmadany and Abduljabbar (1999) considered full state feedback system using multivariable integral control, Karlsson et al. (2001) studied the nonlinear suspension with preview, Yoshimura et al. (2001) and Sam et al. (2002) constructed an active system with the concept of sliding mode control, and Parthasarathy and Srinivasa (2006) studied the active suspension system by applying model reference control.

Chapter 8

Optimal Production Schedule Problem with Ornstein Uhlenbeck Demand Process in a Two Level Supply Chain

8.1 Introduction

This chapter models a supply chain system with Ornstein Uhlenbeck demand process. The Ornstein Uhlenbeck process is a mean-reverting process and by its characteristics, this process is appropriate in modeling the demand of most of our commodities. Even if the demand may be affected by short term fluctuations, the demand will revert back to the long-run equilibrium level. Further, the process is simple enough to have the analytical solution derived. This demand process is seldom considered in the field of supply chain management and has not yet been analytically derived using the Pontryagin's maximum principle. In this chapter, we formulate the single-vendor-single-buyer supply chain system. We extend the work of Dohi et al. (1995) by including the idea of information sharing practice. The problem is modeled with a quadratic cost functional and is solved using Pontryagin's maximum principle. In addition, an approximation method is developed for the no coordination situation.

The main reference for this chapter is Ref. 151.

8.2 The Ornstein Uhlenbeck Demand Process

The Ornstein-Uhlenbeck process is a mean-reverting process governed by the equation

$$dX_t = \mu(\hat{X} - X_t)dt + \sigma dW_t \quad (8.2.1)$$

where X_t is the stochastic variable, \hat{X} is the equilibrium level of X_t , μ is the velocity of the process, σ is the diffusion parameter, and $\{W_t : t \geq 0\}$ is a one dimensional Wiener process. The Ornstein-Uhlenbeck process is a stationary process with Gaussian and Markovian properties. Three sample paths of the Ornstein-Uhlenbeck process are illustrated in figure 8.2.1. In figure 8.2.1, all three sample paths start with an initial value of $X_0 = 30$ with velocity $\mu = 5$. The equilibrium level \hat{X} and the diffusion rate σ for paths OU01, OU02 and OU03 are 25, 30, and 35, and 0.5, 1.0, and 2.0 respectively.

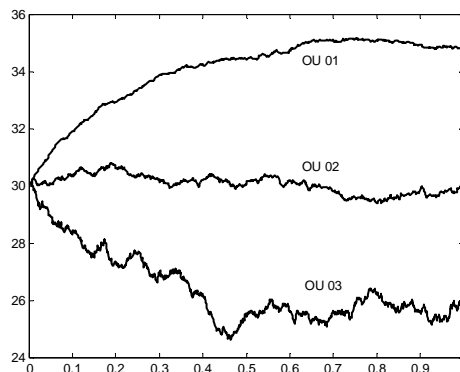


Figure 8.2.1 Sample paths of the Ornstein Uhlenbeck process

8.3 Effect of Information Sharing in a Two-Level Supply Chain

In this section, firstly, we consider the case of co-ordination connection between the two echelons (i.e. with information sharing), such that the upper level has full knowledge regarding the demand pattern and the production schedule faced by the lower level. Secondly, we consider the case of no information sharing situation, whereby the upper echelon needs to estimate its own production schedule based upon the lower echelon's order and such information can only be obtained through previous records. Therefore, the upper level should apply some estimation techniques to predict its future production and inventory levels. An approximation method is developed and by using such method, both the lower and upper echelons optimal production policy can be analytically obtained. In this approximation method, the time horizon is divided into sub-intervals. The demand of the upper level in each sub-interval is approximated by taking the integral average of the past production rate of the lower level over the previous sub-intervals.

8.3.1 Lower Level's Problem

Let $P(t)$, $I(t)$ and $D(t)$ be the rate of production, the inventory level, and the demand rate at time t . Let P^* , I^* , and \hat{D} be the ideal rate of production, ideal inventory level and the saturated demand rate respectively. Let $w(t)$ be a one

8.3 Effect of Information Sharing in a Two-Level Supply Chain

dimensional Wiener process. Let c_p and c_I be the penalty costs deviated away from the ideal values.

The problem of the lower level can be stated as follows:

$$\text{Min } J = \int_0^1 \left[c_p (P - P^*)^2 + c_I (I - I^*)^2 \right] ds \quad (8.3.1.1)$$

such that

$$\dot{I} = P - D \quad (8.3.1.2)$$

$$dD = c_D (\hat{D} - D) dt + \sigma dw(t) \quad (8.3.1.3)$$

where c_D is a constant.

Let

$$x(t) = (I(t), D(t))^T, \quad (8.3.1.4)$$

then

$$dx(t) = Ax(t)dt + BP(t)dt + Cdt + \hat{E}dw(t), \quad (8.3.1.5)$$

where

$$A = \begin{bmatrix} 0 & -1 \\ 0 & -c_D \end{bmatrix}; \quad B = \begin{bmatrix} 1 \\ 0 \end{bmatrix}; \quad C = \begin{bmatrix} 0 \\ c_D \hat{D} \end{bmatrix}; \quad \hat{E} = \begin{bmatrix} 0 \\ \sigma \end{bmatrix}. \quad (8.3.1.6)$$

Let

$$\mu = E \begin{bmatrix} I(t) \\ D(t) \end{bmatrix}, \quad (8.3.1.7)$$

where E denotes the expected value.

Then

8.3 Effect of Information Sharing in a Two-Level Supply Chain

$$\frac{d\mu(t)}{dt} = A\mu(t) + BP(t) + C \quad (8.3.1.8)$$

$$x(t) = e^{At}x(0) + \int_0^t e^{A(t-\tau)}(BP(\tau) + C)d\tau + \int_0^t e^{A(t-\tau)}\hat{E}dw(\tau) \quad (8.3.1.9)$$

Thus

$$\mu(t) = e^{At}x(0) + \int_0^t e^{A(t-\tau)}(BP(\tau) + C)d\tau \quad (8.3.1.10)$$

Let

$$\Psi(t) = E\left[(x(t) - \mu(t))(x(t) - \mu(t))^T\right] \quad (8.3.1.11)$$

Then

$$\begin{aligned} \Psi(t) &= \begin{pmatrix} \Psi_{11}(t) & \Psi_{12}(t) \\ \Psi_{21}(t) & \Psi_{22}(t) \end{pmatrix} \\ &= \begin{pmatrix} E(I(t) - \mu_1)^2 & E[(I(t) - \mu_1)(D(t) - \mu_2)] \\ E[(I(t) - \mu_1)(D(t) - \mu_2)] & E(D(t) - \mu_2)^2 \end{pmatrix} \end{aligned} \quad (8.3.1.12)$$

Moreover

$$\begin{aligned} \Psi(t) &= \int_0^t e^{A(t-\tau)}\hat{E}\theta(\hat{E})^T(e^{A(t-\tau)})^T d\tau \\ &= \int_0^t e^{A(t-\tau)}\begin{pmatrix} 0 & 0 \\ 0 & \sigma^2 \end{pmatrix}(e^{A(t-\tau)})^T \theta d\tau \end{aligned} \quad (8.3.1.13)$$

The expected value of J is

$$\begin{aligned} E(J) &= \int_0^1 c_P(P - P^*)^2 ds + \int_0^1 c_I I^{*2} ds - \\ &\quad \int_0^1 2c_I I^* \mu_1(s) ds + \int_0^1 c_I \mu_1^2(s) ds + \int_0^1 c_I \Psi_{11}(s) ds \end{aligned} \quad (8.3.1.14)$$

To find the optimal production rate, we let

$$H = c_P(P - P^*)^2 - 2c_I I^* \mu_1 + c_I \mu_1^2 + \lambda_1(P - \mu_2) + \lambda_2 c_D(\hat{D} - \mu_2) \quad (8.3.1.15)$$

8.3 Effect of Information Sharing in a Two-Level Supply Chain

By setting $\frac{\partial H}{\partial P} = 0$, we get

$$P = P^* - \frac{\lambda_1}{2c_p}, \quad (8.3.1.16)$$

$$\dot{\lambda}_1 = -\frac{\partial H}{\partial \mu_1} = 2c_I I^* - 2c_I \mu_1 \quad (8.3.1.17)$$

and

$$\ddot{\lambda}_1 = -2c_I \dot{\mu}_1 = -2c_I (P - \mu_2) = \frac{c_I}{c_p} \lambda_1 - 2c_I P^* + 2c_I \mu_2. \quad (8.3.1.18)$$

Together with the initial and boundary conditions

$$\mu_1(0) = I(0); \quad (8.3.1.19)$$

$$\mu_2(0) = D(0); \quad (8.3.1.20)$$

$$\dot{\lambda}_1(0) = 2c_I (I^* - I(0)); \quad (8.3.1.21)$$

$$\lambda_1(1) = 0. \quad (8.3.1.22)$$

We obtain

$$\lambda_1(t) = A_1 e^{\left(\sqrt{\frac{c_I}{c_p}}\right)t} + A_2 e^{-\left(\sqrt{\frac{c_I}{c_p}}\right)t} + \frac{2c_I (D(0) - \hat{D})}{c_D^2 - (c_I / c_p)} e^{-c_D t} + 2c_p (P^* - \hat{D}) \quad (8.3.1.23)$$

and

$$P(t) = A_3 e^{\left(\sqrt{\frac{c_I}{c_p}}\right)t} + A_4 e^{-\left(\sqrt{\frac{c_I}{c_p}}\right)t} + A_5 e^{-c_D t} + \hat{D} \quad (8.3.1.24)$$

where the A_i s are constants which can be easily determined.

8.3.2 Higher Level's Problem (with full information)

Let $\hat{P}(t)$ and $\hat{I}(t)$ be the rate of production and the inventory level at any time t .

8.3 Effect of Information Sharing in a Two-Level Supply Chain

Let $\hat{P}^*(t)$ and $\hat{I}^*(t)$ be the ideal production rate and ideal inventory level. The problem of the higher level's problem can be stated as

$$J = \int_0^1 \left[\hat{c}_p (\hat{P} - \hat{P}^*)^2 + \hat{c}_I (\hat{I} - \hat{I}^*)^2 \right] dt \quad (8.3.2.1)$$

such that

$$\dot{\hat{I}} = \hat{P} - P, \quad (8.3.2.2)$$

where P is the optimal production rate of the lower level.

To find the optimal production rate, we set

$$H = \hat{c}_p (\hat{P} - \hat{P}^*)^2 + \hat{c}_I (\hat{I} - \hat{I}^*)^2 + \lambda (\hat{P} - P) \quad (8.3.2.3)$$

By setting $\frac{\partial H}{\partial \hat{P}} = 0$, we get

$$\hat{P} = \hat{P}^* - \frac{\lambda}{2\hat{c}_p}, \quad (8.3.2.4)$$

where

$$\dot{\lambda} = -\frac{\partial H}{\partial \hat{I}} = 2\hat{c}_I (\hat{I}^* - \hat{I}) \quad (8.3.2.5)$$

By using (8.3.2.5), (8.3.2.2), (8.3.2.4) and (8.3.1.24), we get

$$\begin{aligned} \ddot{\lambda} &= 2\hat{c}_I \left(P - \hat{P}^* + \frac{\lambda}{2\hat{c}_p} \right) \\ &= 2\hat{c}_I \left(A_3 e^{\left(\sqrt{\frac{c_I}{c_p}}\right)t} + A_4 e^{-\left(\sqrt{\frac{c_I}{c_p}}\right)t} + A_5 e^{-c_D t} + \hat{D} - \hat{P}^* + \frac{\lambda}{2\hat{c}_p} \right) \end{aligned} \quad (8.3.2.6)$$

$$\dot{\lambda}(0) = 2\hat{c}_I (\hat{I}^* - \hat{I}(0)) \quad (8.3.2.7)$$

$$\lambda(1) = 0 \quad (8.3.2.8)$$

By solving (8.3.2.6) – (8.3.2.8), we get $\lambda(t)$. The optimal production $\hat{P}(t)$

which can be obtained from (8.3.2.4) has the form

$$\hat{P}(t) = B_1 e^{\left(\sqrt{\frac{c_I}{c_P}}\right)t} + B_2 e^{-\left(\sqrt{\frac{c_I}{c_P}}\right)t} + B_3 e^{\left(\sqrt{\frac{\hat{c}_I}{\hat{c}_P}}\right)t} + B_4 e^{-\left(\sqrt{\frac{\hat{c}_I}{\hat{c}_P}}\right)t} + B_5 e^{-c_D t} + B_6. \quad (8.3.2.9)$$

8.3.3 The Approximation Procedure

In this sub-section, we consider the higher level's problem without information sharing practice. Same as before, the optimal production rate of the lower level has the form

$$P(t) = A_3 e^{\left(\sqrt{\frac{c_I}{c_P}}\right)t} + A_4 e^{-\left(\sqrt{\frac{c_I}{c_P}}\right)t} + A_5 e^{-c_D t} + \hat{D} \quad (8.3.3.1)$$

However, the higher level does not know what $P(t)$ is, except for the past values.

Let $uint(1), uint(2), \dots, uint(10)$ be the estimated value of $P(t)$ from one knot point to another. More precisely,

$$\begin{aligned} uint(1) &= P(0) \\ uint(2) &= \frac{1}{0.1} \int_0^{0.1} P(t) dt, \\ uint(3) &= \frac{1}{0.1} \int_{0.1}^{0.2} P(t) dt, \\ &\vdots \\ uint(10) &= \frac{1}{0.1} \int_{0.8}^{0.9} P(t) dt. \end{aligned} \quad (8.3.3.2)$$

Thus,

8.3 Effect of Information Sharing in a Two-Level Supply Chain

$$uint(1) = A_3 + A_4 + A_5 + \hat{D} \quad \text{and} \quad (8.3.3.3)$$

$$uint(i) = \frac{1}{0.1} \left[A_3 \sqrt{\frac{c_P}{c_I}} \left(e^{\sqrt{\frac{c_I}{c_P}}(0.1)(i-1)} - e^{\sqrt{\frac{c_I}{c_P}}(0.1)(i-2)} \right) - \right. \\ \left. A_4 \sqrt{\frac{c_P}{c_I}} \left(e^{-\sqrt{\frac{c_I}{c_P}}(0.1)(i-1)} - e^{-\sqrt{\frac{c_I}{c_P}}(0.1)(i-2)} \right) \right] - \\ \frac{1}{0.1} \frac{A_5}{c_D} \left[\left(e^{-c_D(0.1)(i-1)} - e^{-c_D(0.1)(i-2)} \right) \right] + \hat{D} \quad (8.3.3.4)$$

for $i = 2, 3, \dots, 10$.

Thus, the higher level solves the problem 10 times.

$$\text{Min} \int_{0.1(i-1)}^{0.1(i)} \left[\hat{c}_P \left(\hat{P} - \hat{P}^* \right)^2 + \hat{c}_I \left(I_E - \hat{I}^* \right)^2 \right] dt \quad (8.3.3.5)$$

such that

$$\hat{I}_E = \hat{P}^i(t) - uint(i) \quad \text{for } i = 1, 2, \dots, 10. \quad (8.3.3.6)$$

where \hat{I}_E is the estimated value of the inventory level of the higher level at time t .

(The true value of the inventory is given by $\hat{I}_T = \hat{P}^i(t) - P(t)$.)

However, due to the fact that $P(t)$ is not available to the higher level except the

past values, the higher level can only estimate its future inventory level. Same

as before, the optimal production rate is

$$\hat{P}^i(t) = \hat{P}^* - \frac{\hat{\lambda}^i(t)}{2\hat{c}_P}, \quad t \in (0.1(i-1), 0.1i] \quad (8.3.3.7)$$

where

$$\hat{\lambda}^i(t) = 2\hat{c}_I \left(\hat{I}^* - I_E \right), \quad t \in (0.1(i-1), 0.1i] \quad (8.3.3.8)$$

Thus,

$$\ddot{\hat{\lambda}}^i(t) = 2\hat{c}_l \left(uint(i) - \hat{P}^* + \frac{\hat{\lambda}^i}{2\hat{c}_p} \right) \quad (8.3.3.9)$$

$$\dot{\hat{\lambda}}^i(0.1(i-1)) = 2\hat{c}_l \left(\hat{I}^* - \hat{I}_T((0.1)(i-1)) \right) \quad (8.3.3.10)$$

$$\hat{\lambda}^i(0.1i) = 0, \quad (8.3.3.11)$$

where $\hat{\lambda}^i$ denotes the i^{th} co-state.

Note that at $t = 0.1(i-1)$, $\hat{I}_T(0.1(i-1))$, the true inventory level at time $0.1(i-1)$, can be observed by the higher level. Thus, the higher level can solve the system (8.3.3.9) – (8.3.3.11).

The method of finding the optimal production rate of the upper level by the approximated method without knowing $\hat{I}_T(0.1(i-1))$ explicitly can be stated as follow:

Let

$$\hat{\lambda}_{\text{homo}}^i = K_i e^{\left(\sqrt{\frac{\hat{c}_l}{\hat{c}_p}}\right)t} + L_i e^{-\left(\sqrt{\frac{\hat{c}_l}{\hat{c}_p}}\right)t} \quad (8.3.3.12)$$

$$\hat{\lambda}_{\text{part}}^i = 2\hat{c}_p \left[\hat{P}^* - uint(i) \right] \quad (8.3.3.13)$$

be the homogeneous and particular solution of $\hat{\lambda}^i$. To get K_i and L_i , we use (8.3.3.10) and (8.3.3.11). That is,

$$K_i e^{\sqrt{\frac{\hat{c}_l}{\hat{c}_p}}(0.1)(i-1)} - L_i e^{-\sqrt{\frac{\hat{c}_l}{\hat{c}_p}}(0.1)(i-1)} = 2\hat{c}_l \left(\hat{I}^* - \hat{I}_T((0.1)(i-1)) \right) \sqrt{\frac{\hat{c}_p}{\hat{c}_l}} \quad (8.3.3.14)$$

$$K_i e^{\sqrt{\frac{\hat{c}_l}{\hat{c}_p}}(0.1i)} + L_i e^{-\sqrt{\frac{\hat{c}_l}{\hat{c}_p}}(0.1i)} = 2\hat{c}_p \left(uint(i) - \hat{P}^* \right) \quad (8.3.3.15)$$

8.3 Effect of Information Sharing in a Two-Level Supply Chain

Now, to solve the above system, we need to find $\hat{I}_T((0.1)(i-1))$. For $i = 1$, $\hat{I}_T((0.1)(i-1)) = \hat{I}(0)$, which is given. Thus we can find K_1 and L_1 by solving (8.3.3.14) and (8.3.3.15) simultaneously. Hence, $\hat{\lambda}^1(t)$ can be found from (8.3.3.12) and (8.3.3.13). Thus $\hat{P}^1(t)$ can be found from (8.3.3.7). By solving

$$\dot{\hat{I}}_T = \hat{P}^1(t) - P(t) \quad (8.3.3.16)$$

$$\hat{I}_T(0) = \hat{I}(0) \quad (8.3.3.17)$$

and using (8.3.3.1), we can find $\hat{I}_T(0.1)$. Hence with $\hat{I}_T(0.1)$ known, we are able to determine $\hat{\lambda}^2(t)$, $\hat{\lambda}^3(t)$, ..., $\hat{\lambda}^{10}(t)$ recursively. Hence $\hat{P}^i(t)$ can be found for all $i = 1, 2, \dots, 10$.

8.4 Vendor Managed Inventory (VMI) Co-ordination

In section 8.3, the buyer chooses the production/ordering schedule that minimizes the total cost; while the vendor minimizes his own based upon the decision made by the buyer. However, even with information sharing, this may not be beneficiary to the supply chain as a whole. Researchers such as Banerjee and Banerjee (1992) examined a better coordination through an introduction of the electronic data interchange (EDI) technology. They considered an EDI-based vendor-managed inventory (VMI) system. All related information

and activities (i.e. demand history, shipping schedule, payment invoice, etc.) can be shared through the synchronized database. The use of EDI facilitates a more accurate demand forecast and a better relationship between echelons in the supply chain. Under VMI, the vendor would have a full knowledge on the demand pattern and the vendor can use the information to design a better production strategy that minimizes the cost incurred for the whole supply chain system. The vendor would be responsible for the replenishment ordering process.

In our model, the VMI coordination can be formulated as follows:

$$\text{Min } J = \int_0^1 \left[c_p (P - P^*)^2 + c_I (I - I^*)^2 + \hat{c}_p (\hat{P} - \hat{P}^*)^2 + \hat{c}_I (\hat{I} - \hat{I}^*)^2 \right] ds \quad (8.4.1)$$

subject to

$$\dot{I} = P - D \quad (8.4.2)$$

$$\dot{\hat{I}} = \hat{P} - P \quad (8.4.3)$$

8.5 Numerical Results and Discussions

Four numerical examples are included and the cost parameters are tabulated in table 8.5.1. The solutions for the VMI coordination are obtained by the aid of

MISER3; while the solutions for the Non-VMI are obtained from the analytical solutions in section 8.3.

Set	Lower Level				Upper Level				Demand		Initial Conditions		
	c_P	c_I	P^*	I^*	\hat{c}_P	\hat{c}_I	\hat{P}^*	\hat{I}^*	c_D	\hat{D}	$I(0)$	$\hat{I}(0)$	$D(0)$
01	10	10	30	30	20	10	30	30	5	35	25	25	25
02	10	10	30	20	20	10	30	20	5	35	25	25	25
03	10	10	30	30	20	10	30	30	5	35	35	35	30
04	10	10	50	35	20	10	50	40	10	45	35	35	30

Table 8.5.1 Cost parameters for the four numerical examples.

Tables 8.5.2 shows the cost borne by the lower level under the Non-VMI and VMI models. For non-VMI models, the cost borne by the lower level is the same for both with and without information sharing. For all 4 datasets, the lower level is worse off under the VMI scheme. This result confirms with previous research findings that the upper level would transfer a portion of his cost to the lower level. Table 8.5.3 shows the cost incurred by the upper level. With information sharing, the upper level can save about 15% – 17% for the first 3 datasets and save 30% for dataset 4. With VMI coordination, the upper level can save an additional of 20% – 30%. Table 8.5.4 depicts similar information for the total system cost. The lower level should realize that it does not worth to share the demand information to the upper level since such sharing only benefits the upper level. Therefore, some kinds of price-discount schemes are

necessary for the upper level in order to entice the lower level to share its demand information, as well as the cost parameters for the VMI coordination. Figures 8.5.1 – 8.5.4 demonstrate the optimal trajectory for the upper level’s production, lower level’s production, upper level’s inventory, and lower level’s inventory respectively.

Set	Non VMI	VMI	% Saved
01	265.12	314.08	-18.47%
02	147.54	185.90	-26.01%
03	105.39	141.43	-34.20%
04	125.64	140.63	-11.93%

Table 8.5.2 Cost borne by the lower level obtained for the four numerical examples.

Set	Non VMI		% Saved (w/ sharing)	VMI	% Saved (vs. VMI)	
	No Sharing	With Sharing			No Sharing	With Sharing
01	419.63	346.62	17.40%	250.84	40.22%	27.63%
02	368.57	311.52	15.48%	208.14	43.53%	33.19%
03	328.73	282.47	14.07%	194.29	40.90%	31.22%
04	190.34	133.76	29.72%	103.44	45.65%	22.67%

Table 8.5.3 Cost borne by the upper level obtained for the four numerical examples.

Set	Non VMI		% Saved (w/ sharing)	VMI	% Saved (vs. VMI)	
	No Sharing	With Sharing			No Sharing	With Sharing
01	684.76	611.74	10.66%	564.93	17.50%	7.65%
02	516.11	459.05	11.06%	394.04	23.65%	14.16%
03	434.11	387.86	10.66%	335.72	22.67%	13.44%
04	315.97	259.40	17.90%	244.08	22.75%	5.91%

Table 8.5.4 Total Cost obtained for the four numerical examples.

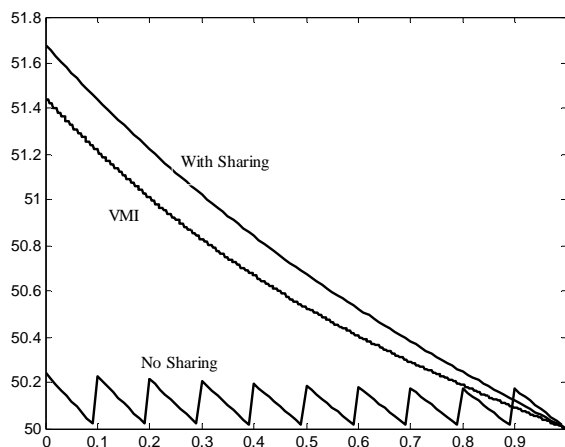


Figure 8.5.1 Optimal Trajectory – Upper level's production (set 04)

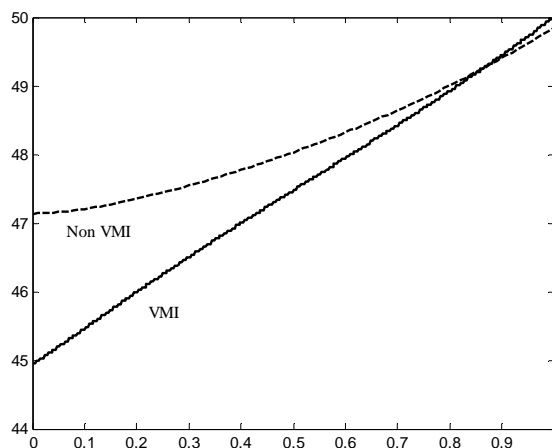


Figure 8.5.2 Optimal Trajectory – Lower level's production (set 04)

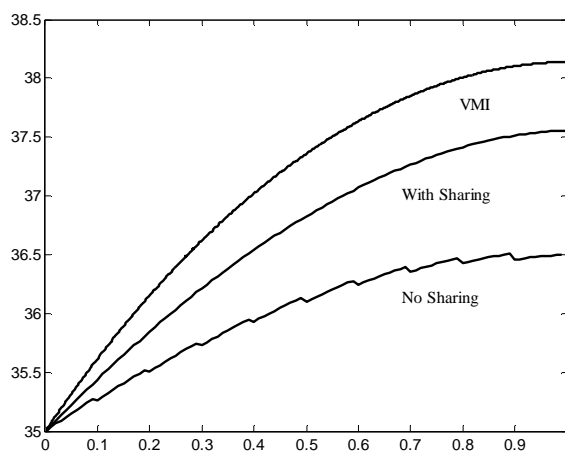


Figure 8.5.3 Optimal Trajectory – Upper level's inventory (set 04)

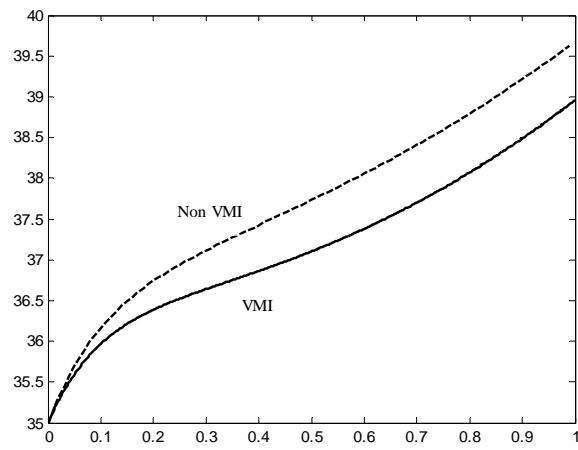


Figure 8.5.4 Optimal Trajectory – Lower level's inventory (set 04)

Chapter 9

The Isoperimetric Pillar Problem

9.1 Introduction

In this chapter, an extension to the isoperimetric problem is considered. The problem is to find an enclosed cross-sectional/base region of a pillar defined by a simple closed curve of fixed perimeter, such that the volume of the pillar, bounded above by a given surface, is maximized. The problem is posed as an optimal control problem and solved by MISER3. Solutions to single pillar and multiple pillars cases are considered. The results to the isoperimetric pillar problem provide useful information in the optimal shape of pillar building in construction design.

The main reference for this chapter is Ref. 100.

9.2 The Isoperimetric Problem

The isoperimetric problem is commonly stated as follows:

Among all bounded region in \mathbb{R}^2 with fixed perimeter P ,
determine the shape of the region bounded by a simple
closed curve such that the enclosed area is the greatest.

Equivalently, the problem can be stated as its dual as:

Among all region bounded by a simple closed curve
with fixed area A , determine the shape of the region
that required the least perimeter.

The problem was first considered by Steiner in 1838, who showed that if a solution exists, the shape should be convex and symmetric. Among all regions, the circle is the only shape that is perfectly convex and symmetrical. Mathematically, the problem can be expressed as an inequality well known as the isoperimetric inequality,

$$4\pi A \leq P^2, \quad (9.2.1)$$

with equality if the region is a circle. Several proofs have been attempted are some are presented in Treibergs (2002).

More formally, the isoperimetric inequality is expressed as:

Denote $\Omega \subset \mathbb{R}^2$ be a compact domain with piecewise C^1 boundary, and let $A(\Omega)$ be the area of Ω and $L(\partial\Omega)$ be the length (perimeter) of the boundary of Ω , then

$$4\pi A(\Omega) \leq L^2(\partial\Omega) \quad (9.2.2)$$

with equality if Ω is a disk.

9.3 Green's Theorem

Green's theorem is a higher-dimension analogous to the Fundamental Theorem of Calculus which applies to regions in the plane. The theorem relates a line integral along a simple closed curve C to a double integral over a closed region R , where $C = \partial R$.

Let R be a simple region in the plane with a piecewise smooth, simple closed boundary ∂R . Further, if $M(x, y)$ and $N(x, y)$ have continuous partial derivatives on an open region containing R , then Green's theorem states that

$$\oint_{\partial R} M(x, y)dx + N(x, y)dy = \iint_R \left(\frac{\partial N}{\partial x} - \frac{\partial M}{\partial y} \right) dA \quad (9.3.1)$$

Here, we consider only the positive orientation of ∂R : One moves in the counter-clockwise direction along the outer loop of ∂R ; while moves in the clockwise direction along the inner loop (if there is any holes) of ∂R . That means as one moves along ∂R , the region R is always on the left.

9.4 Problem Description

In mathematical formulation, the isoperimetric problem (Dido's problem) is stated as follow:

Among all simple closed curves in \mathbb{R}^2 , find a set of parametric equations $x = x(t)$, $y = y(t)$ for $t \in [t_1, t_2]$ that maximizes the functional

$$J = \int_{t_1}^{t_2} (xy' - x'y) dt \quad \text{subject to} \quad L = \int_{t_1}^{t_2} \sqrt{(x')^2 + (y')^2} dt \quad (9.4.1)$$

with conditions

$$x(t_1) = x(t_2), y(t_1) = y(t_2). \quad (9.4.2)$$

In (9.4.1), L is the fixed perimeter. Condition (9.4.2) ensures that the traced solution is a closed curve.

Given a surface S of equation, $z = f(x, y) \geq 0$, in the xy -plane. Let a simple

closed curve C , parametrized by $\begin{cases} x = x(t) \\ y = y(t) \end{cases}$ for $t \in [0,1]$ with terminal

conditions

$$\begin{cases} x(0) = x(1) \\ y(0) = y(1) \end{cases}, \quad (9.4.3)$$

be the boundary of the region R . The length of C is assumed to be fixed and is equal to 2π , so that

$$\int_0^1 \sqrt{\left(\frac{dx}{dt}\right)^2 + \left(\frac{dy}{dt}\right)^2} dt = 2\pi \quad (9.4.4)$$

The volume of the pillar over region R and bounded above by S is given by

$$\iint_R f(x, y) dx dy. \quad (9.4.5)$$

It is easy to transform the double integral objective function into a single integral

that can be handled by MISER3. Green's Theorem could be used to perform

such transformation. According to Green's Theorem, with appropriate

functions $g_1(x, y)$ and $g_2(x, y)$, (9.4.5) can be written as

$$\oint_C g_1(x, y)dx + g_2(x, y)dy = \int_0^1 \left[g_1(x, y) \left(\frac{dx}{dt} \right) + g_2(x, y) \left(\frac{dy}{dt} \right) \right] dt \quad (9.4.6)$$

along C in the counterclockwise direction, where the condition

$$\frac{\partial g_2(x, y)}{\partial x} - \frac{\partial g_1(x, y)}{\partial y} = f(x, y) \quad (9.4.7)$$

must be satisfied.

Suppose the simple closed curve C is traced out by $\mathbf{r}(t) = x(t)\mathbf{i} + y(t)\mathbf{j}$ in the

xy -plane (Figure 9.4.1). For C to have positive orientation, the tangent vector

$\mathbf{T}(t) = \frac{dx(t)}{dt}\mathbf{i} + \frac{dy(t)}{dt}\mathbf{j}$ should point in the counterclockwise direction and the

normal vector \mathbf{n} should point upward (the positive direction of the z -axis).

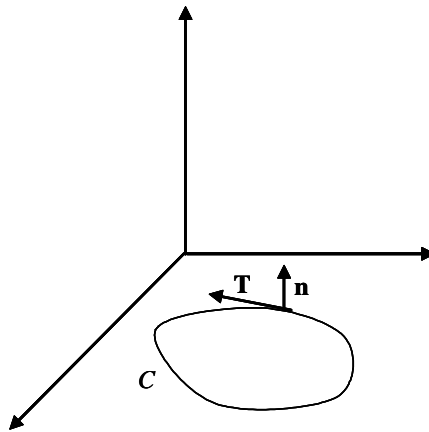


Figure 9.4.1 A simple closed curve with positive orientation.

The normal vector \mathbf{n} is determined by

$$\begin{vmatrix} \mathbf{i} & \mathbf{j} & \mathbf{k} \\ x(t) & y(t) & 0 \\ dx/dt & dy/dt & 0 \end{vmatrix} = \left(x(t) \frac{dy}{dt} - y(t) \frac{dx}{dt} \right) \mathbf{k} \quad (9.4.8)$$

and hence, the condition

$$x(t)\left(\frac{dy}{dt}\right) - y(t)\left(\frac{dx}{dt}\right) \geq 0 \quad \text{for all } t \in [0,1] \quad (9.4.9)$$

is imposed to ensure that C is traversed in the counterclockwise direction.

The problem is to find a pillar of maximum volume, having a fixed perimeter (cross-sectional) of 2π and bounded above by the surface S over a region R in the xy -plane. The control variables are the two time-derivatives:

$$\frac{dx}{dt} = u_1 \quad \text{and} \quad \frac{dy}{dt} = u_2. \quad (9.4.10)$$

For the single-pillar case, the corresponding optimal control problem is to maximize the cost functional (9.4.6) governed by the dynamics of (9.4.10) subject to constraints (9.4.4) and (9.4.9), with terminal conditions (9.4.3).

9.5 Analytic Solution – One Pillar, Flat Surface

One pillar problem:

For the one pillar problem, for simplicity, we consider the ceiling

$S = f(x_1, x_2) = 2$ over the region $R \in \mathbb{R}^2$. The problem (P1) can be stated as

follows:

$$\text{Max } J(\mathbf{x}, \mathbf{u}) = \int_0^1 (-u_1 x_2 + u_2 x_1) dt$$

subject to

$$\dot{x}_1 = u_1$$

$$\dot{x}_2 = u_2$$

$$\dot{x}_3 = \sqrt{u_1^2 + u_2^2}$$

$$x_1 u_2 - x_2 u_1 \geq 0$$

$$x_1(0) = x_1^{(0)}, \quad x_2(0) = x_2^{(0)}, \quad x_3(0) = 0$$

$$x_1(1) = x_1^{(0)}, \quad x_2(1) = x_2^{(0)}, \quad x_3(1) = L$$

Using Pontryagin Maximum Principle, we solve the problem as follows:

The Hamiltonian is

$$H = -u_1 x_2 + u_2 x_1 + \lambda_1 u_1 + \lambda_2 u_2 + \lambda_3 \sqrt{u_1^2 + u_2^2}, \quad (9.5.1)$$

and the Lagrangian is

$$L = H + \mu_1 (x_1 u_2 - x_2 u_1). \quad (9.5.2)$$

The adjoint equations are

$$\dot{\lambda}_1 = -\frac{\partial L}{\partial x_1} = -u_2 - \mu_1 u_2 \quad (9.5.3)$$

$$\dot{\lambda}_2 = -\frac{\partial L}{\partial x_2} = u_1 + \mu_1 u_1 \quad (9.5.4)$$

with transversality conditions

$$\lambda_1(1) = c_1, \quad \lambda_2(1) = c_2 \quad (9.5.5)$$

where c_1 and c_2 are constants.

The optimal trajectory must satisfy

$$\frac{\partial L}{\partial u_1} = -x_2 + \lambda_1 + \lambda_3 u_1 (u_1^2 + u_2^2)^{-\frac{1}{2}} - \mu_1 x_2 = 0 \quad (9.5.6)$$

and

$$\frac{\partial L}{\partial u_2} = x_1 + \lambda_2 + \lambda_3 u_2 (u_1^2 + u_2^2)^{-\frac{1}{2}} + \mu_1 x_1 = 0. \quad (9.5.7)$$

Also μ_1 should also satisfy the complementary slackness conditions

$$\mu_1 \geq 0 \quad (9.5.8)$$

and

$$\mu_1 (x_1 u_2 - x_2 u_1) = 0. \quad (9.5.9)$$

By considering the objective function and the traversal condition in (P1), together with the complementary slackness condition (9.5.9), we can deduce that $\mu_1 = 0$ or otherwise the objective function becomes zero.

The adjoint equations then become

$$\dot{\lambda}_1 = -\frac{\partial L}{\partial x_1} = -u_2 = -\dot{x}_2 \quad (9.5.10)$$

$$\dot{\lambda}_2 = -\frac{\partial L}{\partial x_2} = u_1 = \dot{x}_1 \quad (9.5.11)$$

and subsequently, we have

$$\lambda_1(t) + d_1 = -x_2(t) \quad \text{and} \quad \lambda_2(t) + d_2 = x_1(t) \quad (9.5.12)$$

where d_1 and d_2 are constants.

Substitute (9.5.12) into (9.5.6) and (9.5.7) and after some rearrangements, the following system of equations is obtained

$$\begin{aligned} \lambda_3 \dot{x}_1 (\dot{x}_1^2 + \dot{x}_2^2)^{-\frac{1}{2}} &= 2x_2 + d_1 \\ \lambda_3 \dot{x}_2 (\dot{x}_1^2 + \dot{x}_2^2)^{-\frac{1}{2}} &= -2x_1 + d_2 \end{aligned} \quad (9.5.13)$$

Assume $\lambda_3 (\dot{x}_1^2 + \dot{x}_2^2)^{-\frac{1}{2}} \neq 0$ (later from the solution that this assumption is valid

and $\lambda_3 (\dot{x}_1^2 + \dot{x}_2^2)^{\frac{1}{2}} = \frac{-1}{\pi}$ and by solving (9.5.13) yields

$$\left(x_1 - \frac{d_2}{2} \right)^2 + \left(x_2 + \frac{d_1}{2} \right)^2 = E \quad (9.5.14)$$

where $E = \frac{L^2}{4\pi^2}$ is a constant.

The relationship (9.5.14) shows that the cross sectional area of the pillar is a

circle centered at $\left(\frac{d_2}{2}, -\frac{d_1}{2} \right)$ with radius \sqrt{E} . By parametrized x_1 and x_2

in terms of time t , and consider the boundary conditions, we obtain

$$x_1(t) = \frac{L}{2\pi} \cos(2\pi t) + \frac{d_2}{2},$$

$$x_2(t) = \frac{L}{2\pi} \sin(2\pi t) - \frac{d_1}{2},$$

$$d_1 = -2x_2^{(0)},$$

$$d_2 = 2x_1^{(0)} - \frac{L}{\pi},$$

and the solution of (P1) can be summarized as

Optimal state trajectory:
$$\mathbf{x}^*(t) = \begin{bmatrix} \frac{L}{2\pi} \cos(2\pi t) + x_1^{(0)} - \frac{L}{2\pi} \\ \frac{L}{2\pi} \sin(2\pi t) + x_2^{(0)} \\ Lt \end{bmatrix}$$

Optimal control:
$$\mathbf{u}^*(t) = \begin{bmatrix} -L \sin(2\pi t) \\ L \cos(2\pi t) \end{bmatrix}$$

Adjoint equations:
$$\lambda^*(t) = \begin{bmatrix} -\frac{L}{2\pi} \sin(2\pi t) - x_2^{(0)} \\ \frac{L}{2\pi} \cos(2\pi t) - x_1^{(0)} + \frac{L}{2\pi} \\ -\frac{L}{\pi} \end{bmatrix}$$

Optimal Objective Value: $J(\mathbf{x}^*, \mathbf{u}^*) = \frac{L^2}{2\pi}$, as expected.

For non-flat surfaces or multi-pillar problems, analytical solutions may not be easily obtained.

9.6 Multi-Pillar Problem

For the multi-pillar case, the major difficulty is to ensure that the cross-sectional region of any pillars should not be overlapped. To overcome this problem, we set up a closed “separation” region to encircle each cross-sectional region. This “separation” region should enclose the cross-sectional region as tight as possible and possess an easy-to-handle formula. For example, in a two-pillar case (Pillars P_1 and P_2), the separation region $\Sigma = \{(x_1, x_2) | x_1 \geq 0, x_2 \geq 0\}$ where $P_1 \in \Sigma$ and $P_2 \notin \Sigma$ is not a good choice since the optimal locations of the two pillars can both be in the quadrant Σ ; on the other hand, to enclose a hexagonal-shaped pillar, the tightest separation region is obviously the same hexagonal-shaped as for the pillar. However, the formula for this region is too

complicated to be embedded as constraint for the problem. Among all closed separation regions, the elliptic equation should be the most appropriate.

Therefore, elliptic equations are used as the constraints to separate any two regions in the multi-pillar problem. For an n -pillar case, elliptic bound is imposed on any of the $(n-1)$ cross-sectional regions. The elliptic equation (E_i)

is given by

$$E_i : \frac{(x_i - h_i)^2}{a_i^2} + \frac{(y_i - k_i)^2}{b_i^2} = 1. \quad (9.6.1)$$

In (9.6.1), the point (h_i, k_i) is the centre of the ellipse, a_i and b_i correspond to the two axes (major and minor axes). The subscript i denotes the bound on region i .

The numerical values of the four parameters $(h_i, k_i, a_i$ and $b_i)$ are the system parameters determined by MISER3.

Figure 9.6.1 illustrates the three-pillar case: two ellipses E_1 and E_2 are added as constraints:

- (i) Pillar region R_1 is bounded inside ellipse E_1 .
- (ii) Pillar region R_2 is bounded inside ellipse E_2 but outside E_1 .
- (iii) Pillar region R_3 is bounded outside both ellipses E_1 and E_2 .

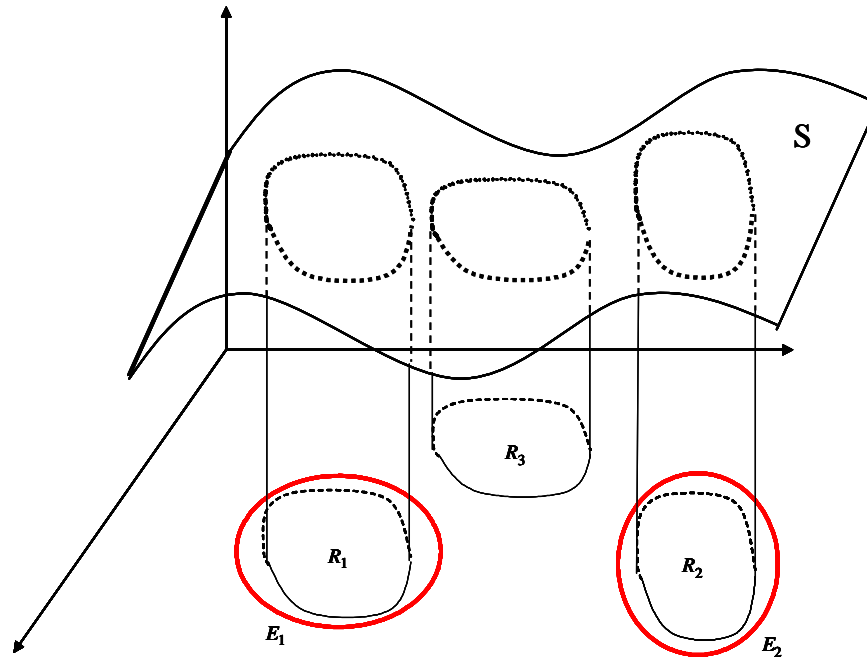


Figure 9.6.1 Illustration of the three-pillar case.

Two pillars problem:

Reconsider the situation as in the one-pillar case with ceiling $S = f(x_1, x_2) = 2$.

We define three more state variables, two more control variables, and two more system parameters for the second pillar. In addition, one more constraint for the transversal requirement and for the separation regions, two extra constraints and four system parameters are imposed. The problem (P2) is then stated as follows:

$$\text{Max } J(\mathbf{x}, \mathbf{u}) = \int_0^1 (-u_1 x_2 + u_2 x_1 - u_3 x_4 + u_4 x_3) dt$$

subject to

$$\dot{x}_1 = u_1; \quad \dot{x}_2 = u_2; \quad \dot{x}_3 = u_3; \quad \dot{x}_4 = u_4;$$

$$\dot{x}_5 = \sqrt{u_1^2 + u_2^2} ; \quad \dot{x}_6 = \sqrt{u_3^2 + u_4^2}$$

$$x_1 u_2 - x_2 u_1 \geq 0$$

$$x_3 u_4 - x_4 u_3 \geq 0$$

$$1 - \frac{(x_1 - z_1)^2}{z_3} + \frac{(x_2 - z_2)^2}{z_4} \geq 0$$

$$\frac{(x_3 - z_1)^2}{z_3} + \frac{(x_4 - z_2)^2}{z_4} - 1 \geq 0$$

$$x_i(0) = x_i^0 \quad \forall i = 1, \dots, 6,$$

$$x_i(1) = x_i^0 \quad \forall i = 1, \dots, 4, \quad x_5(1) = 2\pi, \quad x_6(1) = 2\pi$$

n-pillar problem:

The set up is the same as in the two-pillar problem and only differed by additional constraints. For an n -pillar problem, the total number of variables needed is $(11n - 4)$ and the number of constraints needed is $\frac{1}{2}(n^2 + 3n - 2)$.

The following table demonstrates the values for $n = 1, 2, 3,$ and 4 :

n	# of state variables	# of control variables	# of system variables	# of constraints
1	3	2	2	1
2	6	4	8	4
3	9	6	14	8
4	12	8	20	13

9.7 Illustrative Examples

Four surfaces (including the flat surface) are considered:

(i) $S_1 : f(x_1, x_2) = 2$ (flat surface)

(ii) $S_2 : f(x_1, x_2) = 2 + \cos(x_1)$

(iii) $S_3 : f(x_1, x_2) = 2 + \cos(x_1) + \sin(x_2)$

(iv) $S_4 : f(x_1, x_2) = 1 + \cos(x_1^2 + x_2)$

The constant terms for surfaces S_2 , S_3 , and S_4 are added to ensure the surfaces are bounded below by $f(x_1, x_2) = 0$. For every problem, 9 knot points are used as the initial run and gradually increased to 65 knot points as the final solution. Except for surface S_4 which we intentionally complicated the problem, the location of any pillar can be anywhere in the x_1x_2 plane.

Figure 9.7.1 and 9.7.2 illustrate the solution to 2-pillar and 3-pillar cases respectively corresponding to surface S_1 . As expected, the optimal shape of every pillar is a circle. For surface S_2 , a 3-D plot of the surface is shown in Figure 9.7.3 and a 2-D contour plot (with contour lines) of the surface in Figure 9.7.4. Solutions to 2-pillar and 3-pillar cases (with contour lines) are shown in Figure 9.7.5 and Figure 9.7.6 respectively. For surface S_3 , relevant figures are depicted in Figures 9.7.7 to Figures 9.7.11

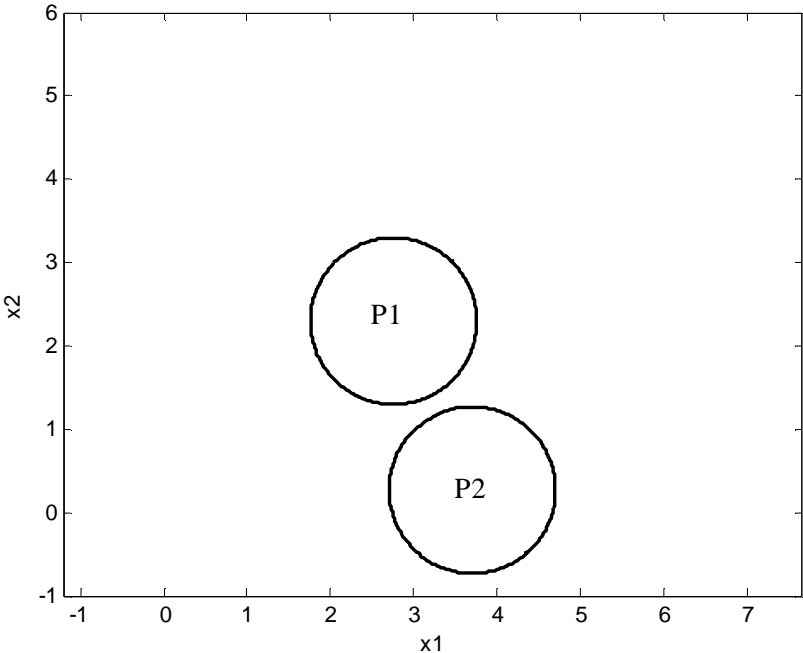


Figure 9.7.1 Optimal location of two pillars bounded above by surface S_1 .

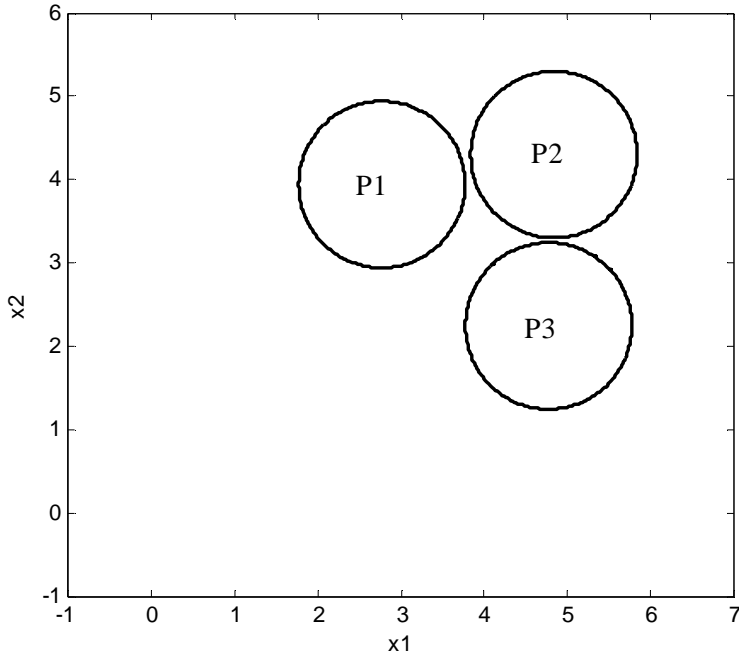


Figure 9.7.2 Optimal location of three pillars bounded above by surface S_1 .

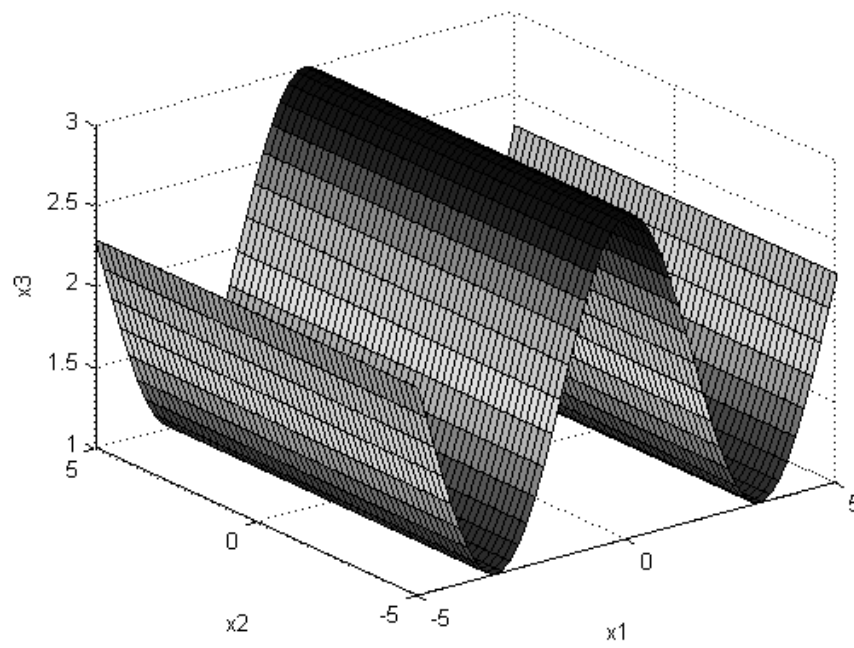


Figure 9.7.3 3-D plot of surface S_2 .

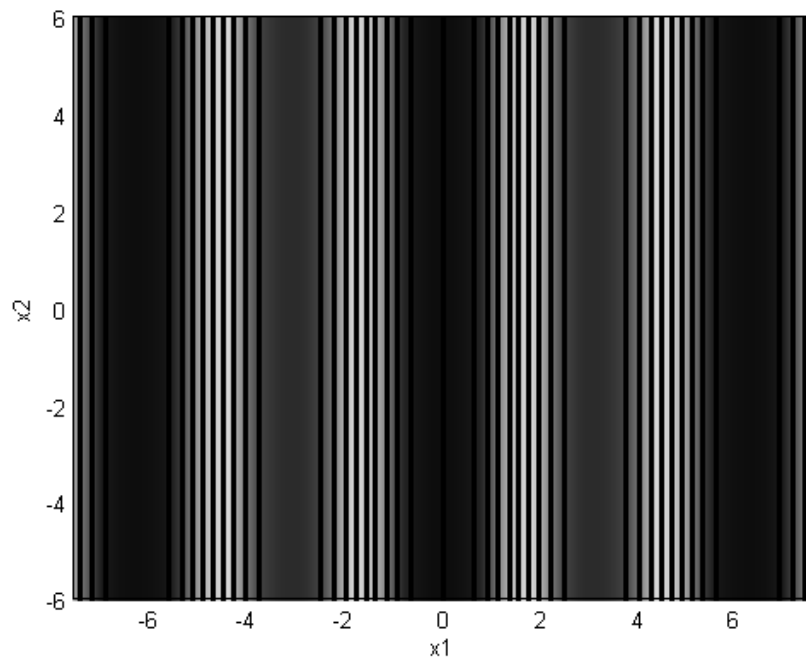


Figure 9.7.4 Contour plot of surface S_2 .

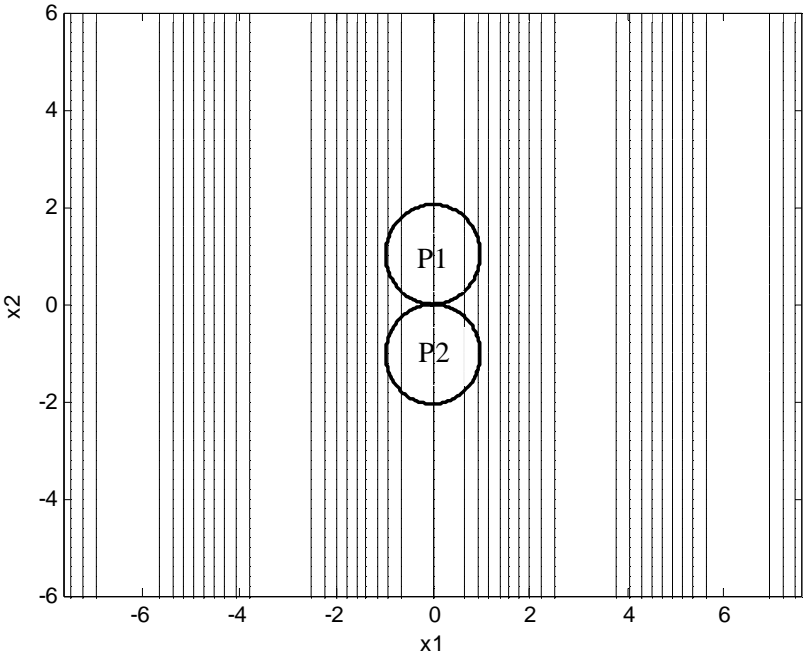


Figure 9.7.5 Optimal location of two pillars bounded above by surface S_2 .

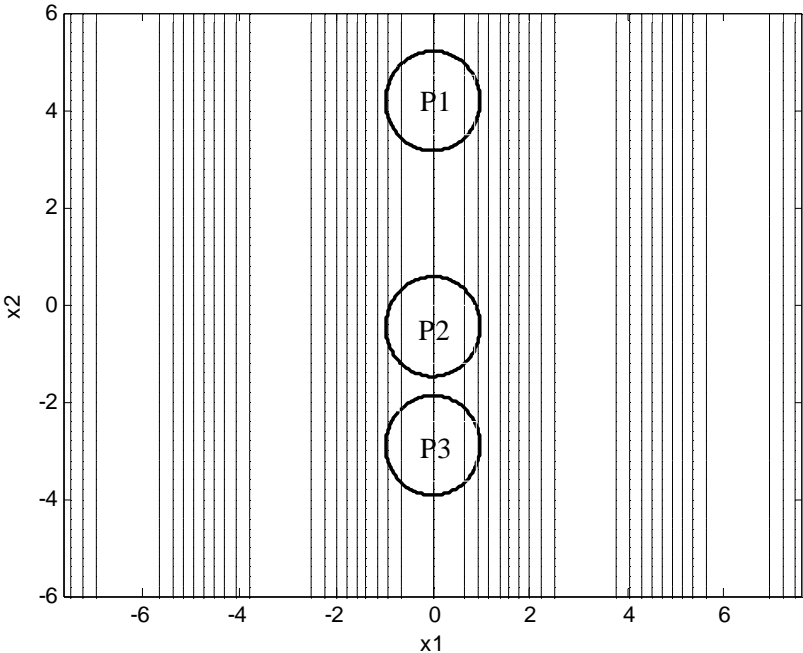


Figure 9.7.6 Optimal location of three pillars bounded above by surface S_2 .

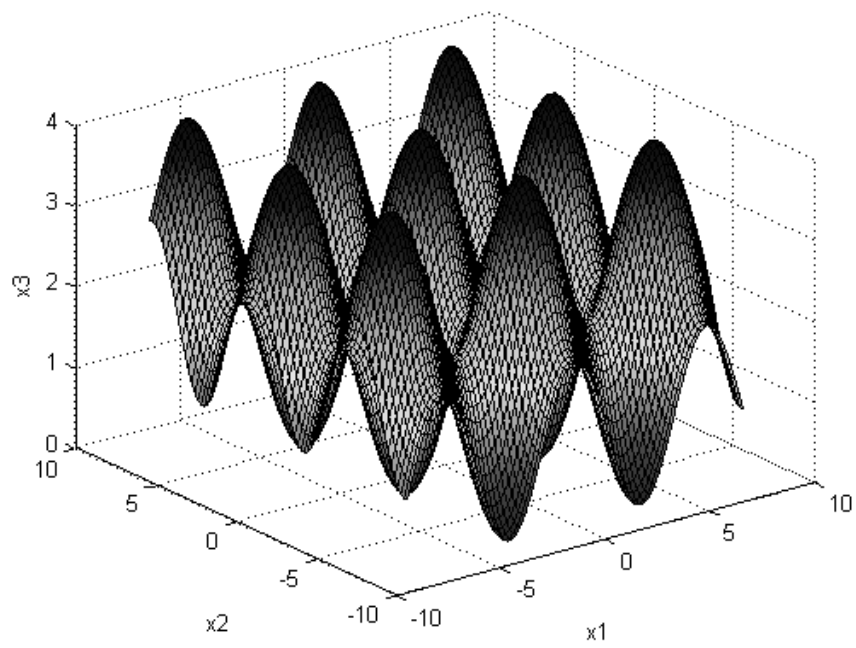


Figure 9.7.7 3-D plot of surface S_3 .

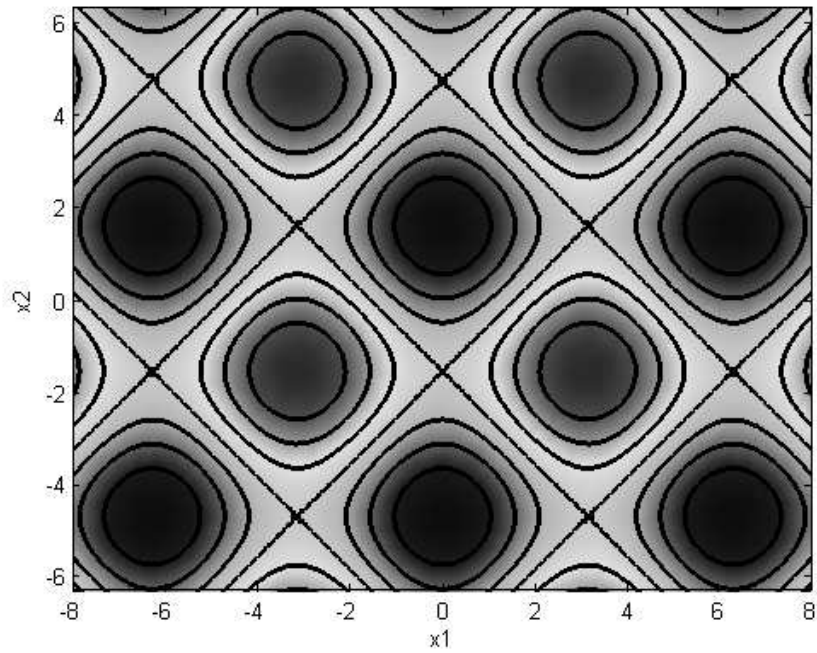


Figure 9.7.8 Contour plot of surface S_3 .

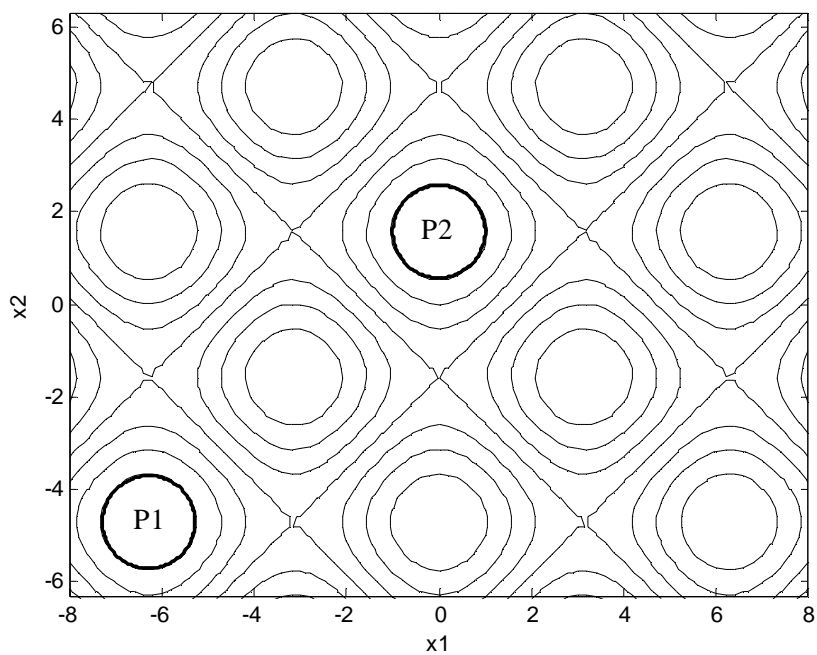


Figure 9.7.9 Optimal location of two pillars bounded above by surface S_3 .

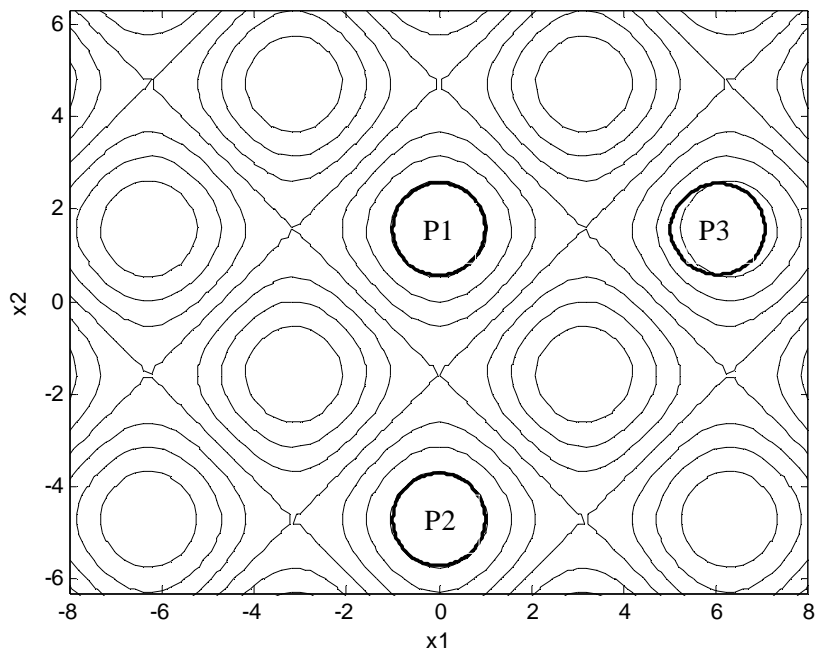


Figure 9.7.10 Optimal location of three pillars bounded above by surface S_3 .

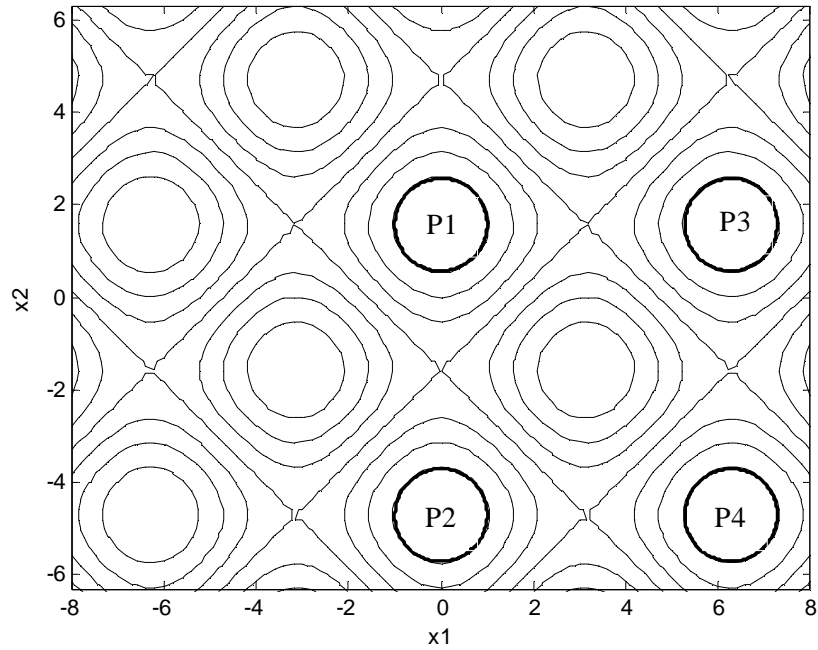


Figure 9.7.11 Optimal location of four pillars bounded above by surface S_3 .

For surface S_4 , we complicated the problem by restricting the location of the pillars. All the pillars must be located in $\Omega = \{(x_1, x_2) \mid -3 \leq x_1 \leq 3, -3 \leq x_2 \leq 3\}$.

The purpose of this restriction is to test whether MISER3 can successfully search for the maximum. For n -pillar problem, such restrictions transformed into MISER3 as:

$$\begin{aligned} 3 - x_i &\geq 0 & i = 1, \dots, 2n \\ 3 + x_i &\geq 0 & i = 1, \dots, 2n \end{aligned} \quad , \quad (9.7.1)$$

an additional of $4n$ equations.

Relevant figures are shown in Figures 9.7.12 to Figures 9.7.16. For this

problem, the elliptic separable regions are also depicted in the figures. The equation of each elliptic separable region is tabulated in Table 9.7.1.

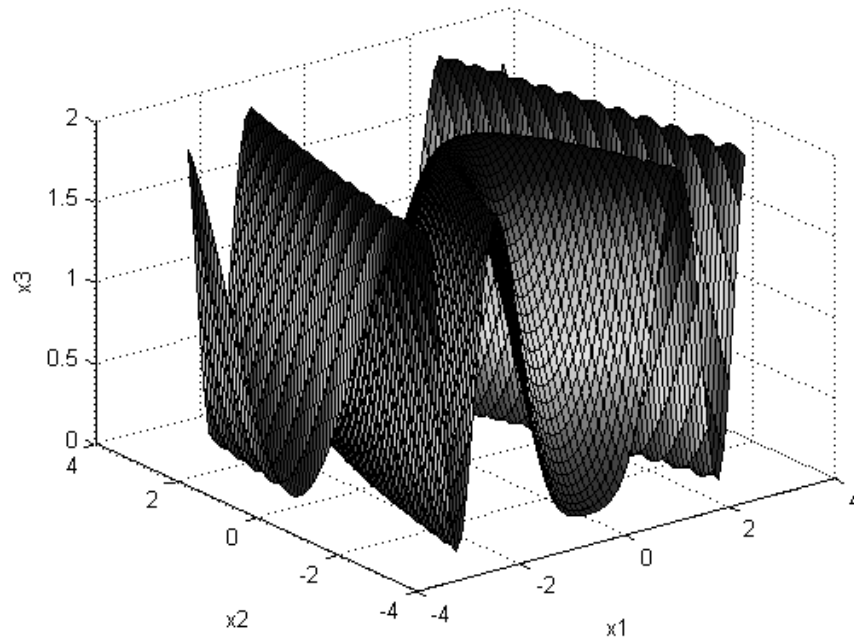


Figure 9.7.12 3-D plot of surface S_4 .

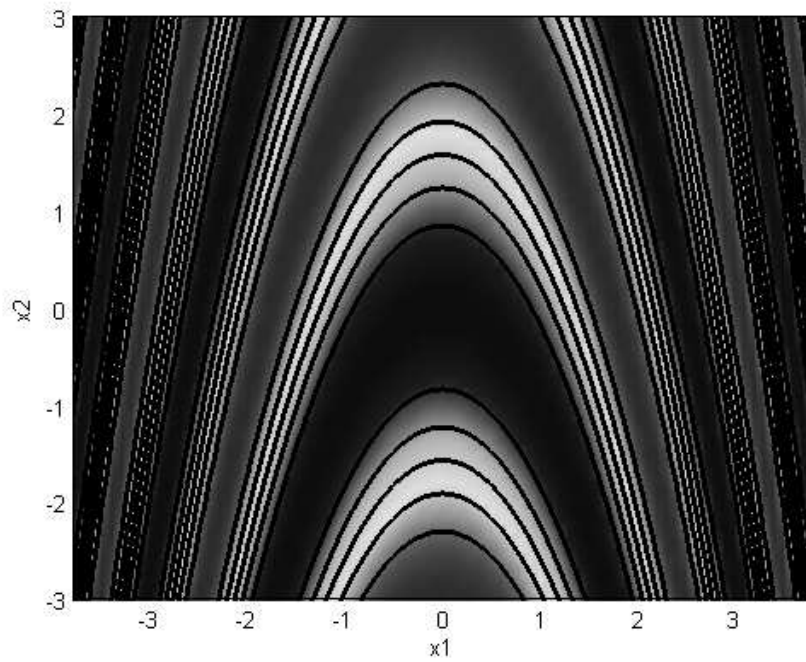


Figure 9.7.13 Contour plot of surface S_4 .

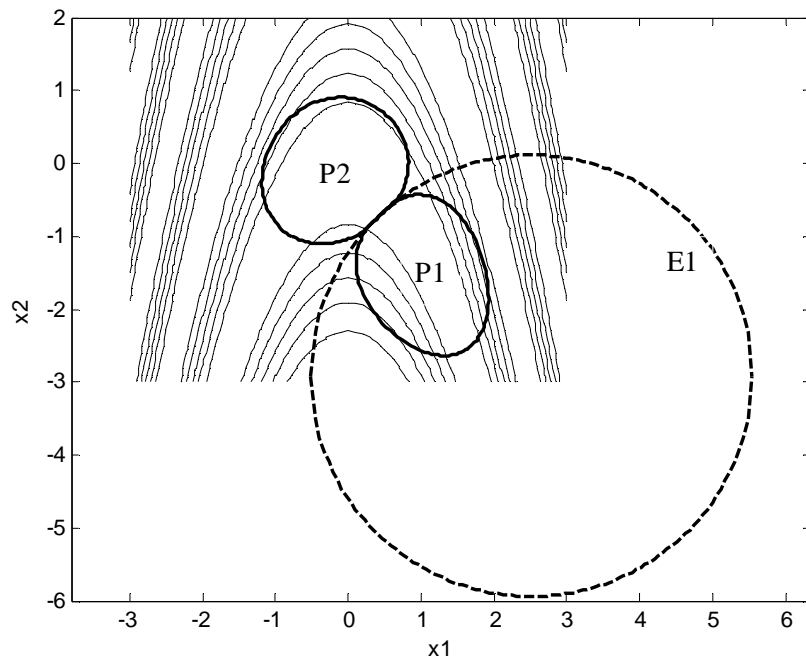


Figure 9.7.14 Optimal location of two pillars bounded above by surface S_4 .

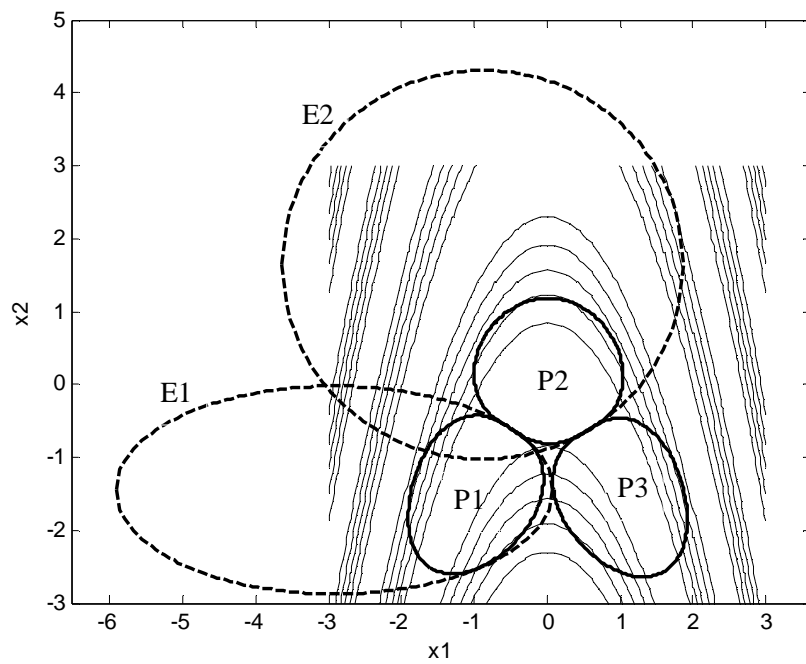


Figure 9.7.15 Optimal location of three pillars bounded above by surface S_4 .

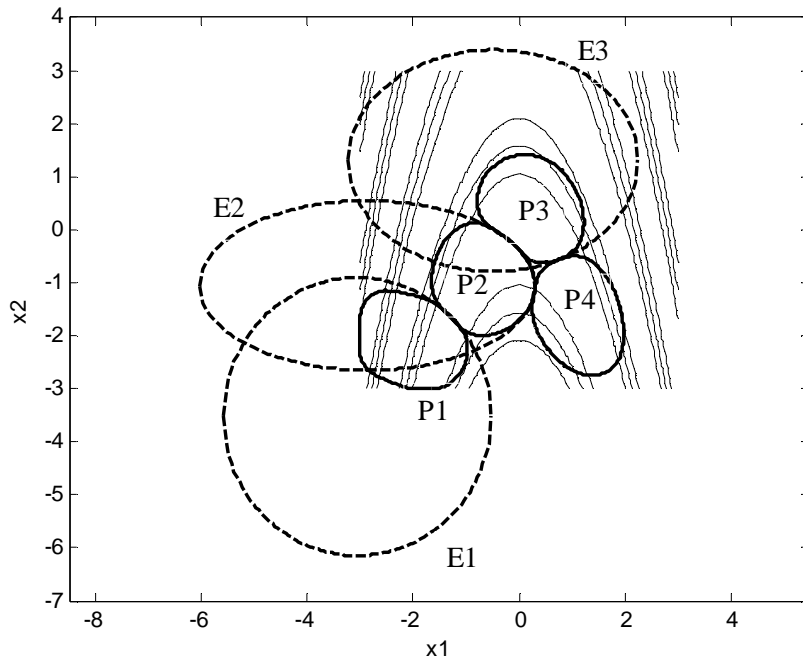


Figure 9.7.16 Optimal location of four pillars bounded above by surface S_4 .

No. of Pillars	Equations of the elliptic separable regions
2	E1: $\frac{(x_1 - 2.5155)^2}{9.1724} + \frac{(x_2 + 2.9131)^2}{9.1633} = 1$
3	E1: $\frac{(x_1 + 2.9199)^2}{9.0101} + \frac{(x_2 + 1.4475)^2}{2.0305} = 1$
	E2: $\frac{(x_1 + 0.8858)^2}{7.5709} + \frac{(x_2 - 1.6412)^2}{7.1175} = 1$
4	E1: $\frac{(x_1 + 3.0513)^2}{6.3926} + \frac{(x_2 + 3.5241)^2}{6.8695} = 1$
	E2: $\frac{(x_1 + 2.8619)^2}{9.9995} + \frac{(x_2 + 1.0547)^2}{2.5623} = 1$
	E3: $\frac{(x_1 + 0.4838)^2}{7.4740} + \frac{(x_2 - 1.2999)^2}{4.3682} = 1$

Table 9.7.1 Equations of the elliptic separable region for surface S_4 .

9.8 Discussion

For surfaces S_1 , S_2 , and S_3 , the location of the pillars depends on the initial starting point for each pillar, and search for maximum volume within its neighborhood to form the shape. As seen from the contour plots of surfaces S_2 , and S_3 (Figures 9.7.4, and 9.7.8), each “maximum” region is perfectly symmetric that it is of no astonishment that the optimal shape of the pillars are all circular. Even for the 4-pillar case, MISER3 can successfully identify the maximum regions. Due to the perfect symmetry, exact numerical values of the volume of the pillars can be evaluated and the results are compared to the one obtained through MISER3 in Table 9.8.1. The volume of one pillar for each surface can be computed using double integration:

$$(i) \quad S_1 : 2 \int_{-1}^1 \int_0^{\sqrt{1-x^2}} 2dy \, dx = 6.283185$$

$$(ii) \quad S_2 : 2 \int_{-1}^1 \int_0^{\sqrt{1-x^2}} (2 + \cos(x)) dy \, dx = 9.048105$$

$$(iii) \quad S_3 : 2 \int_{-1}^1 \int_{\pi/2}^{\left(\sqrt{1-x^2} + \frac{\pi}{2}\right)} (2 + \cos(x) + \sin(y)) dy \, dx = 11.813024.$$

For surface S_4 , we would expect the pillars to be located within the “maximum” parabolic-shaped region illustrated at the bottom half in Figure 9.7.13. This is demonstrated in the 2-pillar and 3-pillar cases. For 4-pillar problem, the

position of pillars P1, P2 and P3 should be of no doubt that they are at the “near-optimal” location. There is no space for the fourth pillar, P4, to be located entirely in the parabolic-shaped region. Therefore MISER3 needs to search for another location for pillar P4 and places the pillar at the lower left corner of the bounded region, at which a portion of the boundary of P4 hits the bounds of $\Omega = \{(x_1, x_2) \mid -3 \leq x_1 \leq 3, -3 \leq x_2 \leq 3\}$.

Surface	No. of Pillars	MISER3 Results	Analytical Results	Percentage Error
S_1	2	12.5563	12.5664	-0.08%
S_1	3	18.8344	18.8496	-0.08%
S_2	2	18.1012	18.0962	0.03%
S_2	3	27.1517	27.1443	0.03%
S_3	2	23.6082	23.6260	-0.08%
S_3	3	35.3195	35.4391	-0.34%
S_3	4	47.2165	47.2521	-0.08%
S_4	2	10.3680	NA	NA
S_4	3	14.9530	NA	NA
S_4	4	18.0600	NA	NA

Table 9.8.1 MISER3 performance compared to the actual results.

Chapter 10

Control Parametrization Enhancing Technique and Simulation on the Design of a Flexible Rotating Beam

10.1 Introduction

This chapter considers a rotating beam which carries an end mass and rotates in a vertical plane under the effect of gravity by means of a time-varying driving torque. Tangential coordinate system and the moving coordinate system are used in system modeling. Due to the highly nonlinear and coupled characteristics of the system, a relative description method is used to represent the motion of the beam and the motion equations are set up by using the relative motion variables. Finite element shape functions of a cantilever beam (Zou et al., 2003) are used as the displacement shape functions in this study. Lagrangian Formulation and Raleigh-Ritz approach (Fung et al., 2004) are employed to derive the governing equations of motion of the nonlinear time-varying system. Simulations are carried out to identify the characteristics of the PCLD treated beam. The problem is then posed as a continuous-time optimal control problem for the ACLD treatment and solved by MISER3. The objective function is to minimize the transverse deflection of a moving beam, the

input voltage to the piezoelectric (PZT) actuator, and the thickness of the constraining layer and the viscoelastic material layer. Such a computational optimal control approach is a novel technique in the design of the ACLD treated rotating beam. In addition, the accurate time of the switching points are determined which has not been considered in previous similar researches.

The main references for this chapter are Ref. 103 and 104.

Notation:

\mathbf{A} rotational transformation matrix	\mathbf{Q}_p generalized forces associated with piezoelectric layer
A_i cross-sectional area of i^{th} layer	\mathbf{Q}_v generalized inertial force
b width of beam	t time
d_{31} piezo-electric strain constant of piezo-actuator	u_i longitudinal extension of i^{th} layer in the moving coordinate system
E_i Young's modulus of i^{th} layer	V potential energy of ACLD treated beam
G_2^* complex shear modulus of visco-elastic core	V_c input voltage
G_2' shear (storage) modulus of G_2^*	w transverse deflection of beam in the moving coordinate system
h_i thickness of i^{th} layer	γ shear strain of visco-elastic core
I_i moment of inertia of i^{th} layer	η loss factor of G_2^*
\mathbf{K} stiffness matrix of ACLD system	ρ_i density of i^{th} layer
l length of beam	τ driving torque
Q_g generalized forces associated with gravity	

10.2 Optimal Control and CPET

Consider a dynamic process governed by a set of non-linear differential

equations, and subjected to a set of constraints on the fixed interval $(0, t_f]$,

where t_f denotes terminal time. A typical optimal control problem can be

converted into the following general format for MISER3 computation:

Problem (P)

Minimize

$$g_0(\mathbf{u}, \mathbf{z}) = \Phi_0(\mathbf{x}(t_f), \mathbf{z}) + \int_0^{t_f} L_0(\mathbf{x}(t), \mathbf{u}(t), \mathbf{z}) dt \quad (10.2.1)$$

such that

$$\frac{d\mathbf{x}(t)}{dt} = \dot{\mathbf{x}}(t) = \mathbf{f}(t, \mathbf{x}(t), \mathbf{u}(t), \mathbf{z}) \quad (10.2.2)$$

with initial condition

$$\mathbf{x}(0) = \mathbf{x}^0(\mathbf{z}) \quad (10.2.3)$$

subject to canonical constraints

$$g_i(\mathbf{u}, \mathbf{z}) = \Phi_i(\mathbf{x}(t_f), \mathbf{z}) + \int_0^{t_f} L_i(\mathbf{x}(t), \mathbf{u}(t), \mathbf{z}) dt \begin{cases} = 0 & \text{for } i=1, \dots, N_e \\ \geq 0 & \text{for } i=N_e+1, \dots, N \end{cases} \quad (10.2.4)$$

where $\mathbf{x} = [x_1 \ \dots \ x_n]^T \in \mathbb{R}^n$ is the state vector and $\mathbf{u} = [u_1 \ \dots \ u_r]^T \in \mathbb{R}^r$ is

the control vector. The state and control variables are normally governed by a

set of ODE equations in the time interval $(0, t_f]$. The vector

$\mathbf{z} = [z_1 \ \dots \ z_m]^T \in \mathbb{R}^m$ is the system parameter vector which is independent of

time t ; $\mathbf{f} : \mathbb{R}^1 \times \mathbb{R}^n \times \mathbb{R}^r \times \mathbb{R}^m \mapsto \mathbb{R}^n$ is the set of predetermined non-linear

functions continuously differentiable within all its

arguments; $\Phi_i \in \mathbb{R}^n \times \mathbb{R}^m \mapsto \mathbb{R}^1$ and $L_i \in \mathbb{R}^n \times \mathbb{R}^r \times \mathbb{R}^m \mapsto \mathbb{R}^1$ are combined as the canonical constraints g_i .

The control parametrization enhancing technique allows the accurate computation of the switching times without the assumption of pure bang-bang type optimal controls. By defining an additional variable s , CPET maps the original time scale $t \in [0, t_f]$ to a new scale $s \in [0, M]$, for some positive integer M , by the following conversion:

$$\frac{dt}{ds} = v(s) \geq 0 \tag{10.2.5}$$

and

$$\int_0^M v(s) ds = t_f \tag{10.2.6}$$

where $v(s) \in \mathbb{R}^1$ is the enhancing control. $v(s)$ belongs to the set of non-negative piecewise constant functions defined on $[0, M]$ with integer fixed knot points located at $\{1, 2, 3, \dots, M-1\}$. Hence, the time of the switching points can be accurately calculated by:

$$t_{s'} = \int_0^{s'} v(s) ds \tag{10.2.7}$$

where $s' \in \{1, 2, 3, \dots, M-1\}$ denotes the switching time in the s -domain.

Under CPET transformation, problem (P) becomes:

Problem (P_{CPET})

Min

$$g_0(\mathbf{u}, \mathbf{z}, v) = \Phi_0(\mathbf{x}(M), \mathbf{z}) + \int_0^M v(s)L_0(\mathbf{x}(s), \mathbf{u}(s), \mathbf{z})ds \quad (10.2.8)$$

such that

$$\begin{aligned} \frac{d\mathbf{x}(t)}{ds} &= (d\mathbf{x}(t)/dt)(dt(s)/ds) \\ &= v(s)\mathbf{f}(t(s), \mathbf{x}(t(s)), \mathbf{u}(t(s)), \mathbf{z}) \\ &= v(s)\mathbf{f}(s, \mathbf{x}(s), \mathbf{u}(s), \mathbf{z}) \end{aligned} \quad (10.2.9)$$

with initial condition

$$\mathbf{x}(0) = \mathbf{x}^0(\mathbf{z}) \quad (10.2.10)$$

subject to canonical constraints

$$g_i(\mathbf{u}, \mathbf{z}, v) = \Phi_i(\mathbf{x}(M), \mathbf{z}) + \int_0^M v(s)L_i(\mathbf{x}(s), \mathbf{u}(s), \mathbf{z})ds \begin{cases} = 0 & \text{for } i=1, \dots, N_e \\ \geq 0 & \text{for } i=N_e+1, \dots, N \end{cases} \quad (10.2.11)$$

Detailed transformation technique and control parametrization can be found in (Teo et al., 1991).

10.3 Dynamics of the ACLD Treated Beam

We consider a flexible rotating beam which carries an end mass rotating in a vertical plane under the effect of gravity by means of a time-varying driving torque via ACLD treatment. An ACLD treated beam is a three-layer beam-like structure – a piezo-electric constraining layer covered as the top layer, visco-elastic layer sandwiched in the middle, and the beam as the bottom layer. Input voltage is applied to the piezo layer. While with no active control, the

ACLD beam is simply a PCLD beam (i.e. the constraining layer in the PCLD treatment acts as a dummy piezoelectric layer). A schematic diagram for the sandwiched beam is depicted in Figure 10.3.1. Details explanations regarding Figure 10.3.1 can be found in Baz and Ro (1995) and Zou (2003).

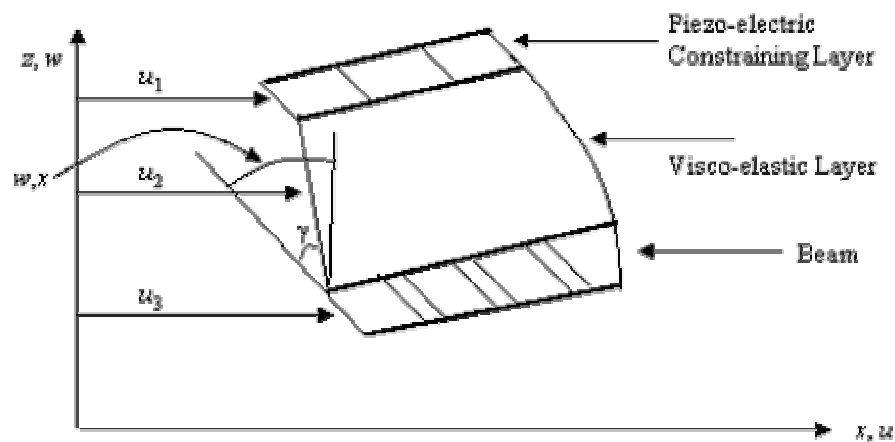


Figure 10.3.1 Section of Sandwiched Beam

The following four assumptions are imposed for the modeling (Zou et al., 2003).

1. Longitudinal and transverse motions are considered for all layers.
2. The transverse displacement at any point on the cross section of the beam is the same.
3. The shear deformation is considered for the viscoelastic material (VEM) layer only.
4. The density and thickness are constant throughout the length of the beam.

In this study, the beam moves in a vertical plane (XZ plane) under the effect of gravity by means of a time-varying driving torque τ . Figure 10.3.2 shows the relationship between the inertia co-ordinate system (XOZ), with position vector r_i , and the moving co-ordinate system (xOz), with position vector r'_i .

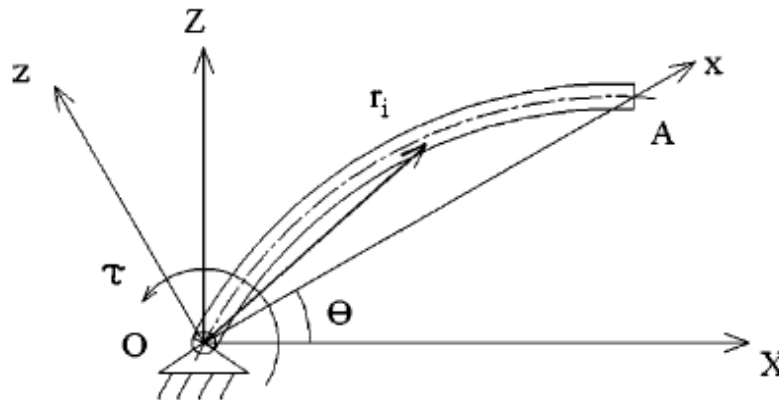


Figure 10.3.2 Co-ordinate Systems

The rotational transformation matrix, \mathbf{A} , is defined as:

$$\mathbf{A} = \begin{bmatrix} \cos \theta & -\sin \theta \\ \sin \theta & \cos \theta \end{bmatrix} \quad (10.3.1)$$

where θ is the angle between axes OX and Ox.

The position vector in each co-ordinate system is related by:

$$r_i = \mathbf{A}r'_i, \text{ where } r'_i = \mathbf{u}_{oi} + \mathbf{u}_{fi} \quad (10.3.2)$$

$$\mathbf{u}_{oi} = \begin{bmatrix} x \\ 0 \end{bmatrix} \text{ and } \mathbf{u}_{fi} = \begin{bmatrix} u_i \\ w \end{bmatrix}. \quad (10.3.3)$$

\mathbf{u}_{oi} denotes the initial position vector, with no deflection and

\mathbf{u}_{fi} denotes the elastic displacement vector.

The deformation of the i^{th} layer is obtained by Rayleigh-Ritz method, which is expressed by the following matrix:

$$\mathbf{u}_{fi} = \begin{bmatrix} \frac{x}{l} & 0 & 0 \\ 0 & 3\frac{x^2}{l^2} - 2\frac{x^3}{l^3} & l(\frac{x^3}{l^3} - \frac{x^2}{l^2}) \end{bmatrix} \begin{bmatrix} q_{fli} \\ q_{f2} \\ q_{f3} \end{bmatrix} \quad (10.3.4)$$

where q_{fli} is the longitudinal displacement of the i th layer at the end point; q_{f2} and q_{f3} represent w and $\frac{\partial w}{\partial x}$ respectively.

The independent generalized coordinates of the system is given by

$$\mathbf{q} = [\theta \quad q_{f11} \quad q_{f2} \quad q_{f3}]^T, \quad (10.3.5)$$

which serves part of the state vector in our optimal control formulation.

The following system governing matrix differential equation is obtained via Lagrangian formulation and Raleigh-Ritz approach (Zou et al. 2003).

Expressions for various terms of the equation are given in Appendix 10.A.

$$\mathbf{M}\ddot{\mathbf{q}} + \mathbf{K}\mathbf{q} = \mathbf{Q}_F + \mathbf{Q}_g + \mathbf{Q}_v + \mathbf{Q}_p \quad (10.3.6)$$

where

$$\mathbf{Q}_g = -\frac{\partial V}{\partial \mathbf{q}} \quad (10.3.7)$$

$$\mathbf{Q}_v = \frac{\partial}{\partial \mathbf{q}} \left(\frac{1}{2} \dot{\mathbf{q}}^T \mathbf{M} \dot{\mathbf{q}} \right) - \dot{\mathbf{M}} \dot{\mathbf{q}} \quad (10.3.8)$$

$$\mathbf{Q}_F = [\tau \quad 0 \quad 0 \quad 0]^T \quad (10.3.9)$$

$$\tau = 0.5 \exp(-120t). \quad (10.3.10)$$

The generalized forces associated with the piezo-electric actuator (PZT), \mathbf{Q}_p , is included in the above equation for ACLD treatment. For PCLD treatment, the \mathbf{Q}_p term is dropped. The derivation of \mathbf{Q}_p is given in Appendix 10.B.

10.4 Optimal Control Formulation of the ACLD Treated Beam

Consider the ACLD treated beam together with the state differential equations stated in section 10.3, the state vector \mathbf{x} is defined as $[\mathbf{q}^T \dot{\mathbf{q}}^T]^T$ and the feedback control V_c is expressed in terms of the state variables, $V_c = \mathbf{u}^T \mathbf{x}$.

\mathbf{u}^T is a row vector with entries $[0 \ 0 \ u_3(t) \ 0 \ 0 \ 0 \ u_7(t) \ 0]$ where $u_i(t)$ denotes the i^{th} element in \mathbf{u} . The two entries, $u_3(t)$ and $u_7(t)$, correspond to the deflection w and deflection rate \dot{w} respectively, forming a PD controller with $V_c = u_3(t)w + u_7(t)\dot{w}$.

The objective is to minimize

$$\int_0^{0.125} [(1 \times 10^{11})x_3^2(t) + V_c^2]dt + 100 \sum_{i=1}^2 \rho_i h_i \quad (10.4.1)$$

subject to the dynamics in Eq (10.3.6) – (10.3.10) with initial condition $\mathbf{x}(0) = \mathbf{0}$.

The weighted cost functional (10.4.1) aims to minimize tracking error of the beam with minimal input voltage V_c , while keeping the total treatment weight to be as low as possible. The weightings in (10.4.1) are used to balance the diversion of the units among the three terms, $x_3^2(t)$, V_c^2 and $\sum_{i=1}^2 \rho_i h_i$, and to

apply different degrees of importance to the three criteria. The h_i s are considered as the system parameters to be determined by MISER3.

10.5 Numerical Simulations and Results

For comparison purpose, the same sandwiched beam structure is used for both the PCLD and ACLD treatments. The following physical parameters in appropriate SI units are used in the analysis:

$$l=0.2616; b=0.0127; h_3=22.86 \times 10^{-4}; \rho_1=7600; \rho_2=1000; \rho_3=2700;$$

$$E_1=63 \times 10^9; G_2=5 \times 10^4; E_3=70 \times 10^9; \eta=1.0; g=9.8; m=0.0005;$$

10.5.1 Numerical Simulations of the PCLD System

To identify the characteristics of the dynamic system (Eq 10.3.6), various simulations are carried out under PCLD treatment (i.e. no active control is applied to the PZT layer).

(i) *Effects of varying the thickness of the constraining layer*

The effect of the thickness of the constraining layer h_1 is depicted in Figure 10.5.1. With a fixed thickness on the VEM layer h_2 of 1.00×10^{-4} m, simulation on the damping behavior are carried out with $h_1=2.00 \times 10^{-4}$ m, 4.00×10^{-4} m, and 8.00×10^{-4} m. As illustrated in Figure 10.5.1, the transverse deflection decreases

as the thickness of the constraining layer increases. There are significant improvements on the vibration amplitude and the damping performance by doubling the thickness of the constraining layer.

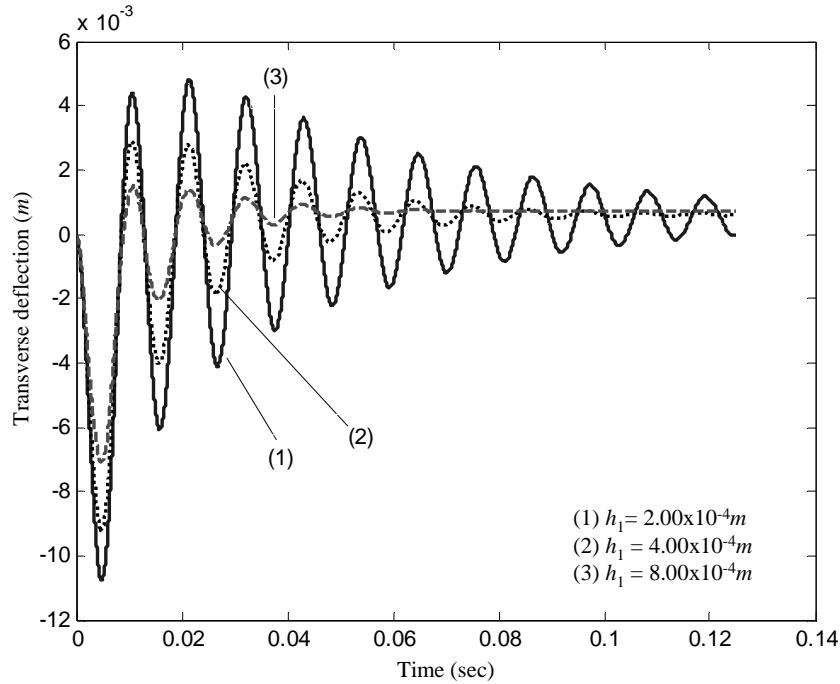


Figure 10.5.1 Effect of the thickness of the constraining layer with $h_2 = 1.00 \times 10^{-4} \text{m}$

(ii) *Effects of varying the thickness of the viscoelastic material layer*

The effect of the thickness of the viscoelastic material (VEM) layer h_2 is depicted in Figure 10.5.2. With a fixed thickness on the constraining layer h_1 of $4.00 \times 10^{-4} \text{m}$, simulation on the damping behavior are carried out with $h_2 = 1.00 \times 10^{-4} \text{m}$, $2.00 \times 10^{-4} \text{m}$, and $4.00 \times 10^{-4} \text{m}$. As shown in Figure 10.5.2, the transverse deflection decreases as the thickness of the VEM layer decreases. There is slight improvement on the vibration amplitude as the thickness of the

VEM layer is reduced. However, it seems there is no significant improvement on the damping performance by varying the thickness of the VEM layer.

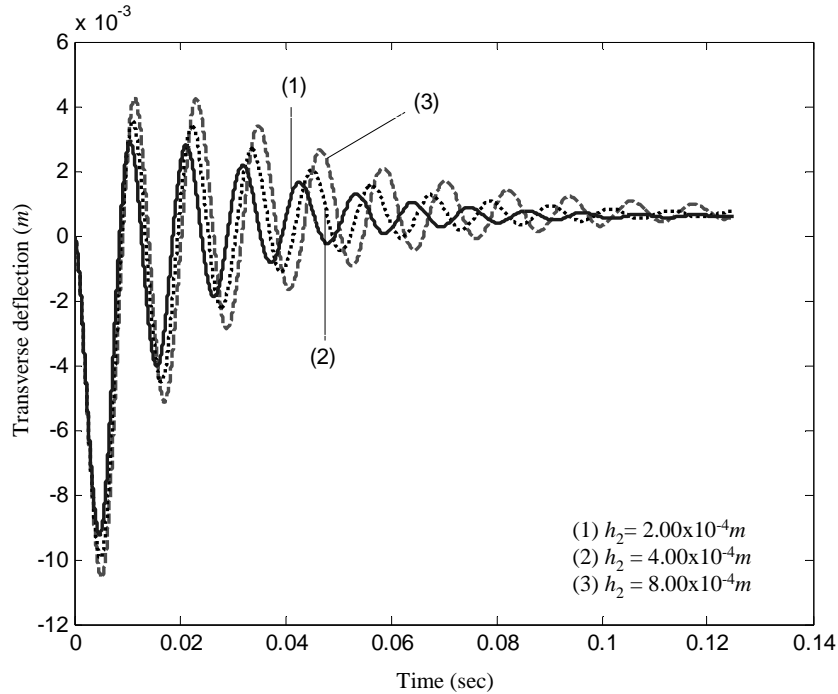


Figure 10.5.2 Effect of the thickness of the VEM layer with $h_1 = 4.00 \times 10^{-4} \text{m}$

(iii) *Effects of varying the thickness of the two layers by fixing the ratio of the two layers*

By fixing the ratio of the thickness of the two layers, the effect of the thickness of the constraining layer h_1 and the VEM layer h_2 is depicted in figures 10.5.3 – 10.5.5. Ratio of $h_1/h_2 = 4, 1, \text{ and } 1/4$ are simulated. In all of the three cases, the amplitude of the transverse deflection and the damping performance of the beam decrease as the thickness of the two layers increase. Moreover, comparing the ratio h_1/h_2 , the largest ratio ($h_1/h_2 = 4$) has substantial improvements in terms of the transverse deflection and the damping performance

compared to the results of the other two smaller ratios. For the two smaller ratios ($h_1/h_2 = 1$, and $1/4$), however, there is no significant difference in term of either the transverse deflection or the damping performance.

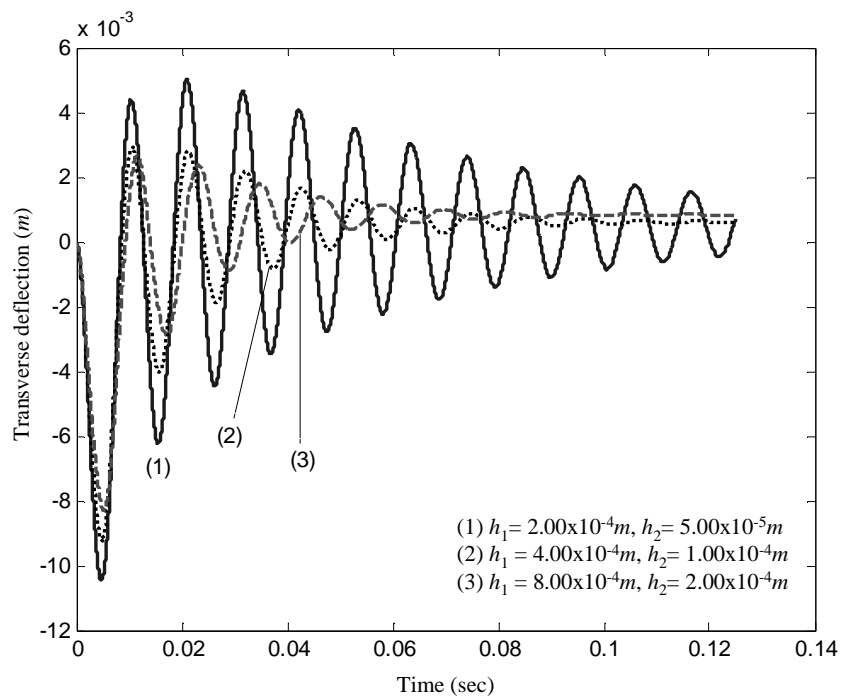


Figure 10.5.3 Effect of the ratio of the thickness of the constraining layer and the VEM layer ($h_1/h_2 = 4$)

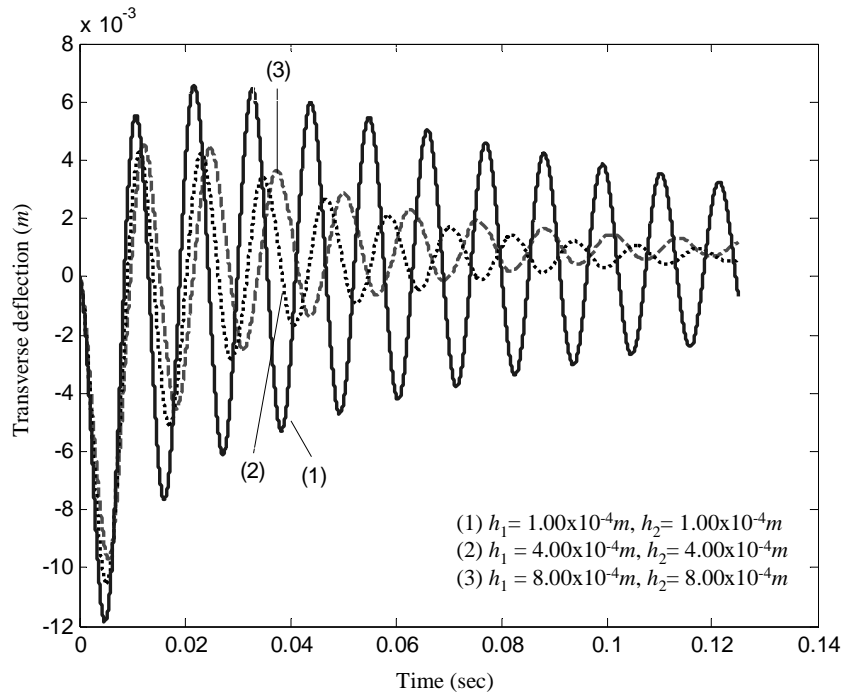


Figure 10.5.4 Effect of the ratio of the thickness of the constraining layer and the VEM layer ($h_1 / h_2 = 1$)

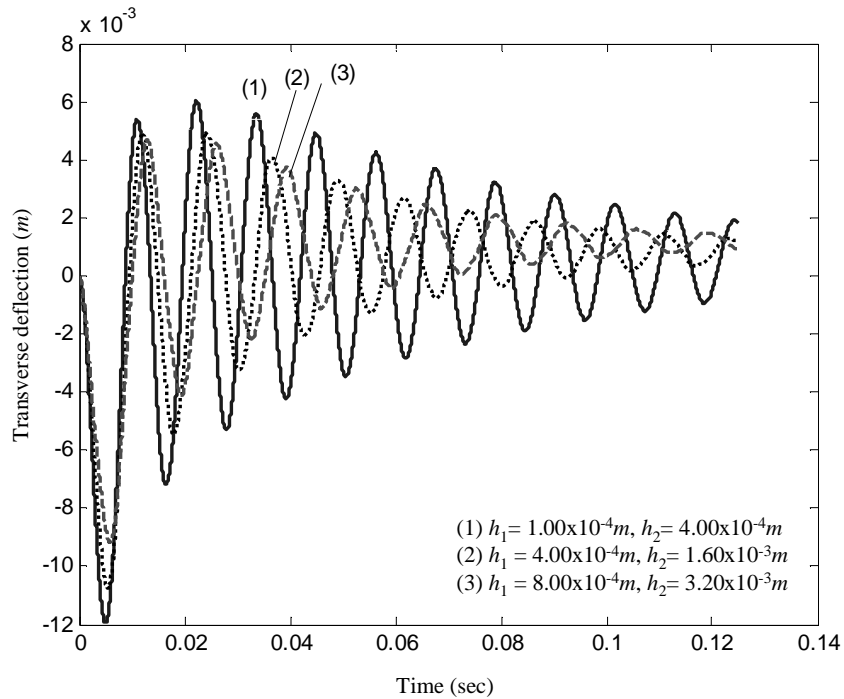


Figure 10.5.5 Effect of the ratio of the thickness of the constraining layer and the VEM layer ($h_1 / h_2 = 1/4$)

10.5.2 Results of the ACLD system

Consider the formulation in section 10.3 under CPET, the problem is solved by MISER3 in MATLAB6.5 platform. The time horizon is partitioned into 2 and 4 with equal subintervals and convergence is obtained with high accuracy in each case. The optimal objective value is 6.5610×10^3 for 2-partition case and 6.5377×10^3 for 4-partition case. Results obtained for the two system parameters are 4.00×10^{-4} m for the constraining layer and 1.00×10^{-4} m for the VEM layer. Relevant plots for the solutions are depicted in Figure 10.5.6 to Figure 10.5.15 in appropriate SI units. The optimal trajectories for the transverse deflection w and the control V_c are depicted in Figures 10.5.6 and 10.5.7 respectively for the constant gain PD controller, in Figures 10.5.8 and 10.5.9 respectively for the 2-partition case (variable gain with one switching), and in Figures 10.5.12 and 10.5.13 respectively for the 4-partition case (variable gain with three switchings). As noticed from Figure 10.5.8 and Figure 10.5.12, the performance of the transverse deflection for the 4-partition case are similar to those of the 2-partition case. For all cases, the amplitude of the deflection is improved substantially compared to that of the PCLD treatment. Comparing the ACLD treatment in the constant gain and the one switching cases, the deflection of the beam is further reduced by allowing one switching in the

control gains. Results also demonstrate that a slight improvement is obtained by increasing the number of switchings to 3, i.e. the 4-partition case.

Figures 10.5.7, 10.5.9 and 10.5.13 show the optimal input voltage as a function of time. Optimal solutions suggest an input voltage, high in magnitude, at the very beginning, and exponentially decrease afterwards until reaching zero near the end of the time horizon. Comparing the optimal input voltage in the constant gain and the one switching cases, a larger input voltage is required for the constant gain PD controller. That means by allowing one switching in the control gains, control effort is reduced. The time histories of the two optimal control gains for the 2-partition case are depicted in Figures 10.5.10 and 10.5.11. For clarity, the plots are zoomed near the time when the switching occurs ($t = 1.09 \times 10^{-3}$ sec). Comparing the optimal input voltage in the one switching case and the three-switching case, a higher input voltage is needed for the three-switching case at the beginning; while a lesser control effort is required subsequently. The time histories of the two optimal control gains for the three-switching case are depicted in Figures 10.5.14 and 10.5.15. Optimal solutions suggest the switching occurs at $t = 4.97 \times 10^{-3}$ sec, 0.119 sec, and 0.124 sec for the three-switching case. The optimal switching times occur at the very beginning or near the end of the time horizon, which are reasonable. If there is

any switching occurred during the midst of the time horizon, such a sudden change in the control gains may produce an abrupt change in the input to the PZT layer, thus increasing the magnitude of the transverse deflection.

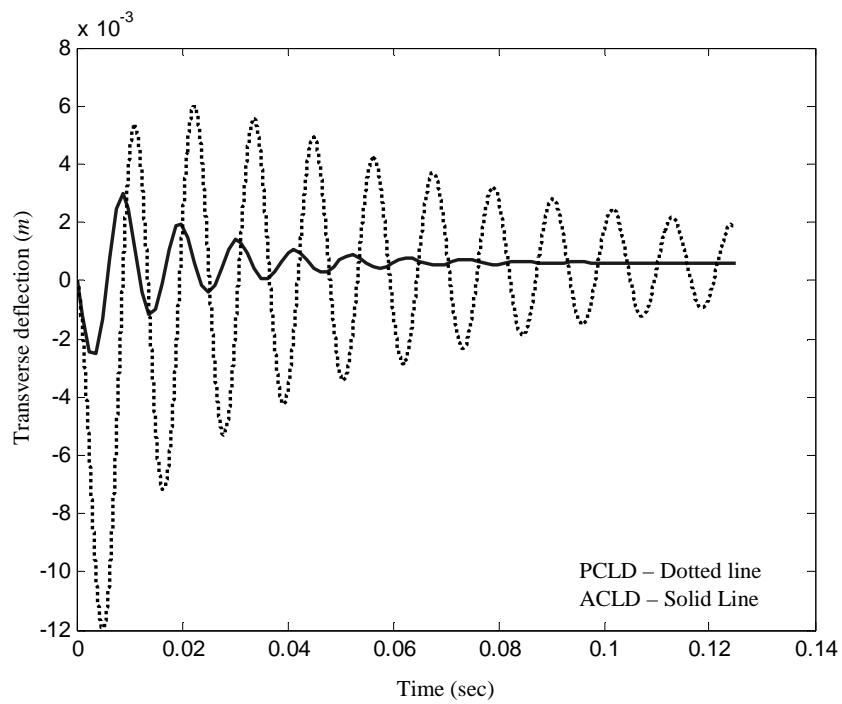


Figure 10.5.6 Transverse Deflection w (constant gain PD controller)

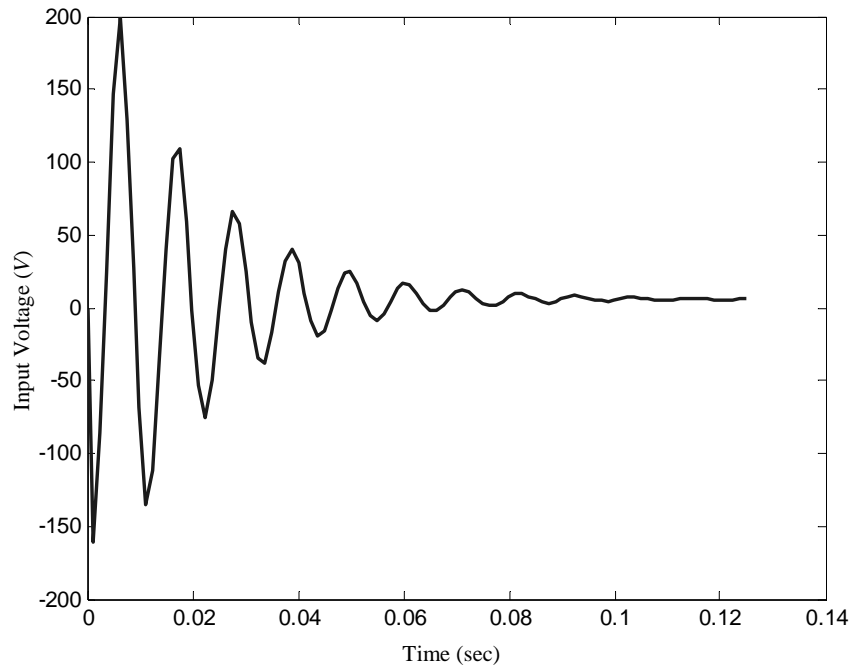


Figure 10.5.7 Input Voltage V_c (constant gain PD controller)

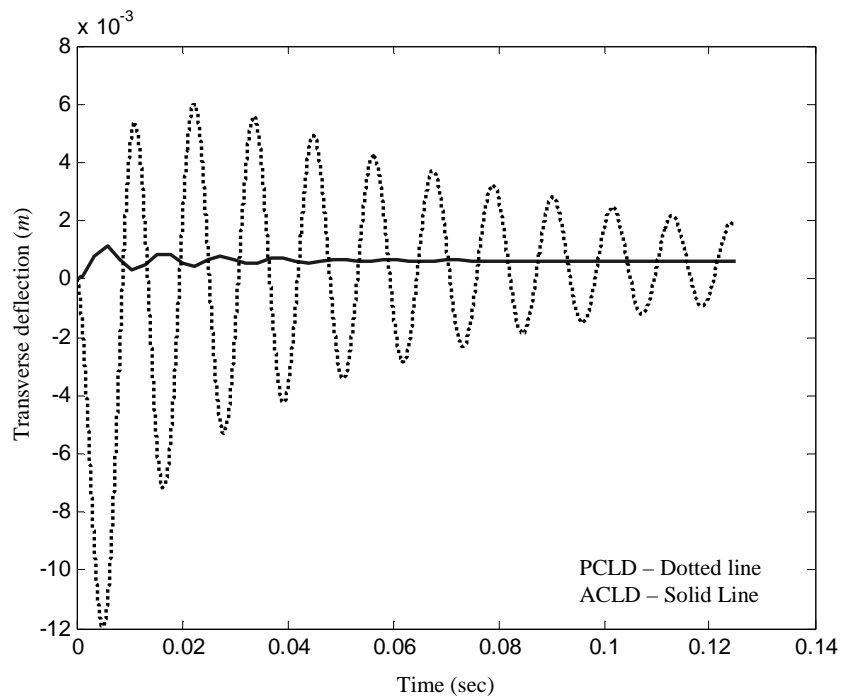


Figure 10.5.8 Transverse Deflection w (2-partition)

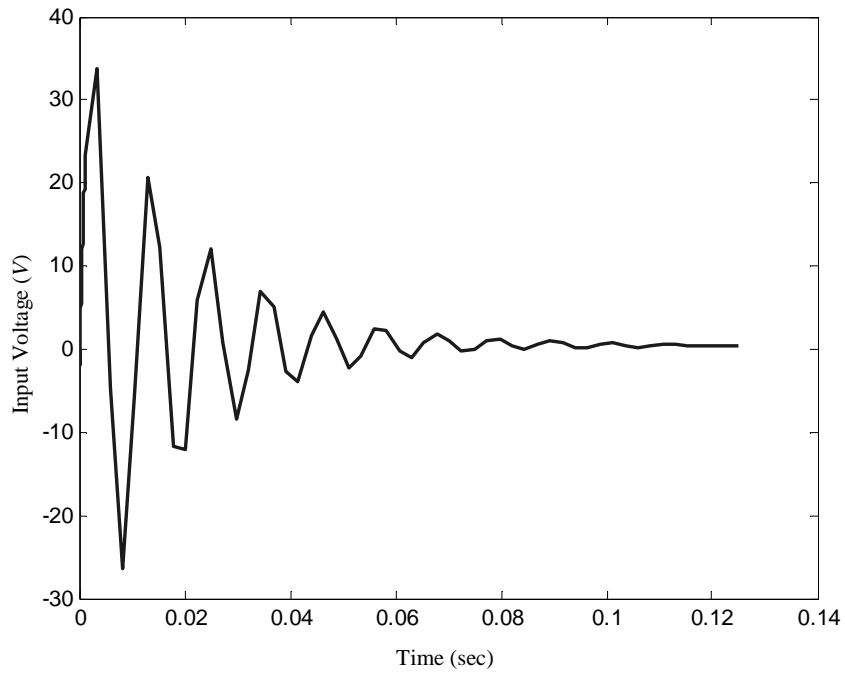


Figure 10.5.9 Input Voltage V_c (2-partition)

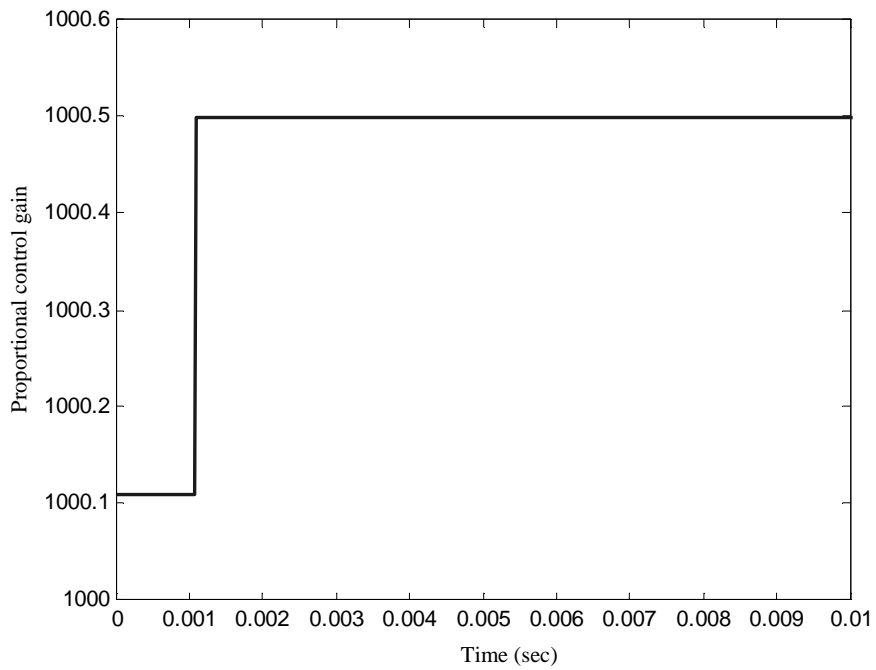


Figure 10.5.10 Optimal Control Gain u_3 (2-partition) (proportional control gain)

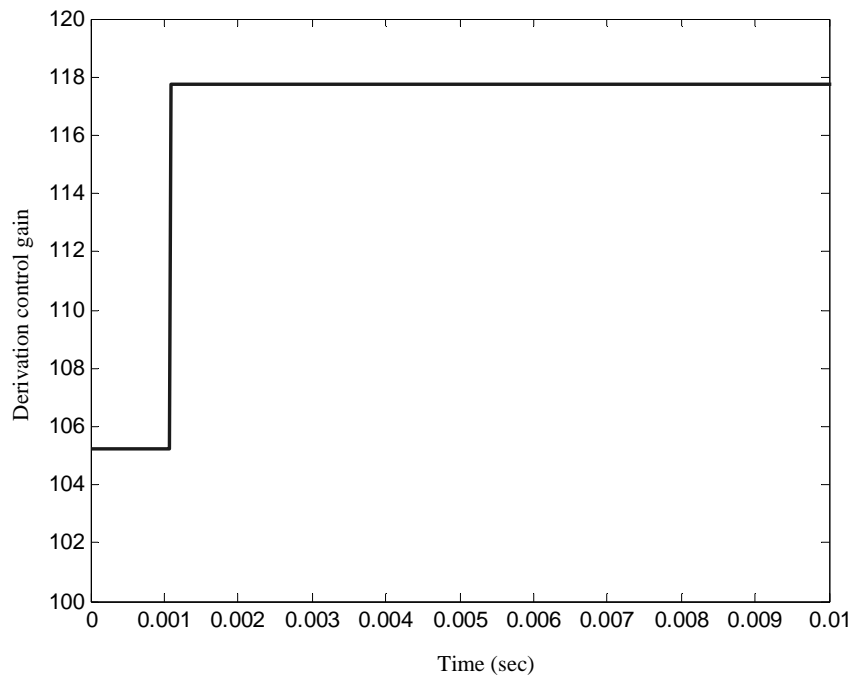


Figure 10.5.11 Optimal Control Gain u_7 (2-partition) (derivative control gain)

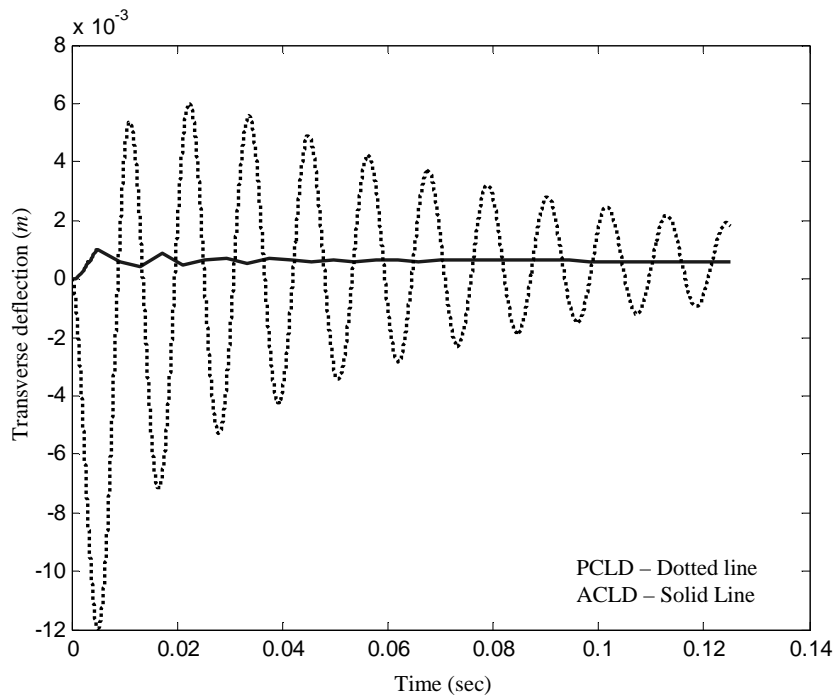


Figure 10.5.12 Transverse Deflection w (4-partition)

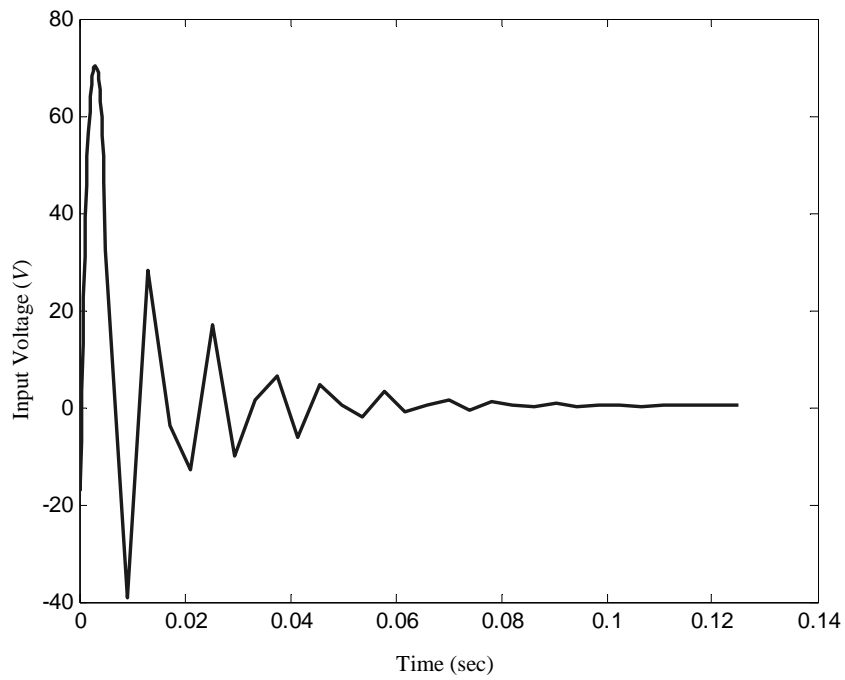


Figure 10.5.13 Input Voltage V_c (4-partition)

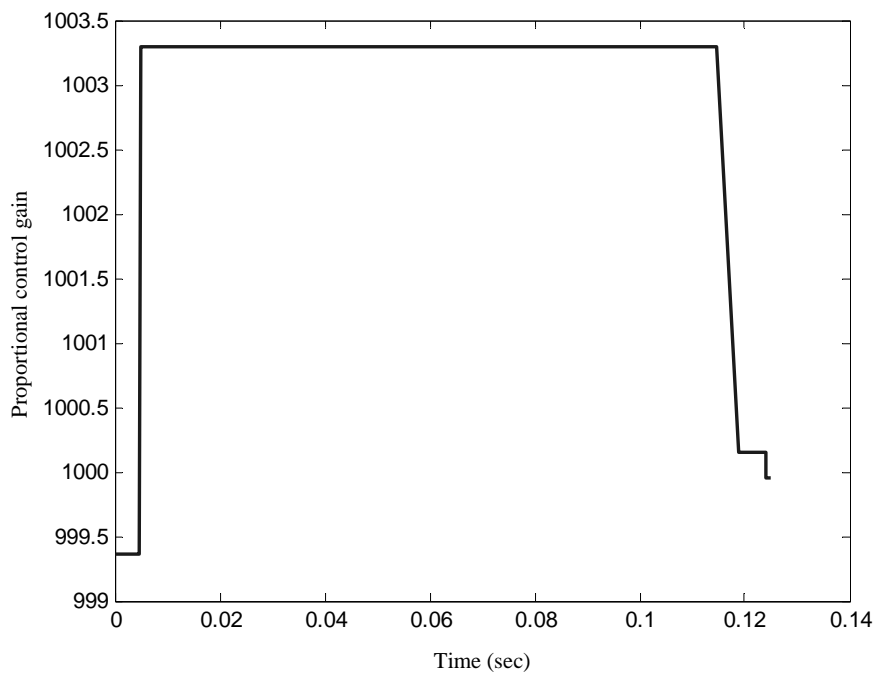


Figure 10.5.14 Optimal Control Gain u_3 (4-partition) (proportional control gain)

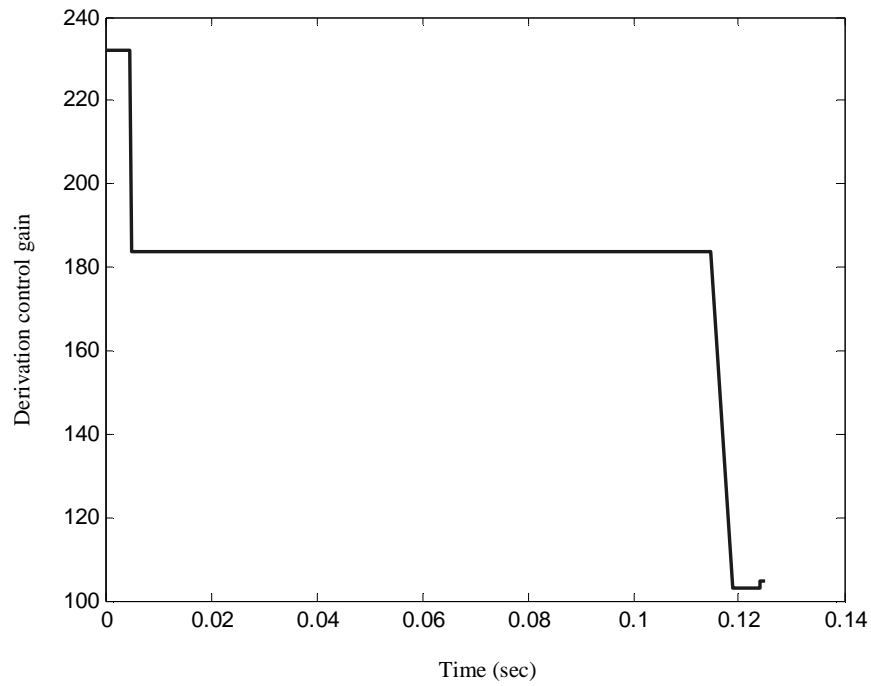


Figure 10.5.15 Optimal Control Gain u_7 (4-partition) (derivative control gain)

Appendix 10.A – Equation for the PCLD System

The mass terms are expressed by

$$\mathbf{M} = \begin{bmatrix} m_{\theta\theta} & \mathbf{m}_{\theta f} \\ \mathbf{m}_{\theta f}^T & \mathbf{m}^f \end{bmatrix} \quad (10.A1)$$

$$m_{\theta\theta} = \sum_{i=1}^3 \bar{m}_i \int_0^l [w^2 + (x + u_i)^2] dx + ml^2 \quad (10.A2)$$

where

$$\bar{m}_i = \rho_i A_i;$$

$$\mathbf{m}_{\theta f} = [m_{\theta 1} \quad m_{\theta 2} \quad m_{\theta 3}]; \quad (10.A3)$$

$$m_{\theta 1} = -(\bar{m}_1 + \frac{\bar{m}_2}{2}) \int_0^l w \Phi_u dx;$$

$$\begin{aligned}
 m_{\theta 2} &= -(\bar{m}_3 + \frac{\bar{m}_2}{2}) \int_0^l w \Phi_u dx ; \\
 m_{\theta 3} &= \sum_{i=1}^3 \bar{m}_i \int_0^l (x + u_i) \Phi_{w2} dx - \frac{\bar{m}_2}{2} \int_0^l d_1 w \Phi_{w2,x} dx ; \\
 \Phi_u &= \xi ; \\
 \Phi_{w1} &= 3\xi^2 - 2\xi^3 ; \\
 \Phi_{w2} &= l(\xi^3 - \xi^2) . \\
 \mathbf{m}^f &= \begin{bmatrix} m_{11}^f & m_{12}^f & m_{13}^f \\ m_{21}^f & m_{22}^f & m_{23}^f \\ m_{31}^f & m_{32}^f & m_{33}^f \end{bmatrix} , \tag{10.A4}
 \end{aligned}$$

where

$$\begin{aligned}
 m_{11}^f &= (\bar{m}_1 + \frac{\bar{m}_2}{4}) \int_0^l \Phi_u^2 dx ; \\
 m_{12}^f &= m_{21}^f = \frac{\bar{m}_2}{4} \int_0^l \Phi_u^2 dx ; \\
 m_{13}^f &= m_{23}^f = m_{31}^f = m_{32}^f = \frac{\bar{m}_2}{4} \int_0^l d_1 \Phi_u \Phi_{w2,x} dx ; \\
 m_{22}^f &= (\bar{m}_3 + \frac{\bar{m}_2}{4}) \int_0^l \Phi_u^2 dx ; \\
 m_{33}^f &= \sum_{i=1}^3 \bar{m}_i \int_0^l \Phi_{w2}^2 dx + \bar{m}_2 \int_0^l (\frac{d_1}{2} \Phi_{w2,x})^2 dx ;
 \end{aligned}$$

The stiffness terms are expressed by

$$\mathbf{K} = \begin{bmatrix} \mathbf{0} & \mathbf{0} \\ \mathbf{0} & \mathbf{k}^f \end{bmatrix} \tag{10.A5}$$

$$\mathbf{k}^f = \begin{bmatrix} k_{11}^f & k_{12}^f & k_{13}^f \\ k_{21}^f & k_{22}^f & k_{23}^f \\ k_{31}^f & k_{32}^f & k_{33}^f \end{bmatrix} , \tag{10.A6}$$

where

$$k_{11}^f = (k_{12} + \frac{k_{22}}{4}) \int_0^l \Phi_{u,x}^2 dx + g_2^* \int_0^l \Phi_u^2 dx ;$$

$$\begin{aligned}
 k_{12}^f &= k_{21}^f = \frac{k_{22}}{4} \int_0^l \Phi_{u,x}^2 dx - g_2^* \int_0^l \Phi_u^2 dx; \\
 k_{13}^f &= k_{31}^f = \frac{k_{22}}{4} \int_0^l d_1 \Phi_{u,x} \Phi_{w2,xx} dx - g_2^* \int_0^l d \Phi_u \Phi_{w2,x} dx; \\
 k_{22}^f &= (k_{32} + \frac{k_{22}}{4}) \int_0^l \Phi_{u,x}^2 dx - g_2^* \int_0^l \Phi_u^2 dx; \\
 k_{23}^f &= k_{32}^f = \frac{k_{22}}{4} \int_0^l d_1 \Phi_{u,x} \Phi_{w2,xx} dx - g_2^* \int_0^l d \Phi_u \Phi_{w2,x} dx; \\
 k_{33}^f &= (k_t + k_{22} d_1^2) \int_0^l \Phi_{w2,xx}^2 dx + g_2^* \int_0^l (d \Phi_{w2,x})^2 dx; \\
 k_t &= \sum_{i=1}^3 E_i I_i; \quad k_{i1} = E_i I_i; \quad k_{i2} = E_i A_i; \quad g_2^* = \frac{G_2^* A_2}{h_2^2}
 \end{aligned}$$

G_2^* is the complex shear modulus of the VEM, and $G_2^* = G_2'(1 + \eta i)$ where G_2' is the shear storage modulus of the VEM and η is the loss factor of the VEM .

The potential energy of the ACLD treated beam is given by

$$V = mgl \sin \theta + \frac{1}{2} \sum_{i=1}^3 r_i A_i l^2 g \sin \theta + \sum_{i=1}^3 r_i A_i g \cos \theta \int_0^l w dx \quad (10.A7)$$

Appendix 10.B – Derivation for Q_p

For ACLD treatment, an external control is inserted into the system, namely Q_p , the piezoelectric force.

The workdone is given by

$$\delta W_p = Q_p \delta q \quad (10.B1)$$

and

$$\delta W_p = E_1 A_1 \int_0^L \varepsilon_p \delta u_1 dx \quad (10.B2)$$

where

$$\varepsilon_p = \frac{d_{31}}{h_1} V_c;$$

V_c is the input voltage, and

$$d_{31} = 18.6 \times 10^{-11}.$$

Combining (10.B1) and (10.B2) gives

$$\mathbf{Q}_p = \begin{bmatrix} 0 & \frac{E_1 b l}{2} d_{31} V_c & 0 & 0 \end{bmatrix} \quad (10.B3)$$

Chapter 11

Optimal Control Strategy for a Nonlinear Quarter–Car Suspension Model with State Depending ODE Class

11.1 Introduction

This chapter considers a nonlinear model of quarter-car suspension problem. Such a system has been a popular issue in road vehicle applications. There are number of suspension systems developed with active suspension control strategy design. We adopt the model similar to the one in Sam et. al. (2002) with a state dependent ODE system of equations. This class of problem is difficult to solve since we do not know in advance when the system jump from one system to another. There does not exist any method for solving this class of problem in the vehicle suspension literature. By applying the control parametrization enhancing transform (CPET), the problem can easily be solved by MISER3. A numerical example is provided to illustrate the method used.

The main reference for this chapter is Ref. 101.

11.2 State Dependent Optimal Control Problem

Consider the following state equation:

$$\frac{d\mathbf{x}}{dt} = \begin{cases} f_1(\mathbf{x}(t), \mathbf{u}(t)) & \text{if } \mathbf{x}(t) \in \Omega_1 \\ f_2(\mathbf{x}(t), \mathbf{u}(t)) & \text{if } \mathbf{x}(t) \in \Omega_2 \\ \vdots & \\ f_m(\mathbf{x}(t), \mathbf{u}(t)) & \text{if } \mathbf{x}(t) \in \Omega_m \end{cases} \quad (11.2.1)$$

$$\mathbf{x}(0) = \hat{\mathbf{x}} \quad (11.2.2)$$

where $\mathbf{x}(t) \in \mathbb{R}^n$ is the state vector, $\mathbf{u}(t) \in \mathbb{R}^m$ is the control vector and $f_i(\mathbf{x}, \mathbf{u}) : \mathbb{R}^n \times \mathbb{R}^m \rightarrow \mathbb{R}^n$ is a continuous differentiable function with respect to each of its arguments in Ω_i . Moreover we assume that if \mathbf{x} enters Ω_i for any $i \in \{1, 2, \dots, m\}$, it will remain inside Ω_i for a finite time interval.

Let us also impose the continuous state inequality constraint to the problem, namely:

$$h(x(t)) \geq 0 \quad \text{for } t \in [0, T] \quad (11.2.3)$$

where h is continuously differentiable with respect to its component, and T is the final time. The ‘ $\varepsilon - \tau$ ’ algorithm is used to deal with the continuous state inequality constraints (Teo et al., 1991)

The objective function to be minimized is

$$J(u) = \int_0^T L_0(x(t), u(t)) dt, \quad (11.2.4)$$

where L_0 is continuously differentiable with respect to its components.

The optimal control problem, denoted by (P) can be stated as follow:

Subject to the system (11.2.1), (11.2.2) and the constraint (11.2.3), find an optimal step function control u^* such that $J(u^*)$ is a minimum over the set of

all step-function controls $u(t)$.

11.3 The Computational Method with Enhanced Switching

Controls

Consider the one-dimensional ODE analogous to (11.2.1),

$$\frac{dx}{dt} = \begin{cases} f_1(x) & x \in [\alpha_1, \alpha_2) \\ f_2(x) & x \in [\alpha_2, \alpha_3) \\ \vdots & \vdots \\ f_m(x) & x \in [\alpha_m, \infty) \end{cases}, \quad (11.3.1)$$

the interval $[\alpha_i, \alpha_{i+1})$, for $i = 1, 2, \dots, m-1$, can be written as a single

continuously differentiable function $g_i(x)$ as follow:

$$g_i(x) = (\alpha_i - x)(x - \alpha_{i+1}) \geq 0 \quad (11.3.2)$$

The inequality (11.3.2) ensures that x is in the interval $[\alpha_i, \alpha_{i+1})$.

The intervals in (11.3.1) can be combined as:

$$g(x) = (\alpha_1 - x)(x - \alpha_2)\hat{u}_1 + (\alpha_2 - x)(x - \alpha_3)\hat{u}_2 + \dots + (x - \alpha_m)\hat{u}_m \geq 0 \quad (11.3.3)$$

where \hat{u}_i s are the enhanced switching controls which takes on value of either 0

or 1. Since x can only be in one and only one of the intervals $[\alpha_i, \alpha_{i+1})$, only

one of the \hat{u}_i s equals to 1 and the rest are all 0 at any single time. Hence, the

state dependent ODE system of equations (11.3.1) can be reformulated as

11.3 The Computational Method with Enhanced Switching Controls

$$\frac{dx}{dt} = f_1 \hat{u}_1 + f_2 \hat{u}_2 + \dots + f_n \hat{u}_n \quad (11.3.4)$$

with constraints (11.3.3),

$$\sum_{i=1}^m \hat{u}_i = 1, \text{ and} \quad (11.3.5)$$

$$\hat{u}_i = \{0,1\}. \quad (11.3.6)$$

Nevertheless, the problem cannot be solved by MISER3 since the enhancing controls in (11.3.6) are 0-1 discrete variables. To handle such discrete-valued constraint, Lee et. al. (1998) developed a statistical variance type of functional constraint:

$$\text{variance}(\hat{u}_1, \hat{u}_2, \dots, \hat{u}_m) = \frac{1}{12} \quad (11.3.7)$$

where

$$\text{variance}(\hat{u}_1, \hat{u}_2, \dots, \hat{u}_m) = \sum_{i=1}^m \hat{u}_i \left(i^2 - i + \frac{1}{3} \right) - \left[\sum_{i=1}^m \hat{u}_i \left(i - \frac{1}{2} \right) \right]^2. \quad (11.3.8)$$

However, it is difficult to force the \hat{u}_i s to satisfy the all-time continuous equality constraint (11.3.7). Thus, (11.3.7) is “relaxed” by

$$\text{variance}(\hat{u}_1, \hat{u}_2, \dots, \hat{u}_m) \leq \frac{1}{12} + \beta \quad (11.3.9)$$

with $\beta > 0$. We first set $\beta = 1$ and obtain a feasible solution of the state dependent ODE optimal control problem. Then, use that feasible solution as an initial guess for the same problem but with a reduced value of β (i.e. 0.5β).

The process is repeated until β is closed to zero.

11.4 Optimal Control Formulation of the Vehicle Suspension Problem

Problem

This section considers a quarter vehicle model similar to the one in Sam et al. (2002). A schematic diagram is depicted in Figure. 11.4.1. In the diagram, x_1 denoted tyre deformation, x_2 denoted suspension deflection, x_3 and x_4 denotes the wheel velocity and the body velocity respectively.

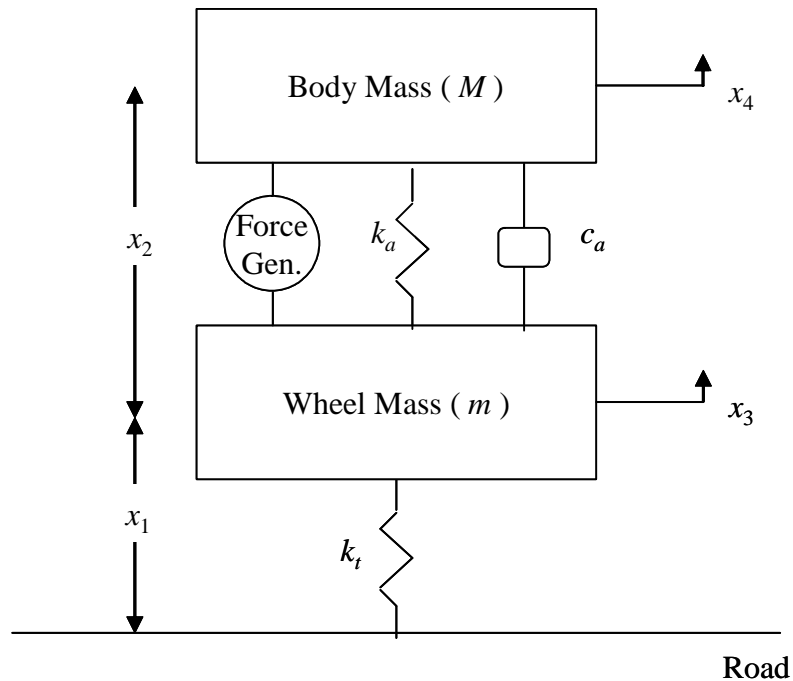


Figure 11.4.1 A schematic diagram for the vehicle suspension model.

The following system governing differential equation is obtained via Newton's law of motion:

11.4 Optimal Control Formulation of the Vehicle Suspension Problem

$$\dot{x}_1 = x_3 \quad (11.4.1)$$

$$\dot{x}_2 = -x_3 + x_4 \quad (11.4.2)$$

$$\dot{x}_3 = \frac{-f(x_1)}{m} + \frac{k_a}{m}x_2 - \frac{c_a}{m}x_3 + \frac{c_a}{m}x_4 - \frac{u(t)}{M} \quad (11.4.3)$$

$$\dot{x}_4 = \frac{-k_a}{M}x_2 + \frac{c_a}{M}x_3 - \frac{c_a}{M}x_4 + \frac{u(t)}{M} \quad (11.4.4)$$

where $f(x_1)$ is the linear tyre force function given as follow:

$$f(x_1) = \begin{cases} k_t x_1 & x_1 \leq \frac{(M+m) \times g}{k_t} \\ (M+m) \times g & x_1 > \frac{(M+m) \times g}{k_t} \end{cases} \quad (11.4.5)$$

In (11.4.1) – (11.4.5), k_a and k_t are the spring coefficients; c_a is the damping coefficient; m is the wheel mass; M is the body mass; and g is the force of gravity.

This suspension system is controlled by the force generator, denotes by the control u .

The objective is to minimize

$$\int_0^2 (400000x_1^2 + 30000x_2^2 + \dot{x}_4^2) dt \quad (11.4.6)$$

subject to the dynamics in Eq (11.4.1) – (11.4.5). The cost functional (11.4.6)

aims to minimize the effect of the tyre deformation, suspension deflection and

the body acceleration. In addition to the above, we also impose bounds for the

11.4 Optimal Control Formulation of the Vehicle Suspension Problem

tyre deformation and the suspension deflection variables:

$$-0.025 \leq x_1 \leq 0.025 \quad (11.4.7)$$

and

$$-0.1 \leq x_2 \leq 0.1 \quad (11.4.8)$$

Apply the solution method introduced in section 11.3 together with the control

parametrization enhancing technique (CPET), the problem becomes (P^{CPET}):

$$\text{Min} \int_0^N (400000x_1^2 + 30000x_2^2 + \dot{x}_4^2)v(s)ds \quad (11.4.9)$$

such that

$$\hat{\mathbf{x}} = v(s)\dot{\mathbf{x}}, \quad (11.4.10)$$

where $\dot{\mathbf{x}} = [\dot{x}_1 \ \dot{x}_2 \ \dot{x}_3 \ \dot{x}_4]^T$ as defined in (11.4.1) – (11.4.5)

subject to canonical constraints

$$\int_0^N v(s)ds = 2.0 \quad (11.4.11)$$

all-time continuous state inequality constraints

$$x_1 + 0.025 \geq 0 \quad (11.4.12)$$

$$0.025 - x_1 \geq 0 \quad (11.4.13)$$

$$x_2 + 0.1 \geq 0 \quad (11.4.14)$$

$$0.1 - x_2 \geq 0 \quad (11.4.15)$$

and the constraints for the enhanced switching controls

$$\hat{u}_1 + \hat{u}_2 = 1 \quad (11.4.16)$$

11.4 Optimal Control Formulation of the Vehicle Suspension Problem

$$\left(\frac{(M+m) \times g}{k_t} - x_1 \right) \hat{u}_1 + \left(x_1 - \frac{(M+m) \times g}{k_t} \right) \hat{u}_2 \geq 0 \quad (11.4.17)$$

$$\frac{1}{12} + \beta - \text{variance}(\hat{u}_1, \hat{u}_2) \geq 0 \quad (11.4.18)$$

A state dependent optimal control problem (P^{CPET}) is formed by (11.4.11) – (11.4.18) and in the form that (P^{CPET}) can be solved by MISER3.

11.5 Numerical Results

The following physical parameters in appropriate SI units are used in our analysis:

$$k_t = 300000; k_a = 16812; c_a = 1000; m = 59; M = 290; g = 9.81$$

and the objective is to minimize

$$\int_0^2 (400000x_1^2 + 30000x_2^2 + \dot{x}_4^2) dt$$

with initial conditions $\mathbf{x}(0) = [0.0225, -0.01, 0, 0]^T$.

Applying the solution method together with CPET, we obtain the plots of the optimal state trajectories, $x_1(t)$ – the tyre deformation and $x_2(t)$ – the suspension deflection, against time in Figures 11.5.1 and 11.5.2 respectively.

Both the states variables are well within their associated bounds. The purpose of active vehicle suspension design is to provide a smooth and comfortable ride.

This can be accomplished by minimizing the effect of the tyre deformation,

suspension deflection and the body acceleration. The tyre deformation decreases significantly at the beginning and maintain near zero throughout the rest of the time horizon. The suspension deflection fluctuates around zero with a decrease in magnitude. Figure 11.5.3 is a zoomed plot for the tyre deformation at the very beginning for clarity. Figures 11.5.4 and 11.5.5 are zoomed plots for the two enhanced switching controls. From the figures, we can also accurately determine the time of the switching on the tyre force function $f(x_1)$:

$$f(x_1) = \begin{cases} k_t x_1 & t \geq 2.005 \times 10^{-2} \\ (M + m) \times g & t < 2.005 \times 10^{-2} \end{cases} \quad (11.5.1)$$

Figure 11.5.6 depicted the graph of the body acceleration vs. time. The body acceleration changes rapidly at the beginning of the ride but is quickly minimized near zero, which ensure better ride comfort.

Another Numerical Example (a non-flat road surface)

In this example, we consider a non-flat road surface with equation

$$r(t) = 0.05(1 - \cos(\pi + \pi t)). \quad (11.5.2)$$

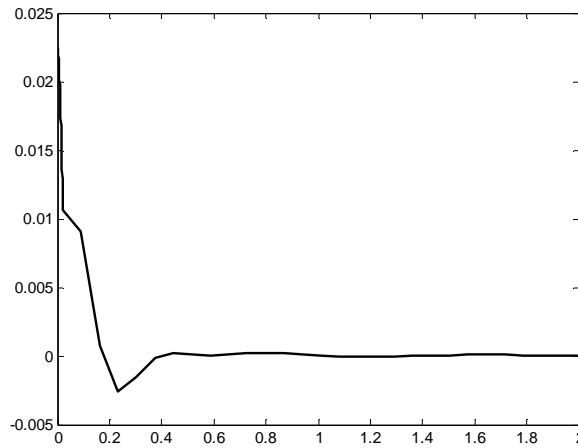


Figure 11.5.1 The tyre deformation, $x_1(t)$. (Flat Road Surface)

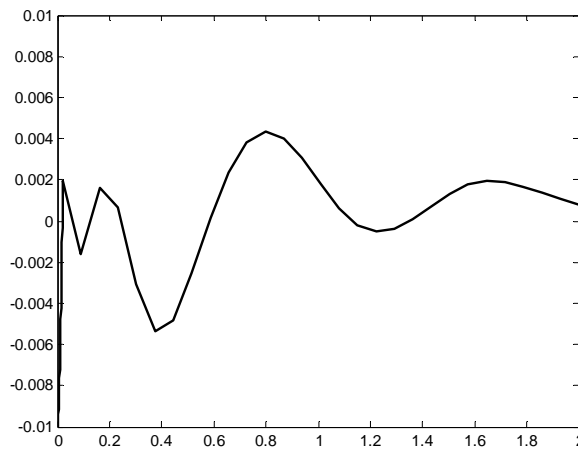


Figure 11.5.2 The suspension deflection, $x_2(t)$. (Flat Road Surface)

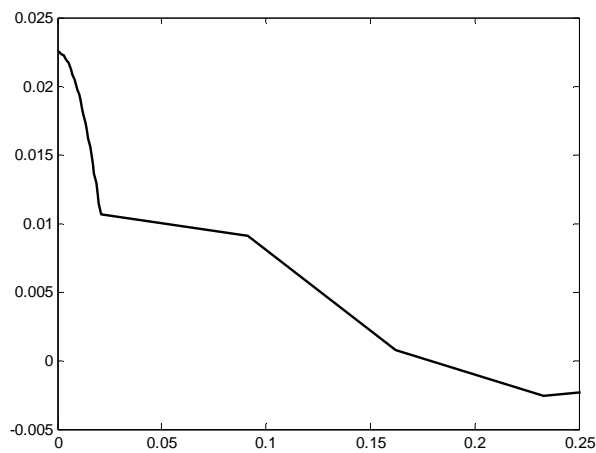


Figure 11.5.3 Zoomed plot of the tyre deformation, $x_1(t)$. (Flat Road Surface)

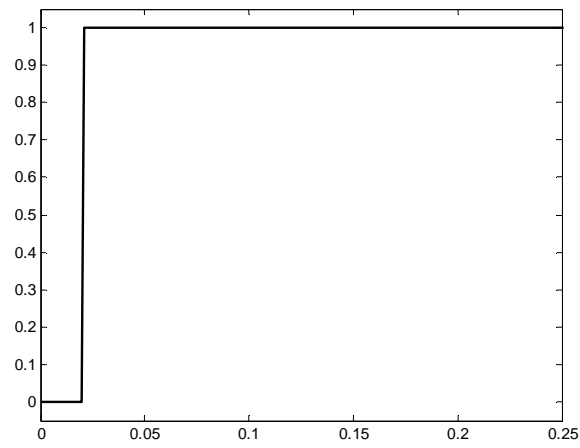


Figure 11.5.4 Zoomed plot of the enhanced switching control, $\hat{u}_1(t)$. (Flat Road Surface)

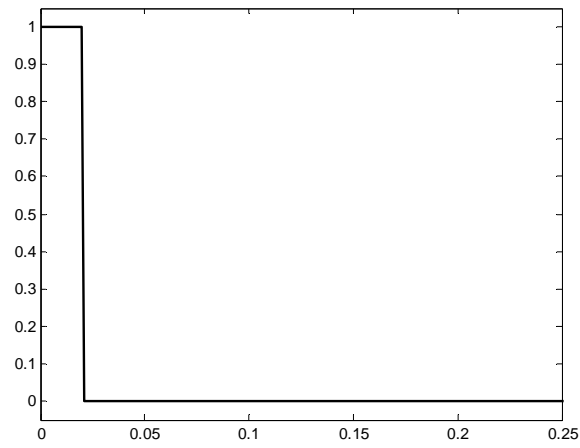


Figure 11.5.5 Zoomed plot of the enhanced switching control, $\hat{u}_2(t)$. (Flat Road Surface)

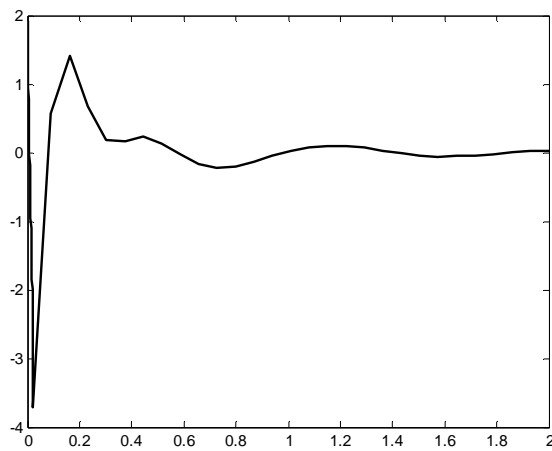


Figure 11.5.6 The body acceleration, $\dot{x}_4(t)$. (Flat Road Surface)

A slight modification to (11.4.1) is required to model this non-flat road surface:

$$\dot{x}_1 = x_3 - \dot{r}(t) = x_3 - 0.05\pi(\sin(\pi + \pi t)) \quad (11.5.3)$$

The problem is then solved by MISER3 and relevant figures are depicted in figures 11.5.7 – 11.5.10. In this example, the tyre deformation decreases significantly at the beginning and maintain near zero throughout the rest of the time horizon (similar to the one for the flat road surface). The suspension deflection fluctuates around zero at the beginning and then shifted away from zero near the end. The body acceleration changes rapidly at the beginning of the ride but then try to stabilize near zero at the end. Although the suspension deflection fluctuates away from zero, the body acceleration seems to be quite steady that this should ensure better ride comfort.

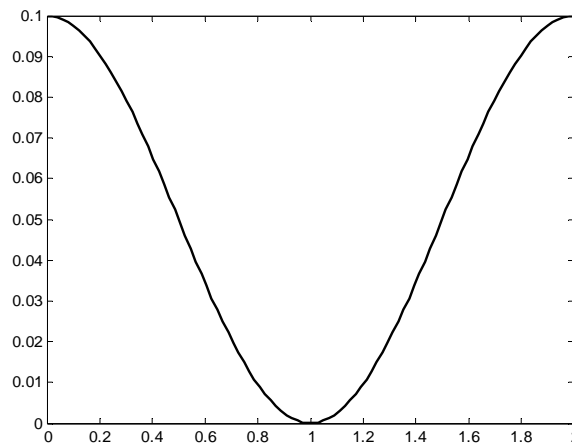


Figure 11.5.7 The non-flat surface

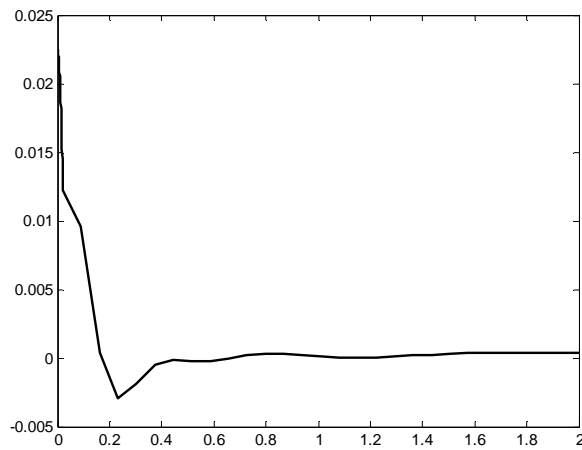


Figure 11.5.8 The tyre deformation, $x_1(t)$. (Non-flat Road Surface)

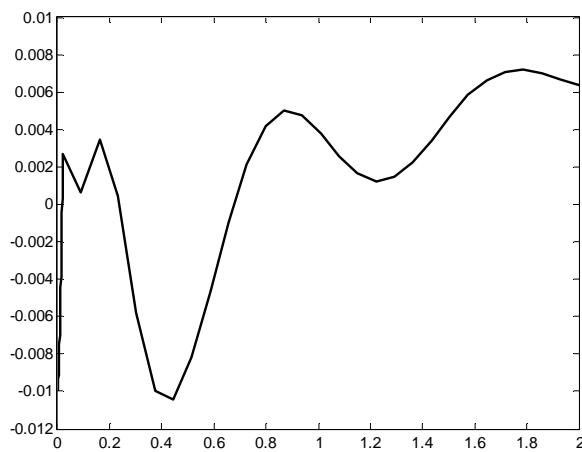


Figure 11.5.9 The suspension deflection, $x_2(t)$. (Non-flat Road Surface)

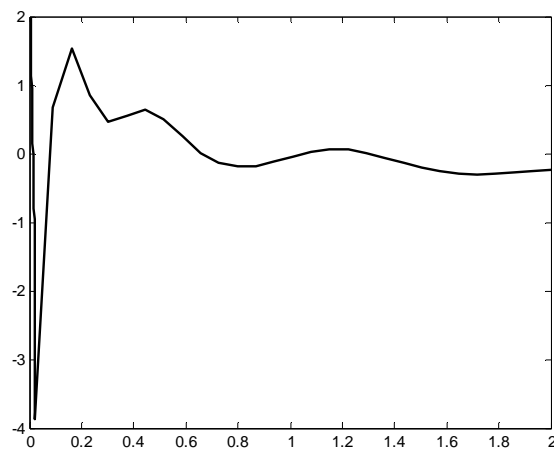


Figure 11.5.10 The body acceleration, $\dot{x}_4(t)$. (Non-flat Road Surface)

Chapter 12

Concluding Remarks and Future Research Directions

12.1 Part I: Co-ordinated Supply Chain Model

This part of the thesis further explores the synchronized cycles model. Some enhancements on the model are developed and limitations of the model are discussed through numerical examples. A novel investigation in the vendor-buyer's cost proportion on the effect of co-ordination model is presented and the situation when the co-ordination work in terms of vendor-buyer's cost proportion is discussed. This investigation is not common in previous studies. Further, according to Sarmah et al. (2006) there was very little work available on the modeling of vendor inventory depletion with heterogeneous buyers. This part of the thesis not only tackles the vendor inventory depletion model but also develops a supply chain model by including vehicle scheduling with heterogeneous buyers. The thesis also investigates demand heterogeneity among buyers, e.g. different values of mean demand, variance and skewness, which has not been considered in previous researches. The numerical results show that the demand heterogeneity does make a difference in the total system cost, the performance of supply chain models, and the co-ordination decisions.

Chapter 4 applies meta-heuristics to obtain “near-optimal” solutions to the synchronized cycles algorithm. A modified genetic algorithm (GA) with two sets of mutation rates is developed. The global mutation rate, same as the non-uniform mutation rate in Cheung et al (2001, 2005), applies to the whole population and decreases as the GA evolves. The local mutation rate applies to a single chromosome within a population, the lowest rate applied to the fittest chromosome and the highest applied to the worst according to their fitness values (i.e. the total system cost of the synchronized cycles model). With the non-uniform local mutation rate the GA can evolve faster towards the “near-optimal” solution. Even with homogeneous population, the non-uniform local mutation rate can be applied to the same chromosome for more constructive local searches. Simulated annealing (SA) is also considered. Comparing the results of the GA and the SA, GA yields a better solution in most of the trials but SA converges faster in terms of computational time. This leads to the design of a hybrid meta-heuristic that combines the pros of GA and SA, namely the genetic algorithm-simulated annealing (GASA) heuristic. Numerical examples show that GASA provide better “near-optimal” solutions than the one obtained by the synchronized cycles algorithm. The solutions obtained by the GASA are compared to the “optimal” solution using “reduced enumerative search”.

GASA is capable of obtaining a better solution compared to the SCA, and requires far less computational time. Therefore, the meta-heuristic (GASA) developed in this chapter can act as benchmarks for the SCA or other algorithms attempted to solve similar supply chain models.

In chapter 5, sensitivity on the total cost improvement of the SCA over the independent policy is examined. The change in standard parameters (i.e. demand, transportation cost, ordering cost, buyer's holding cost, vendor's set-up cost and vendor's holding cost) of the model, and the proportion borne by the vendor under independent policy are investigated. In addition, reasonable bounds on certain decision variables are developed in order to enhance the synchronized cycles algorithm. Extensions of the synchronized cycles model is considered by introducing transportation costs of trucks with and without limited capacities. Numerical results reveal that the synchronized cycles model out-performs the independent policy in terms of both shipment scheduling and the total system cost by its "synchronization" characteristic.

Chapter 6 investigates demand heterogeneity among buyers on the effect of total system cost, such an analysis is a novel analysis in the field of supply chain

management. The three supply chain models, the independent model, the common cycle model and the synchronized cycles model, are compared. The total cost for the common cycle model is insensitive to the deviation effect; while the total costs for the independent model and the synchronized cycles model decrease as the deviation increases. Further, as the deviation increases, the synchronized cycles model seems to out-perform the independent model at a lesser degree. However, the deviation effect cannot be totally eliminated.

Numerical experiments are carried out to identify conditions when the demand heterogeneity, e.g. different values of mean demand, variance and skewness, work well for the co-ordination models. The results are summarized and presented in section 6.4 and tables 6.4.3 – 6.4.4. Compared to the independent policy, the synchronized cycles model is more better off if there are relatively more buyers, lower mean demand, and lower demand variance. The skewness does not affect the differences between the independent policy and the synchronized cycles model.

The study on demand heterogeneity of buyers is only at the infancy stage. For further research, more explorations can be considered regarding this issue in supply chain co-ordination models. Moreover, a study of stochastic version of

the synchronized cycles model can be conducted.

12.2 Part II: Optimal Control Problems

This part of the thesis consists of four open problems in different areas. The optimal control software package, MISER3, has been intensively used to tackle the problems effectively with high accuracy. Optimal control techniques have been developed and applied to solve the mathematical and computational difficulties encountered by the problems. Numerical examples are provided to demonstrate the effectiveness of the methods. All the results obtained are significant.

In chapter 8, optimal control approach is used to obtain the optimal production schedule for a single-vendor-single-buyer supply chain system with Ornstein Uhlenbeck demand process. This demand process is seldom considered in the field of supply chain management. Both the inventory level and production level for the two echelons are analytically solved using Pontryagin's maximum principle. In addition, an approximation method is developed for non-cooperative situation. In this chapter, three different levels of information

sharing practices – decentralized level (with no information sharing), co-ordinated level (with information sharing), and centralized level (VMI) – are compared. From the results, the lower level is worse off under the VMI scheme. This result confirms with previous research findings that the upper level would transfer a portion of his cost to the lower level. However the total system cost has substantial savings. Hence, under the VMI co-ordination, the lower level should realize that it does not worth to share the demand information to the upper level since such sharing only benefits the upper level. Therefore, some kinds of price-discount schemes are necessary for the upper level in order to entice the lower level to share its demand information, as well as the cost parameters for the VMI coordination. For further research, a more practical and reality situation can be considered: (*i*) inventory and production constraints can be imposed; (*ii*) the model can be extended to multi-vendor-multi-buyer system; and (*iii*) inclusion of the production and delivery lead times.

Chapter 9 considers the maximum volume pillar problem which can be considered as an extension for the Dido's problem. Green's Theorem is applied in the formulation of the problem such that the problem can be transformed into canonical form handled by MISER3. For the case of multiple pillars, a novel

elliptic separation technique is successfully used to ensure that the cross-sectional regions of any pillars are separated. The major difficulty in solving this kind of optimal control problem is to deal with the “all-time” continuous inequality constraint. Unlike most of the existing optimal control problems, the n -pillar problem solely consists of “all-time” inequality constraints and thus a large amount of effort, in terms of numerical computation, is needed to overcome the difficulties. The results to the isoperimetric pillar problem provide useful information in the optimal shape of pillar building in construction design. An interesting and challenging future investigation regarding this kind of problems can be the isoparmetric pillar problem – different shapes of pillars having equal perimeter of the base area, equal surface area, and equal volume.

In chapter 10, simulations and optimal control approach are introduced in solving the vibration damping problem of a vertically flexible rotating beam under the effect of gravity. Consider the PCLD treated beam, simulation results suggest the use of a thicker constraining layer and a thinner VEM layer to minimize deflection. For ACLD treatment, the problem is solved successfully using MISER3, despite the fact that highly complicated non-linear differential equations are introduced. The solution to the optimal problem yields a

substantial improvement in the damping performance and lesser tracking deflection of the beam. Switching times of the controls can be accurately determined by the use of CPET. The results also demonstrates that variable control gains with one and three switchings applied to the ACLD treated beam result in better damping performance and reduced control effort. Further research can be focused on the study of placing multiple actuators with different dimensions. The CPET technique may also be extended to determine the optimal number of piezoelectric actuators, dimension of each actuator, and their locations on the beam.

Chapter 11 considers a nonlinear model of vehicle suspension problem with state dependent ordinary differential equations. Computational method by using enhanced switching controls in solving this kind of problem is described. Numerical examples for flat and non-flat road surfaces are presented. From the outputs, the magnitudes of tyre deformation and suspension deflection are reduced significantly at the beginning of the ride. This guarantees better road handling. Further, the body acceleration is also reduced dramatically to ensure better ride comfort. Therefore it can be concluded that the active suspension system designed with enhanced switching controls is quite effective in providing

a smoother and more comfortable ride. For further investigation, the model can be extended to include more complex state dependent ODEs applying to the full vehicle suspension problem.

Appendix - Datasets

Set 01 (5 Buyers; $S_v = 250$; $h = 0.005$)

<i>Buyer i</i>	<i>d_i</i>	<i>C_i</i>	<i>A_i</i>	<i>h_i</i>
1	8	40	20	0.008
2	15	40	15	0.009
3	10	40	6	0.010
4	5	40	10	0.010
5	20	40	18	0.007

Set 02 – Set 11 (15 Buyers; $S_v = 250$; $h = 0.003$)

Set 02

<i>Buyer i</i>	<i>d_i</i>	<i>C_i</i>	<i>A_i</i>	<i>h_i</i>
1	8	1	21	0.008
2	15	1	14	0.009
3	10	1	7	0.010
4	5	1	15	0.010
5	20	1	6	0.007
6	31	1	2	0.045
7	5	1	10	0.021
8	14	1	15	0.050
9	12	1	7	0.044
10	9	1	6	0.080
11	20	1	9	0.092
12	4	1	12	0.032
13	5	1	7	0.011
14	28	1	12	0.060
15	2	1	11	0.072

Set 03

<i>Buyer i</i>	<i>d_i</i>	<i>C_i</i>	<i>A_i</i>	<i>h_i</i>
1	3	19	7	0.018
2	32	21	15	0.048
3	16	12	16	0.062
4	2	13	20	0.031
5	8	20	18	0.013
6	31	26	13	0.100
7	3	12	8	0.072
8	32	13	8	0.010
9	1	18	7	0.053
10	37	17	12	0.065
11	11	22	24	0.045
12	15	16	19	0.015
13	5	24	22	0.084
14	34	15	3	0.081
15	26	6	12	0.030

Set 04

<i>Buyer i</i>	<i>d_i</i>	<i>C_i</i>	<i>A_i</i>	<i>h_i</i>
1	21	22	9	0.076
2	25	30	14	0.050
3	25	25	23	0.046
4	26	22	16	0.069
5	15	15	19	0.011
6	6	4	10	0.091
7	2	20	24	0.011
8	27	11	8	0.067
9	6	5	16	0.026
10	10	18	6	0.059
11	20	25	8	0.068
12	39	21	20	0.065
13	28	30	21	0.039
14	31	29	6	0.051
15	37	2	19	0.040

Set 05

<i>Buyer i</i>	<i>d_i</i>	<i>C_i</i>	<i>A_i</i>	<i>h_i</i>
1	22	11	4	0.016
2	20	17	20	0.093
3	27	8	4	0.072
4	14	18	8	0.052
5	35	2	7	0.032
6	15	18	16	0.037
7	32	22	20	0.078
8	28	29	3	0.071
9	21	23	24	0.035
10	30	23	19	0.064
11	6	13	19	0.027
12	10	20	5	0.005
13	38	25	7	0.021
14	15	3	11	0.088
15	34	29	6	0.057

Set 06

<i>Buyer i</i>	<i>d_i</i>	<i>C_i</i>	<i>A_i</i>	<i>h_i</i>
1	16	28	10	0.096
2	38	19	3	0.084
3	3	8	22	0.079
4	2	27	5	0.045
5	9	16	5	0.082
6	23	22	25	0.079
7	33	13	18	0.079
8	37	29	2	0.020
9	4	3	9	0.074
10	37	17	21	0.006
11	35	9	23	0.096
12	3	26	1	0.070
13	21	11	19	0.083
14	17	21	14	0.036
15	8	2	6	0.049

Set 07

<i>Buyer i</i>	<i>d_i</i>	<i>C_i</i>	<i>A_i</i>	<i>h_i</i>
1	10	11	7	0.087
2	9	15	8	0.076
3	40	14	20	0.074
4	36	17	3	0.094
5	33	19	14	0.083
6	14	4	9	0.043
7	1	27	5	0.007
8	39	23	6	0.008
9	4	24	22	0.072
10	7	25	13	0.061
11	18	21	5	0.092
12	28	7	2	0.086
13	7	9	7	0.038
14	9	19	17	0.034
15	4	17	17	0.020

Set 08

<i>Buyer i</i>	<i>d_i</i>	<i>C_i</i>	<i>A_i</i>	<i>h_i</i>
1	2	2	4	0.006
2	4	3	22	0.034
3	24	9	5	0.041
4	6	13	16	0.041
5	20	15	24	0.038
6	4	28	21	0.030
7	27	18	23	0.061
8	20	10	21	0.016
9	6	15	3	0.026
10	5	18	7	0.087
11	2	5	20	0.078
12	2	25	23	0.045
13	8	29	6	0.055
14	7	18	1	0.009
15	15	1	19	0.089

Set 09

<i>Buyer i</i>	<i>d_i</i>	<i>C_i</i>	<i>A_i</i>	<i>h_i</i>
1	20	25	15	0.037
2	20	19	14	0.043
3	28	22	4	0.058
4	18	3	23	0.041
5	3	13	10	0.086
6	38	12	22	0.039
7	17	5	21	0.090
8	5	25	8	0.021
9	14	26	20	0.098
10	36	14	17	0.042
11	14	29	5	0.022
12	35	5	10	0.049
13	7	27	18	0.031
14	15	24	4	0.075
15	16	14	3	0.061

Set 10

<i>Buyer i</i>	<i>d_i</i>	<i>C_i</i>	<i>A_i</i>	<i>h_i</i>
1	32	19	2	0.006
2	25	29	22	0.063
3	24	20	21	0.051
4	17	8	10	0.011
5	10	11	12	0.020
6	24	6	20	0.023
7	21	15	22	0.031
8	8	13	6	0.010
9	19	14	16	0.091
10	28	19	15	0.073
11	26	3	10	0.015
12	12	10	15	0.087
13	13	19	6	0.046
14	32	6	16	0.050
15	39	19	25	0.029

Set 11

<i>Buyer i</i>	<i>d_i</i>	<i>C_i</i>	<i>A_i</i>	<i>h_i</i>
1	35	8	1	0.022
2	19	18	1	0.060
3	33	16	23	0.072
4	33	14	11	0.095
5	33	17	23	0.018
6	39	29	17	0.081
7	27	11	20	0.008
8	16	13	19	0.025
9	33	10	1	0.034
10	31	13	7	0.079
11	36	9	7	0.054
12	39	12	16	0.060
13	27	16	23	0.030
14	9	22	12	0.009
15	6	10	13	0.042

Set 12 – Set 21 (30 Buyers; $S_y = 3,000$; $h = 0.0028$)

Set 12

Buyer <i>i</i>	<i>d_i</i>	<i>C_i</i>	<i>A_i</i>	<i>h_i</i>	Buyer <i>i</i>	<i>d_i</i>	<i>C_i</i>	<i>A_i</i>	<i>h_i</i>
1	8	1	21	0.008	16	13	1	9	0.003
2	15	1	14	0.009	17	7	1	10	0.033
3	10	1	7	0.010	18	15	1	18	0.067
4	5	1	15	0.010	19	23	1	17	0.087
5	20	1	6	0.007	20	9	1	17	0.050
6	31	1	2	0.045	21	26	1	18	0.023
7	5	1	10	0.021	22	19	1	8	0.049
8	14	1	15	0.050	23	3	1	10	0.005
9	12	1	7	0.044	24	18	1	16	0.062
10	9	1	6	0.080	25	5	1	6	0.041
11	20	1	9	0.092	26	11	1	3	0.091
12	4	1	12	0.032	27	5	1	2	0.013
13	5	1	7	0.011	28	27	1	7	0.002
14	28	1	12	0.060	29	33	1	8	0.055
15	2	1	11	0.072	30	17	1	17	0.008

Set 13

Buyer <i>i</i>	<i>d_i</i>	<i>C_i</i>	<i>A_i</i>	<i>h_i</i>	Buyer <i>i</i>	<i>d_i</i>	<i>C_i</i>	<i>A_i</i>	<i>h_i</i>
1	16	16	23	0.167	16	25	24	28	0.434
2	37	16	35	0.207	17	27	29	32	0.620
3	11	6	3	0.449	18	5	8	15	0.575
4	17	23	24	0.511	19	32	11	36	0.446
5	47	25	17	0.326	20	19	15	7	0.570
6	29	19	27	0.226	21	33	7	24	0.525
7	29	30	4	0.763	22	38	12	6	0.064
8	37	22	31	0.444	23	13	12	33	0.690
9	13	16	30	0.260	24	47	23	12	0.016
10	39	10	25	0.517	25	25	27	37	0.787
11	30	5	18	0.334	26	45	11	4	0.142
12	34	19	33	0.178	27	46	4	12	0.216
13	32	14	39	0.368	28	16	20	25	0.243
14	4	2	32	0.615	29	34	10	18	0.350
15	20	9	37	0.135	30	27	6	35	0.496

Set 14

<i>Buyer i</i>	<i>d_i</i>	<i>C_i</i>	<i>A_i</i>	<i>h_i</i>	<i>Buyer i</i>	<i>d_i</i>	<i>C_i</i>	<i>A_i</i>	<i>h_i</i>
1	33	2	2	0.120	16	47	3	29	0.186
2	25	12	10	0.273	17	26	6	16	0.763
3	10	1	38	0.424	18	29	19	32	0.007
4	4	3	31	0.298	19	11	1	23	0.126
5	35	9	28	0.064	20	22	15	34	0.184
6	31	4	16	0.715	21	11	14	18	0.474
7	41	27	29	0.183	22	3	17	26	0.421
8	4	7	1	0.214	23	45	12	30	0.433
9	46	8	7	0.284	24	34	17	32	0.171
10	33	12	31	0.245	25	50	28	24	0.197
11	28	27	16	0.028	26	42	5	18	0.577
12	18	5	5	0.332	27	5	14	6	0.037
13	42	29	14	0.200	28	45	27	6	0.315
14	40	11	11	0.376	29	50	7	35	0.161
15	43	13	34	0.461	30	10	19	17	0.594

Set 15

<i>Buyer i</i>	<i>d_i</i>	<i>C_i</i>	<i>A_i</i>	<i>h_i</i>	<i>Buyer i</i>	<i>d_i</i>	<i>C_i</i>	<i>A_i</i>	<i>h_i</i>
1	48	15	32	0.222	16	28	5	8	0.555
2	21	30	26	0.714	17	45	11	39	0.604
3	21	15	34	0.228	18	31	5	17	0.228
4	16	8	18	0.374	19	20	7	28	0.483
5	20	18	16	0.437	20	26	29	4	0.456
6	35	12	26	0.014	21	29	3	12	0.585
7	27	14	34	0.627	22	37	25	6	0.689
8	45	3	7	0.737	23	19	16	27	0.277
9	5	15	34	0.221	24	9	25	11	0.751
10	13	24	4	0.153	25	12	21	19	0.259
11	40	23	5	0.379	26	29	18	34	0.493
12	38	6	13	0.200	27	27	5	28	0.455
13	22	16	37	0.035	28	5	7	28	0.532
14	24	22	3	0.179	29	45	25	16	0.431
15	20	24	17	0.452	30	47	13	27	0.087

Set 16

<i>Buyer i</i>	<i>d_i</i>	<i>C_i</i>	<i>A_i</i>	<i>h_i</i>	<i>Buyer i</i>	<i>d_i</i>	<i>C_i</i>	<i>A_i</i>	<i>h_i</i>
1	3	12	16	0.253	16	4	23	25	0.629
2	11	11	19	0.195	17	38	21	15	0.016
3	49	25	15	0.016	18	31	14	20	0.121
4	21	3	14	0.733	19	47	27	4	0.402
5	7	25	24	0.166	20	32	18	10	0.465
6	27	9	22	0.128	21	18	17	37	0.437
7	23	14	9	0.541	22	12	19	30	0.482
8	6	2	19	0.607	23	40	15	1	0.511
9	19	21	29	0.179	24	13	29	23	0.069
10	2	25	21	0.506	25	34	18	24	0.645
11	49	10	22	0.284	26	6	7	21	0.425
12	6	13	27	0.647	27	37	7	25	0.167
13	30	17	3	0.506	28	26	7	10	0.690
14	12	22	38	0.775	29	21	23	13	0.039
15	44	5	17	0.165	30	49	22	23	0.679

Set 17

<i>Buyer i</i>	<i>d_i</i>	<i>C_i</i>	<i>A_i</i>	<i>h_i</i>	<i>Buyer i</i>	<i>d_i</i>	<i>C_i</i>	<i>A_i</i>	<i>h_i</i>
1	48	29	8	0.436	16	16	11	4	0.330
2	34	18	20	0.200	17	37	7	16	0.174
3	12	9	35	0.614	18	9	12	33	0.378
4	45	16	3	0.401	19	6	27	15	0.725
5	23	24	11	0.764	20	31	22	6	0.029
6	2	24	9	0.095	21	3	29	9	0.746
7	28	26	24	0.677	22	44	25	33	0.738
8	20	30	29	0.186	23	5	24	15	0.040
9	3	16	29	0.448	24	22	8	19	0.271
10	5	24	8	0.157	25	48	9	14	0.253
11	20	5	26	0.372	26	30	9	20	0.416
12	38	19	10	0.511	27	40	5	6	0.165
13	42	28	13	0.085	28	12	4	37	0.266
14	27	25	25	0.629	29	12	19	31	0.709
15	17	7	1	0.314	30	14	12	15	0.119

Set 18

<i>Buyer i</i>	<i>d_i</i>	<i>C_i</i>	<i>A_i</i>	<i>h_i</i>	<i>Buyer i</i>	<i>d_i</i>	<i>C_i</i>	<i>A_i</i>	<i>h_i</i>
1	24	16	21	0.609	16	36	28	25	0.122
2	19	18	5	0.771	17	48	19	36	0.313
3	28	10	36	0.005	18	23	23	16	0.663
4	10	16	18	0.213	19	18	5	22	0.223
5	7	21	27	0.097	20	48	5	4	0.372
6	34	14	2	0.611	21	11	20	23	0.014
7	24	7	12	0.229	22	39	18	16	0.400
8	16	22	14	0.675	23	23	12	4	0.154
9	37	20	38	0.107	24	24	6	23	0.720
10	35	25	3	0.448	25	12	23	36	0.604
11	45	15	23	0.107	26	32	2	13	0.068
12	35	25	39	0.346	27	17	16	3	0.689
13	15	30	29	0.010	28	12	14	28	0.573
14	12	12	22	0.052	29	35	26	11	0.143
15	15	18	5	0.031	30	37	22	39	0.716

Set 19

<i>Buyer i</i>	<i>d_i</i>	<i>C_i</i>	<i>A_i</i>	<i>h_i</i>	<i>Buyer i</i>	<i>d_i</i>	<i>C_i</i>	<i>A_i</i>	<i>h_i</i>
1	13	3	23	0.619	16	11	26	11	0.574
2	30	18	30	0.021	17	5	21	29	0.779
3	45	9	14	0.678	18	27	20	2	0.258
4	28	5	39	0.268	19	18	30	25	0.399
5	48	12	16	0.275	20	18	12	21	0.706
6	26	29	33	0.446	21	42	23	39	0.071
7	22	5	29	0.535	22	49	12	27	0.329
8	45	22	22	0.084	23	33	14	22	0.153
9	46	3	2	0.492	24	40	24	17	0.624
10	10	18	22	0.516	25	45	2	27	0.166
11	45	14	7	0.017	26	35	26	4	0.713
12	42	27	31	0.007	27	9	1	19	0.266
13	35	11	3	0.777	28	47	30	24	0.169
14	47	21	24	0.193	29	2	14	26	0.322
15	41	16	11	0.749	30	29	10	31	0.279

Set 20

<i>Buyer i</i>	<i>d_i</i>	<i>C_i</i>	<i>A_i</i>	<i>h_i</i>	<i>Buyer i</i>	<i>d_i</i>	<i>C_i</i>	<i>A_i</i>	<i>h_i</i>
1	26	1	14	0.465	16	32	18	35	0.544
2	2	21	9	0.028	17	26	21	36	0.305
3	47	30	26	0.483	18	20	4	3	0.320
4	19	7	8	0.027	19	12	9	29	0.546
5	29	18	3	0.211	20	5	21	4	0.142
6	24	15	14	0.297	21	22	14	40	0.660
7	3	25	7	0.506	22	14	28	8	0.700
8	48	23	17	0.198	23	22	28	19	0.132
9	31	13	37	0.155	24	14	27	10	0.383
10	6	25	6	0.296	25	32	26	22	0.506
11	28	16	36	0.063	26	3	16	12	0.765
12	18	3	19	0.006	27	3	10	22	0.209
13	18	6	29	0.559	28	48	10	39	0.297
14	37	20	6	0.091	29	39	27	15	0.236
15	3	10	8	0.609	30	24	11	30	0.734

Set 21

<i>Buyer i</i>	<i>d_i</i>	<i>C_i</i>	<i>A_i</i>	<i>h_i</i>	<i>Buyer i</i>	<i>d_i</i>	<i>C_i</i>	<i>A_i</i>	<i>h_i</i>
1	20	21	13	0.553	16	35	29	22	0.576
2	39	12	15	0.214	17	27	19	12	0.174
3	18	15	21	0.644	18	17	8	2	0.545
4	36	11	28	0.355	19	3	29	26	0.174
5	8	15	25	0.132	20	19	8	39	0.295
6	11	18	33	0.506	21	32	16	7	0.314
7	20	29	18	0.778	22	4	26	9	0.252
8	17	7	17	0.064	23	2	2	35	0.249
9	15	30	14	0.511	24	19	11	5	0.466
10	10	9	30	0.548	25	27	27	37	0.514
11	29	4	29	0.691	26	4	2	8	0.689
12	19	19	2	0.259	27	27	9	26	0.486
13	27	19	29	0.769	28	15	6	27	0.024
14	32	3	16	0.493	29	18	8	38	0.570
15	14	3	16	0.384	30	35	10	25	0.713

Set 22 – Set 24 (50 Buyers; $S_y = 5,000$; $h = 0.0028$)

Set 22

<i>Buyer i</i>	<i>d_i</i>	<i>C_i</i>	<i>A_i</i>	<i>h_i</i>	<i>Buyer i</i>	<i>d_i</i>	<i>C_i</i>	<i>A_i</i>	<i>h_i</i>
1	26	10	8	0.147	26	21	18	17	0.081
2	6	5	19	0.203	27	1	13	26	0.977
3	49	27	7	0.548	28	31	22	14	0.003
4	3	14	26	0.874	29	48	6	5	0.152
5	11	24	22	0.324	30	48	4	22	0.873
6	15	17	24	0.522	31	4	26	28	0.119
7	26	12	21	0.160	32	13	11	8	0.500
8	48	17	20	0.998	33	7	9	11	0.271
9	33	10	1	0.183	34	42	11	6	0.960
10	24	16	4	0.471	35	14	4	10	0.383
11	18	21	11	0.964	36	20	16	39	0.155
12	20	24	27	0.876	37	16	20	22	0.677
13	16	15	22	0.791	38	24	10	14	0.196
14	30	8	17	0.977	39	37	17	26	0.576
15	32	12	2	0.735	40	45	29	20	0.110
16	1	9	10	0.887	41	2	26	4	0.076
17	7	11	5	0.094	42	37	7	16	0.282
18	2	11	1	0.484	43	16	2	29	0.446
19	20	13	5	0.857	44	34	26	23	0.047
20	31	17	18	0.170	45	47	25	20	0.987
21	29	26	11	0.708	46	15	14	17	0.358
22	24	24	19	0.361	47	33	15	10	0.817
23	7	7	12	0.952	48	31	1	18	0.112
24	21	14	22	0.277	49	35	20	27	0.659
25	22	22	15	0.438	50	20	2	5	0.606

Set 23

<i>Buyer i</i>	<i>d_i</i>	<i>C_i</i>	<i>A_i</i>	<i>h_i</i>	<i>Buyer i</i>	<i>d_i</i>	<i>C_i</i>	<i>A_i</i>	<i>h_i</i>
1	81	9	37	0.094	26	114	22	36	0.490
2	8	7	17	0.743	27	98	4	39	0.065
3	67	6	13	0.118	28	71	22	9	0.225
4	51	26	11	0.670	29	105	13	23	0.487
5	81	14	5	0.656	30	65	14	37	0.704
6	49	10	15	0.004	31	85	14	40	0.447
7	61	7	9	0.045	32	23	25	22	0.570
8	39	6	13	0.775	33	2	25	10	0.028
9	28	23	25	0.228	34	73	4	36	0.064
10	14	14	11	0.514	35	12	30	19	0.496
11	39	16	20	0.480	36	34	20	26	0.582
12	65	26	22	0.594	37	56	29	13	0.533
13	108	9	34	0.038	38	101	11	33	0.350
14	106	27	5	0.525	39	7	27	20	0.592
15	2	15	20	0.715	40	84	20	37	0.101
16	45	24	3	0.394	41	5	16	31	0.139
17	80	28	15	0.163	42	24	15	26	0.757
18	30	2	5	0.612	43	69	5	34	0.318
19	110	5	8	0.064	44	39	17	17	0.148
20	21	10	39	0.792	45	19	15	35	0.098
21	6	20	9	0.601	46	45	2	4	0.744
22	118	27	39	0.641	47	94	15	19	0.769
23	14	28	21	0.212	48	68	9	13	0.307
24	43	10	33	0.736	49	26	16	5	0.537
25	43	6	34	0.564	50	96	1	8	0.304

Set 24

<i>Buyer i</i>	<i>d_i</i>	<i>C_i</i>	<i>A_i</i>	<i>h_i</i>	<i>Buyer i</i>	<i>d_i</i>	<i>C_i</i>	<i>A_i</i>	<i>h_i</i>
1	104	29	13	0.339	26	30	14	4	0.358
2	78	23	40	0.766	27	27	16	16	0.750
3	35	16	32	0.609	28	102	17	36	0.307
4	62	11	23	0.733	29	56	5	18	0.280
5	73	23	38	0.169	30	68	14	18	0.064
6	104	19	37	0.694	31	116	8	37	0.485
7	25	24	26	0.625	32	70	15	17	0.144
8	85	2	10	0.372	33	5	2	2	0.564
9	17	15	34	0.778	34	33	29	27	0.643
10	75	18	37	0.679	35	55	16	15	0.630
11	103	10	24	0.638	36	1	15	11	0.671
12	48	12	20	0.603	37	109	25	3	0.609
13	14	28	24	0.611	38	43	21	10	0.176
14	26	16	21	0.332	39	30	23	29	0.408
15	55	26	30	0.051	40	7	7	8	0.550
16	72	8	35	0.491	41	113	12	24	0.139
17	70	15	35	0.705	42	51	13	24	0.776
18	10	15	14	0.151	43	14	1	24	0.475
19	19	5	39	0.417	44	95	9	35	0.449
20	108	15	15	0.228	45	94	2	11	0.232
21	90	21	13	0.614	46	53	16	4	0.581
22	64	26	15	0.403	47	106	14	35	0.316
23	26	22	35	0.629	48	87	11	1	0.519
24	69	9	34	0.705	49	45	22	5	0.168
25	3	18	21	0.217	50	74	19	9	0.170

References

1. Ali, M.M. and Storey, C., 1996, The Optimal Control of Vehicle Suspension System, Proceedings of the 2nd International Conference on Adaptive Computing in Engineering Design and Control, edited by I.C. Parmee, 167-173.
2. Ali, M.M., 2000, A Feedback Controller Design Methodology for Vehicle Suspension System, Proceedings of the International Workshop on Multi-disciplinary Design Optimization (MDO), edited by J. Snyman and K. Craig, 26-36.
3. Aliyu, M.D.S., and Andifani, A.A., 1999, Multi-Item-Multi-Plant Inventory Control of Production Systems with Shortages/Backorders, International Journal of Systems Science, 30(5), 533-539.
4. Alleyne, A., and Hedrick, J.K., 1992, Nonlinear Control of a Quarter Car Active Suspension, Proceeding of the 1992 American Control Conference, Chicago IL, 21-25.
5. Ando, Y., and Suzuki, M., 1996, Control of Active Suspension System Using the Singular Perturbation Method, Control Engineering Practice, 4(3), 287-293.
6. Ansoff, H.I., and Slevin, D.P., 1968, Comments on Professor Forrester's Industrial Dynamics - After the First Decade. Management Science, 14(9), 600.
7. Apostol, T.M., and Mnatsakanian, M.A., 2004, Isoperimetric and Isoparametric Problems, The American Mathematical Monthly, 111(2), 118-136.
8. Artle, R., and Berglund, S., 1959, A Note on Manufacturers' Choice of Distribution Channels, Management Science, 5, 460-471.
9. Axsater, S., 1985, Control Theory Concepts in Production and Inventory Control, International Journal of Systems Science, 16(2), 161-169.
10. Bainum, P.M., and Xu, J.K., 1995, Calibration of Tip Position During Maneuvers of Space-Robotic Systems, Journal of Astronautical Sciences, 43(1), 1-23.
11. Ballou, R.H., 1999, Business Logistics Management : Planning, Organizing, and Controlling the Supply Chain (London: Prentice Hall).
12. Banerjee, A., 1986, A Joint Economic-Lot-Size Model for Purchaser and Vendor, Decision Sciences, 17(3), 292-311.
13. Banerjee, A., and Banerjee, S., 1992, Coordinated, Orderless Inventory Replenishment for a Single Supplier and Multiple Buyers Through

- Electronic Data Interchange, *International Journal of Technology Management*, 7, 328-336.
14. Banerjee, A., and Burton, J.S., 1994, Coordinated vs. Independent Inventory Replenishment Policies for a Vendor and Multiple Buyers, *International Journal of Production Economics*, 35, 215-222.
 15. Baumol, W.J., and Vinod, H.D., 1970, An Inventory Theoretic Model of Freight Transport Demand, *Management Science*, 16(7), 413-421.
 16. Baz, A., and Ro, J., 1995, Optimum Design and Control of Active Constrained Layer Damping, *Journal of Vibration and Acoustics*, 117 supp., 135-144.
 17. Baz, A., and Ro, J., 2001, Vibration Control of Rotating Beams with Active Constrained Layer Damping, *Smart Materials and Structures*, 10, 112-120.
 18. Bellman, R., and Cooke, K.L., 1963, *Differential-Difference Equations* (New York: Academic Press).
 19. Bensoussan, A., Nissen, G., and Tapiero, C.S., 1975, Optimum Inventory and Product Quality Control with Deterministic and Stochastic Deterioration – An Application of Distributed Parameters Control Systems, *IEEE Transaction on Automatic Control*, 20(3), 407-412.
 20. Bouazara, M., and Richard, M.J., 2001, An Optimization Method Designed to Improve 3-D Vehicle Comfort and Road Holding Capability Through The Use of Active and Semi-Active Suspensions, *European Journal of Mechanics – A*, 20, 509-520.
 21. Boyaci, T., and Gallego, G., 2002, Coordinating Pricing and Inventory Replenishment Policies for One Wholesaler and One or More Geographically Dispersed Retailers, *International Journal of Production Economics*, 77, 95-111.
 22. Bradshaw, A., and Daintith, D., 1976, Synthesis of Control Policies for Cascaded Production Inventory Systems, *International Journal of Systems Science*, 7(9), 1053-1070.
 23. Braglia, M., and Zavanella L., Modelling an Industrial Strategy for Inventory Management in Supply Chains: The ‘Consignment Stock’ Case, *International Journal of Production Research*, 41(16), 3793-3808.
 24. Bylka, S., 1999, A Dynamic Model for the Single-Vendor Multi-Buyer Problem, *International Journal of Production Economics*, 59, 297-304.
 25. Cerny, V., 1985, A Thermodynamical Approach to the Travelling Salesman Problem: An Efficient Simulation Algorithm, *Journal of Optimization Theory and Applications*, 45, 41-51.

26. Chan, Chi-kin, Cheung, B.K.S., and Langevin, A., 2003, A., Solving the Multi-Buyer Joint Replenishment Problem with a Modified Genetic Algorithm, *Transportation Research, Part B*, Vol. 37, 291-299.
27. Chan, Chi-kin and Kingsman, B.G., 2005, A Co-ordinated Single-vendor Multi-buyer Supply Chain Model: Synchronization of Ordering and Production Cycles, *Successful Strategies in Supply Chain Management*, Idea Group Publishing, U.S.A., 1-27.
28. Chan, Chi-kin, and Kingsman B.G., 2007, Co-ordination in a Single-vendor Multi-buyer Supply Chain by Synchronizing Delivery and Production Cycles, *Transportation Research, Part E: Logistics and Transportation Review*, 43, 90-111.
29. Chen, F., Federgruen, A., and Zheng Y.S., 2001, Coordination Mechanisms for a Distribution System with One Supplier and Multiple Retailers, *Management Sciences*, 47(5), 693-708.
30. Cheung, B.K.S, 2005, Genetic Algorithm and Other Meta-Heuristics – The Essential Tools for Solving Modern Supply Chain Management Problems in “Successful Strategies in Supply Chain Management” eds: C.K. Chan and H.W.J. Lee, 144-173, (Idea Group Publishing, PA).
31. Cheung, B.K.S., Langevin, A., and Villeneuve, B., 2001, High Performing Evolutionary Techniques for Solving Complex Location Problems in Industrial System Design, *Journal of Intelligent Manufacturing*, 12, 455-466.
32. Christy, D.P., and Grout, J.R., 1994, Safeguarding Supply Chain Relationships, *International Journal of Production Economics*, 36(3), 233-242.
33. Coyle, J.J., Bardi, E.J., and Langley, C.J., 2003, *The Management of Business Logistics: A Supply Chain Perspective* (Ohio : South-Western/Thomson Learning).
34. Craven, B.D., 1995, *Control and Optimization* (London : Chapman & Hall).
35. Dejonckheere, J., Disney, S.M., Lambrecht, M.R., and Towill, D.R., 2003, The Impact of Information Enrichment on the Bullwhip Effect in Supply Chains: A Control Engineering Perspective, To Be Appear in the *European Journal of Operational Research*.
36. Dejonckheere, J., Disney, S.M., Lambrecht, M.R., Towill, D.R., 2003, Measuring and Avoiding the Bullwhip Effect: A Control Theoretic Approach, *European Journal of Operational Research*, 147(3), 567-590.
37. Disney S.M., and Towill, D.R., 2003, On the Bullwhip and Inventory Variance Produced by an Ordering Policy, *Omega*, 31(3), 157-167.

38. Disney, S.M., and Towill, D.R., 2002, A Discrete Transfer Function Model to Determine the Dynamic Stability of a Vendor Managed Inventory Supply Chain, *International Journal of Production Research*, 40(1), 179-204.
39. Dohi T., Kaio N., and Osaki S., 1995, Optimal Production Planning Under Diffusion Demand Pattern, *Mathematical and Computer Modelling*, 21(11), 35-46.
40. Dorf, R.C., and Bishop, R.H., 2001, *Modern Control Systems* (New Jersey, Prentice Hall).
41. Drezner, Z., and Wesolowsky, G.O., 1989, Multi-Buyer Discount Pricing, *European Journal of Operational Research*, 40, 38-42.
42. Elmadany, M.M., and Abduljabbar Z.S., 1999, Linear Quadratic Gaussian Control of a Quarter-Car Suspension, *Vehicle System Dynamics*, 32, 479-497.
43. Elmaghraby, S.E., 1966, *The Design of Production Systems* (New York: Reinhold).
44. Esmailzadeh, E., and Taghirad, H.D., 1998, Active Vehicle Suspension with Optimal State-Feedback Control, *International Journal of Modelling and Simulation*, 18(3), 228-238.
45. Fasana, A., and Marchesiello, S., 2001, Rayleigh-Ritz Analysis of Sandwich Beams, *Journal of Sound and Vibration*, 241(4), 643-652.
46. Forrester, J.W., 1961, *Industrial Dynamics* (Cambridge MA: MIT Press).
47. Frankline, G.F., Powell, J.D., and A. Emami-Naeini, 2002, *Feedback Control of Dynamic Systems* (London: Prentice Hall).
48. Frost, G.P., Gordon, T.J., Howell, M.N., and Wu, Q.H., 1996, Moderated Reinforcement Learning of Active and Semi-Active Vehicle Suspension Control Laws, *Proceedings of the Institution of Mechanical Engineers*, 210, 249-257.
49. Fruhauf, F., Kasper, R., and Luckel, J.L., 1985, Design of an Active Suspension for a Passenger Vehicle Model Using Input Processes with Time Delays, *Vehicle System Dynamics*, 15, 126-138
50. Fung, E.H.K., and Yau, D.T.W., 2004, Vibration Characteristics of a Rotating Flexible Arm with ACLD Treatment, *Journal of Sound and Vibration*, 269(1-2), 165-182.
51. Fung, E.H.K., Zou, J.Q., and Lee, H.W.J., 2004, Lagrangian Formulation of Rotating Beam with Active Constrained Layer Damping in Time Domain Analysis, *Journal of Mechanical Design*, 126(2), 359-364.
52. Goldberg, D.E, 1989, *Genetic Algorithms in Search, Optimization &*

- Machine Learning (Addison Wesley).
53. Gonedes, N.J., and Lieber, Z., 1974, Production Planning for a Stochastic Demand Process, *Operations Research*, 22(4), 771-787.
 54. Gordon, T.J., and Best, M.C., 1994, Dynamic Optimization of Nonlinear Semi-Active Suspension Controllers, *International Conference on Control* (Conventry, UK), 1, 332-337.
 55. Gordon, T.J., Marsh, C., and Milsted, M.G., 1991, A Comparison of Adaptive LQG and Nonlinear Controllers for Vehicle Suspension Systems, *Vehicle System Dynamics*, 20, 321-340.
 56. Goulliaev, V.I., and Zavrazhina, T.V., 2001, Dynamics of a Flexible Multi-Link Cosmic Robot Manipulator, *Journal of Sound and Vibration*, 243(4), 641-657.
 57. Goyal, S.K., 1976, An Integrated Inventory Model for a Single Supplier-single Customer Problem. *International Journal of Production Research*, 15(1), 107-111.
 58. Goyal, S.K., 1988, A Joint Economic-Lot-Size Model for Purchaser and Vendor: A Comment, *Decision Sciences*, 19, 236-241.
 59. Goyal, S.K., 1995, A One-Vendor Multi-Buyer Integrated Inventory Model: A Comment, *European Journal of Operational Research*, 82, 209-210.
 60. Goyal, S.K., 2000, On Improving the Single-Vendor Single-Buyer Integrated Production-Inventory Model with a Generalized Policy, *European Journal of Operational Research*, 125, 429-430.
 61. Goyal, S.K., and Gupta, Y.P., 1989, Integrated Inventory Models: The Buyer-vendor coordination, *European Journal of Operational Research*, 41(3), 261-269.
 62. Goyal, S.K., and Srinivasan, G., 1992, The Individually Responsible and Rational Decision Approach to Economic Lot Sizes for One Vendor and Many Purchasers: A Comment, *Decision Sciences*, 21(3), 492-506.
 63. Gurnani, H., 2001, A Study of Quantity Discount Pricing Models with Different Ordering Structures: Order Coordination, Order Consolidation, and Multi-Tier Ordering Hierarchy, *International Journal of Production Economics*, 72, 203-225.
 64. Hac, A., 1985, Suspension Optimization of a 2-DOF Vehicle Model Using a Stochastic Optimal Control Technique', *Journal of Sound and Vibration*, 100(3), 343-357.
 65. Hac, A., 1987, Adaptive Control for Vehicle Suspension, *Vehicle System Dynamic*, 16, 57-74.
 66. Harpaz, G., Lee, W.Y., and Winkler, R.L., 1982, Learning, Experimentation,

- and the Optimal Output Decisions of a Competitive Firm, *Management Science*, 28(6), 589-603.
67. Hau, L.C., and Fung E.H.K., 2004, Effect of ACLD Treatment Configuration on Damping Performance of a Flexible Beam, *Journal of Sound and Vibration*, 269(3-5), 549-567.
 68. Heath, T.L., 1956, *Euclid – The Thirteen Books of The Elements*, New York: Dover Publications, 2nd edition.
 69. Hill, R.M., 1997, The Single-Vendor Single-Buyer Integrated Production-Inventory Model with a Generalised Policy, *European Journal of Operational Research*, 97, 493-499.
 70. Hill, R.M., 1999, The Optimal Production and Shipment Policy for the Single-Vendor Single-Buyer Integrated Production-Inventory Problem, *International Journal of Production Research*, 37(11), 2463-2475.
 71. Hill, R.M., and Omar, M., 2006, Another Look at the Single-Vendor Single-Buyer Integrated Production-Inventory Problem, *International Journal of Production Research*, 44(4), 791-800.
 72. Hocking, L.M., 1991, *Optimal Control: An Introduction to the Theory with Applications* (New York : Clarendon Press).
 73. Holland, J.H., 1975, *Adaptation in Natural and Artificial Systems*, (Michigan Press)
 74. Hrovat, D., 1990, Optimal Active Suspension Structures for Quarter-Car Vehicle Models, *Automatica*, 26(5), 845-860.
 75. Hrovat, D., 1997, Survey of Advanced Suspension Developments and Related Optimal Control Applications, *Automatica*, 33(10), 1781-1817.
 76. Jennings, L.S., Fisher, M.E, Teo, K.L., and Goh, C.J., 1990, *MISER3 Optimal Control Software: Theory and User Manual*, EMCROSS (Pty) Ltd.
 77. Jennings, L.S., Fisher, M.E, Teo, K.L., and Goh, C.J. (2004). *MISER3 Optimal Control Software: Version 3. Theory and User Manual*. (<http://www.maths.uwa.edu.au/~les/miser3.3.html>)
 78. Joglekar, P., and Tharthare, S., 1990, The Individually Responsible and Rational Decision Approach to Economic Lot Sizes for One Vendor and Many Purchasers, *Decision Sciences*, 21(3), 492-506.
 79. Johnson, G.D., and Thompson, H.E., 1975, Optimality of Myopic Inventory Policies for Certain Dependent Demand Process, *Management Science*, 21(11), 1303-1307.
 80. Karlsson, N., Dahleht, M., and Hrovat D., 2001, Nonlinear Active Suspension with Preview, *Proceedings of the American Control Conference*, Arlington, VA, 2640-2645.

81. Karmark, U.S., and Patel, N.R., 1977, The One-Period, N-Location Distribution Problem, *Naval Research Logistics Quarterly*, 24(4), 559-575.
82. Kelle, P., and Akbulut, A., 2005, The Role of ERP tools in Supply Chain Information Sharing, Cooperation, and Cost Optimization, *International Journal of Production Economics*, 93-94, 41-52.
83. Kim, K.H., and Hwang, H., 1988, An Incremental Discount Pricing Schedule with Multiple Customers and Single Price Break, *European Journal of Operational Research*, 35, 71-79.
84. Kirkpatrick, S., and Gelatt, C.D., and Vecchi, M.P., 1983, Optimization by Simulated Annealing, *Science*, 220, 4598, 671-680.
85. Klastorin, T.D., Moinzadeh, K., and Son, J., 2002, Coordinating orders in Supply Chains Through Price Discounts, *IIE Transactions*, 34, 679-689.
86. Kline, M., 1972, *Mathematical Thought From Ancient to Modern Times*, New York: Oxford University Press.
87. Kogan, K., Leu, Y.Y., and Perkins, J.R., 2002, Parallel-Machine, Multiple-Product-Type, Continuous-Time Scheduling: Decomposable Cases, *IIE Transactions*, 34(1), 11-22.
88. Kolmogorov, A.N., and Yushkevich, A.P., 1998, *Mathematics of the 19th Century*, Vol. 3, Boston: Birkhäuser Verlag.
89. Lal, R., and Staelin, R., 1984, An Approach for Developing an Optimal Discount Pricing Policy, *Management Science*, 30(12), 1524-1539.
90. Lam, M.J., Inman, D.J., and Saunders, W.R., 2000, Hybrid Damping Models Using the Golla-Hughes-McTarvish Method with Internally Balanced Model Reduction and Output Feedback, *Smart Materials and Structures*, 9, 362-371.
91. Lee, H.L., and Rosenblatt, M.J., 1986, A Generalized Quantity Discount Pricing Model to Increase Supplier's Profits, *Management Science*, 32, 1177-1185
92. Lee, H.W.J., Ali, M., and Wong, K.H., 2004, Global Optimization for a Class of Optimal Discrete-Valued Control Problems, *Dynamics of Continuous Discrete and Impulsive Systems Series B*, 11, 735-756.
93. Lee, H.W.J., and Teo, K.L., 2003, Control Parametrization Enhancing Technique for Solving a Special ODE Class with State Dependent Switch, *Journal of Optimization Theory and Applications*, 118(1), 55-66.
94. Lee, H.W.J., Cai, X.Q., and Teo, K.L., 2001a, Optimal Control Approach to Manpower Planning Problem, *Mathematical Problems in Engineering*, 7, 155-175.

95. Lee, H.W.J., Lee, W.R., Wang, S., and Teo, K.L., 2001b, Construction of Sub-Optimal Feedback Control for Chaotic Systems Using B-Spline with Optimally Chosen Knot Points, *International Journal of Bifurcation and Chaos in Applied Science and Engineering*, 11(9), 2375-2387.
96. Lee, H.W.J., Teo, K.L., and Cai, X.Q., 1998, An Optimal Control Approach to Nonlinear Mixed Integer Programming Problems, *Computers and Mathematics with Applications*, 36, 87-105.
97. Lee, H.W.J., Teo, K.L., and Lim, A.E.B., 2001c, Sensor Scheduling in Continuous Time, *Automatica*, 37, 2017-2023.
98. Lee, H.W.J., Teo, K.L., Rehbock, V. and Jennings, L.S., 1999, Control Parametrization Enhancing Technique for Optimal Discrete-Valued Control Problems, *Automatica*, 35(8), 1401-1407.
99. Lee, H.W.J., Teo, K.L., Rehbock, V., and Jennings, L.S., 1997, Control Parametrization Enhancing Technique for Time Optimal Control Problems, *Dynamic Systems and Applications*, 6, 243-262.
100. Lee, Y.C.E., and Lee, H.W.J., Optimal Control Solutions to the Maximum Volume Isoperimetric Pillars Problem, *Automatica*, *accepted*.
101. Lee, Y.C.E., and Lee, H.W.J., Enhanced State-dependent Switching Control for Quarter-car Suspension Model, *submitted*.
102. Lee, Y.C.E., Chan, Chi Kin, and Hou, S.H., 2006, The Effects of Demand Distribution Among Buyers on Co-ordination in a Single-Vendor-Multi-Buyer Supply Chain, *Conference proceedings in International Workshop on Successful Strategies in Supply Chain Management, Hong Kong, January 5-6*, 157-166.
103. Lee, Y.C.E., Fung, E.H.K., and Lee, H.W.J., Control Parametrization Enhancing Technique and Simulation on the Design of a Flexible Rotating Beam, *Journal of Optimization Theory and Applications*, 136(2), 2008.
104. Lee, Y.C.E., Fung, E.H.K., Zou, J.Q., and Lee, H.W.J., 2004, A Computational Optimal Control Approach to the Design of a Flexible Rotating Beam With Active Constrained Layer Damping, *Proceedings of IMECE2004, ASME International Mechanical Engineering Congress and Exposition, Anaheim, California, November 13-19*, proceeding in the form of CD-ROM, IMECE2004-62205.
105. Leigh, J.R., 1992, *Control Theory: A Guided Tour* (London : the Institution of Electrical Engineers).
106. Lesieutre, G.A., and Lee, U., 1996, A Finite Element for Beams Having Segmented Active Constrained Layers with Frequency-Dependent

- Viscoelastics, *Smart Materials and Structures*, 5, 615-627.
107. Lewis, F.L., 1992, *Applied Optimal Control & Estimation: Digital Design & Implementation* (New Jersey, Prentice Hall).
108. Lieber, Z., 1973, An Extension to Modigliani and Hohn's Planning Horizon Results, *Management Science*, 20(3), 319-330.
109. Lu, L., 1995, A One-Vendor Multi-Buyer Integrated Inventory Model, *European Journal of Operational Research*, 81, 312-323.
110. Marshall, J.E., Gorecki, H., Korytowski, A., and Walton, K., 1992, *Time-Delay Systems: Stability and Performance Criteria with Applications* (New York : Ellis Horwood).
111. Melachrinoudis, E., and Min, H., 2002, The Dynamic Relocation and Phase-Out of a Hybrid, Two-Echelon Plant/Warehousing Facility: A Multiple Objective Approach, *European Journal of Operational Research*, 123(1), 1-15.
112. Midler, J.L., 1969, A Stochastic Multiperiod Multimode Transportation Model, *Transportation Science*, 3(1), 8-29.
113. Miller, B.L., 1986, Scarf's State Reduction Method, Flexibility, and a Dependent Demand Inventory Model, *Operations Research*, 34(1), 83-90.
114. Mishra, A.K., 2004, Selective Discount for Supplier-Buyer Coordination Using Common Replenishment Epochs, *European Journal of Operational Research*, 153, 751-756.
115. Monahan, J.P., 1984, A quantity Discount Model to Increase Vendor Profits, *Management Science*, 30, 720-726.
116. Niculescu, S.I., Verriest, E.I., Dugard, L., and Dion, J.M., 1997, Stability and Robust Stability of Time-Delay Systems: A Guided Tour. In Dugard, L., and Verriest, E.I. (Eds), 1998, *Stability and Control of Time-Delay Systems* (London: Springer-Verlag), 1-71.
117. Ogata, K., 2002, *Modern Control Engineering* (New Jersey, Prentice Hall).
118. Parthasarathy, S.S., and Srinivasa, Y. G., 2006, Design of an Active Suspension System for a Quarter-Car Road Vehicle Model Using Model Reference Control, *Journal of Systems & Control Engineering*, 220(2), 91-107.
119. Porter, B., and Bradshaw, A., 1974, Modal Control of Production Inventory Systems Using Piecewise Constant Control Policies, *International Journal of Systems Science*, 5(8), 733-742.
120. Porter, B., and Taylor, F., 1972, Modal Control of Production Inventory Systems, *International Journal of Systems Science*, 3(3), 325-331.
121. Riddalls. C.E., Johanson, B.I., Axtell, C.M., Bennett S., and Clegg., C.,

- 2002, Quantifying the Effects of Trust in Supply Chain During Promotional Periods, *International Journal of logistics: Research and Applications*, 5(3), 257-274.
122. Riddalls., C.E., and Bennett S., 2001, The Optimal Control of Batched Production and Its Effect on Demand Amplification, *International Journal of Production Economics*, 72(2), 159-168.
123. Riddalls., C.E., and Bennett, S., 2002, The Stability of Supply Chains. *International Journal of Production Research*, 40(2), 459-475.
124. Riddalls, C.E., Bennett, S., and Tipi, N.S., 2000, Modelling the Dynamics of Supply Chains. *International Journal of Systems Science*, 31(8), 969-976.
125. Ritoré, M., and Ros, A., 2002, Some Updates on Isoperimetric Problems, *Mathematical Intelligencer*, 24(3), 9-14.
126. Sam, Y.M., Osman, H.S., Ghani, R.A., 2002, Proportional-Integral Sliding Mode Control of a Quarter Car Active Suspension, *Proceedings of IEEE TENCON02, Beijing*, 1630-1633.
127. Sarmah, S.P., Acharya, D., and Goyal, S.K., 2006, Buyer Vendor Coordination Models in Supply Chain Management, *European Journal of Operational Research*, 175, 1-15.
128. Schneeweiss, C.A., 1971, Smoothing Production by Inventory – An Application of the Wiener Filtering Theory, *Management Science*, 17(7), 472-483.
129. Sethi, S.P., and Thompson, G.L., 2000, *Optimal Control Theory : Applications to Management Science and Economics* (Boston: Kluwer Academic Publishers).
130. Siegel, A., 2002, A Dido Problem as Modernized by Fejes Tóth, *Discrete & Computational Geometry*, 27(3), 227-238.
131. Simchi-Levi, D., Kaminsky, P., and Simchi-Levi, E., 2003, *Designing and Managing the Supply Chain : Concepts, Strategies, and Case Studies* (New York : McGraw-Hill)
132. Simon, H.A., 1952, On the Application of Servomechanism Theory in the Study of Production Control, 20(2), 247-268.
133. Smykay, E.W., Bowersox, D.J., and Mossman, F.H., 1961, *Physical Distribution Management Logistics Problems of the Firm* (New York: Macmillan).
134. Serman, J.D., 1989, Modeling Managerial Behavior: Misperceptions of Feedback in a Dynamic Decision Making Experiment, *Management Science*, 35(3), 321-339.
135. Sussmann, H.J., and Williems, J.C., 1997, 300 Years of Optimal Control:

- From the Brachystochrone to the Maximum Principle, *IEEE Control Systems*, 17(3), 32-44.
136. Suzuki, J., 2002, *A History of Mathematics*, Upper Saddle River, New Jersey: Prentice Hall.
137. Teo, K.L., Goh, C.J., Wong, K.H., 1991, *A Unified Computational Approach to Optimal Control Problems* (England : Longman Scientific and Technical).
138. Toffner-Clausen, S., 1996, *System Identification and Robust Control: A Case Study Approach* (New York : Springer).
139. Towill, D. R., Naim, M. M., and Wikner, J., 1992, *Industrial Dynamics Simulation Models in the Design of Supply Chains*, *International Journal of Physical Distribution & Logistics Management*, 22(5), 3-13.
140. Towill, D.R., 1991, *Supply Chain Dynamics*, *International Journal of Computer Integrated Manufacturing*, 4(4), 197-208.
141. Treiberg, A., 2002, *Inequalities that Imply the Isoperimetric Inequality*, <http://www.math.utah.edu/~treiberg/isoperim/isop.pdf>.
142. Tustin, A., 1953, *The Mechanism of Economic Systems* (London: William Heinemann).
143. Tzafestas, S., and Kapsiotis, G., 1994, *Coordinated Control of Manufacturing/Supply Chains Using Multi-Level Techniques*, *Computer Integrated Manufacturing Systems*, 7(3), 206-212.
144. Valentini, G., and Zavanella L., 2003, *The Consignment Stock of Inventories: Industrial Case and Performance Analysis*, *International Journal of Production Economics*, 81-82, 215-224.
145. Veinott, A.F., 1965, *Optimal Policy for a Multi-Product, Dynamic, Non-Stationary Inventory Problem*, *Management Science*, 12(3), 206-222.
146. Viswanathan, S., 1998, *Optimal Strategy for the Integrated Vendor-Buyer Inventory Model*, *European Journal of Operational Research*, 105, 38-42.
147. Viswanathan, S., and Piplani, R., 2001, *Coordinating Supply Chain Inventories Through Common Replenishment Epochs*, *European Journal of Operational Research*, 129, 277-286.
148. Wang, Q., 2002, *Determination of Suppliers' Optimal Quantity Discount Schedules with Heterogeneous Buyers*, *Naval Research Logistics*, 49(1), 46-59.
149. Waters, D., 2003, *Logistics: An Introduction to Supply Chain Management* (New York: Palgrave Macmillan).
150. Wong, K.H., Chan, C.K., and Lee, H.W.J., 2006, *Optimal Feedback*

- Production for a Single-Echelon Supply Chain, to appear in Journal of Discrete and Continuous Dynamical Systems.
151. Wong, K.H., Lee, Y.C.E., and Lee, H.W.J., Effect of Information Sharing in a Two-Level Supply Chain with Ornstein Uhlenbeck Demand Process, *submitted*.
 152. Woo, Y.Y., Hsu, S.L., and Wu, S., 2001, An Integrated Inventory Model for a Single Vendor and Multiple Buyers with Ordering Cost Reduction, *International Journal of Production Economics*, 73, 203-215.
 153. Xu, J.K., and Bainum, P.M., 1995, Dynamics of Flexible Multi-Link Robot Arms with Mass Center Offset”, *Acta Astronautica*, 36(2), 99-111.
 154. Yang, T.W., Xu., W.L., and Tso, S.K., 2001, Dynamic Modeling Based on Real-Time Deflection Measurement and Compensation Control for Flexible Multi-Link Manipulators, *Dynamics and Control*, 11(1), 5-24.
 155. Yoshimura, T., Kume, A., Kurimoto, M., and Hino, J., 2001, Construction of an Active Suspension System of a Quarter Car Model Using the Concept of Sliding Mode Control, *Journal of Sound and Vibration*, 239(2), 187-199.
 156. Zahir, S., and Sarker, R., 1991 Joint Economic Ordering Policies of Multiple Wholesalers and a Single Manufacturer with Price-Dependent Demand Functions, *Journal of the Operational Research Society*, 42(2), 157-164.
 157. Zheng, Y.S., 1994, Optimal Control Policy for Stochastic Inventory Systems with Markovian Discount Opportunities, *Operations Research*, 42(4), 721-738.
 158. Zou, J.Q., Fung, E.H.K., and Lee, H.W.J., 2003, Dynamic Analysis of a Flexible Manipulator with Passive Constrained Layer Damping, 2003 ASME International Mechanical Engineering Congress & Exposition, Washington, D.C., IMECE2003-41246.